Characterisation of the Acto-MyoA motor complex in *Toxoplasma gondii*

by

Dipl.Biol.
Saskia Marcia Egarter

Submitted in fulfilment of the requirements for the
Degree of Doctor of Philosophy

Institute of Infection, Immunity & Inflammation
College of Medical, Veterinary & Life Science
University of Glasgow

2014

Abstract

In apicomplexan parasites, the machinery required for gliding motility is located between the plasma membrane and the Inner Membrane Complex (IMC). This type of motility depends on the regulated polymerisation and depolymerisation of actin and a multi-subunit complex, known as the Myosin A motor complex. This complex consists of the myosin heavy chain A (MyoA), the myosin light chain 1 (MLC1), the essential light chain 1 (ELC1) and three gliding-associated proteins (GAP40, GAP45 and GAP50). Gliding motility is thought to be essential for host cell egress and linked to active, parasite driven penetration of the host cell. Many components of this complex are extensively studied using either the ddFKBP system or the tetracycline-inducible knockdown system (Tet-system). Strikingly, while depletion of *myoA* has no impact on IMC formation, overexpression of the tail domain of MyoA results in a severe IMC biogenesis phenotype. In order to investigate this issue, conditional knockout (KO) mutants of the interacting partners of MyoA-tail were generated using the conditional site-specific DiCre recombination system. Indeed, GAP40 and GAP50 were identified as being essential for parasite replication and having a crucial role during IMC biogenesis. This is the first evidence showing that components of the MyoA motor complex fulfil essential functions during IMC formation and thus are not exclusively important for gliding motility dependant processes.

Several components of the MyoA motor complex were characterised using the Tet-system and showed a complete block in gliding motility, but not in host cell invasion. While it is possible that leaky expression of the gene in the knockdown mutants is responsible for this uncoupling of gliding motility and invasion, it remains feasible that different mechanisms are involved in these two processes. In order to shed light on this issue, conditional KOs for the Acto-MyoA motor complex were generated in this study and their functions during gliding dependent processes thoroughly analysed. Intriguingly, while depletion of individual components of this complex caused a severe block in host cell egress, gliding motility and host cell penetration were decreased, but not blocked, demonstrating an important, but not essential role of the Acto-MyoA motor complex during these processes. Altogether, this study raises questions of our current view of what drives gliding motility and invasion and supports the argument for critical revision of the linear motor model.

Table of contents

List of tables

List of figures

Acknowledgements

At this point, I would like to say a big thank you to everyone who actively supported me during my PhD. A very special and sincere thanks goes to my supervisor, Prof. Markus Meißner. I am grateful for the opportunity to do my PhD in his laboratory, for all his support and advice over the last years. His excitement for science is simply infectious (although sometimes challenging ☺) and I enjoyed the enthusiastic discussions.

I am thankful to my assessors from Glasgow, Prof. Mike Barrett and Dr Lisa Ranford-Cartwright for their advices and valuable suggestions to my projects.

The Meißner group was a great place to be and I want to thank all the past and present members for their help and support whenever it was needed and the fun time inside and outside the lab. Sincere thanks goes to Nicole. I am truly going to miss all of our "how is it gliding and how does it invade" discussions. Many thanks goes to all my little proofreading helpers, Jacqueline, Robyn and Ellie, who had to face the new rules for English grammar I invented ☺. I would like to thank Manu for always having a friendly ear, helping me in the lab especially in the beginning of my PhD and for giving me countless personal and scientific advice. I would also like to acknowledge Dr. Gurman Pall for all his effort and assistance with administrational problems and Dr. Volodymyr Nechyporuk-Zloy for his assistance in microscopy. I want to thank Jennifer, who contributed to some of the data presented here. Thanks to Jamie for keeping up with a too worrying flatmate and telling me countless time "You'll be fine" especially during the last month of writing. I am certain my favourite KO is in good hands ☺

Very big thanks go to everyone on level 6 of the GBRC. It was a pleasure to be part of such an amazing work environment.

Mein ganz besonderer Dank gilt meinen Eltern, meinen Schwestern und Sebastian, ohne deren Unterstützung, Hilfe und Liebe ich nicht soweit gekommen wäre. DANKE!

Publications arising from this work

The following published paper contains work presented in this thesis:

Andenmatten, N., **S. Egarter**, A. J. Jackson, N. Jullien, J. P. Herman and M. Meissner (2013). "Conditional genome engineering in *Toxoplasma gondii* uncovers alternative invasion mechanisms." Nat Methods **10**(2): 125-127.

Egarter, S., N. Andenmatten, A. J. Jackson, J. A. Whitelaw, G. Pall, J. A. Black, D. J. Ferguson, I. Tardieux, A. Mogilner and M. Meissner (2014). "The Toxoplasma Acto-MyoA Motor Complex Is Important but Not Essential for Gliding Motility and Host Cell Invasion." PLoS One **9**(3): e91819.

Author's Declaration

I, Saskia Marcia Egarter hereby declare that I am the sole author of this thesis and performed all of the work presented, with the following exceptions:

Chapter 3:

- Complementation analysis of MyoA-tail was counted by Prof Markus Meissner

- EM analysis was performed in collaboration with Prof David JP Ferguson from the University of Oxford, United Kingdom

Chapter 4:

- Analytical PCR and Western blot of *gap45* KO was performed by Jennifer Ann Black under my supervision

- Live microscopy of wildtype and *myoA* KO parasites to measure gliding speed was performed by Dr Nicole Andenmatten

- EM analysis was performed in collaboration with Prof David JP Ferguson from the University of Oxford, United Kingdom

Chapter 5:

- EM analysis was performed in collaboration with Prof David JP Ferguson from the University of Oxford, United Kingdom

……

Saskia M. Egarter

Abbreviations/ Definitions

°C	degree Celsius
6-TX	6-thioxanthine
aa	amino acid
AGE	Agarose gel electrophoresis
AMA1	apical membrane antigen 1
Amp	Ampicillin
ATP	adenosine triphosphate
BLAST	Basic-Local-Alignment-Search-Tool
bp	base pair
BSA	bovine serume albumine
Ca^{2+}	calcium
CAT	chloramphenicol acetyltransferase
cDNA	complementary deoxyribonucleic acid
CDPK	calcium-dependent protein kinase
CIP	calf intestinal phosphatase
C-terminal	carboxy terminal
CytD or CD	Cytochalasin D
dd	destabilisation domain
DHFR	dihydrofolate reductase
DiCre	dimerisable Cre
DMEM	Dulbecco's Modified Eagle's Medium
DMSO	dimethyl sulfoxide
DN	dominant negative
DNA	deoxyribonucleic acid
dNTP	deoxynucleoside 5'-triphosphate
E. coli	*Escherichia coli*
e.g.	exempli gratia (for example)
ECL	enhanced chemiluminescence
EDTA	ethylene diamine tetraacetic acid
EGTA	ethylene glycol tetraacetic acid
ELC	Endosomal like compartment
ELC1	essential light chain 1
EM	electron microscopy
ER	endoplasmatic reticulum
EtOH	Ethanol
FBS	Fetal bovine serum
fw	Forward
g	Gram
GAP	glideosome associated protein
gDNA	genomic deoxyribonucleic acid
GFP	green fluorecent protein
GOI	gene of interest
GPI	Glycophosphatidylinositol
GRASP	Golgi re-assembly stacking protein

GSH	Glutathione
h	Hour
H_2O	Water
HEPES	4-(2-Hydroxyethyl)-piperazineethanesulphonic acid
HFF	human foreskin fibroblast
HRP	horseradish peroxidase
HSP	heat shock protein
hx or hxgprt	hypoxanthine-xanthine-guanine phosphoribosyl transferase
IFA	immunofluorescence analysis
IMC	inner membrane complex
IPTG	isopropyl-O-D-thiogalactopyranoside
kbp	kilo base pair
KD	Knockdown
kDa	kilo Dalton
KO	Knockout
LB	Luria-Bertani
loxP	Locus crossover in P1
M	Molar
MCS	multiple cloning site
mg	Milligram
MIC	micronemal protein
min	Minute
ml	millilitre
MLC	myosin light chain
mM	Milimolar
MPA	mycophenolic acid
mRNA	messenger ribonucleic acid
MT	Microtubule
Myo	Myosin
NCBI	National Center for Biotechnology Information
ng	Nanogram
nm	nanometer
N-terminal	amino terminal
o/n	over night
ORF	open reading frame
P. berghei or *Pb*	*Plasmodium berghei*
P. falciparum or *Pf*	*Plasmodium falciparum*
PBS	phosphate buffered saline
PCR	polymerase chain reaction
PFA	paraformaldehyde
PM	plasma membrane
POI	protein of interest
PV	parasitophorous vacuole
PVM	parasitophorous membrane
qPCR	quantitative polymerase chain reaction
RFP	red fluorescent protein

RNA	ribonucleic acid
RON	rhoptry neck protein
ROP	rhoptry protein
rpm	revolutions per min
RT	room temperature
rv	Reverse
s	Second
SAG1	surface antigen 1
SD	standard deviation
SDS-PAGE	sodium dodecyl sulfate polyacrylamide gel electrophoresis
SEM	standard of the mean
SOC	super optimal broth with catabolite repression
spp.	Species
SSR	Site specific recombination
t	Time
T. gondii or *Tg*	*Toxoplasma gondii*
TAE	tris-acetate-EDTA
Taq	thermos aquaticus
TEMED	N,N,N',N'-tetramethylethylenediamine
TJ	tight junction
TM	transmembrane
Tris	tris [hydroxymethyl] aminomethane
U	Unit
UTR	Untranslated region
UV	Ultraviolet
V	Volt
v/v	volume/volume percentage
w/v	weight/volume percentage
WB	Western blot
WHO	World health organisation
WT	wild-type
x	Fold
Xan	xanthosine monophosphate
X-Gal	5-bromo-4-chloro-3-indoyl-ß-D-Galactopyranoside
YFP	yellow fluorescent protein
µg	microgram
µl	Microliter
µm	micrometer
µM	Micromolar

1 Introduction

1.1 The phylum Apicomplexa

Apicomplexan parasites belong to a large group of obligate intracellular parasites, which can cause severe diseases in humans and animals and thus are of great veterinary and medical importance. This phylum contains over 5,000 species of parasitic protozoa (Levine 1988). One of the most lethal parasites is *Plasmodium falciparum* the causative agent of malaria, with almost 207 million cases of disease and a mortality rate of over half a million per year (World Health Organization (WHO) December 2013). Other apicomplexan parasites such as *Eimeria spp.* (causes coccidiosis in poultry), *Babesia spp.*, *Neospora spp.* (causes of spontaneous abortion in cattle) and *Theileria spp.* effect livestock and can cause immense economic losses. *Cryptosporidium spp.* is able to infect humans and cause severe gastrointestinal illnesses resulting in fatal, opportunistic infections in HIV/AIDS patients. One of the most widespread parasites is *Toxoplasma gondii* with about one third of the world's population infected (Hill *et al.* 2005), with the frequency of infection rising with increased age. This parasite can cause debilitating, life threatening complications in immunocompromised individuals and affects foetal development during pregnancy.

1.2 General overview of *Toxoplasma gondii*

T. gondii was isolated for the first time from the North African rodent *Ctenodactylus gundi* by the French scientists Nicolle and Manceaux in 1908 (Nicolle and Manceaux 1908, Nicolle and Manceaux 1909, Ferguson 2009). It can infect any nucleated cell of warm-blooded vertebrates. After an acute infection phase tachyzoites differentiate into slow growing bradyzoites which form tissue cysts that persist in the host. *T. gondii* forms three infectious stages: sporozoites (sexual form found in oocysts), bradyzoites (persistent, slow replicating asexual form) and tachyzoites (fast replicating, asexual form). Generally, human infections occur by eating undercooked meat containing tissue cysts or by ingesting contaminated water containing oocysts (Mead *et al.* 1999, de Moura *et al.* 2006, Jones and Dubey 2012).

Infection with *T. gondii* is asymptomatic or causes mild symptoms, such as headache and fever in healthy people. In contrast, infection in immune-suppressed people can have much more serious consequences (Suzuki *et al.* 1996). According to the WHO up to 35 million people are infected with AIDS worldwide. Toxoplasmosis is one of the leading causes of death in HIV-infected people. Due to the impairment of the immune system, persistent cysts are reactivated and toxoplasmosis can break out. Cysts formed within brain tissue can cause severe lesions that subsequently lead to encephalitis and are fatal if left untreated. Women infected with toxoplasmosis for the first time while pregnant have a high risk of congenital transfer, whereby the parasite is passed from mother to the embryo (McLeod *et al.* 2012). The risk of such a transfer increases towards the end of the pregnancy. This might result in multiple organ damage to the developing embryo. Furthermore, the risk of miscarriage is increased. *T. gondii* is responsible for more spontaneous abortions than any other food borne pathogen.

During an acute infection, common drug treatments include antifolates such as sulfadiazine and pyrimethamine (Montoya and Liesenfeld 2004). Furthermore, spiramycin can be used to treat pregnant women before the twentieth week of pregnancy (Schoondermark-Van de Ven *et al.* 1994). No current drugs or vaccines are active against the bradyzoite stage of *T. gondii* showing there is a need for the development of effective, well-tolerated drugs to treat toxoplasmosis.

1.3 Life cycle of *Toxoplasma gondii*

T. gondii has a facultative *heteroxen* life cycle, in which sexual and asexual reproduction occurs in two different hosts. Asexual replication occurs in intermediate hosts whereas sexual reproduction takes place in the definitive host. All warm-blooded vertebrates serve as intermediate hosts, while the sexual life cycle is restricted to members of the Felidae family. Unlike most other Apicomplexa, *T. gondii* has no need to go through the sexual cycle before transmission to a new host *(Su et al. 2002)*. The complete life cycle (Figure 1-1) was first described with the discovery of sexual stages in the small intestine of cats in 1970 (Hutchison *et al.* 1969, Dubey *et al.* 1970).

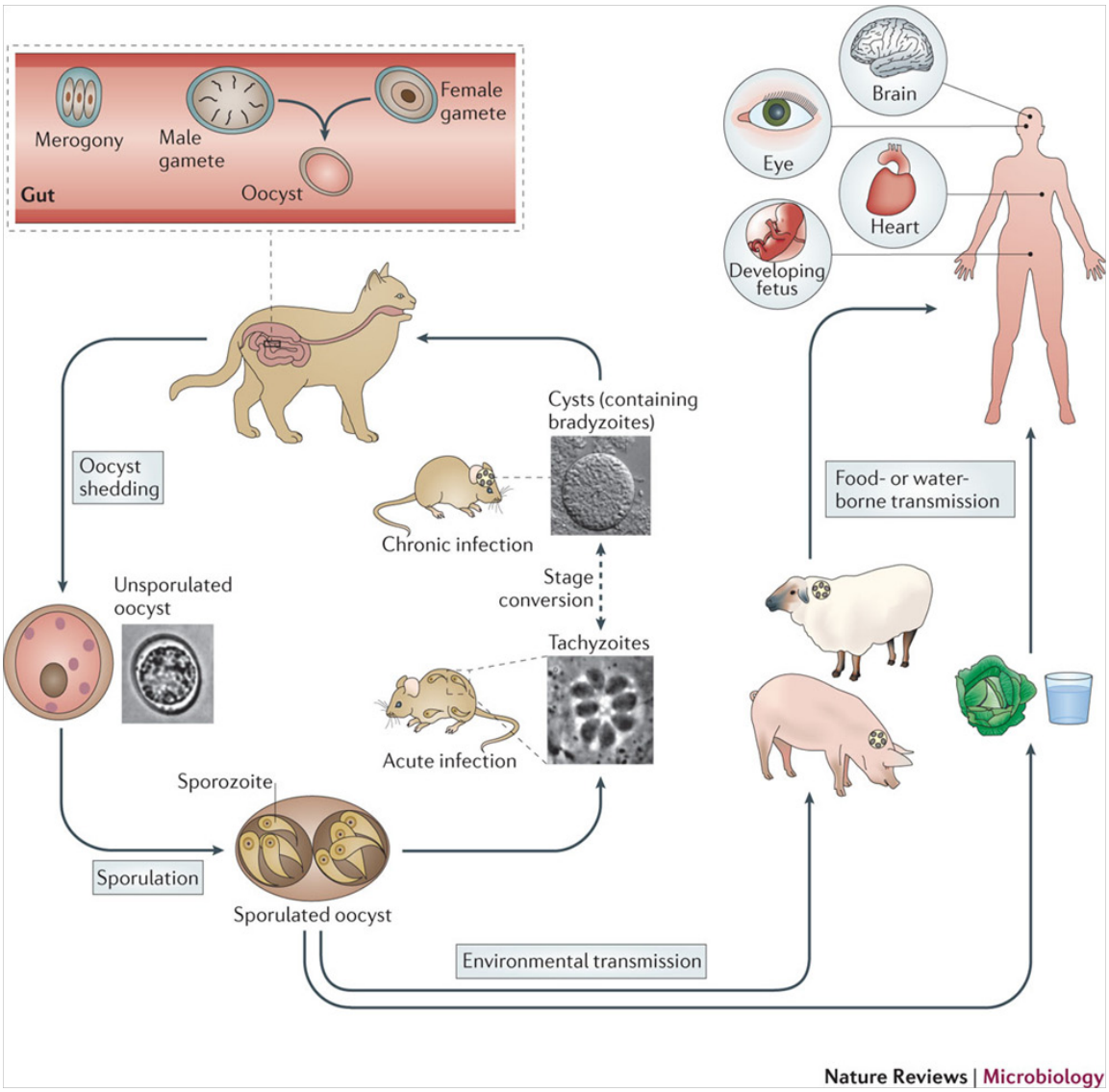

Figure 1-1: The life cycle of *Toxoplasma gondii*. The sexual reproduction of *T. gondii* occurs in the cat that serves as a definite host, while the asexual replication can take place in any warm-blooded vertebrate as intermediate hosts. Within the gut of the cat, male and female gametes are formed and their fusion leads to the production of diploid oocysts. Those oocysts are then shed in the faeces of the cat where sporulation occurs under the right conditions. They can be taken up by intermediate hosts. Once within the intestines of the intermediate host sporozoites are released whereupon they enter sub epithelial cells and begin their asexual reproduction. Acute infections are denoted by fast replicating tachyzoites whereas long-termed chronic infections are characterised by slow growing, cyst forming bradyzoites. Figure reprinted from Hunter and Sibley (2012).

1.3.1 Life cycle in the definitive host

Cats can acquire *T. gondii* by ingesting any of the three infectious stages: bradyzoites (form cysts in infected tissue), tachyzoites or sporozoite-containing oocysts. Of these, the bradyzoite-induced infection is the most transmissive as most cats infected shed oocysts, whereas only 30 % of cats infected with tachyzoites or oocysts shed the latter (Miller *et al.* 1972, Dubey and Frenkel 1976). The bradyzoite-induced sexual live cycle is the only one studied in detail. After tissue cysts containing bradyzoites are taken up, the cyst wall is digested

by proteolytic enzymes in the stomach and the bradyzoites penetrate the intestinal epithelium undergoing several steps of morphogenesis. Five morphologically distinct stages are known before gametocyte formation occurs. The first two stages divide by endodyogeny (two daughter cells are formed within the mother cell) followed by three rounds of endopolygeny (multiple rounds of DNA replication and mitosis before budding takes place).

After asexual development is completed, merozoites commence gamete formation. Merozoites develop to either male (microgametocyte) or female (macrogametocyte) gametocytes. While microgametogony results in the formation of multiple (15-30) microgametes, macrogametogony leads to the formation of a single macrogamete. The male gamete is flagellated and swims to the female gamete for fertilisation. This process is called gamogony and results in a diploid zygote that develops to haploid oocysts by meiosis. Finally, the infected epithelial cells rupture and unsporulated oocysts are released into the lumen and millions of unsporulated oocysts are shed with the feces (Dubey 2001). If the environmental conditions of humidity, aeration and ambient temperature are optimal oocysts can sporulate in 1 day (Dubey *et al*. 1970, Dubey *et al*. 1970). During sporulation, two sporocysts are formed containing four sporozoites each. Sporulated oocysts can maintain their infectivity for up to a year if temperature and humidity are suitable (Dubey 1997, Dubey *et al*. 2011).

1.3.2 Lytic cycle of *Toxoplasma gondii*

The life cycle in intermediate hosts is exclusively asexual and begins after oral uptake of oocysts. Upon reaching the intestine, sporozoites are released and enter the epithelium of the intestinal lumen where they transform into tachyzoites which are distributed throughout the body. Asexual reproduction can be divided into two distinct phases of growth depending if the infection is acute or chronic. During the first phase, fast and repetitive divisions take place. Parasites during these stages are termed tachyzoites (greek: tachos=fast). Whilst in the acute infection stage, the parasites are able to pass tissue barriers (e.g. the placenta).

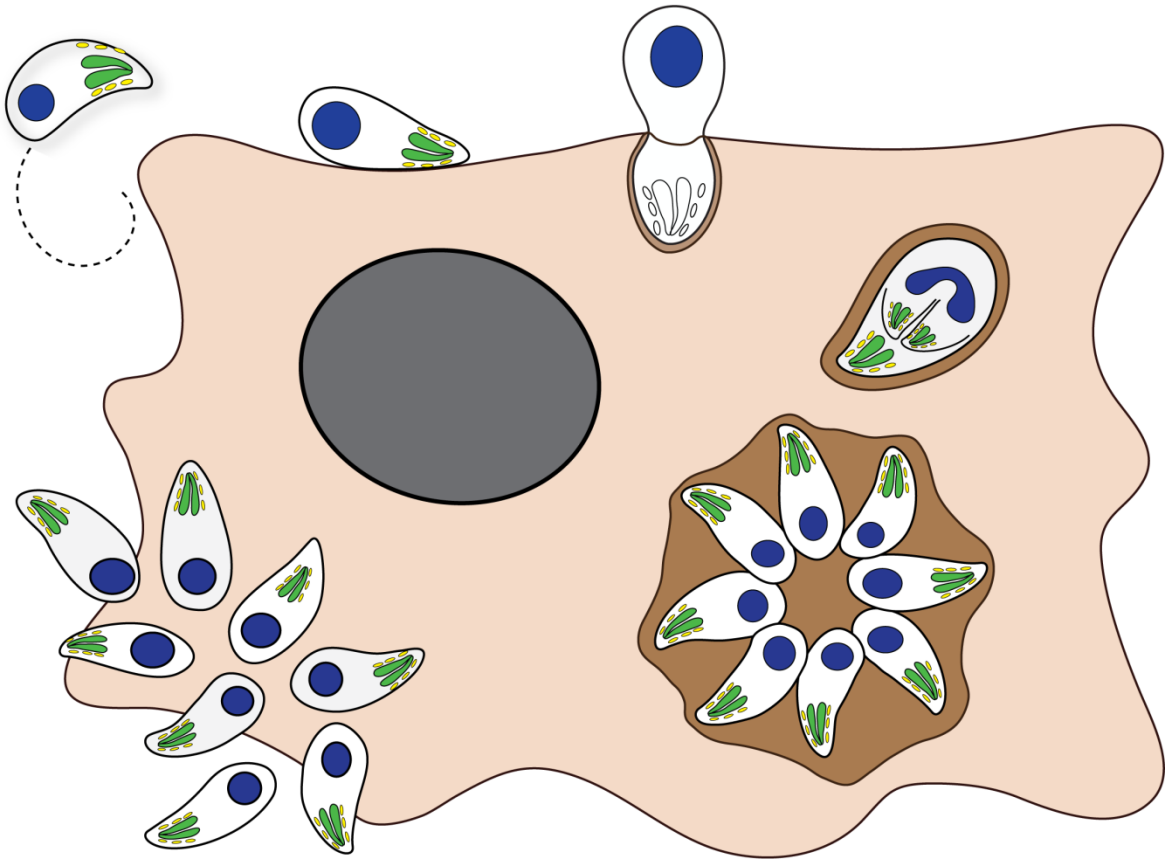

Figure 1-2: The lytic cycle of *Toxoplasma gondii*. After egressing the host cells, *T. gondii* tachyzoites move to neighbouring cells using gliding motility. Following attachment to the host cell surface, the parasites actively invade the cell through a tight junction. While penetrating the cell, a parasitophorous vacuole (PV) is formed around the parasite. That way, protected from the host trafficking system, *T. gondii* starts replicating by endodyogeny. After several rounds of replication, when 16-64 parasites are within the PV, the tachyzoites egress from the host cell migrating to surrounding cells ready to start the cycle again. Figure inspired by Soldati and Meissner (2004).

In order to fulfil this rapid division a chronological order of processes takes place, called the lytic cycle (Black and Boothroyd 2000) (Figure 1-2). This cycle has five consecutive or/and simultaneous steps: (1) attachment, (2) invasion, (3) vacuole formation, (4) replication and (5) egress. The cycle starts with the attachment of the parasite to the host cell. This step is subdivided in an initial, loose attachment, followed by reorientation of the parasites, so that it faces the host cell with its apical end, before attaching more strongly to allow invasion (for more detailed information see chapter 1.9.3). During invasion the parasitophorous vacuole membrane encapsulates the parasite. Replication proceeds by endodyogeny (see chapter 1.6.1) until a signal is received that triggers egress (see chapter 1.9.2), which results in lyses of the host cell and release of motile tachyzoites. These parasites migrate and invade neighbouring cells to start the cycle from the beginning.

Once an immune response is initiated by the host, the proliferative stage ends, the tachyzoites invade new cells and start to develop slowly. In this second phase of development, the last generation of tachyzoites develops into the lifelong stages. A membrane is formed that surrounds the cysts, in which thousands of bradyzoites (Greek: brady = slow) divide very slowly. These tissue cysts are mainly found in brain, skeletal or heart muscles (Lyons *et al*. 2002). These stages can have a lifelong persistence and they remain infective if they enter a new host. Generally, tissue cysts are the final stage of asexual reproduction. After uptake through another intermediate host, the asexual development cycle starts again. If the lifelong stages enter a host that is a member of the Felidae family, a new round of the sexual reproduction begins (Dubey 1997).

1.4 *Toxoplasma gondii* as a model organism

T. gondii serves as an important model system for analysing specific conserved features of apicomplexan biology. This is because of the ease of culturing this parasite, its fast propagation speed and the amenability to genetic modifications (see chapter 1.4.1 and 1.4.2). For instance, a feasible, continuous *in vitro* cultivation method for *Cryptosporidium* spp. has not yet been developed and procedures for cryopreservation and the efficient generation of mature, infectious oocysts are not available at present (Coulliette *et al*. 2006, Karanis and Aldeyarbi 2011, Bessoff *et al*. 2013). *In vitro* culturing of asexual *Plasmodium falciparum* was introduced almost 40 years ago. However, after subsequent developments transfection is still an inefficient process (Haynes *et al*. 1976, Trager and Jensen 1976). The transfection efficiency is very low, episomes are maintained for a long time and isolation of stable lines need month long drug cycling periods (O'Donnell *et al*. 2001). Another limitation is that *Plasmodium* parasites are restricted to distinct cell types like hepatocytes and erythrocytes. In contrast, *T. gondii* invades virtually any nucleated vertebrate cell, making it easy to maintain constantly *in vitro* (Kim and Weiss 2004). Transfections are a straightforward task and non-integrated episomal DNA will get lost after a short time period. Well-established mouse models exist for *in vivo* studies as well (Dubey 1997, Chtanova *et al*. 2009, Gregg *et al*. 2013).

1.4.1 The genome of *Toxoplasma gondii*

With exception of the diploid unsporulated oocyst, the genome of *Toxoplasma gondii* is haploid and has been completely sequenced. *T. gondii* has 14 chromosomes and a genome size of 65 Mb (Sibley and Boothroyd 1992, Kissinger *et al*. 2003, Khan *et al*. 2005, Gajria *et al*. 2008). This is more than the double of the genome size of *Plasmodium falciparum* despite the same number of chromosomes (Khan *et al*. 2005). This difference is due to a lower gene density and a higher numbers of introns per gene. An additional difference exists concerning the GC content of the DNA. The GC content of *T. gondii* is 52 %, while the one of *P. falciparum* is at about 19 % (Pain *et al*. 2005). Additionally, most genes in *T. gondii* occur as single copies. Thus, the analysis of the function of particular genes can be easily carried out using a full set of reverse genetic tools.

1.4.2 Reverse genetics in *Toxoplasma gondii*

The first successful transient and stable transfections in *T. gondii* were reported in 1993 using a genetically altered Dihydrofolate reductase (*dhfrts*) as a selectable marker (Donald and Roos 1993, Soldati and Boothroyd 1993). Consecutively, analysis of the parasites using reverse genetic approaches became feasible. For stable transfections, selection markers such as the Uracil phosphoribosyltransferase (UPRT; (Donald and Roos 1995)), the hypoxanthine-xanthine-guanine phosphoribosyl transferase (HXGPRT; (Donald *et al*. 1996)) and the Chloramphenicol acetyltransferase ((CAT); (Kim *et al*. 1993)) are used. Reporter genes like *lacZ* and fluorescence proteins, such as GFP, can be introduced for studying these parasites (Soldati and Boothroyd 1993, Seeber and Boothroyd 1996, Striepen *et al*. 1998, Striepen *et al*. 1998, Kim *et al*. 2001). Random integration of DNA into the genome was used for insertional mutagenesis to identify developmental specific genes and promoters. Using homologous recombination, genes can be inactivated by replacement of the gene of interest (GOI) through a selection marker (Kim *et al*. 1993). This principle is only achievable with non-essential genes.

To analyse the function of essential genes ectopic gene regulation systems such as the tetracycline-repressor system (Meissner *et al*. 2001) or the transactivator-

system (Meissner *et al*. 2002) are used. The tetracycline (Tet) inducible transactivator system regulates expression on transcriptional level (Gossen and Bujard 1992). This system works with a Tet responsive promoter (TRE), where the Tet operator (TetO) sequences are located upstream of a minimal promoter. Binding of Tet dependant transactivator (tTA) to the TRE switches on transcription of the respective GOI, while the presence of the inducer anhydrotetracycline (ATc) abolishes binding of tTA to TetO, thus inactivating transcription. This system was successfully optimised for the use in *T. gondii* to generate conditional knockdowns of GOIs (see Figure 1-3A) (Meissner *et al*. 2002, Meissner and Soldati 2005, Kessler *et al*. 2008). The establishment of a parasite line expressing TATi in a *Δku80* background allowed targeted replacement of the endogenous promoter by the Tet-inducible promoter by homologous recombination (Sheiner *et al*. 2011). This approach has been successfully transferred for use in *Plasmodium berghei* to analyse blood-stage essential genes (Pino *et al*. 2012).

Another possibility is based on the destabilization-domain (dd) system. The ddFKBP-system allows rapid regulation of protein stability. This system was originally developed in mammalian cells (Banaszynski *et al*. 2006). A ligand responsive destabilisation domain, based on the 12 kDa sized rapamycin-binding protein (FKBP12) is fused in frame of the protein of interest (POI). As ligand serves the cell permeable, rapamycin analogue Shield-1. The dd domain has a high instability in the absence of the ligand which leads to protein degradation. However, addition of the ligand results in protein stabilisation (see Figure 1-3B). After adapting this system for use in apicomplexan parasites (Armstrong and Goldberg 2007, Herm-Gotz *et al*. 2007) it has been extremely well explored for the regulated expression of dominant negative mutants and for the generation of overexpression mutants (Herm-Gotz *et al*. 2007, Agop-Nersesian *et al*. 2009, Breinich *et al*. 2009, van Dooren *et al*. 2009, Agop-Nersesian *et al*. 2010, Daher *et al*. 2010, Kremer *et al*. 2013, Pieperhoff *et al*. 2013).

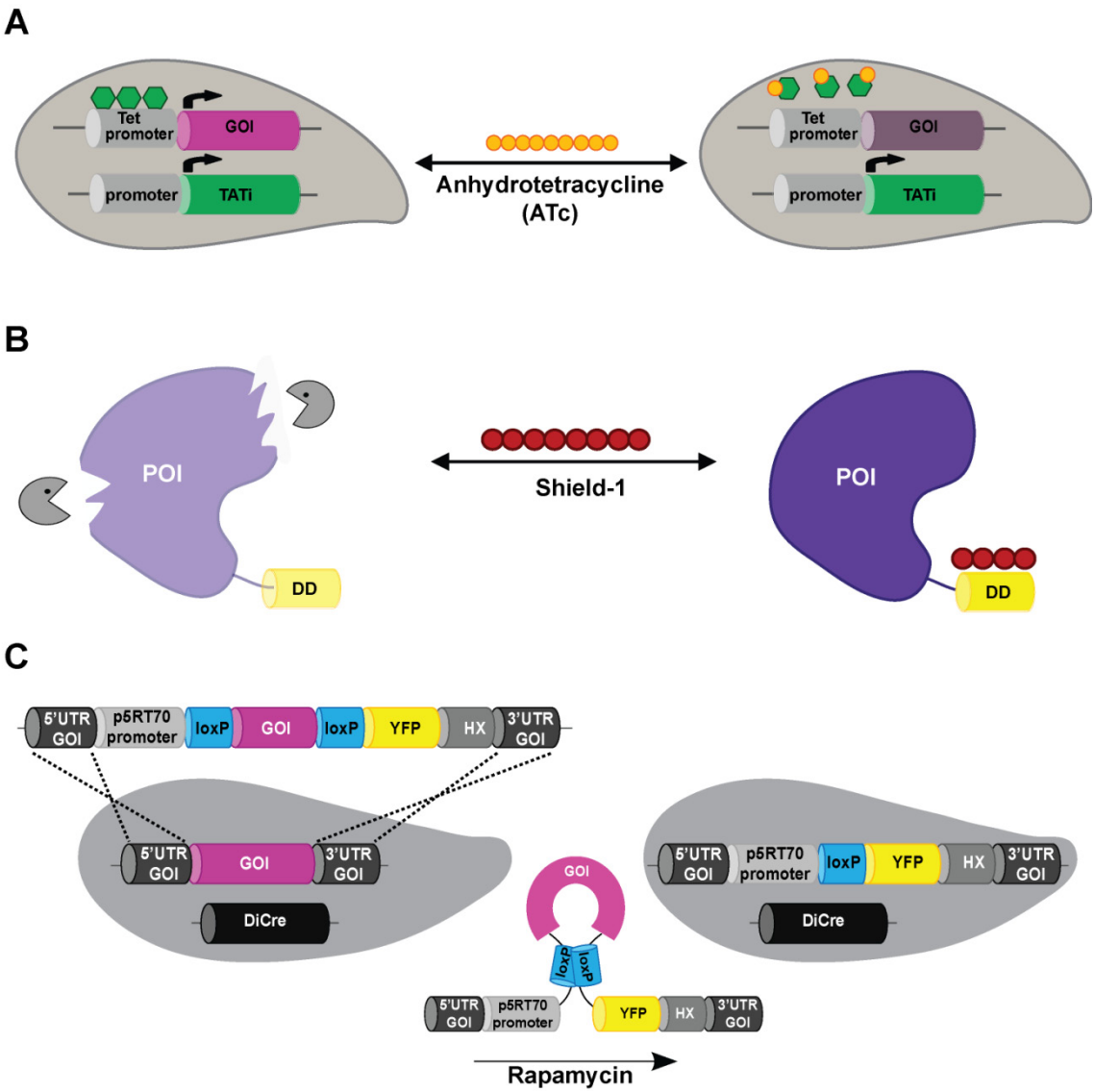

Figure 1-3: Reverse genetic toolbox in *Toxoplasma gondii*. (A) Scheme of the tetracycline inducible transactivator system. The TATi transactivator (green) binds to Tet-operator DNA repeats and recruits the transcription machinery that leads to gene expression. Addition of ATc (orange) interferes with the interaction of TATi with the promoter resulting in no transcription. B) Functional principle of the ddFKBP-system. The fusion of a destabilisation domain (DD; yellow) to the protein of interest (POI) allows for regulation of protein levels through the addition of the ligand shield-1 (red). The DD domain is highly unstable in the absence of the ligand which leads to protein degradation. C) Model of the Cre recombinase inducible Knockout system (DiCre-system). The cDNA of the gene of interest (GOI) is flanked by two loxP sites. After homologous recombination into the endogenous locus of the GOI and expression of the Cre recombinase the loxP sites recombine and the cDNA is excised which leads to a conditional Knockout of the GOI. Figure reprinted from Andenmatten *et al.* (2013).

A further strategy to create mutants for essential genes is the use of site-specific recombination systems like Cre/LoxP. The approach of this system is to flank a gene of interest with specific recognition sites for particular recombinases (Brecht *et al.* 1999). Cre recombinases catalyse the recombination between two loxP sites of 34 bp sequences. Depending on the orientation of these loxP sites, the DNA in between is either excised or inverted, thus leading to gene knockouts or translocation. The Cre recombinase activity can be

regulated by ligand controlled systems such as the recently developed dimerizable Cre (DiCre) system (Jullien *et al*. 2003, Jullien *et al*. 2007). This system was successfully introduced to manipulate the genome of apicomplexan parasites such as *Toxoplasma gondii* (Andenmatten *et al*. 2013) and *Plasmodium falciparum* (Collins *et al*. 2013). The mechanism of this system is based on splitting of the Cre recombinase in two inactive fragments. Each of the fragments is fused to a rapamycin-binding protein (FRB and FKBP12). Addition of the ligand rapamycin results in dimerisation of the two inactive Cre fragments, thus leading to the reconstitution of Cre activity (see Figure 1-3C) (Jullien *et al*. 2007).

With the generation of parasites lacking the *ku80* gene for non-homologous end joining (Fox *et al*. 2009, Huynh and Carruthers 2009), targeting to specific genetic loci has become reasonably straightforward. This allows endogenous gene tagging, one-step promoter swapping for conditional gene knockdowns, gene knockouts, and allelic replacement via homologous recombination (Mital *et al*. 2005, Sheiner *et al*. 2011, Andenmatten *et al*. 2013).

1.5 Morphology of *Toxoplasma gondii*

The tachyzoite is a crescent shaped parasite with a size of 2 x 7 µm which is more pointed towards the apical end and rounded towards the basal end (Dubey *et al*. 1998). A set of eukaryotic organelles is present *in T. gondii* (see Figure 1-4) comprised of nucleus, endoplasmic reticulum (ER), a single mitochondrion and a single Golgi stack (Joiner and Roos 2002, Pelletier *et al*. 2002). A unique organelle of the Apicomplexa is the apicoplast, a non-photosynthetic plastid obtained via secondary endosymbiosis by uptake of an eukaryotic red algae (see chapter 1.5.3) (Kohler *et al*. 1997, Foth and McFadden 2003, Waller *et al*. 2003). Additionally a new vacuolar compartment or plant-like vacuole (VAC or PLV) has recently been discovered (Miranda *et al*. 2010). This vacuole comprises a sodium hydrogen exchanger (NHE3) which is believed to be important for invasion and osmoregulation (Francia *et al*. 2011). Apicomplexan parasites evolved a special organelle complex (apical complex) at the apical end giving the phylum its name (Morrissette and Sibley 2002).

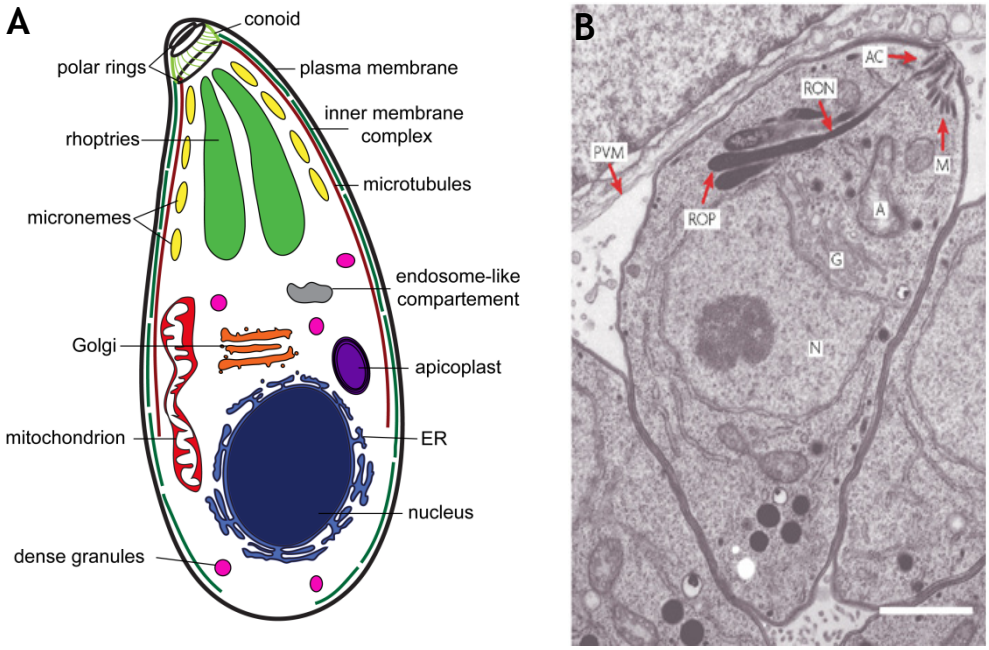

Figure 1-4: Ultrastructure of Toxoplasma gondii. A) A tachyzoite is surrounded by the plasma membrane (in black), the IMC (in dark green) and a network of microtubules (in dark red). Located at the apical end are the polar rings, the conoid (in light green) and secretory organelles, micronemes (in yellow) and rhoptries (in green). Dense granules are distributed uniformly in the cytoplasm (in pink). In the centre of the parasite are the apicoplast (in purple), the single Golgi stack (in orange), a single tubular mitochondrion (in red) and the endosome-like compartment (in grey). The nucleus is surrounded by the ER (in blue) and located at the basal end of the parasites. Picture inspired by Agop-Nersesian *et al*. (2010). B) Electron micrograph of a tachyzoite inside a parasitophorous vacuole membrane (PVM). Depicted is the apical cytoskeleton (AC) micronemes (M), rhoptry bulbs (ROP) and rhoptry necks (RON). Other organelles of the parasite are the nucleus (N), the Golgi apparatus (G) and the apicoplast (A). The scale bar represents 0.5 µm. Reprint of Boothroyd and Dubremetz (2008).

1.5.1 Apical complex

The apical complex consists of an intriguing structure called the conoid, two intraconoidal microtubules, two polar rings and secretory organelles including the rhoptries, micronemes and dense granules (see chapter 1.5.2) (Morrissette and Sibley 2002). The conoid, which resembles a truncated cone, is adjoined by two polar rings and made up of 14 spirally wound fibres of a novel α-tubulin polymer. It extends and retracts as the tachyozoite migrates, via gliding motility, and is postulated to be involved in the invasion process (Hu *et al*. 2002). The mechanism for this protrusion is not yet known, despite the ability to mimic the process by altering parasite cytosolic calcium concentrations, with calcium ionophores and calcium chelators, or by treating parasites with actin inhibitors (Mondragon and Frixione 1996, Pezzella *et al*. 1997, Stommel *et al*. 1997, Del Carmen *et al*. 2009).

1.5.2 Secretory organelles

1.5.2.1 Rhoptries

The rhoptries belong to the secretory organelles of apicomplexan parasites. Tachyzoites usually possess 8-12 of these specialised organelles that are club-shaped with a bulbous body and a narrow electron-dense neck and claim up to 30 % of the parasite volume with a size of approximately 2.5 µm (Dubey *et al*. 1998, Dubremetz 2007). Their anchorage is mediated by the palmitoylated Armadillo Repeat Protein (ARO) to the apical pole of the parasite (Beck *et al*. 2013, Mueller *et al*. 2013). Rhoptries are compartmentalised and their protein content can be divided in two distinct subgroups depending on their function and localisation. Located to the neck of the rhoptry organelle are the so called rhoptry neck proteins (RONs) which are the first rhoptry proteins secreted (Bradley et al 2005). Four of those proteins, RON2,4,5 and 8, have a role during tight junction formation (see chapters 1.9.3) and form a complex with the micronemal protein AMA1 (apical membrane antigen-1) (Mital *et al*. 2005, Besteiro *et al*. 2009, Tonkin *et al*. 2011, Tyler *et al*. 2011). The rhoptry bulb proteins (ROP) are situated in the bulbous part of these organelles. ROPs play a number of roles, such as helping to form the parasitophorous vacuole (PV) and PV membrane (Boothroyd and Dubremetz 2008), acting as virulence factors by hijacking host cellular functions (Saeij *et al*. 2006, Taylor *et al*. 2006, Saeij *et al*. 2007), and manipulating host responses by altering host actin disassembly and invasion kinetics (Delorme-Walker *et al*. 2012).

1.5.2.2 Micronemes

The smallest of the secretory organelles are the elliptical shaped micronemes with an internal size of 75 nm x 150 nm (Carruthers and Tomley 2008). The quantity of micronemes varies between species and developmental stages, but approximately 50-100 micronemes are enriched at the apical end of *Toxoplasma*. Recently, with the discovery of different vesicular routes and content of micronemes, these organelles were divided into two different subsets (Kremer *et al*. 2013). The micronemes contain many proteins which possess adhesive domains important for gliding motility, attachment, invasion and egress. These processes depend on the regulated secretion of micronemal proteins coupled to changes of the intracellular calcium levels. While there is usually a low level of

constitutive secretion, high levels of cytoplasmic calcium have been reported before invasion and egress (Moudy *et al*. 2001) (Silvia Moreno, 12th congress of toxoplasmosis, 2013). Treatment of *T. gondii* with ethanol, acetaldehyde or calcium ionophore (A23187) can artificially trigger microneme discharge by increasing the calcium levels (Carruthers *et al*. 1999, Carruthers and Sibley 1999, Moudy *et al*. 2001).

1.5.2.3 Dense granules

Dense granules form the third class of secretory organelles. They derived their name because of their high electron density. Approximately 20 of these 200 nm large organelles are distributed throughout the cytosol (Mercier *et al*. 2005). After invading the host cell, the dense granules release their content into the PV suggesting a role in its establishment, maintenance and modification (Mercier *et al*. 2002, Gendrin *et al*. 2010). So far 24 dense granule proteins have been identified, these localise to the PV space and membranous structures such as the PV membrane or the membranous nanotubular network (Mercier *et al*. 1993, Mercier *et al*. 2002, Ahn *et al*. 2005, Bougdour *et al*. 2013, Braun *et al*. 2013). Two dense granule proteins, gra16 and gra24, were identified having regulatory functions on host cell signalling pathways (Bougdour *et al*. 2013, Braun *et al*. 2013).

1.5.3 The Apicoplast

Two organelles are present in apicomplexan parasites that derive from endosymbiosis, a single mitochondrion and a relict non-photosynthetic plastid, the apicoplast. The latter is a feature of Alveolates and was obtained via secondary endosymbiosis by uptake of a eukaryotic red algae (Kohler *et al*. 1997, Foth and McFadden 2003, Waller *et al*. 2003, Sheiner *et al*. 2011). The apicoplast has its own genome of 35 kb (Wilson *et al*. 1996, Lim and McFadden 2010) and is surrounded by four membranes. The outermost membrane of the apicoplast is derived from the endomembrane system of the host apicomplexan ancestor. The periplastid membrane which is the second outermost membrane originates from the plasma membrane of the red algal symbiont. The inner two membranes descend from the outer and inner membranes of the primary plastids of red algae (McFadden *et al*. 1996, Roos *et al*. 2002, van Dooren and Striepen 2013).

This plastid is involved in several important metabolic functions, (a) isoprenoid precursors (Wiesner and Jomaa 2007, Seeber and Soldati-Favre 2010, Baumeister *et al*. 2011, Nair *et al*. 2011), (b) type II fatty acids (Waller *et al*. 1998, Mazumdar *et al*. 2006, Ramakrishnan *et al*. 2012) (c) synthesis of heme (van Dooren *et al*. 2012, Koreny *et al*. 2013), and (d) iron-sulfur cluster [Fe-S] synthesis (Lim and McFadden 2010, Kumar *et al*. 2011, Gisselberg *et al*. 2013). Although many of those functions display critical roles for apicomplexan parasites, not all of them are of essential nature for parasite survival even differing within the Apicomplexa. Fosmidomycin is a drug targeting the apicoplast isoprenoid synthesis pathway. While *Plasmodium* spp. shows high sensitivity to this drug (Jomaa *et al*. 1999) the growth of *Toxoplasma* tachyzoites is not majorly affected, likely due to drug inaccessibility to the apicoplast (Baumeister *et al*. 2011, Nair *et al*. 2011). Furthermore, supplementation of isopentenyl phosphate (IPP) can rescue *Plasmodium falciparum* blood stages treated with fosmidomycin or lacking an apicoplast (Yeh and DeRisi 2011). Taken together these data indicate the isoprenoid pathways are essential for both apicomplexan protists (Nair *et al*. 2011, Yeh and DeRisi 2011). In contrast to this, synthesis of fatty acids seems essential for the growth of *T. gondii* tachyzoites and *Plasmodium* liver stages but not *Plasmodium* erythrocytic or mosquito stages (Mazumdar *et al*. 2006, Vaughan *et al*. 2009). Several drugs affect apicoplast segregation which results in a so called delayed death phenotype (Fichera *et al*. 1995, Fichera and Roos 1997, Dahl and Rosenthal 2008). After drug addition parasites replicate typically and form large vacuoles. However, not all parasites possessed an apicoplast and after re-invasion only parasites that obtained an apicoplast were able to replicate while parasites lacking this organelle died. Furthermore, apicoplast segregation mutants verified that the apicoplast is an essential organelle for parasites survival and indeed leads to a delayed death phenotype, but only one apicoplast per vacuole is required for replication (He *et al*. 2001).

1.6 Cell division and Assembly of the Cytoskeleton

1.6.1 Replication of *Toxoplasma gondii* by endodyogeny

Apicomplexan parasites replicate by the formation of daughter parasites within a mother cell. This process is termed endodyogeny, endopolygeny or schizogony

depending on the number of daughter cells formed and the timing of nuclear division. *T. gondii* tachyzoites divide by endodyogeny, also known as internal daughter budding (Sheffield and Melton 1968, Hu *et al*. 2002). Mitosis and daughter cell formation occur simultaneously and after duplication of the organelles, they are separated to the daughter parasites (Figure 1-5).

First, the Golgi apparatus is enlarged and duplicated late in G1 phase (Pelletier *et al*. 2002). Second, the centrioles migrate around the nucleus prior their division early in S1-phase, ensuring the polarity of the daughter parasites (Figure 1-5B; centriole: green staining IFA images 1-3) (Hartmann *et al*. 2006, Nishi *et al*. 2008). Following this, DNA is replicated and the centrioles migrate back to the apical pole of the parasite. Synchronously with the nucleus, the apicoplast divides (Figure 1-5B; apicoplast: red staining in IFA images 2,4,5) (Striepen *et al*. 2000). Late in S1 phase, the earliest components of the cytoskeleton are build and the internal daughter budding begins (Tilney and Tilney 1996, Radke *et al*. 2001, White *et al*. 2005, Hu 2008, Agop-Nersesian *et al*. 2010). The development of the conoid marks the formation of the cytoskeleton of the daughter cell (Hu *et al*. 2006). Concurrently, spindle poles and intranuclear microtubules are formed. Afterwards, the assembly of the Inner Membrane Complex (IMC) of the daughter parasites is initialised (Figure 1-5B; IMC: green staining in IFA images 4-7) (Mann and Beckers 2001) and followed by distribution of organelles to the forming daughter buds. To these organelles belong the nucleus, apicoplast and endoplasmic reticulum (Hager *et al*. 1999, Striepen *et al*. 2000, Hu *et al*. 2002). Similar to the apicoplast, the mitochondrion is not autonomously replicated. During early replication the mitochondrion forms branches but its integration into the growing daughter parasites occurs late during replication (Nishi *et al*. 2008). The last step of cytokinesis involves separation of all organelles between the two daughter parasites and completion of IMC formation. Following, the apical organelles of the mother cell are degraded and the plasma membrane of the mother cell is adopted by the daughter parasites. A residual body is left, which contains material such as maternal micronemes, rhoptries and parts of the mitochondrion (Nishi *et al*. 2008). The synthesis of the micronemes and rhoptries occurs *de novo* in the forming daughter parasites (Sheffield and Melton 1968, Nishi *et al*. 2008).The generation time of *T. gondii* tachyzoites depends on the

culture conditions and varies between six and seven hours (Radke *et al*. 2001, Gubbels *et al*. 2008).

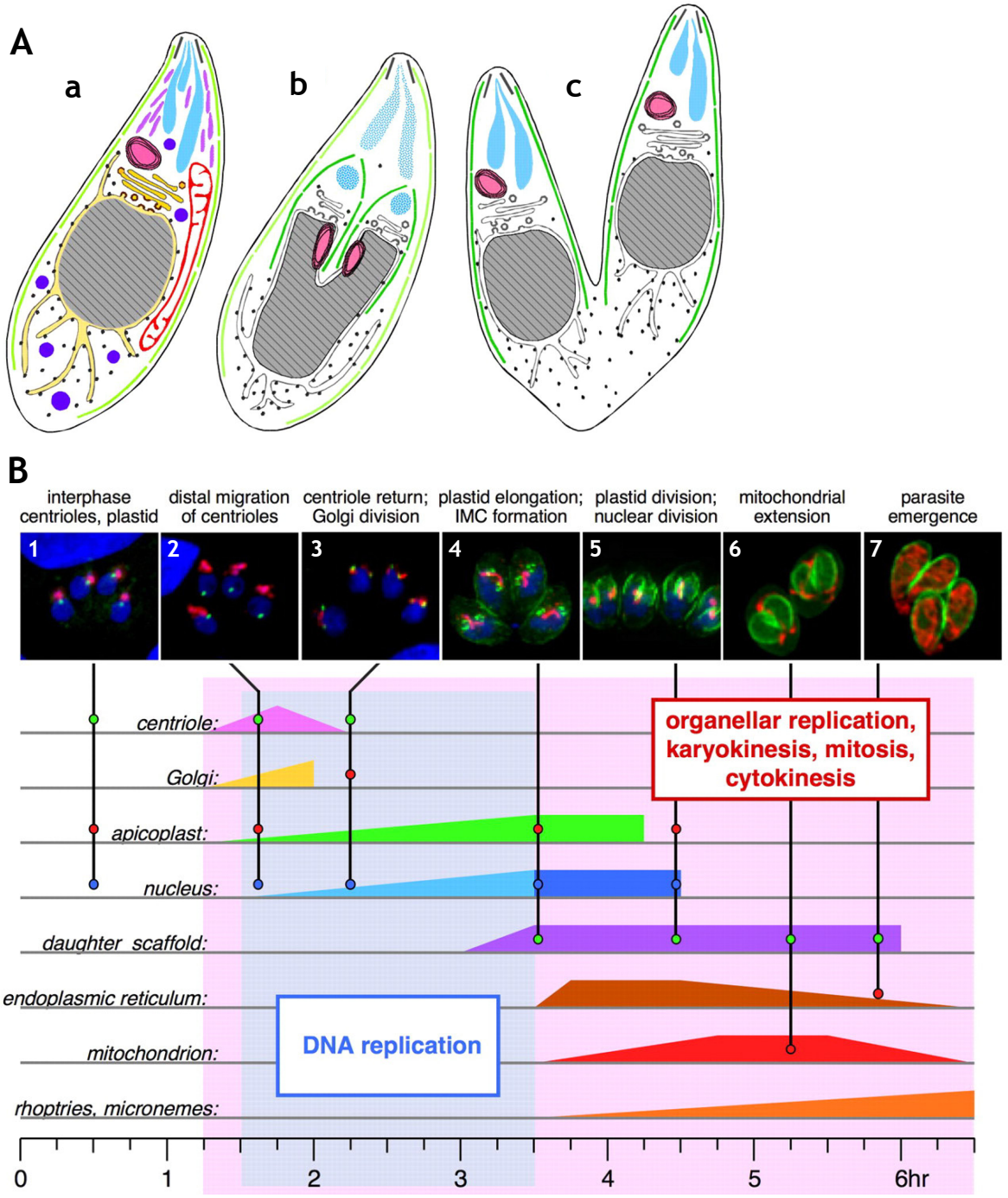

Figure 1-5: Replication of *Toxoplasma gondii* by endodyogeny. (A) Illustration of different phases of *T. gondii* tachyzoites during endodyogeny. a) Figure of the interphase. The following organelles are shown from the apical to basal end: the conoid (black lines), inner-membrane complex (light green lines), rhoptries (turquoise), micronemes (purple), dense granules (blue), apicoplast (pink), mitochondrion (red), Golgi (dark yellow) and nucleus (grey), encircled by endoplasmic reticulum (light yellow). b) Formation of the daughter parasites. Division of the Golgi and apicoplast organelles which are separated into the developing daughter cells and development of the daughter IMC (green). The maternal rhoptries are degraded and newly synthesised in the daughter parasites. c) Further development of the daughter IMC and the plasma membrane is obtained from the mother cell. (B) Chronology of biogenesis and division of organelles. The timeline displays coordinated events during *T. gondii* replication. IFAs show the appearance of several organelles and the main morphological changes during division. Modified and reprinted from Nishi *et al*. (2008).

While the chronological processes of endodyogeny have been well characterised by live cell imaging (Hu 2008, Nishi *et al*. 2008), the molecular mechanisms of organelle biogenesis and division are largely unknown. Recently, some components with a key role during biogenesis of secretory organelles, as well as maturation of the IMC, have been characterised. Three dynamin-related-proteins, DrpA, DrpB and DrpC were identified in the genome of *T. gondii* and DrpA and DrpB were characterised in detail (Breinich *et al*. 2009, van Dooren *et al*. 2009). DrpB accumulates close to the Golgi-apparatus, but this accumulation dissipates during replication. DrpB has a role during the biogenesis of the secretory organelles, micronemes and rhoptries (Breinich *et al*. 2009). DrpA is essential for the growth of *T. gondii* and the segregation of the apicoplast (van Dooren *et al*. 2009). In former studies the GTPase Rab11A was shown to be involved in the maturation of the IMC as well as regulating an essential step during cytokinesis (Agop-Nersesian *et al*. 2009) that occurs after biogenesis of the secretory organelles.

1.6.2 Components of the Cytoskeleton

Four further tubulin-containing structures exist additional to the conoid. The apical polar ring belongs to one of the three microtubule organising centres (MTOC). The minus ends of 22 subpellicular microtubules originate from this polar ring. These spiral in a left handed direction, terminate approximately two thirds of the way down the parasite and are responsible for its crescent shape. (Nichols and Chiappino 1987, Hu *et al*. 2002). The non-dynamic subpellicular microtubules are extremely stable, remaining intact even after extended treatment with the microtubule destabilising dinitroaniline herbicide, Oryzalin (Stokkermans *et al*. 1996, Morrissette *et al*. 2004). Inside the conoid lies a pair of short intraconoidal microtubules stemming from the outmost apical end and finishing precisely posterior to the conoid. Two further tubulin-comprising structures are found in the centrioles and spindle microtubules, which function during parasite replication organizing the mitotic spindle to coordinate chromosome segregation (Hu *et al*. 2002, Morrissette and Sibley 2002).

One of the components of the cytoskeleton in *Toxoplasma gondii* is the pellicle. This is made up of the outer plasma membrane and the beneath lying IMC, which is composed of two membranes (Mann and Beckers 2001). The pellicle is thought

to provide mechanical strength and structural stability to the parasite (Anderson-White *et al*. 2011). The IMC comprises of flattened membranous sacs called alveoli, which are a feature of the Alveolata, it spans the entire length of the parasites and gaps are only found at the apical and posterior end. Located on the cytoplasmic side of the IMC is a meshwork of intermediate filament-proteins called the subpellicular network (Anderson-White *et al*. 2011). The role of the IMC is giving structure to the cell, forming a scaffold for daughter parasite assembly, and serving as a support for motility mediated by the MyoA motor complex (Mann and Beckers 2001, Gaskins *et al*. 2004).

The IMC can be divided in subcompartments defined by the composition of proteins within the alveoli as can be seen by IMC subcompartment proteins (ISPs). ISP1 can be visualised at the apical cap of the IMC, while ISP2 and ISP4 localises to the middle part of the IMC and ISP3 can be found at the central and basal part of the IMC membranes (Beck *et al*. 2010, Fung *et al*. 2012) (Figure 1-6A). Another protein group that show distinct localisations to particular regions are the gliding associated proteins (GAPs). While GAP45 can be detected along the whole length of the parasite with exception of the apical cap, GAP70 can only be visualised apically and GAP80 is only detected at the basal end (Frenal *et al*. 2010, Jacot and Soldati-Favre 2012) (Figure 1-6A).

The anterior pole is called the apical cap and numerous proteins are localised to this region (Figure 1-6B). One of these proteins is the meshwork component IMC15 that belongs to the family of alveoli proteins (Anderson-White *et al*. 2011). This protein is the earliest detectable cytoskeleton protein during daughter cell assembly. It was assumed that because of its early expression IMC15 might play a role during the organisation of early parasite development (Anderson-White *et al*. 2012). Similar to IMC15, Centrin2 and Ring1 (RNG1) are found at the apical tip of the parasite. The precise function of these proteins at the extreme apical end is not known yet, although RNG1 is thought to be essential (Tran *et al*. 2010). RNG1 is localised beneath the extended conoid and only appears late in replication, just before mother parasite disassembly. Membrane occupation and recognition nexus 1 (MORN1) is another ring like structure found at the apical end of *T. gondii* visualised early during daughter cell budding (Gubbels *et al*. 2006, Hu 2008). Additional to their apical localisation, MORN1, IMC15 and Centrin2 are found in the basal complex.

Electron microscopy on the basal complex shows that two electron dense structures exist within the basal complex, the basal inner ring and basal inner collar (Anderson-White *et al*. 2011). The function of this complex is unknown, however, it was speculated that it could have a role in resisting mechanical stress during host cell invasion (Gubbels *et al*. 2006, Hu *et al*. 2006, Hu 2008).

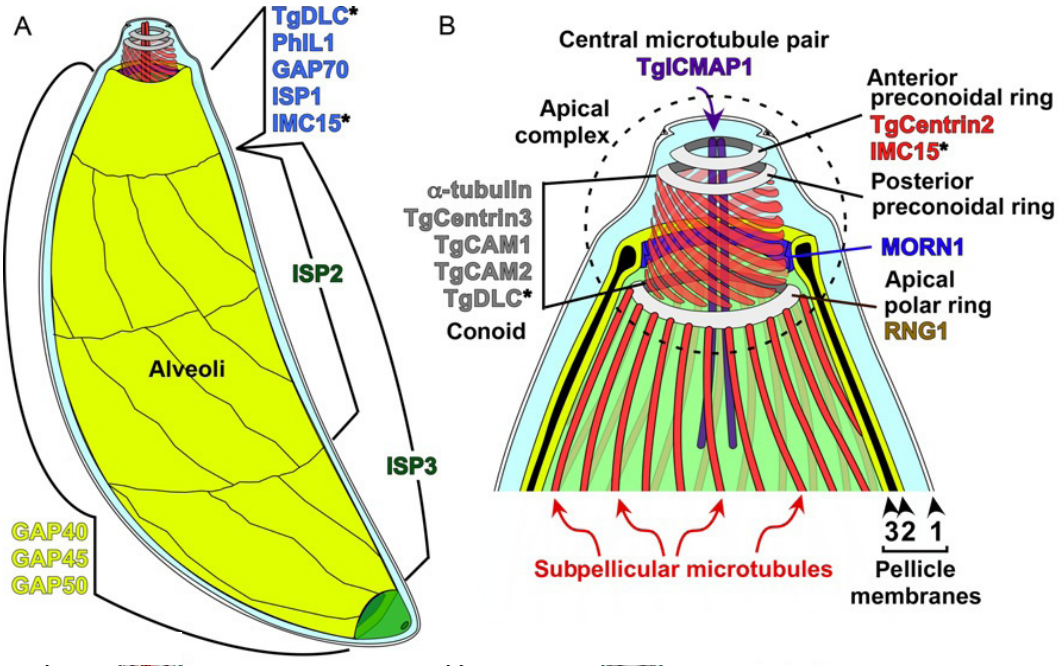

Figure 1-6: Schematic illustration of cytoskeleton structures in *Toxoplasma gondii*. (A) Beneath the plasma membrane are the alveolar vesicles, here pictured in yellow. These alveolar vesicle are subdivided into different sections which is demonstrated by localisation of the indicated proteins to distinct sections of the alveolar vesicles The apical cap represents the most unique alveolar vesicle whose components are indicated by blue labelling. (B) Representation of the subpellicular microtubules and the conoid and their associated structures. Components known to localise to these structures are indicated. Other structures are marked and named in the panel by matching colours. Reprinted from Anderson-White *et al*. (2012).

1.6.3 Coordinated assembly of the cytoskeleton

The assembly of the cytoskeleton is a well-orchestrated process that can be divided into four different periods: Initiation of budding, early budding, mid budding and late budding (Anderson-White *et al*. 2012). Initiation of budding begins after centrosome duplication where the DNA content is 1.2N. The centrosome plays an important role for the coordination of the mitotic and the cytokinetic cycle (Gubbels *et al*. 2008). The centrosomes themselves are very dynamic and co-localise early during the initiation phase with IMC15 and the small GTPase Rab11B. These observations make IMC15 and Rab11B the earliest markers for daughter cell budding (Anderson-White *et al*. 2012). The actin-like protein 1 (ALP1) can be visualised during the bud initiation process as well,

suggesting a role during the early stages of daughter cell assembly (Gordon *et al*. 2008). The termination of the bud initiation step can be monitored by the accumulation of MORN1 on the daughter buds (Gubbels *et al*. 2008). Additionally, the subpellicular microtubules and the conoid are formed during this phase (Hu *et al*. 2006, Agop-Nersesian *et al*. 2010). Those early structures of the IMC and MTs serve as a scaffold for the next steps of daughter cell budding.

The early budding stage is identified as beginning by the appearance of the IMC subcompartment proteins ISP1-3 (Beck *et al*. 2010). During this phase, at a DNA content of 1.8N, additional elements are identified within the daughter cells. These include IMC proteins, IMC1 and IMC3, and components of the MyoA motor complex, the gliding associated proteins GAP40 and GAP50. (Gaskins *et al*. 2004, Frenal *et al*. 2010).

After these early components are assembled the middle budding phase begins. It is typified by the elongation of the daughter parasite cytoskeleton towards the basal end. The basal end of the growing daughter cells is marked by MORN1 protein. It is suspected that first the apical end of the parasite is formed then the cytoskeleton scaffold grows in direction of the basal end. This is because ISP1 remains apical while the cytoskeleton grows in the direction of the midpoint of budding (Beck *et al*. 2010). CAM1 and CAM2 are proteins with two EF-hand calcium binding domains each localising to the MT region of the conoid at the midpoint of budding (Hu *et al*. 2006, Anderson-White *et al*. 2012). At this stage the IMC proteins, IMC5, 8, 9 and 13, are relocated from the periphery of the growing daughter parasites to the basal ends where MORN1 can be visualised (Anderson-White *et al*. 2011). The exact mechanism of basal complex constriction is currently unknown, however, it is suspected that Centrin2 might drive constriction of the basal complex (Hu 2008). This is because Centrin2 is Ca^{2+} dependant, filament forming and contractile, and begins to assemble at the basal complex at the same time IMC5,8 ,9 and 13 change their location to this complex (Anderson-White *et al*. 2011).

Maturation of the daughter cell occurs during the late budding phase while the cytoskeleton of the mother parasites is disassembled. A marker of this period is RNG1 that localises to the apical polar ring and can be detected just before the mother cell's cytoskeleton breaks down (Tran *et al*. 2010). The plasma

membrane of the mother cell is integrated into the pellicle of the newly formed daughter cells in a Rab11A dependant manner (Agop-Nersesian *et al*. 2009).The MyoA motor complex is then incorporated between the plasma membrane and the IMC of the nascent daughter parasites.

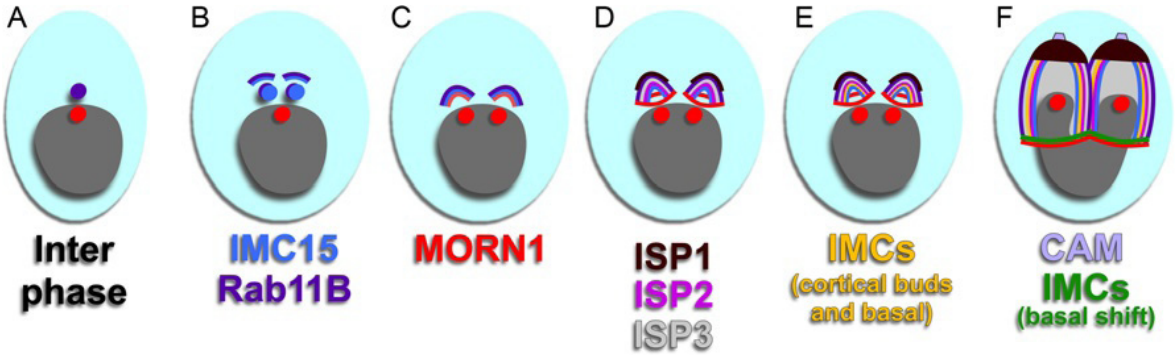

Figure 1-7: Time line of the budding process. Time improves from panel A to F. In (A) the interphase (G1 phase) is depicted where no budding occurs. (B+C) describe the budding initiation with Rab11B and IMC15 build first followed by MORN1. The early budding is shown in (D+E) where the ISP proteins are formed prior to the first IMC proteins and gliding associated proteins. (F) illustrates the end of the early budding process and the transition to mid budding. Components correspond to the text colours below the panels respectively. Reprinted from Anderson-White *et al*. (2012).

1.7 Myosin motor complexes

1.7.1 Motor proteins in general

The majority of active transport processes in the cell are driven by three types of molecular motors: myosins, kinesins and dyneins (Ross *et al*. 2008). These motor proteins all utilise ATP hydrolysis to generate movement which arises from a conformational change in the globular head domain (Schliwa and Woehlke 2003, Okten and Schliwa 2007). Kinesins and dyneins utilise microtubules to generate movement and move to the plus- or the minus-end of the microtubule, respectively (Vallee and Sheetz 1996). Dyneins can be classed into two groups: cytoplasmic and axonemal dynein. Axonemal dynein is responsible for the ATP-driven movement of flagella and cilia (Gibbons and Rowe 1965). Cytoplasmic dynein is responsible for minus end-directed transport (Vallee and Sheetz 1996) and for transport from the endoplasmic reticulum to the Golgi apparatus (Vaughan 2005). Kinesins play a role in the distribution of the chromosomes during mitosis and meiosis and are involved in the transport of organelles, vesicles, RNA and protein complexes (Goldstein 2001). Unconventional myosin motors use actin filaments for their transport. They move toward the plus end of the filaments. Myosins and kinesins bind to the actin track via their head

domain, which has an ATP-binding site. The tail domain, which is highly variable in sequence, is responsible for specific binding to its cargo. In order to perform movements on a cellular and molecular level, several protein-regulated processes are required within the cell.

1.7.2 General overview and structure of myosins

Myosins are actin-dependent molecular motors that have several functionally important roles. Though best known for co-ordinating muscle contractions myosins are also involved in cellular movement, cytokinesis, phagocytosis, endocytosis, exocytosis and vesicle transport (Mermall *et al.* 1998). The myosin structure is composed of a heavy and a light chain. The heavy chain has a highly conserved head domain responsible for binding to actin and for ATPase activity. The neck domain interacts with the myosin light chains and functions as a lever that can change the conformation of the ATP binding pocket. The variable tail region binds the motor protein to its specific cargo and thus, varies markedly in its structure as each tail domain is functionally specific for its respective cargo. Conventional myosins have a shared amino acid motif in which a negatively charged amino acid or a phosphorylation-modifiable amino acid is located 16 amino acids up/downstream of a conserved DALAK sequence. This sequence motif is referred to as "TEDS rule" (Bement and Mooseker 1995). The binding site of the neck domain also displays a conserved sequence known as the IQ motif. Myosin activity is regulated through calmodulin or calmodulin-like light chains linked to bivalent Ca^{2+} molecules (Sellers and Goodson 1995). Apicomplexans however possess many unconventional myosins that do not follow those rules. More details on these apicomplexan myosins are outlined below.

1.7.3 Myosins in Apicomplexa

T. gondii has, with 11 open reading frames, the largest collection of unconventional myosin heavy chains within apicomplexan parasites identified so far. Six myosins are present in both *P. falciparum* and *Cryptosporidium parvum* (Gardner *et al.* 2002, Abrahamsen *et al.* 2004). Many apicomplexan myosins belong to class XIV of the myosin superfamily. This superfamily is divided into four subclasses, with the subclass XIVd consisting solely of myosins of the ciliates *Tetrahymena thermophila* (Foth *et al.* 2006). In *T. gondii* class XIV is comprised

of the following six myosins, MyoA, MyoB/C, MyoD, MyoE and MyoH (Foth *et al*. 2006). MyoA and MyoD belong to the subclass XIVa and localise to the plasma membrane of the parasite (Hettmann *et al*. 2000). MyoB, -C and -E are assigned to the subclass XIVb.

MyoA is the most well characterised apicomplexan myosin due to its role in gliding motility, invasion and egress. MyoA homologues are also found in all known apicomplexan parasites (Heintzelman and Schwartzman 1997, Pinder *et al*. 1998, Matuschewski *et al*. 2001, Foth *et al*. 2006). As Myo A is involved in so many important processes it will be discussed in more detail (see chapter 1.7.4.1). MyoB and MyoC are encoded by a single gene that is alternatively spliced. The two distinct mRNAs encode for the two myosins that have identical head and neck domains and differ only in their tail region (Delbac *et al*. 2001). MyoB is generated when the last intron remains unspliced. MyoB is naturally expressed at very low levels in bradyzoites but not at all in tachyzoites (Delbac *et al*. 2001). Overexpression of MyoB in tachyzoites shows a punctuated and cytoplasmic distribution. Additionally, large residual bodies and morphological replication defects can be observed after overexpression of MyoB. MyoC is formed by splicing of the last intron. MyoC is the predominant isoform expressed in tachyzoites. Localised to the apical and basal rings of *T. gondii,* MyoC is thought to play roles during daughter cell formation (Delbac *et al*. 2001).

Found in all coccidians, MyoD is the closest myosin to MyoA in *Toxoplasma* concerning sequence homology (55% identity and 70% similarity), peripheral localisation, and biophysical characteristics (Foth *et al*. 2006, Herm-Gotz *et al*. 2006). It is thought that MyoD has emerged from gene duplication of MyoA and is dispensable for tachyzoites as a conventional gene knockout could be maintained in this parasite stage with no effects on gliding motility, invasion or virulence in mice (Herm-Gotz *et al*. 2006). Recently, an interaction between MyoD and the myosin light chain 2 (MLC2) has been demonstrated (Polonais *et al*. 2011). More prominently expressed in bradyzoites, MyoD might have a more important function in this cyst forming stage.

MyoF belongs to the class XXII myosins and contains WD40 repeats (Foth *et al*. 2006). Recently an interaction between MyoF and the *Toxoplasma gondii* armadillo repeats only protein (ARO) has been shown. The authors suggest a

model where the MyoF motor complex associates with ARO at the rhoptry membrane, targeting it to the apical end of the parasite (Mueller *et al*. 2013). Finally, an important role of MyoF for centrosome positioning and inheritance of the apicoplast has been identified (Jacot *et al*. 2013). MyoH has been assigned to class XIVc, and has a tail domain similar to the α-tubulin suppressor 1 (ATS1) and the related regulator of chromosome condensation 1 (RCC1) of other myosins (Foth *et al*. 2006). Recently the localisation of this myosin to the apical ring of the conoid has been discovered implicating a role in conoid protrusion (Graindorge 2013). MyoE is only expressed in bradyzoites and its function is not yet known (Delbac *et al*. 2001). Also unknown is the precise function of the MyTH4 domain containing myosin, MyoG (Foth *et al*. 2006). Likewise of unknown function are the remaining myosins, MyoI, MyoJ and MyoK. As there are 11 myosin-heavy-chains in *Toxoplasma gondii* and only 7 myosin-light-chains, MLC1 and other MLCs are likely to have multiple myosin-heavy-chain interaction partners.

1.7.4 Myosin A motor complex

The movement of *T. gondii* tachyzoites does not occur through cilia, pseudopodia or lamellipodia. Instead, *T. gondii* moves by a unique mechanism called gliding motility. The mechanism of gliding motility is driven by an actin-myosin motor (Keeley and Soldati 2004) which is located in the supra-alveolar space and anchored to the IMC (Soldati and Meissner 2004). The components of this motor form a complex, which consists of the myosin-heavy chain A (MyoA), the myosin-light chain 1 (MLC1), the essential light chain 1 (ELC1) and three gliding-associated proteins (GAP45, GAP50 and GAP40) (Herm-Gotz *et al*. 2002, Gaskins *et al*. 2004, Frenal *et al*. 2010). The MyoA motor complex is part of the apicomplexan gliding and invasion machinery. Other factors of this machinery are the actin track on which the motor complex moves, and the bridging molecules, AMA1 and MIC2 that were believed to connect the acto-myosin system with the parasite cytoskeleton and extracellular substrate (see Figure 1-8) (Harper *et al*. 2004, Mital *et al*. 2005, Huynh and Carruthers 2006, Sheiner *et al*. 2010, Lamarque *et al*. 2011). Although in vitro interaction studies suggested that aldolase could provide the link between actin and adhesin, recent data revealed that aldolase is not the linker between the Acto-MyoA

motor and the adhesions, therefore how the interplay of these proteins occurs is not known yet (Shen and Sibley 2014).

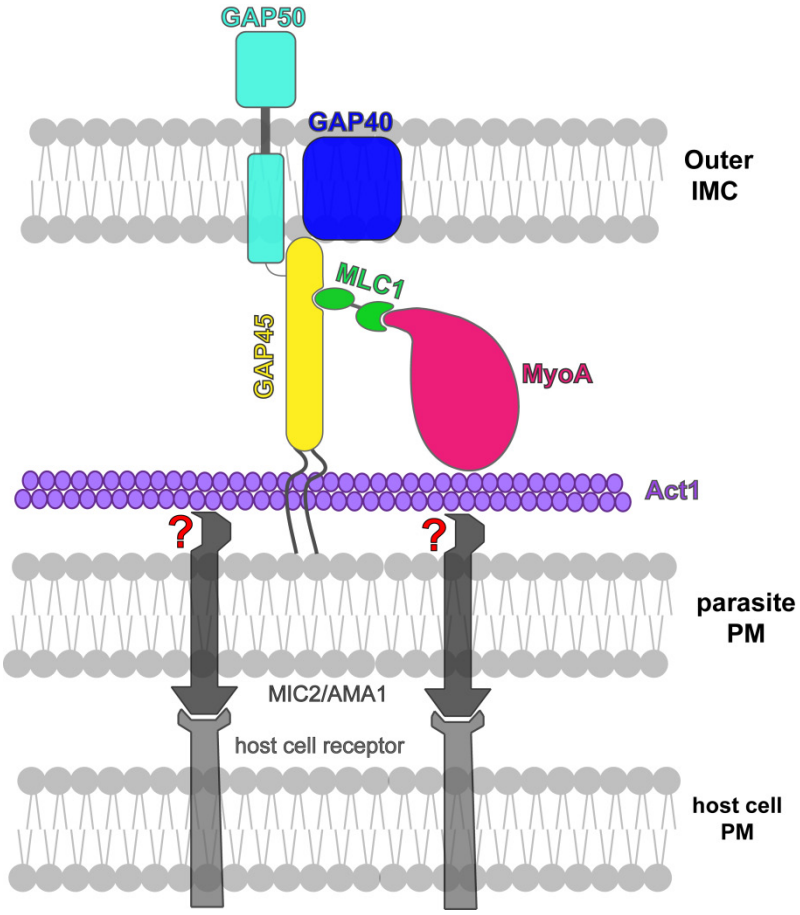

Figure 1-8: Gliding and invasion machinery of *T. gondii*: The MyoA motor complex consists of MyoA, MLC1 and the IMC interacting proteins GAP40, GAP45, and GAP50 Together the MyoA motor complex is connected to F- actin, IMC and PM. The mechanical forces of the actin translocation are transferred to the substrate or host cell plasma membrane via adhesive transmembrane proteins such as MIC2 and AMA1. Therefore redistribution and subsequent shedding of the adhesins translates into a forward motion.

1.7.4.1 Toxoplasma Myosin A

While many *T. gondii* myosins still need to be functionally characterised in depth, MyoA has been well described. This fast, single headed myosin has a molecular weight of roughly 93 kDa and is anchored through GAP45 with the IMC and plasma membrane. MyoA possesses certain unusual structures. Its motor domain has only 23-34 % identity to other myosins and the neck/tail domain is very short (Heintzelman and Schwartzman 1997). Furthermore, MyoA does not follow the TEDS rule (Bement and Mooseker 1995). Transient kinetic assays show that N-terminally tagged MyoA move with a step size of 5.3 nm and a velocity of 5.2 µm/sec towards the plus end of actin filaments (Herm-Gotz *et al.* 2002).

The locomotion of MyoA along actin filaments is non-processive and shows the behaviour of a low duty ratio motor. Duty ratio is the fraction of time that a motor is attached to its filament. This means MyoA spends only little time tightly bound to actin during ATP catalysis (Herm-Gotz *et al*. 2002, Heaslip *et al*. 2010, Dharan and Farago 2012). Other myosins with low duty ratios (5 %) are skeletal myosins that need to respond rapidly for muscle contraction. High duty ratio motors (70 %) like Myosin V function in long distance transport of cargo (Tyska and Warshaw 2002, De La Cruz and Ostap 2004). It has been shown that the duty ratio of MyoA was extremely low with 0.77 % (Heaslip *et al*. 2010). The reason for this low duty ratio of MyoA is not known yet, but the combination of this feature with the high amount of globular actin may reflect the motility level of *Toxoplasma*. Highly motile parasites like *Dictyostelium* have high monomeric to filamentous actin ratio, whereas slow organisms like yeast have less globular actin (Karpova *et al*. 1995). Therefore, a low duty ratio with high actin turnover could elucidate the fast and vigorous processes of gliding motility and invasion in *Toxoplasma*.

Using a tetracycline inducible conditional knockdown, MyoA has been shown to be important for gliding motility, host cell invasion and egress of *T. gondii* (Meissner *et al*. 2002). Very recently it has been shown that although MyoA plays a crucial role during these processes, its function is not of essential nature since a knockout of MyoA remains viable indefinitely (Andenmatten *et al*. 2013). Furthermore, MLC1 has been identified as the regulatory light chain of MyoA (Herm-Gotz *et al*. 2002). A truncated version of MyoA (removal of the last 53 amino acid residues at the C-terminus; contain an IQ motif (QxxxR)) could no longer interact with MLC1 and was non-functional in an *in vitro* motility assays (Herm-Gotz *et al*. 2002). Additionally, mutation of two arginines within the last 22 amino acid into alanines abolishes peripheral localisation of MyoA, indicating that those residues are required for MLC1 binding (Hettmann *et al*. 2000).

1.7.4.2 MyoA associated proteins

The MyoA motor complex comprises several gliding associated proteins (GAPs) that fulfil functions in localising the MyoA motor complex to the space between the IMC and the plasma membrane (Gaskins *et al*. 2004). GAP45, one of the first GAP identified, has been shown to interact with the IMC based on experiments

using *Clostridium septicum* α–toxin that causes swelling of the plasma membrane from the IMC (Wichroski *et al*. 2002). Recently a more detailed characterisation of GAP45 displayed that GAP45 is anchored to both the IMC via palmitoylation of the C-terminus and the plasma membrane via myristoylation and palmitoylation of the N-terminus (Frenal *et al*. 2010). As the C-terminus of GAP45 is interacting with the N-terminus of MLC1, which itself interacts with MyoA through its C-terminus, GAP45 has a major role in anchoring the whole complex to the IMC. A conditional knockdown of *gap45* showed crucial effects on gliding motility, invasion and egress, but no significant role during replication (Frenal *et al*. 2010). The interaction of GAP45 with the IMC occurs via the integral membrane protein GAP50, another gliding associated protein, whose exact function is not determined yet (Gaskins *et al*. 2004). Other identified GAPs are GAP40, GAP70 and GAP80. While GAP40 has nine transmembrane spanning domains and localises to the IMC of mature and immature parasites, GAP70 and GAP80 can be found at the apical cap and posterior end, respectively (Frenal *et al*. 2010, Jacot and Soldati-Favre 2012, Jacot 2013). Because GAP70 is dispensable in tachyzoites it was suggested that it has no important role during this cell stage or that GAP45 can functionally replace it. Indeed a genome database search has revealed that GAP45 and GAP70 have conserved N-and C-terminal regions and differ mainly in their coiled-coil domain which is significant longer in GAP70 compared to GAP45 (Frenal *et al*. 2010).

1.7.4.3 Regulatory and essential light chains in *Toxoplasma gondii*

Usually myosin light chains resemble calmodulin-like proteins with EF-hand motifs recognising and binding Ca^{2+} ions. In *T.gondii* those motifs are degenerate and no longer react with Ca^{2+} (Herm-Gotz *et al*. 2002, Gifford *et al*. 2007, Polonais *et al*. 2011). Moreover, two different classes of light chains exist: regulatory light chains (RLCs) and essential light chains (ELCs). MLC1 is the first myosin light chain identified in *T. gondii* (Herm-Gotz *et al*. 2002). Recently six further genes were discovered coding for EF-hand contain proteins, meaning myosin light chains (named MLC2 to MLC7) (Polonais *et al*. 2011). Endogenous tagging of these MLCs displayed different, specific subcellular localisations. MLC2 can initially be visualised at the periphery of tachyzoites. Furthermore, a direct interaction of MLC2 with MyoD is demonstrated in this study (Polonais *et al*. 2011). MLC3 and MLC7 show a cytosolic distribution whereas MLC4 is localised

around the nucleus, potentially with vesicles close to the parasite endoplasmic reticulum. While both MLC5 and MLC6 are found to be located at the conoid, only MLC5 is localised at the nucleus as well (Hu *et al*. 2006, Polonais *et al*. 2011). The exact biological function of these myosin light chains is unknown. Recently uncovered was the existence of the calmodulin-like essential light chain ELC1 which interacts with MyoA (Nebl *et al*. 2011). Upon stimulation of Ca^{2+} signalling pathways the interaction of MyoA with ELC1 is upregulated, although the precise function of ELC1 is not known so far (Nebl *et al*. 2011). The most studied myosin light chain represents MLC1. It was first described through co-purification with MyoA and possesses a unique N-terminal extension of roughly 79 amino acids not found in calmodulin or other myosin light chains, and a C-terminus comprised mainly of four degenerate EF-hand motifs (Herm-Gotz *et al*. 2002).

There are generally two ways to regulate myosin activity and function in many organisms. While the first way involves calcium-dependant phosphorylation of the RLC, the second possibility is binding of Ca^{2+} ions to the EF hand motif of the ELC. Usually both light chains bind together to the IQ motif of the involved myosin providing structural stability (Rayment *et al*. 1993, Xie *et al*. 1994). However, in apicomplexan parasites the influences of regulatory and essential light chains on myosin motor activity is not completely resolved. The calcium-dependent protein kinase PfCDPK1 phosphorylates two serine residues of *P. falciparum* myosin tail interacting protein (PfMTIP) which is the orthologue of MLC1 (Green *et al*. 2008). The two main phosphorylation sites were identified as Ser_{47} and Ser_{51}, which are in close vicinity to Ser_{55} and Ser_{57} in the N-terminus of MLC1. Two additional phophorylation sites, Thr_{98} and Ser_{132}, located in the C-terminus of MLC1 were later identified as being dependent on Ca^{2+} stimulation (Nebl *et al*. 2011). Interestingly, phosphorylation of distinct serine residues of PfMTIP causes it to bind less tightly to PfMyoA, suggesting that these posttranslational modifications of the light chain can ultimately influence myosin heavy chain activity and function (Douse *et al*. 2012).

1.7.5 Assembly and functions of the MyosinA motor complex

The assembly of the MyoA motor complex, also referred to as the glideosome, is believed to occur in two steps (Gaskins *et al*. 2004). First MyoA, MLC1 and GAP45

form the proto-glideosome that presumably is delivered to the plasma membrane by Rab11A driven vesicular transport (Agop-Nersesian *et al*. 2009). Afterwards the proto-glideosome associates with the conserved carboxy terminal, cytoplasmic domain of GAP50. The entire complex is anchored to the IMC within cholesterol-rich, detergent-resistant membrane domains (Gaskins *et al*. 2004, Johnson *et al*. 2007). This last step is reliant on dephosphorylation of two serines of GAP45 (Gilk *et al*. 2009), suggesting a possible role for kinases and/or phosphatases in the assembly and activity of the complex. This two-step process also reflects the different localisations of the distinct components during division. GAP50 can be found in the IMC of mature and immature parasites, whereas all parts of the proto-glideosome can only be found in association with the IMC of mature parasites (Gaskins *et al*. 2004).

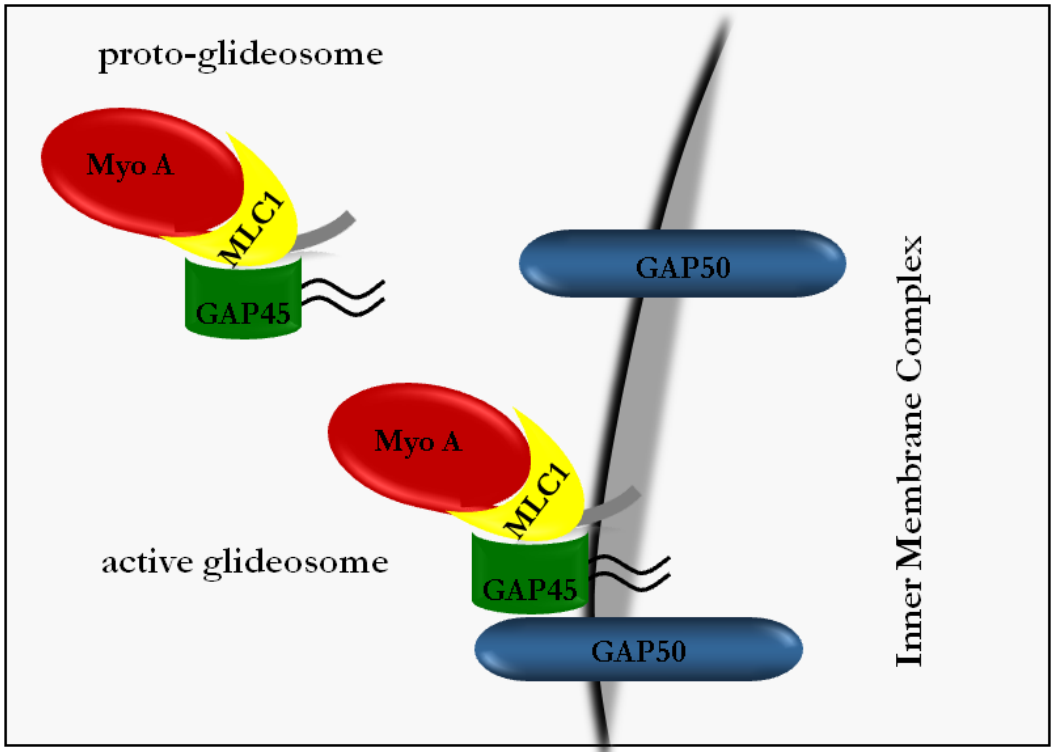

Figure 1-9: Assembly of the Glideosome. The assembly of the glideosome occurs in 2 steps: GAP50 is first directly inserted within the IMC. This is an integral membrane glycoprotein and serves as an anchor for the other components of the glideosome. In the second step, the Proto-glideosome (i.e. MLC1, Myosin A and GAP45) associate with the IMC. This step takes place during replication.

1.8 Actin, actin-like proteins and Actin-related proteins

1.8.1 General overview and structure of Actin in eukaryotes

Actin is a highly conserved, 42 kDa protein that is present as different isoforms: α-, ß- and γ-actin. α-actin is present in muscle cells, whereas ß-actin and γ-actin is found in non-muscle cells and muscle cells (Herman 1993). Both ß- and γ-actin perform several crucial roles in eukaryotes including the formation of stress fibres and driving the locomotion by extension of pseudopods which are used by single-cell organisms to actively migrate. In multicellular organisms cell locomotion is used for various processes such as morphogenetic movements during embryonic development, movement of neurites during development of the nervous system, chemotactic movement of immune cells and fibroblast migration during wound healing. The globular monomeric form of actin is called G-actin whereas the filamentous form is termed F-actin and consists of a chain of G-actin subunits. The prerequisite for pseudopod formation is the assembly of actin filaments at the leading edge of the cell. Actin filaments are highly polarised with the fast growing end termed barbed end (+) and slow growing end pointed end (-). Additionally the turnover of actin in migrating cells is referred to as treadmilling process since actin monomers are preferentially added at the (+) end and removed at the (-) end of the filament (Wanger *et al*. 1985). Moreover, membrane protrusion and therewith motility is directed by extension of the barbed end.

Since cells must be able to adapt to environmental changes rapidly, actin polymerisation and depolymerisation is tightly controlled. Many Actin binding proteins (ABPs) play a role during the rapid regulation of actin dynamics. These proteins possess numerous functions such as actin monomer sequestration, filament capping, filament severing and filament cross-linking (Cooper and Schafer 2000, Pollard and Borisy 2003) (see Figure 1-10). Gelsolin for example is part of a family of actin-severing and actin-capping proteins. Upon calcium activation gelsolin binds to actin filaments and severs the filaments through a coordinated pincer movement (Burtnick *et al*. 1997, Silacci *et al*. 2004). Another ABP is profilin that promotes actin assembly in different ways, for instance it catalysed the exchange of ADP for ATP thus building actin monomers ready to be assembled; it inhibits nucleation of actin filaments and profilin-bound globular

actin cannot be assembled to pointed ends but can bind to barbed ends to elongate the filament (Yarmola and Bubb 2009, Kardos *et al*. 2013). Moreover, Actin depolymerising factor (ADF) and cofilin function in the recycling of globular actin by filament depolymerisation. Unlike profilin, ADF and cofilin preferentially bind to ADP-actin (Kardos *et al*. 2013). The nucleation of actin filaments can be mediated through the Actin-related proteins (Arps), Arp2 and Arp3. The Arp2/3 complex connects the (-) end of a new daughter filament to the side of the mother filament. Additional ADF/cofilin interacts with Arp2/3 complex to facilitate filament disassembly (Blanchoin *et al*. 2000, Pollard and Borisy 2003). Another group of ABPs are formins, which are multidomain regulatory proteins binding to the Arp2/3 complex and the barbed end of actin filaments to promote actin polymerisation (Paul and Pollard 2009, Aspenstrom 2010).

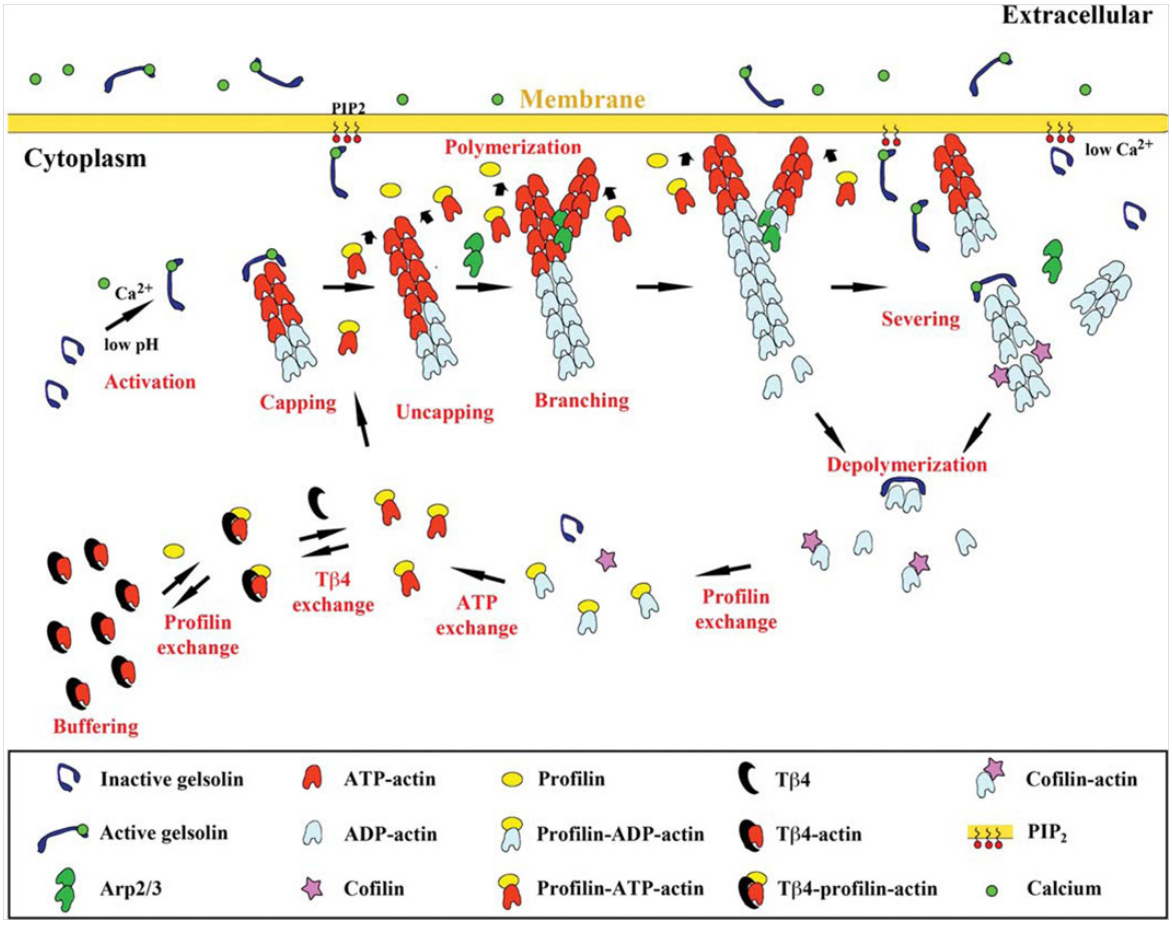

Figure 1-10: Scheme of actin dynamics. The model shows the effect of gelsolin on capping and severing of actin filaments in the cytoplasm. Following, uncapping results in directed polymerization of profilin-ATP-actin at the membrane which causes movement. Through Arp2/3 complex-dependent nucleation the number of barbed ends is increased. Additionally, Gelsolin-capped actin filaments are responsible for pointed-end depolymerization and targeted for cofilin severing. The ADP-actin monomers are recycled into profilin-ATP-actin for additional rounds of polymerization, or retained as an ATP-actin buffer as thymosin-b4-ATP-actin. Figure reprinted from Nag *et al*. (2013).

1.8.2 Actin in apicomplexan parasites

Actin is a crucial protein of nearly all eukaryotic cells. Interestingly, the genome of *Toxoplasma gondii* encodes for only one conventional actin gene, *Act1*. In contrast to other eukaryotic cells, the majority (97 %) of actin in *Toxoplasma* is present as monomers (G-actin) and actin filaments (F-actin) are barely detected shown by a technique that sediments filamentous actin at 100,000 x g (Dobrowolski *et al*. 1997). Furthermore, actin filaments are not detected using standard immunofluorescence assays staining with an antibody against Act1 which displayed a rather diffuse pattern in the cytosol. Moreover, Immuno electron microscopy of Act1 in extracellular parasites showed a localisation of Act1 beneath the plasma membrane closely to the Inner Membrane Complex and in dispersed accumulations in the cytosol (Dobrowolski *et al*. 1997). Nevertheless, studies on actin filaments in *Toxoplasma* and *Plasmodium* filaments uncovered their atypical short nature. Unlike rabbit actin filaments which are roughly 3.5 µm long, filamentous actin in apicomplexan parasites does not exceed 100 nm and forms unstable filaments transiently during gliding motility (Wetzel *et al*. 2003, Schmitz *et al*. 2005, Schuler *et al*. 2005, Sahoo *et al*. 2006).

Comparison of amino acid sequences of actins revealed that *Toxoplasma gondii* Act1 is closely related to *Plasmodium falciparum* actin 1 (PfAct1; 93.1 % identity) and *Cryptosporidium parvum* actin (88.1 % similarity) while it shares 83 % with mammalian ß and γ actin isoforms (Dobrowolski *et al*. 1997). Additionally, there are major differences between the apicomplexan actins and more conventional actins. The changes of several amino acids in *Toxoplasma* actin might contribute to the instability of the filaments by disrupting lateral interactions between the monomers with the filament (Sahoo *et al*. 2006). Additionally, some amino acid substitutions are predicted to change the electrostatic interaction between filaments and to alter the nucleotide-binding pocket which may interfere with ATP hydrolysis. Mutation of these residues leads to the formation of longer and more stable filaments *in vitro* and changes the pattern of gliding motility assays (Skillman *et al*. 2011). Contrary to the conventional actin, actin in *T. gondii* features isodesmic polymerisation and polymerisation kinetics lack a lag phase and critical concentration (Skillman *et al*. 2013). Furthermore, treatment of parasites with Cytochalasin D, which binds

to the barbed end of filaments and blocks further addition of G-actin, and Jasplakinolide, which stabilises filamentous actin and prohibits depolymerisation, interfere with actin polymerization kinetics and alter parasite motility and invasion (Ryning and Remington 1978, Dobrowolski and Sibley 1996, Poupel and Tardieux 1999).

1.8.3 Actin-like - and Actin-related proteins in Apicomplexa

Actin related proteins (Arps) belong to the large actin superfamily of regulatory proteins involved in processes like modulating the cytoskeleton or regulation of chromatin remodelling (Schafer and Schroer 1999). Members of this family possess an actin fold that is divided into two main domains, which are further subdivided (Kabsch and Holmes 1995, Frankel and Mooseker 1996). Those subdomains form the ATP binding pocket, the barbed and pointed end of the monomer and serve as the binding site for actin-binding proteins. Arps have a high homology to conventional actin with the identity ranging from 20-60 %. Moreover, genomic and phylogenetic analyses revealed that ten distinct groups containing an actin domain in apicomplexan parasites and many orthologues to conserved eukaryotic Arps exist (Gordon and Sibley 2005). Surprisingly, none of the apicomplexan genomes encode for Arp2 or Arp3 which are crucial factors for actin dynamics in other eukaryotes. Several apicomplexan specific Arps were identified which are referred to as actin-like proteins (Alps) to distinguish them from members of the Arp family found outside the Apicomplexa. So far Arp and Alp proteins are poorly described within the apicomplexan phylum. Generally, Arps function in regulating microtubule motor activity (Arp1, Arp10, Arp11), actin polymerisation (Arp2, Arp3) and chromatin remodelling (Arp4-9). Three orthologue groups of well described Arps were discovered in *Toxoplasma*, namely Arp1, Arp4 and Arp6. In other eukaryotes Arp1 plays a crucial role as component of the dynactin complex for microtubule motor activity. Arp6 and Arp4 are known nuclear proteins and a role during nuclear division was recently confirmed for *Toxoplasma* Arp4a (Suvorova *et al*. 2012). The other seven groups of actin-related proteins are phylum specific and hence termed Alps. Since Alps are unique to apicomplexan parasites a parasites specific cellular role was suggested (Gordon and Sibley 2005). The *Toxoplasma* genome encodes for six Alp proteins, one of those, Alp8, is even *Toxoplasma* specific. Moreover, Alp1 is with 51 % identity the closest related Arp to Act1. Additionally, a role of Alp1 in IMC

formation during replication was suggested (Gordon *et al*. 2008, Gordon *et al*. 2010).

1.8.4 Actin regulating factors in apicomplexa

As described above actin dynamics are tightly regulated by over 100 regulating proteins in eukaryotes (Pollard and Cooper 2009). However, actin dynamics in apicomplexan parasites are still not as well understood and only a minimal repertoire of actin-binding proteins are present compared to eukaryotes. Nevertheless, this reduced set contains formins, actin depolymerising factor (ADF)/cofilin, cyclase associated protein (CAP), profilin, coronin and capping protein (CP). When a mutated version of actin, which leads to filament stabilisation, is expressed in *T. gondii*, parasites are retarded in motility. This indicates that the amount of actin monomers is very important for this process (Skillman *et al*. 2011). Moreover, this might indicate that G-actin binding proteins like ADF/cofilin, CAP, and profilin, are crucial for keeping actin in the monomeric form.

While *P. falciparum* has two ADF/cofilin isoforms, most other Apicomplexa like *T.gondii* possess only one homologue. Comparison with other ADFs revealed that the amino acids responsible for G-actin binding are conserved while residues for F-actin binding are absent (Allen *et al*. 1997, Mehta and Sibley 2010). Furthermore a conditional knockdown (KD) of *adf* results in accumulation of filamentous actin and changes the gliding motility of *Toxoplasma* to a movement that resembles the one observed after addition of Jasplakinolide. The overall speed of circular and helical gliding was dramatically reduced and ADF KD parasites were not capable of completing a single helical turn. (Mehta and Sibley 2011). Consequently invasion and egress are inhibited by removal of ADF. Another well characterised group of G-actin binding proteins are CAPs which bind to actin with their C-terminus. The CAP homologues in apicomplexan parasites are smaller than the ones found in yeast and vertebrates and the N-terminal and WH2 domain are missing. This suggests their function is limited to monomer sequestration (Hliscs *et al*. 2010). Interestingly, CAP localises to the apical cap region in intracellular *Toxoplasma* parasites whereas it is found in the cytoplasm in extracellular parasites suggesting a role in regulating actin-associated motility of extracellular tachyzoites (Lorestani *et al*. 2012). *In vitro*

assays of *P. berghei* CAP revealed that it is expressed solely in motile stages and that it not essential in the asexual phase of the life cycle. Moreover, depletion of CAP is vital for oocyst development in the mosquito midgut (Hliscs *et al.* 2010). Each apicomplexan species has one identified profilin gene (Kursula *et al.* 2008). Amongst others profilin enhances nucleotide exchange and thereby increases the amount of ATP-actin for polymerisation. In *P. falciparum* profilin is an essential protein with cytosolic localisation in late schizogony (Baum *et al.* 2008). In *Toxoplasma,* profilin (Pfn) weakly binds to G-actin, reduces the nucleotide exchange of actin and influences the ability of formins to stimulate actin polymerisation, therefore indicating a role in monomer sequestering. Further, Pfn is crucial for several processes in the parasite life cycle such as gliding motility, invasion and egress (Plattner *et al.* 2008). In eukaryotes, profilins interact with formins, which facilitate the elongation of actin filaments by recruiting profilin bound G-actin to the barbed end, via a proline rich FH1 domain. The *Toxoplasma* genome encodes for three formin genes (FRM1-3) (Daher *et al.* 2010). While FRM3 is not essential in parasites, FRM1 and FRM2 are crucial for parasite survival. Interestingly lack of FRM1 has only mild effects on parasite motility and invasion, although biochemical assays revealed a role of FRM1 and FRM2 for the assembly of filamentous actin (Skillman *et al.* 2012).

1.9 Motility involved processes

1.9.1 *Toxoplasma* gliding motility

Toxoplasma tachyzoites are motile, invasive stages that are able to migrate on and through tissue by a substrate dependant locomotion referred to as gliding motility. Responsible for this movement is the gliding machinery of the parasite which consists of the MyoA motor complex, parasite actin and transmembrane proteins such as MIC2 and AMA1. The MyoA motor complex is connected to the IMC and the underlying microtubular network. By ATP hydrolysis of the motor protein, MyoA walks along filamentous actin causing actin displacement. The mechanical forces of this actin translocation are redirected to the substrate or host cell plasma membrane with the help of adhesive proteins and result in forward movement of the parasite.

On two dimensional (2D) coated substrates such as fetal bovine serum or poly-L-lysine, tachyzoites use three distinct forms of movement called circular, upright twirling and helical gliding (Hakansson *et al*. 1999). While performing circular gliding the parasite lies on its right side and moves counter clockwise with an average speed of roughly 1.5 µm/sec. Upright twirling occurs when a tachyzoite is orientated upright with its posterior end attached to the substrate while the anterior end is spinning clockwise. The most complex mode of motility is helical gliding. First, the parasite moves forward clockwise for around a body length while concurrently rotating 180 degree around its curved, longitudinal axis until its apical pole upwards. Afterwards the tachyzoite physically re-orientates itself by flipping back into the starting position where it is capable to initiate the next round of helical gliding. It is currently not known what triggers these different motility types, but tachyzoites are able to alter between them. *Plasmodium* sporozoites show comparable types of motility *in vitro* which were termed circular gliding and attached waving. Sporozoites move in mostly counter clockwise circles or attach one end to the substrate surface and perform a waving-like motion (Vanderberg 1974). Moreover, recent studies of the circular gliding of *P. berghei* sporozoites revealed that this movement is performed in a so called stick and slip mechanism (Munter *et al*. 2009). By using reflection interference contrast microscopy and traction force microscopy recurrent turnover of discrete adhesion sites was identified as the fundamental mechanism of this substrate-dependent type of motility. Instead of linear and consequently continuous attachment, translocation and release of adhesion sites, discrete, unevenly distributed formation and disengagement of adhesion sites at the front, centre and rear end of the sporozoite were detected (Munter *et al*. 2009).

The biological relevance of the different motility types on 2D surfaces is still unclear largely because they do not reflect the situation of 3D tissues in *vivo*. Contrary to the waving and circular gliding motility observed on 2D substrates, *Plasmodium* sporozoites and ookinetes move with corkscrew like trajectories in a Matrigel-based 3D environment (Akaki and Dvorak 2005, Volkmann *et al*. 2012). The observed moving pattern in 3D studies more likely resembles *in vivo* situations where sporozoites traverse enormous distances before invading hepatocytes and follow random paths in the dermis of mice bitten by infected *Anopheles stephensi* mosquitoes (Frevert *et al*. 2005, Amino *et al*. 2006, Amino

et al. 2008). Strikingly, an exclusively corkscrew-like motility pattern was very recently discovered on *T. gondii* tachyzoites in 3D motility assays although three motility forms exist in 2D assays (Leung *et al*. 2014).

1.9.2 *Toxoplasma* egress out of host cells

Apart from invasion the egress process is also an important step for the survival and propagation of intracellular parasites. Akin to invasion, parasite motility is essential for parasite egress. Cytochalasin D (CD) almost eliminates gliding motility and CD treated parasites were not able to exit the host cell after being artificially triggered with calcium Ionophore (Shaw *et al*. 2000, Moudy *et al*. 2001). Calcium ionophore increases intracellular calcium levels that lead to microneme discharges and following to the disruption of the parasitophorous vacuole membrane (PVM). More specific micronemes release a perforin like protein, PLP1 that disrupts the PVM enabling the parasite to exit (Kafsack *et al*. 2009, Roiko and Carruthers 2013). Elevated calcium levels are a prerequisite for egress and recent studies demonstrate a role of calcium dependant protein kinase 3 (CDPK3) during the egress process. (Garrison *et al*. 2012, Lourido *et al*. 2012, McCoy *et al*. 2012). Those studies revealed that CDPK3 is exclusively required for egress and only needed for microneme secretion when triggered by distinct stimuli. Moreover, CDPK3 is part of a calcium dependant signalling pathway that is induced upon alteration of environmental potassium levels after cell damage or permeabilisation. Additionally CDPK3 localises to the periphery of the parasites and is not needed for gliding motility or invasion. Consistent with those results, scanning electron microscopy revealed that tachyzoites exit cells in a comparable way to invasion (Caldas *et al*. 2010) and therefore egress is not passively as a consequence of cell rupture. After disruption of the PVM the parasites escape into the cytoplasm of the host cell where parasite factors disrupt the host cytoskeleton and plasma membrane resulting in exit from the lysed cell using their own gliding motility system (Chandramohanadas *et al*. 2009, Kafsack *et al*. 2009, Roiko and Carruthers 2013).

1.9.3 Invasion of *Toxoplasma gondii* is a multistep process

In apicomplexan parasites, invasion of host cells is an active process composed of multiple steps that are well regulated and orchestrated. After initially

attaching to the host cells, *Toxoplasma* re-orientates itself to form a tight junction before actively penetrating its host (Carruthers and Boothroyd 2007). This whole process is very rapid and completed within 15-30 seconds (Morisaki *et al*. 1995). The surface of *T. gondii* is covered by a family of GPI-anchored surface antigens (SAGs) and SAG-related sequence proteins (SRS). Six of these proteins are expressed in tachyzoites (SAG1-3 and SRS1-3) and distributed evenly over the surface (Lekutis *et al*. 2001, Jung *et al*. 2004). Both protein groups are implicated to participate in the initial attachment process through lectin-carbohydrate interactions. Agreeing with this, SAG3 deficient parasites show a 50 % decrease in host cell attachment (Dzierszinski *et al*. 2000). Moreover SAG1 and SAG3 were found to interact with heparin and other proteoglycans of the host cell (Jacquet *et al*. 2001, Azzouz *et al*. 2013). The frequency and overall distribution of SAG proteins all over the surface of the parasite positions those proteins ideally for low-affinity lateral interaction with the host cell surface. This circumstance would allow the parasites to glide along the surface of the host cell to scan for optimal invasion sites (Carruthers and Boothroyd 2007). The invasion process is highly polarised since *Toxoplasma* solely uses its apical tip to initiate invasion. Due to the fact that SAG proteins are distributed regularly over the surface, another protein group, located at the apical surface and named micronemal proteins (MICs), was attributed with the firm apical attachment. Several MICs possess adhesive domains mediating protein-protein or protein-carbohydrate interactions. After the invasion process has been initiated, micronemes are secreted in a calcium-dependant manner through the apical tip which strengthens the attachment. Furthermore, parasites lacking the calcium-dependant protein kinase 1 (CDPK1) showed less MIC2 secretion and were strongly decreased in host cell attachment (Lourido *et al*. 2010). This strong apical attachment is also referred to as intimate attachment since the parasite and the host cell are only 6 nm apart (Carruthers and Boothroyd 2007). Several micronemal proteins such as MIC2 and AMA1 were implicated to play a role for intimidate attachment (Brossier and David Sibley 2005, Mital *et al*. 2005, Huynh and Carruthers 2006). Simultaneous to the intimate apical attachment, the parasite re-orientates itself so the extruded conoid is facing the target cell. AMA1 now interacts with several RON proteins (RON2,4,5 and 8) to form a unique, ring-like structure termed tight junction (TJ) (Alexander *et al*. 2005, Lebrun *et al*. 2005, Besteiro *et al*. 2009, Straub *et al*. 2009). This TJ can be

visualised as a constriction at the plasma membrane and the components of this complex interact with the host cell cytoskeleton. Interestingly, recent studies revealed that *T. gondii* tachyzoites and *P. berghei* merozoites and sporozoites are still invasive when *ama1* is depleted (Giovannini *et al.* 2011, Bargieri *et al.* 2013). Although *ama1* is not essential for *T. gondii* survival, tachyzoites showed a severe attachment phenotype in the absence of AMA1. Furthermore, parasites lacking *ama1* form a normal RON complex (Giovannini *et al.* 2011, Bargieri *et al.* 2013). While AMA1 is not required for *P. berghei* sporozoite penetration into hepatocytes, RON4 plays an important role during this process (Giovannini *et al.* 2011). RON4 is thought to bind host tubulin and RON8 is implied to interact with host actin (Straub *et al.* 2011, Takemae *et al.* 2013). Furthermore, absence of RON5 disrupts the RON complex at the TJ and RON5 has an importing role during invasion (Beck *et al.* 2014). As the invasion process progresses the TJ migrates from the anterior to the posterior pole of the parasite. This active penetration is thought to be driven by the parasite's own actin-myosin system while the TJ serves as anchor to the host cell. As integral part of this model it is believed that the micronemal proteins MIC2 and AMA1 link the host cell surface to the cytoskeleton of the parasites (Sheiner *et al.* 2011). Further it is believed that Myosin A interacts with Actin and links the adhesive proteins to the Inner Membrane Complex (see Figure 1-8). For this reason, it is understood the parasite moves forward when the MyoA motor walks along actin filament. During the last decade several conditional knockdown mutants were generated using the tetracycline inducible KD system. In agreement with this model depletion of the force transducers, AMA1 and MIC2, lead to a severe invasion phenotype suggesting an important role during this process (Mital *et al.* 2005, Huynh and Carruthers 2006). Furthermore, conditional KD of glideosome components like MyoA, GAP45 and actin-binding proteins such as profilin and formins, resulted in severe decreases in their invasion rates (Meissner *et al.* 2002, Plattner *et al.* 2008, Daher *et al.* 2010, Frenal *et al.* 2010). Surprisingly none of the above mentioned mutants showed a complete abolishment of invasion. This was attributed to background expression of the respective gene or alternatively a different or additional invasion mechanism is in place that does not rely on the gliding machinery.

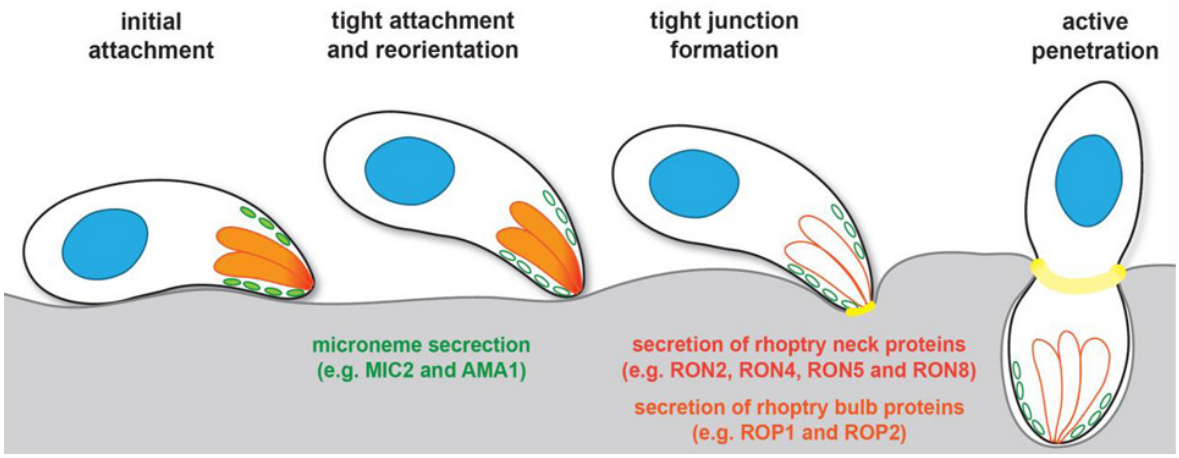

Figure 1-11: Model of the invasion process of *Toxoplasma gondii*. First the parasite loosely attaches to the host cell via cell surface adhesins like SAG1. Afterwards micronemal proteins such as MIC2 and AMA1 (depicted in green) are secreted to the surface of the parasites to form a tight interaction of the apical end of the tachyzoite and the host cell. In doing so the parasite simultaneously re-orientates itself. Next penetration is initiated by the formation of a tight junction (yellow). Therefore rhoptry neck protein (dark orange) and AMA1 are secreted into the host cell where they form a structure with host cell proteins that serves as anchor for the active penetration. At the same time ropthry bulb proteins (light orange) are secreted into the parasitophorous vacuole (Figure kindly provided by Dr Nicole Andenmatten).

1.9.4 Involvement of the host cell during the invasion process

Although *Toxoplasma* invasion is thought to be an active parasite driven process, the environment of the host cell is not to be underestimated since apicomplexan parasites are capable of hijacking and modulating host cellular functions (Plattner and Soldati-Favre 2008). Many studies demonstrate that invasion is affected by alteration of cytosolic host factors like ATP, magnesium ions, aquaporins, sugar transporters, host actin and tubulin (Field *et al*. 1992, Chen *et al*. 2004, Chen *et al*. 2005, O'Hara *et al*. 2010, Sweeney *et al*. 2010, Delorme-Walker *et al*. 2012). Moreover, chicken embryo erythrocytes treated with sodium fluoride and potassium cyanide to deplete ATP levels showed a significant decrease in *Toxoplasma* invasion and removal of magnesium ions from red blood cells almost blocked invasion by Plasmodium falciparum merozoites *in vitro* (Kimata and Tanabe 1982, Field *et al*. 1992). Additionally, host cell actin and tubulin are recruited to parasite-host attachment sites. It has been demonstrated that filamentous actin of the host and the host Arp2/3 complex are present at the TJ and RNAi of host cortactin (an actin nucleation factor) results in 50 % decrease of parasite invasion (Gonzalez *et al*. 2009). Likewise, host cell microtubules are recruited to the constriction site and treatment with the microtubule depolymerising drug Nocodazole that affect host cell microtubules at a lower dose than parasite microtubules, showed a slowdown in

TJ formation (Sweeney *et al*. 2010). Toxofilin, an actin-binding protein, that controls actin dynamics through monomer sequestration and barbed-end filament capping, locally upregulates the turnover of actin which increases depolymerisation at the site of entry. As a consequence the host cell actin meshwork is loosened and penetration of the parasite facilitated (Delorme-Walker *et al*. 2012). Furthermore, a high throughput invasion screen using a human siRNA library targeting druggable proteins identified actin regulators that are important for the invasion process. Intriguingly, six of the hits influence parasite invasion by modifying host cell actin dynamics (Gaji *et al*. 2013). Moreover, studies using the actin destabilising drug CD caused a complete block in host cell invasion. Interestingly, three independent studies that were performed to investigate the role of parasite and host cell actin for the invasion process using this drug came to different conclusions (Ryning and Remington 1978, Dobrowolski and Sibley 1996, Gonzalez *et al*. 2009). In the first study the uptake of *Toxoplasma* and heat-killed *Candida* by phagocytic and non-phagocytic cells was compared in the presence of up to 10 µg (=19.7 µM) CD. The results suggest that the host cell actively participates in the invasion process (Ryning and Remington 1978). Within the second study the influence of host cell actin on invasion was re-examined exposing CD-resistant parasites and wild-type parasites to low doses (0.2 µM) of CD during the invasion event. Since CD-resistant parasites had a significantly higher invasion rate compared to wild-type parasites, it was concluded that invasion solely depends on parasite actin and that the host cell is rather passive (Dobrowolski and Sibley 1996). Surprisingly, a third study revealed that the usage of higher concentrations of CD (0.5 µM) is enough to completely block invasion of CD resistant parasites (Gonzalez *et al*. 2009). Conclusively it seems that host cell factors, particularly actin remodelling factors play indeed an important role during the invasion process.

1.10 Aim of study

According to the current view, apicomplexan parasites invade host cells via an active, parasite driven process that is dependent on gliding motility. The driving force for this motility is believed to rely on the parasite's own Acto-MyoA motor complex (Keeley and Soldati 2004), which is located in the supra-alveolar space and anchored to the Inner Membrane Complex and the plasma membrane (Soldati and Meissner 2004). Recent data revealed that several key components

of the gliding machinery (AMA1, MIC2, aldolase) are not essential for parasite invasion (Andenmatten *et al*. 2013, Bargieri *et al*. 2013, Shen and Sibley 2014). The MyoA motor complex consists of the myosin heavy chain A (MyoA), the myosin light chain 1 (MLC1), the essential light chain 1 (ELC1) and three gliding-associated proteins (GAP45, GAP50 and GAP40) (Herm-Gotz *et al*. 2002, Gaskins *et al*. 2004, Frenal *et al*. 2010). It is generally believed that components of the glideosome are not involved in parasite replication, since conditional knockdown mutants for MyoA or GAP45 did not show a defect in intracellular parasite growth (Meissner *et al*. 2002, Frenal *et al*. 2010). However, expression of a dominant negative version of MyoA in *T. gondii* leads to a severe block in host cell invasion and intracellular replication of the parasite (Agop-Nersesian *et al*. 2009). This result implies that one of the interacting partners of this domain has a role in IMC biogenesis. Because of these observations, the aim of this study is to find the actual reason for the phenotype of the Myosin A tail overexpressor by using the DiCre conditional KO system to analyse other components of the Acto-MyoA motor complex. Given recent data as well as data presented in this study, I will evaluate if the Acto-MyoA complex is indeed necessary for gliding motility and host cell invasion, and if different or additional mechanisms exist to generate the driving force for *T. gondii* invasion.

2 Materials and Methods

2.1 Equipment and computer software

Manufacturer	Equipment
Applied biosystems	MicroAmp® Optical 96-Well reaction plate, MicroAmp® optical adhesive film
Applied Precision	DeltaVision® Core microscope
BD biosciences	needles (26 gauge), syringes
BioRad	Agarose gel electrophorese equipment, blotting apparatus (transblot SD and mini transblot Electrophoretic transfer cell), gel documentation system, gene pulser Xcell, Micropulser, SDS-PAGE system, transilluminator
BTX	Elctroporation cuvettes and system (Electro Square Pore 830)
Eppendorf	Thermocycler (Mastercycler Epgradient), thermo mixer compact
GE healthcare	nitrocellulose membrane (Hybond ECL)
Grant	water bath
Heraeus Instruments	Incubator
Kodak	X-ray film cassette, X-ray film (BioMax MR)
Kuehner	shaking incubator (ISF-1-W)
Millipore	water deionising facility
Sanyo	CO_2-incubator tissue culture
Sartorius	analytical balances
Sciquip	Sigma 6K 15 centrifuge (1150 rotor and 12500 rotor)
Stuart	heat block, orbital shaker, roller mixer
Thermo Scientific	centrifuge (sorvall legend XFR), CO_2-incubator tissue culture, Nanodrop spectrophotometer, Table top centrifuge Heraeus Fresco 21, Table top centrifuge Heraeus Pico 21
Zeiss	Axioskop 2 (mot plus) fluorescence microscope with Axiocam MRm CCD camera, Axiovert 40 CFL fluorescence microscope with Axiocam ICc1, Primovert (light microscope)

Table 2-1: Equipment

Manufacturer	Software
AcaClone software	pDraw32
Adobe Systems Inc.	Photoshop CS4, Illustrator CS4
Applied Precision	SoftWoRx suite software, SoftWoRx explorer software
GraphPad software Inc	Prism
Ibis Biosciences	Bioedit
Microsoft Corporation	Windows 7, Microsoft office 2007, 2010
National Institutes of Health	ImageJ 1.34r software
PerkinElmer	Volocity 3D Image Analysis Software
Thomson Scientific	Endnote X6

Table 2-2: Computer software

2.2 Consumables, biological and chemical reagents

2.2.1 Chemicals

Manufacturer	Chemical reagent
Clontech	Shield-1
Fisher Scientific	Bovine serum albumin, ethylene diamine tetraacetic acid, glycerol, glycine, methanol, N-N-dimethylformamide, D-(+)-Glucose, dimethyl sulfoxide, Tris, sodium chloride, hyperchloric acid, Na_2EDTA
Formedium	Tryptone, yeast extract
Invivogen	Phleomycin
Life technologies	phosphate buffered saline, trypsin/EDTA (0.05%), DNaseI, NuPage SDS loading buffer and reducing agent, sodium bicarbonate, ultrapure agarose
Marvel	milk powder (semi skimmed)
Melford	agar, dithiothreitol, IPTG, X-Gal
National diagnostics	Tris Glycine SDS PAGE Buffer (10X)
Phenix research products	GelRed nucleic acid gel stain
Riedel-de Haën	$MgSO_4$* $7H_2O$, potassium hydroxide, paraformaldehyde
Roche	protease inhibitor
Sigma	ammonium persulfate, ampicillin sodium salt,

	bromophenol blue sodium salt, casein hydrosylate, Dulbecco's Modified Eagle Medium, ficoll, mycophenolic acid, ethylene glycol tetraacetic acid, gentamicin, ponceau S, pyrimethamine, isopropanol, sodium dodecyl sulphate, N,N,N',N'-tetramethylethylenediamine, triton X-100, rapamycin, beta mercaptoethanol, xanthine, chloramphenicol, calcium ionophore A23187, tween20, giemsa stain, L-Glutathione reduced, adenosine 5'-triphosphate disodium salt hydrate, glutamine, 30% acryl-bisacrylamide mix, sodium deoxychoate, K_2HPO_4, magnesium chloride
Southern Biotech	Fluoromount G (with and without DAPI)
VWR	$CaCl_2$*$2H_2O$, glacial acetic acid, ethanol, HEPES, potassium chloride, Na_2HPO_4, KH_2PO_4
Zeiss	Immersion oil

Table 2-3: Consumables

2.2.2 Enzymes and kits

Manufacturer	Enzyme/Kit
GE healthcare	ECL detection kit
Life technologies	Platinum Taq DNA Polymerase High Fidelity, SuperScript® II Reverse Transcriptase
New England Biolabs	All restriction endonucleases and associated buffers, T4 DNA ligase, Taq DNA polymerase, alkaline Phosphatase Calf Intestinal (CIP)
Promega	pGEM®-T Easy vectors system, SV Total RNA Isolation System
Qiagen	Qiaprep spin miniprep kit, Plasmid midi kit, MinElute PCR purification kit, MinElute gel extraction kit, DNeasy blood and tissue kit
Roche	High Pure PCR Product Purification Kit

Table 2-4: Enzymes and kits

2.2.3 Ladders

Ladder	Manufacturer	Application
1 kb Plus DNA-Ladder	Invitrogen	AGE
Page Ruler Prestained Protein Ladder	Fermentas	SDS-PAGE

Table 2-5: Ladders

2.3 Antibodies

Antibody	Species	Dilution IFA	Dilution WB	Source
Actin (TgActin1)	R	1:1250		David Sibley
ACTN05(C4)) ab3280	M	1:500		ABCAM
TgAct1	M	1:100		Dominique Soldati
Actin (TgAct1)	R			Jake Baum
P.falciparum Act1	R	1:1000		Artur Scherf
P. falciparum Act1	R	1:500		Artur Scherf
Aldolase	R		1:10,000	David Sibley
AMA-1	M	1:500		Gary Ward
Apicoplast G2-Trx	R	1:500		Lilach Sheiner
Apicoplast HSP60	R	1:1000		Lilach Sheiner
Catalase	R		1:3000	Dominique Soldati
c-Myc Rabbit	R	1:200		Santa Cruz, cat # sc-789
c-myc SC-40 SIGMA	M	1:1000		Sigma, cat # M-4439
FKBP12 (DD)(ABR)	R	1:500	1:1000	Affinity Bioreagents, cat # PA1-026A
GAP40				Dominique Soldati
GAP45	R	1:1000	1:10 000	Con Beckers
GAP50	R		1:100	Con Beckers
GFP	M	1:500	1:2000	Roche cat#11841460001
GRA9	R	1:500		Didier Desleea
IMC1	R	1:1500		Con Beckers
proM2AP	R	1:500		Vern Carruthers
MIC2 6D10 new	M	1:500		Vern Carruthers

MIC3 T82C10	M	1:300		Maryse Lebrun
MLC1	R	1:2000	1:10,000	Dominique Soldati
MORN1	R	1:250		Marc-Jan Gubbels
MyoA 114 B	R		1:1000	Markus Meissner
MyoA 109	R	1:200		Gary Ward
RON2 160312	R	1:200		John Boothroyd
RON 4 TS6H1	M	1:1000		Maryse Lebrun
ROP 2,4 T34A7	M	1:500		Jean-François Dubremetz
ROP5 T53E2	M	1:1000		Jean-François Dubremetz
SAG1 T91E5	M	1:2000		Jean-François Dubremetz
Tubulin acetylated	M	1:500		sigma, cat# T6793
Ty rabbit	R	1:250		GenScript, cat# A01004-40
Ty mouse	M	1:10-1:40		Hybridoma
VPI	R	1:500		Vern Carruthers

Table 2-6: Primary antibodies used in this study. R: rabbit; M: mouse; IFA: immunofluorescence analysis; WB: western blot.

Antibody	Dilution	Source
Alexa Fluor 488 goat anti-rabbit	1:3000	Life technologies
Alexa Fluor 488 goat anti-mouse	1:3000	Life technologies
Alexa Fluor 594 goat anti-rabbit	1:3000	Life technologies
Alexa Fluor 594 goat anti-mouse	1:3000	Life technologies
Alexa Fluor 350 goat anti-rabbit	1:1000	Life technologies
Alexa Fluor 350 goat anti-mouse	1:1000	Life technologies
goat anti-rabbit IgG (HRP conjugated)	1:50000	Jackson ImmunoResearch
donkey anti-mouse IgG (HRP conjugated)	1:50000	Jackson ImmunoResearch

Table 2-7: Secondary antibodies

2.4 Oligonucleotides

Oligonucleotides were designed with the assistance of pDraw software and Oligo Calc (http://www.basic.northwestern.edu/biotools/oligocalc.html) in order to

optimise the GC content and to avoid self-complementary of the primer. All oligonucleotides were purchased from Eurofins.

Oligo	Sequence (5'→3')
ECL1-fw	CCGGAATTCCCTTTTTCGACAAAATGACCTGCCCTCCCCGCGTCC
ECL1-rv	CGCATGCATCTTTCAGCAGCATCTTGACAAAGTTGGCGTACTGGA
MLC7-fw	GGGAATTCCCTTTTTCGACAAAATGAGCAACGTCGTTCG
MLC7-rv	CGGATGCATCTCGAGTTGCATTGACTGTTGCGACTC
5'UTRGAP45 rv	CGGAATTCTATAACTTCGTATAATGTATGCTATACGAAGTTATCGAATCGAA AAAGTGCGAAAAAGTTGAGGGGGCGAC
3'UTR GAP45 fw	CCACATGTGCTTCGGGATCTGTGTCTGTATAGCGTGC
3'UTR GAP45rv	GCGCCACATGTCTCATCTGTCATAGTTCCTGG
5'UTR MyoB/C fw	CGGGTACCGCTTCACTGGTTTATCGTGTCACGG
5'UTR MyoB/C rv	GCAAGCTTGAAGTCACAGCCTCTCTCGGAAAACG
3'UTR MyoB/C fw	CCTTAATTAATGCCTTTAAAGTGGACAAGGGTGAATGGACGG
3'UTR MyoB/C rv	GGACTAGTTTGGTTCACGCAAGCGGTGTGTCG
YFP rv	ATGGGCACCACCCCGG
HX fw2	GCTACGACTTCAACGAGATGTTCCGCG
MLC1 3UTR rv2	GCGAGAGCAAGAGTAGAGAAGTCGTCACC
MLC1 5'UTR fw2	CCACACAATGGCTAGACTTGCTGCCC
GAP45 5'UTR fw2	GCACACCGTGAATCTGCTGGT
GAP45 3'UTR rv2	GCCAACTCGTGTGGAACAGACTGTCG
MyoB/C gene fw	TACTTCCAATCCAATTTAATGCCTCCCGCAGTCCGTCAGACGCAATAGATGT TCG
MyoB/C gene rv	TCCTCCACTTCCAATTTTAGCCGGTCTATCCGGCGCACAGGCCTCGAAGC
5'UTR MyoB/C fw2	GCTATCTCAACGGACAACGACTGCG
5'UTR MyoB/C rv2	CGTTGTCTCAGACTTTGC
3'UTR MyoB/C fw2	GCTGCACCACTTCATTATTTCTTCTG
3'UTR MyoB/C rv2	GCCAGAACCCAAAACTCTCCACTCAGACG
5'UTR Act1 fw	CGGGGCCCACACGTAGTCTGCCGCGTGAAGCAGCAG
5'UTR Act1 rv	CGGAATTCTATAACTTCGTATAATGTATGCTATACGAAGTTATCTTACCTATG AAAAAGTGGAAATTATTCGAAAGGAAAACAAAAAGCGTG
Act1 ORF fw (1)	GGGAATTCGACAAAATGGCGGATGAAGAAGTGCAAGCC
Act1 ORF rv (1')	CGTTAATTAAAAGCACTTGCGGTGGACGATGCTCGGG
3'UTR Act1 fw	CGGAGCTCTGATCAGATCTGGATCCTAGGTTAACGCAGTTTGTGGTGTTTTA TCGAGCGCCGAG
3'UTR Act1 rv	CGGAGCTCGCGGCCGCACAATTGCATATGGCTAGCCTGCAGCTCGAGTCTA GAACTAGTTAACCTGGACGCGGAATTGGCGAATCAGCGACATCTTATCACGA
Act1 3'UTR rv (3')	GGCTCAAACATGACACGTGTGC
Act1 5'UTR fw (2)	CGTCACACCCGCTCAGCCAAAGG
GAP50 ORF rv	GGGTTAATTAATTATTTCATGTAGCGAGAGAGACCGTTC
GAP50 ORF fw	CCCAATTGGACAAAATGGCAGGCGCCCCCGTCGCGG
3'UTR GAP50 rv	CCAGGAGCTCTGCCAAAAGTTTTTGGCTGCGGAAGAAAAG
GAP50 3'UTR fw	GGGAGCTCATTGGGGAAAGGGAACTGCGGACCCC
GAP50 5'UTR rv	CGGAATTCTATAACTTCGTATAATGTATGCTATACGAAGTTATAGTTTGGAG TTGGCCGAGAGCAGGAAAACGGTTCCCGAAA
GAP50 5'UTR fw	GGGCCGGCTGCTTGATGAGTCAGCGCATGTATGTGTTTTG
GAP40 3'UTR fw	GGGGAGCTCGCGAGCTGATGCGTTATGTACTTTAAGG

GAP40 3'UTR rv	CCGGAGCTCCGAAGTGGCATGATCAGCGTGTTTTCCCCG
GAP40 5'UTR fw	CGGGCCGGCCAGATAGCCTGTCCACCCTCAGTACGC
GAP40 5'UTR rv	CGAGATCTTATAACTTCGTATAATGTATGCTATACGAAGTTATCCAAACGTCT GAAAAAGGCAGAGGAACTGTGCGAACGCTGG
GAP40 ORF fw	CCGCAATTGAGATCTATGTCGACTCTTCAGGACATTCGCTTG
GAP40 ORF rv	GGGTTAATTAATGCATTAGCTCGAATGGGCTTCGTCGTCAC
GAP50 5'UTR fw2	CCCTGCGTAGCAAAAGTCGGACTC
GAP50 3'UTR rv2	CGAGCATCCGACATCTACCTGTACTGACC
GAP40 3'UTR rv2	CCGCTGGAGAAAACCCAAGTACATTGC
GAP40 5'UTR fw2	GCAGGCTCCATCCAAACCCAAAGTC

Table 2-8: Oligonucleotides used in this study.

2.5 Expression vectors

2.5.1 Plasmids for expression in *E. coli*

Expression vector	Source
pGEM-T Easy vector system	promega
Strataclone vector	Agilent technologies

Table 2-9: Expression plasmid for *E. coli*

2.5.2 Plasmids for expression in *T. gondii*

Expression vector	resistance	Source/reference
GRASP-RFP	CAT	Pfluger *et al.* (2005)
HSP60-RFP	CAT	van Dooren *et al.* (2009)
FNR-RFP	CAT	Striepen *et al.* (2000)
P5RT70mycGFP	HXGPRT	Meissner *et al.* (2001)
pDHFR-TSc3 (referred to as DHFR)	DHFR	Donald and Roos (1993)
pSAG1/ble	Bleomycin	Messina *et al.* (1995)
P5RT70ddFKBPmycMyoA-tail	HXGPRT	Agop-Nersesian *et al.* (2009)
P5RT70tyMyoAfullenght WT	HXGPRT	(Meissner *et al.* 2002)
P5RT70YFPMyoAfullenght WT	CAT	Markus Meissner
P5RT70mycGFPGAP45	HXGPRT	Dominique Soldati
P5RT70GAP50YFP	CAT	Con Beckers
P5RT70ELC1ty	—	this study
P5RT70GAP40ty	HXGPRT	Dominique Soldati

ddFKBPmycRab11A WT	HXGPRT	Agop-Nersesian *et al.* (2009)
ddFKBPmycRab11B WT	HXGPRT	Agop-Nersesian *et al.* (2010)
P5RT70MLC1ty	—	Dominique Soldati
P5RT70MLC7ty	—	this study
loxPMLC1loxP-YFP	HXGPRT	Egarter *et al.* (2014)
loxPAct11loxP-YFP	HXGPRT	Andenmatten *et al.* (2013)
loxPGAP40loxP-YFP	HXGPRT	this study
loxPGAP50loxP-YFP	HXGPRT	this study
loxPGAP45loxP-YFP	HXGPRT	Egarter *et al.* (2014)
Myosin B/C KO	Bleomycin	Egarter *et al.* (2014)

Table 2-10: Expression vectors for *T. gondii*

2.6 Solutions, Buffers, Media, antibiotics and drugs

2.6.1 General Buffers

10X PBS	137 mM NaCl, 2.7 mM KCl, 8 mM Na_2HPO_4, 1.8 mM KH_2PO4 (pH 7.4)

2.6.2 Buffer and media for bacteria culture

LB medium	10 g/l Tryptone, 5 g/l yeast extract, 5 g/l NaCl
LB agar	1.5 % (w/v) agar in LB medium
SOC medium	2 % Tryptone (w/v), 0.5 % yeast extract (w/v), 0.05 % NaCl (w/v), 2.5 mM KCl, 10 mM $MgCl_2$, 20 mM glucose
NYZ broth	5 g/l NaCl, 2 g/l $MgSO_4$*$7H_20$, 5 g/l yeast extract, 10 g/l Casein hydrosylate, pH adjusted to 7.5 with NaOH
Ampicilin (1000X)	100 mg/ml in H_2O
IPTG (100 µl/petri dish)	100 mM IPTG in H_2O
X-Gal (20 µl/petri dish)	50 mg/ml in N,N-dimethylformamide

2.6.3 Buffer and media for tissue culture

$DMEM_{complete}$	500 ml DMEM, 10 % FBS (v/v), 2 mM glutamine, 20 µg/ml gentamicin
Freezing solution	25 % FBS (v/v), 10 % DMSO (v/v) in DMEM
Elektroporation buffer (Cytomix)	10 mM K_2HPO_4/KH_2PO_4, 25 mM HEPES and 2 mM EGTA pH 7.6, 120 mM KCl, 0.15 mM $CaCl_2$, 5 mM $MgCl_2$ with 5 mM KOH adjusted to pH 7.6, 3 mM ATP, 3 mM GSH
Chloramphenicol (1000X)	10 mg/ml in ethanol
MPA (500X)	12.5 mg/ml in methanol
Xanthine (500X)	20 mg/ml, 1M KOH
Pyrimethamine (1000X)	1 mM in ethanol
Phleomycin (4000X)	20 mg/ml in H_2O
Gentamicin (500X)	10 mg/ml in H_2O
Rapamycin (1000X)	50 µM in DMSO
Shield-1 (1000X)	1 mM in 70 % EtOH

2.6.4 Buffers and solutions for phenotypical assays

Giemsa staining solution	10 % Giemsa stain (v/v) in H_2O
IFA fixing solution	4 % PFA (w/v) in PBS
IFA permeabilisation solution	0.2 % triton X-100 (v/v) in PBS
IFA blocking solution	3 % BSA (w/v) in permeabilisation solution
Hanks' balanced salt solution (HBSS) buffer (Gliding buffer)	5.33 mM potassium chloride, 0.44 mM KH_2PO_4, 4.17 mM sodium bicarbonate, 138 mM sodium chloride, 0.338 mM Na_2HPO_4, 1mM EGTA (pH=7.3), 12.5 mM

	HEPES
calcium ionophore A23187 (1000X)	2 mM in DMSO
Egress buffer	2 µM A23187 in DMEM
Phosphate buffer (0.1 M)	10.9g Na_2HPO_4, 3.2 g NaH_2PO_4 in 500 ml H_2O, pH 7.4
EM fixation solution	2.5% Glutaraldehyde (v/v) in Phosphate buffer 0.1 M, pH 7.4

2.6.5 Buffers for DNA analysis

50X TAE	2 M Tris, 0.5 M Na_2EDTA, 5.71 % glacial acetic acid (v/v)
5X DNA loading buffer	15 % Ficoll (v/v), 20 mM EDTA, 0.25 % bromopenol blue (w/v) in H_2O
DNA ladder	150 µl 1kb-Ladder plus (1 µg/µl), 300 µl 5X DNA loading buffer, 1050 µl H_2O

2.6.6 Buffers for protein analysis

RIPA buffer	50 mM Tris-HCl (pH 8), 150 mM sodium chloride, 1 mM EDTA, 50 mM sodium, 0.5% sodium deoxycholate, 0.1 % SDS (w/v), 1 % triton X-100 (v/v)
4X separating gel buffer	1.5 M Tris/ HCl (pH 8.8), 0.4 % SDS (w/v), filtered sterile
Separating gel	8-15 % of 30 % acryl-bisacrylamide mix, 25% 4X separating gel buffer, 0.1 % APS 10 % (w/v), 0.2 % TEMED (v/v)
4X stacking gel buffer	0.5 M Tris/HCl (pH 6.8), 0.4 % SDS (w/v), filtered sterile
Stacking gel	4 % of 30 % acryl-bisacrylamide mix , 25% 4X stacking gel buffer (v/v), 0.2 % APS 10%(w/v), 0.2% TEMED (v/v)

SDS PAGE running buffer	25 mM Tris, 192 mM glycine, 0.1 % (w/v) SDS
Transer buffer for semi-dry blot	48 mM Tris, 39 mM glycine, 20 % methanol (v/v)
Transer buffer for wet blot	48 mM Tris, 39 mM glycine, 20 % methanol (v/v), 0.037 % SDS (w/v)
Blocking solution	0.2 % Tween (v/v), 5 % milk powder (w/v) in PBS
Washing solution	0.2 % Tween (v/v) in PBS

2.7 Organisms

2.7.1 Bacterial strains:

E. coli: XL10-gold, chemically competent, Stratagene

XL1 blue, electrocompetent, Stratagene

2.7.2 T. gondii strain:

RHΔHX: virulent, *hxgprt*-deficient *T. gondii* strain RH (Donald and Roos 1993).

2.7.3 Host cell lineages:

Human foreskin fibroblasts (HFF) (purchased from ATCC)

This cell line has a limited number of cell cycles (~30) and forms only one single layer. Because of this HFF cells were used for the culturing of transient transfected parasites, for limited dilution of stable parasite pools, for microscopic analysis and for distinct experiments.

Vero: (provided by Dominique Soldati)

The Vero lineage was isolated from kidney epithelial cells extracted from an African green monkey. These cells have the ability to grow in several cell layers and are potential immortal, because they lost any contact inhibition. Because of this fact, those cells were used for obtaining high amounts of parasites and to maintain stable clones in culture.

KB100 Cyt1: (Toyama and Toyama 1988, Dobrowolski and Sibley 1996)

Cytochalasin B resistant cell line which also resistant to Cytochalasin D and was used for drug assays.

2.8 Molecular biology

2.8.1 Extraction of genomic DNA from *T. gondii* parasites

To extract genomic DNA from Toxoplasma gondii tachyzoites the DNeasy Blood & Tissue Kit from Qiagen was utilized. The principle of this kit is that the cells are lysed with proteinase K and a silica based membrane with microspin technology provides fast and efficient purification of the genomic DNA. The obtained DNA is free interfering contaminants and enzyme inhibitors and works well for PCR based approaches. Freshly lysed parasites (500 µl to 1 ml) were centrifuged at 1200 rpm for 10 min at RT and washed once with 1x PBS. Afterwards the isolation of genomic DNA was performed according to the manufacturer's manual for cultured cells. The DNA was eluted from the column in 200 µl of molecular grade water.

2.8.2 Isolation of RNA from *T. gondii*

To isolate RNA from *T. gondii* tachyzoites the SV Total RNA Isolation System from Promega was used. Therefore a confluent T175 tissue flask with HFF cell was inoculated with parasites and incubated till the parasites lysed the host cell monolayer completely to avoid cross contamination with host cell material. The freshly lysed tachyzoites (approximately 10^9 parasites) were centrifuged at 1200 rpm for 10 min at 4 °C and washed once with ice cold 1x PBS. The pellet was resuspended in the provided lysis buffer and loaded on five separate columns. Subsequently, the extraction of RNA was performed according to the manufacturer's manual for cultured cells. The RNA was eluted from the column in 50 µl of RNase free water. The RNA was either used immediately or stored without delay at -80 °C.

2.8.3 Reverse transcription (cDNA synthesis)

To generate cDNA the SuperScript® II Reverse Transcriptase (Life technologies) was applied following manufacturers instruction to transcribe purified RNA (see

chapter 2.8.2) into complementary DNA (cDNA). The cDNA was stored at -20°C or directly used for standard PCR to amplify specific cDNA sequences.

2.8.4 Amplification of DNA using Polymerase chain reaction

2.8.4.1 From *T. gondii* genomic DNA, cDNA or plasmid DNA templates

Polymerase chain reaction (PCR) allows the amplification of specific DNA regions *in vitro* using two oligonucleotides that are complementary to the 3' ends of each of the sense and anti-sense strand of the target DNA. The general principle of the PCR process can be divided into 3 steps. During the first step double stranded DNA is denatured into single strands by boiling. In the next step the oligonucletides bind to complementary regions of the target sequence. During the final step the DNA polymerase synthesises a complimentary copy of the target sequence through assembly of deoxynucleotide triphosphates (dNTPs) from the 3'OH end of the used oligonucleotides. This cycle is repeated several times which leads to the exponential amplification of the target sequence. For the amplification the Platinum® Taq DNA Polymerase High Fidelity from Invitrogen was used. This polymerase possesses a 3´→5´ exonuclease with proofreading activity that increases fidelity approximately six times. The reaction was performed in PCR tubes and the composition of the reaction mix was as described in Table 2-11

Component	Final concentration
Template DNA	Approximately 50-200 ng
10X High Fidelity PCR Buffer	1x
10 mM dNTP mixture	0.2 mM each
50 mM MgSO4	2 mM
Sense oligonucleotide	0.2[a]-0.4[b] µM each
Antisense oligonucleotide	0.2[a]-0.4[b] µM each
Platinum® Taq High Fidelity	1.0 unit

[a] genomic and cDNA
[b] plasmid DNA

Table 2-11 General PCR reaction mix.

The reaction occurred in a thermocycler from Eppendorf using the programme described in Table 2-12.

Cycles	Steps	Temperature	Time
1x	Initial denaturation	94°C	5 min
25x-35x	Denaturation Annealing Elongation	94°C 48-65°C* 68°C	30 s 30 s 1 min/kb
1x	Final elongation	68°C	10 min
1x	Cool down	4°C	∞

* the optimal annealing temperature depends on the melting temperature of the primer

Table 2-12: General overview of the thermocycler programme used for PCR.

2.8.4.2 Colony PCR

Colony PCR was performed on bacteria clones to identify correct clones after transformation of ligation reactions. Bacteria colonies served as template for the PCR and the oligonucleotides used were specific to the insert that was integrated into the vector. Before staring the actual PCR reaction a LB-plate, overnight culture tubes (contain LB broth) and PCR tubes were labelled with numbers referring to the bacteria colonies picked. A PCR Master Mix (see Table 2-13) was prepared and pipetted into the PCR tubes. Afterwards single colonies were picked from transformation plates, streaked on the new LB plates, dipped into the PCR tube and transferred to the overnight culture tube. The LB plate and overnight culture were kept on 37°C till colonies were screen using PCR. The PCR programme used is displayed in Table 2-12.

Component	Final concentration
Bacteria colony	-
10X NEB Taq polymerase buffer	1x
10 mM dNTP mixture	0.4 mM each
Sense oligonucleotide	0.4 µM each
Antisense oligonucleotide	0.4 µM each
NEB DNA Taq polymerase	1.0 unit

Table 2-13: PCR reaction mix for colony PCR.

2.8.5 Agarose gel electrophoresis

DNA fragments can be separated by size using agarose gel electrophoresis. DNA fragments are nucleic acid molecules and negatively charged. Therefore, those molecules move towards the anode after applying an electric field. Smaller molecules move faster that larger ones, because they migrate easier through the pores of the agarose gel. The size of the pores can be determined by the concentration of agarose used, whereby the pores get smaller when higher agarose concentration is being used. For gel electrophoresis agarose was dissolved at the required concentration (0.8 % to 2 % w/v) in 1x TAE buffer. To visualise the DNA on the gel, GelRed (Phenix research products) was used. After mixing the DNA sample with 6x loading dye, the electrophoresis was performed in the appropriate amount of 1x TAE buffer according to the manufacturers (Biorad) manual. To determine the size of the DNA band 1 kb plus DNA ladder (Invitrogen) was loaded in a lane next to the sample. The DNA was visualised with the help of a transluminator.

2.8.6 Isolation of DNA fragments from agarose gel or solution

DNA fragments were isolated from agarose gels and solutions using the High Pure PCR Product Purification Kit from Roche Diagnostics GmbH. The purification of DNA fragments occurred according to manufacturer's instruction on silica based technique. The purified DNA was eluted in 30 µl instead of 50 µl of molecular grade water to increase the DNA concentration.

2.8.7 Dephosphorylation of DNA fragments

To minimise the likeliness of self-ligation of endonuclease digested plasmid DNA, Alkaline Phosphatase Calf Intestinal (CIP) can be added. This enzyme catalyses the removal of 5' phosphate residues from DNA, thus avoiding self-ligation of the vector. The ligation of an insert into the CIP treated vector is still possible over the 5' phosphate groups of the insert. After restriction digest of the vector, 10 U of CIP were added for for 1 hour at 37°C for sufficient dephosphorylation. Afterwards, a gel extraction (see chapter 2.8.6) was performed to purify the DNA and remove the alkaline phophatase.

2.8.8 Restriction endonuclease digests

All restriction endonucleases used in this study were purchased from New England Biolabs (NEB) and used with adequate NEB buffer and BSA according to instructions of manufacturer. Almost all digest were performed in an incubator at 37°C for 1h-4h. The only exceptions are digests using ApaI as enzyme. This enzyme requires an incubation temperature of 25°C, so the digest were performed in a heat block for 1h. To analyse plasmids generally 100-500 ng DNA were digested for 1h in a 20 µl digestion mix. For preparative digest 1-5 µg were used for digestion for 2-3 h. After digestion the samples were analysed using agarose gelelectrophoresis.

2.8.9 Ligation of DNA fragments

Ligation is the covalent joining of two DNA fragments through the action of a DNA ligase. This enzyme is derived from the bacteriophage T4 and catalyses the formation of phosphodiester bonds between 5' phosphate and 3' OH ends. For insertion of DNA fragments into *T. gondii* expression plasmids the T4 DNA ligase from NEB was used. To set up a 10 µl ligation mix 1 µl of the enzyme and 1 µl of the supplied 10x ligase buffer were used and the molar ratio of vector and insert was between 1:3 and 1:7. After mixing all components on ice the ligation mix was incubated for 1 hour at 23.5°C. PCR products were ligated into a cloning vector via TA (Thymine, Adenine) cloning using the StrataClone PCR Cloning Kit (Agilent Technologies) following manufacturer's instructions.

2.8.10 Heatshock Transformation of *E.coli*

For transformations of ligation done with the StrataClone PCR Cloning Kit (Agilent Technologies), half of the ligation mix was used. The heat shock transformation into StrataClone SoloPack competent cells occurred according to manufacturer's instructions. After transformation the bacteria were plated on LB Agar plates containing ampicillin and X-Gal. X-Gal was added to allow easy screening for positive colonies. The StrataClone cloning vector contains a reporter gene for ß-galactosidase. Within the open reading frame of ß-galactosidase is the multiple cloning sites where the PCR fragment is inserted. After transformation, bacteria colonies that have the PCR fragment inserted appear white, because the LacZ gene is getting destroyed. Bacteria colonies

without insertion are blue. For all other transformation the whole ligation mix was used and transformed into XL10-Gold Ultracompetent Cells (Agilent Technologies) following the instructions of the manufacturer. The transformation mixture was then plated on LB agar plates and incubated over night at 37°C.

2.8.11 Overnight cultures of *E. coli*

The successful isolation of plasmid DNA requires appropriate amounts of bacteria. For this purpose, sterile LB broth containing ampicillin was inoculated with the respective bacteria clone and incubated over night at 37°C in a shaking incubator with 225 rpm. Afterwards, the bacteria culture was directly used for the isolation of DNA are pelleted and stored at -20°C.

2.8.12 Isolation of plasmid DNA from *E. coli* bacteria

To isolate plasmid DNA bacteria are lysed under alkaline conditions and the released nucleic acids are reversibly denatured. The lysis buffer contains SDS and RNase A, which denatures proteins and degrades RNA. Subsequently, the plasmid DNA is renatured by addition of neutralisation buffer and purified using a silica-gel membrane.

2.8.12.1 Small scale plasmid isolation (Miniprep)

For the isolation of small amounts of plasmid DNA the Qiaprep Spin Miniprep Kit (Qiagen). Therefore single bacteria colonies were picked from agar plates to inoculate 3 ml of LB broth containing ampicillin. The cultures were then grown overnight at 37°C with permanent shaking at 225 rpm. Plasmid DNA was purified according to manufacturer's instructions and eluted in 50 µl water. The general yield was between 5-25 µg of plasmid DNA.

2.8.12.2 Medium scale plasmid isolation (Midiprep)

Large scale purifications were performed using the Plasmid *Plus* Midi Kit (Qiagen). Single bacteria colonies were inoculated in 5 ml LB broth and this so called pre-culture was incubated for approximately 4-6hourat 37°C with constant shaking at 225 rpm. Then, the pre-culture was added to 50 ml of LB

broth and incubated overnight with the same conditions. Plasmid DNA was purified according to manufacturer's instructions and eluted in 200 µl molecular grade water. The typical yield was between 50-300 µg of plasmid DNA.

2.8.13 Ethanol precipitation of DNA

Ethanol precipitation of DNA was performed to concentrate DNA and/or purify nucleic acids from salts. DNA solutions were mixed with 1/10 volume of 3 M sodium acetate pH 5.2 and 2.5 volumes of 100 % ethanol (-20°C cold). The DNA was stored at -20°C for at least 30 minutes. Afterwards, the DNA precipitation mix was centrifuged for 30 min at 13,000 rpm and 4°C. Subsequently, the DNA was washed twice with 70% ethanol to remove residual salts. The supernatant was removed and the pellet air dried. If Ethanol precipitation was performed to concentrate DNA appropriate amount of water was added to resuspend DNA. DNA for transfections was dried under sterile conditions and dissolved in 50 µl sterile Cytomix.

2.8.14 Determination of nucleic acid concentration and purity

The nucleic acid concentrations of samples were measured using a NanoDrop spectrometer (Thermo Scientific) following the instructions of the manufacturer. The NanoDrop can also be used to assess the purity of nucleic acids. The absorbance maxima of nucleic acids and proteins are at 260 and 280 nm respectively. This can be used to determine if a nucleic acids sample is contaminated with proteins. DNA is considered as pure if the 260/280 ratio is about 1.8 whereas RNA is regarded as pure if the ratio is about 2.0. Chemical contaminations, like phenol are detected with the help of an absorbance maximum at 230 nm. Nucleic acids are regarded as pure if the 230/260 nm ratio is between 2.0-2.2.

2.8.15 DNA sequencing and alignments

DNA sequencing was performed by DNA Sequencing & Services in Dundee and GATC biotech in Konstanz. The analysis of obtained DNA sequences was carried out using the function ClustalW of the BioEdit Alignment Editor. To compare sequences of DNA or proteins with existing genes the BLAST (Basic Local

Alignment Search Tool) tool of databases like NCBI (http://www.ncbi.nlm.nih.gov/) and ToxoDB (http://ToxoDB.org/) were used.

2.8.16 Cloning of DNA construct performed in this study

All primers used in this study are listed in Table 2-8. The P5RT70ELC1ty plasmid was generated using P5RT70MLC1ty as parental vector. First the coding region of *elc1* was amplified using the primer set ELC1-fw/rv. The *mlc1* cDNA was replaced by the cDNA of *elc1* (TGME49_269442) EcoRI and NsiI. The construct P5RT70MLC7ty was generated using the same strategy. The cDNA of *mlc7* (TGME49_315780) was amplified using the oligo pair MLC7-fw/rv and integrated in P5RT70MLC7ty via EcoRI and NsiI.

The loxPAct1loxP–YFP–HX construct was created using the subsequent strategy. Initially, the *act1* ORF (TGME49_209030) was amplified from cDNA using the primer set Act1 ORF fw/rv and following the resulting PCR product was cloned into the parental vector p5RT70loxPKillerRedloxPYFP–HX (Andenmatten *et al*. 2013) via EcoRI and PacI. To place *act1* under the control of the endogenous promoter a 2 kb fragment upstream of the start codon of *act1* was amplified from genomic DNA using the primer pair 5'UTR Act1 fw/rv and cloned into the vector using EcoRI and PacI. Last, the *act1* 3'UTR was amplified from genomic DNA using the oligos 3'UTR Act1 fw/rv, and integrated into the final vector using ApaI and EcoRI.

To generate loxPMLC1loxP–YFP-HX the *mlc1* 3'UTR was amplified from genomic DNA using the oligo set 3'UTR MLC1 fw/rv, and the PCR fragment was integrated into p5RT70loxPKillerRedloxPYFP–HX (Andenmatten *et al*. 2013) via SacI. The *mlc1* ORF (TGME49_257680) was amplified from cDNA with the primer pair MLC1 ORF fw/rv, and subsequently cloned into the parental vector using EcoRI and Pac1. To place mlc*1* under the control of the endogenous promoter a 2 kb fragment upstream of the start codon of *mlc1* was amplified from genomic DNA using the oligos 5'UTR MLC1 fw/rv and cloned into the parental vector using EcoRI and ApaI.

The loxPGAP45loxP–YFP–HX construct was created using the strategy described for loxPMLC1loxP–YFP–HX with minor changes. First, the *gap45* ORF

(TGME49_223940) was amplified from cDNA using the oligos GAP45 ORF fw/rv and integrated into the vector with EcoRI/PacI. Next a 2 kb fragment upstream of the start codon was amplified using 5'UTRGAP45 fw/rv and digested with ApaI/EcoRI. Both ORF and endogenous were cloned simultaneously into the parental *vector* p5RT70loxPKillerRedloxPYFP-HX. Finally, the *gap45* 3'UTR was amplified from genomic DNA using the oligo set *3*'UTR GAP45 *fw/rv via PciI*.

The loxPGAP50loxP-YFP-HX construct was generated using the following strategy. Firstly, the *gap50* 3' UTR was amplified from genomic DNA using the primer pair 3'UTR GAP50 fw/rv, and cloned into the parental vector p5RT70loxPKillerRedloxPYFP-HX using SacI. To place *gap50* under the control of the endogenous promoter a 2 kb fragment upstream of the start codon of *gap50* was amplified from genomic DNA using the oligos 5'UTR GAP50 fw/rv and cloned into the vector using EcoRI and NaeI. Finally, the *gap50* ORF (TGME49_219320) was amplified from cDNA using the primers GAP50 ORF fw/rv and the PCR product was cloned into final vector using EcoRI/MfeI and PacI.

To generate loxPGAP40loxP-YFP-HX the *gap40* 3'UTR was amplified from genomic DNA using the primer pair 3'UTR GAP40 fw/rv, and the PCR fragment was cloned into p5RT70loxPKillerRedloxPYFP-HX (Andenmatten *et al*. 2013) via SacI. The *gap40* ORF (TGME49_249850) was amplified from cDNA using the primers GAP40 ORF fw/rv, and was cloned into the parental vector using EcoRI/MfeI and PacI. To position gap40 under the control of the endogenous promoter a 2 kb fragment upstream of the start codon of *gap40* was amplified from genomic DNA using the oligos 5'UTR GAP40 fw/rv and cloned into the parental vector using BglII and NaeI. The BglII restriction site was integrated with the oligo GAP40 ORF fw.

To generate the Myosin B/C KO-*Bleo* construct, the bleomycin selection plasmid pSAG1-BLE was used as parental vector (Messina *et al*. 1995). First the *myob/c* 5'UTR was amplified from genomic DNA using the primer pair 5'UTR MyoB/C fw/rv and integrated into the parental vector via KpnI/HindIII. Afterwards the *myob/c* 3'UTR was cloned into the vector using the oligo pair 3'UTR MyoB/C fw/rv using PacI/SpeI.

2.9 Cell biology

2.9.1 Culturing of host cells

In general all host cells used in this study were maintained in Dulbecco's modified Eagle's medium (DMEM) supplemented with 10% fetal calf serum, 2 mM glutamine and 25 mg/ml gentamicin at 37°C and 5 % CO2 in humid environment. For culturing *Toxoplasma gondii,* Human Foreskin Fibroblasts (HFF) and Vero cells (from African green monkey kidney) were used. HFF cells are primary cell with limited growth due to contact inhibition. Because of their ability to grow only in monolayer HFF cells were mostly used for selection after transfection, limited dilutions to obtain clonal lines as well as immunofluorescence and phenotypical analysis. HFF cells were split once a week in a 1:3 ratio and they can be used up to passage 25. The vero cells are potentially immortal, transformed cell line that lost any contact inhibition leading to the ability that this cell line can grow in many layers on top of each other. So these cells were used when high yields of parasites were needed or to culture stable parasite lines. Vero cells were split every 3-4 days in 1-5 to 1-20 ratios. Cyt-1 KB100 cells were cultures in $DMEM_{complete}$ supplemented with 0.01 µM Cytochalasin D at 37°C and 5 % CO2 and split every 3-4 days in 1:4 ratios.

2.9.2 Culturing of *T. gondii* tachyzoites

Toxoplasma tachyzoites were cultured in Dulbecco's modified Eagle's medium (DMEM) supplemented with 10% fetal calf serum, 2 mM glutamine and 25 mg/ml gentamicin at 37°C and 5 % CO2 in humid environment. Extracellular parasites were inoculated on host cells. They undergo several rounds of replication until they lyse the host cells completely. Extracellular, *T.gondii* tachyzoites are only able to survive up to 24 hours. The parasites need to be transferred to fresh cells. In case intracellular parasites are used to infect fresh cells, the parasites need to be artificially released from the host cells. For this purpose, the host cell layer was detached from tissue culture dish with help of a cell scraper. To destroy the host cells and release the intracellular parasites, the host cells were syringed using a needle with 26 gauge.

2.9.3 Trypsin/EDTA treatment

Trypsin is a protease cleaving distinct peptide bonds. By treatment with Trypsin/EDTA adherent cells can be detached gently from the bottom of culture flasks and neighbouring cells. Therefore, the host cell layer is washed once with 1x PBS to remove the FBS deriving from the culture media, because FBS in inhibiting Trypsin. After addition of Trypsin/EDTA the cells are incubated for 5-10 min at 37°C and 5 % CO_2. Subsequently, the detached cells can be re-suspended in new culture media and be transferred to new culture flasks.

2.9.4 Freezing and defrosting of stabilates

To generate stabilates intracellular parasites were frozen. Therefore, HFF cells were highly infected with Toxoplasma gondii, so that most host cells contain large vacuoles. Infected host cells were treated with 250 µl Trypsin/EDTA to detach them from the dish surface. Afterwards the cells were gently re-suspended in 800 µl of DMEM, transferred to Cryo tubes containing 2x freezing media and immediately frozen at -20°C. After one day the tubes were transferred to -80°C, where they could be stored for a couple of months. For a longer time period frozen cells were transferred to liquid nitrogen.

To defrost stabiliates, they frozen parasites were incubated in a water bath at 37°C till thawed. Afterwards, the parasites were immediately transferred in 15 ml falcon tubes containing 10 ml of media and centrifuged at 1200 rpm for 5 minutes. This step is performed to remove the DMSO included in the freezing media. The parasite pellet was then transferred to confluent HFF cells.

2.9.5 Cell count with Neubauer counting chamber

For some assays a precise amount of parasites is needed. Because of this the amount of parasites was determined using a Neubauer counting chamber. For this purpose *T. gondii* tachyzoites were diluted appropriately and 10 µl were transferred to the counting chamber. Subsequently, cells within a defined area were counted using a light microscope. Afterwards, the amount of cells per 1 ml could be calculated according to the manufacturer's specifications.

2.9.6 Transfection of *T. gondii*

The transfection of DNA in *T. gondii* takes place by electroporation (Soldati and Boothroyd 1993). For this purpose freshly released parasites were centrifuged for 10 min at 1200 rpm and then the pellet was washed once with electroporation buffer (10 mM K_2HPO_4/KH_2PO_4, 25 mM HEPES, 2 mM EGTA pH 7,6, 120 mM KCl, 0,15 mM $CaCl_2$, 5 mM $MgCl_2$). Afterwards the pellet was resuspended in 700 µl electroporation buffer and 30 µl ATP (100 mM) as well as 30 µl GSH (100 mM) were added. 60 µg of the respective DNA was precipitated and dissolved in 50 µl electroporation buffer. For the electroporation two pulses at 1,7 kV for 200 ms were used. Directly after transfection the parasites were put onto a confluent 6 cm dish of HFF cells and transient IFA were set up on a 24 well plate.

For a stable transfection (Donald and Roos 1993) the plasmid DNA has to be linearised prior to precipitation. The insertion of linearised DNA occurs undirected, randomly distributed over the genome and the number of copies per genome is variable. For a successful stable transfection, it is necessary to select the positive parasites by using a respective selection marker. In contrast to transient transfections 10 U of the enzyme used for linearising were added to the transfection mix. In doing so, the genomic DNA is cut undirected and the DNA repair mechanisms are activated. This process is called Restriction Enzyme Mediated Insertion and increases the insertion of DNA in *T. gondii* by up to 400 (Black *et al.* 1995).

To get stable parasites four different selection markers have been used. The parasites were either selected in presence of 25 mg/ml mycophenolic acid and 40 mg/ml xanthine as previously described (Donald *et al.* 1996) or the selection was based on 1 mM pyrimethamine (using a plasmid containing *dhfrts*) (Donald and Roos 1993) or 20 mM chloramphenicol acetyltransferase (CAT) recorded previously (Kim *et al.* 1993) or 5 µg/ml or 50 µg/ml phleomycin (Messina *et al.* 1995). The respective selection marker is added 24 hours post transfection. In average stable parasite pool are obtained within 4 days via *dhfrts* selection, after 5 days using *hxgprt* or phleomycin or after 10 days using CAT selection.

2.9.7 Isolation of a clonal parasite line via limited dilution

The isolation of stable, clonal parasite lines occurred through limited dilution of a stable pool on a 96 well plate. After 5-7 days plaques were formed in the host cell monolayer, whereas one plaque resembles a clonal population. Wells with one plaque indicate a single parasite clone, because only one parasite was initially present in this well. Clonal populations were transferred to 24 well plates, checked with the help of immunofluorescence analysis and further characterised.

2.9.8 Phenotypical analysis to characterise *Toxoplasma*

2.9.8.1 Plaque assay

The growth behaviour of *Toxoplasma* parasites can be investigated by performing a so called plaque assay. As a consequence of several rounds of host cell invasion, intracellular replication and lysis of the infected host cells, plaques (cell free lysis zones) were formed in the host cell monolayer. The size and the number of these plaques mirror the infectivity of the respective parasite strain. To perform a plaque assay, HFF monolayers were usually inoculated with 200 to 500 parasites and incubated for 5-7 days under normal growth conditions. Afterwards, the plaque containing monolayer was fixed with 100 % methanol for 15 minutes and stained with Giemsa for 30 minutes. In case YFP positive KO lines were used, the plaque assay was fixed with 4 % PFA for 20 minutes because methanol destroys YFP. The plaque assays were analysed using a light microscope.

2.9.8.2 Attachment/Invasion assay

The efficiency of *Toxoplasma gondii* to invade host cell was determined performing invasion assays. Therefore, parasites were artificially released from host cells and 5 x 10^6 parasites were inoculated on HFF cells growing in glass cover slips in 24 well plates. Afterwards, the parasites were centrifuged at 250 g for 2,5 minutes to settle them on top of the host cells. Subsequently, the parasites were allowed to invade for 30 minutes to 4 hours depending on the strain. After washing the cover slips for 3 times in PBS to remove not and loosely attached parasites, the parasites were fixed with 4 % PFA for 20 minutes. To be

able to distinguish between extra- and intracellular parasites an immunofluorescence assay was performed using SAG1 antibody. Without permeabilising the cells only attached parasites are stained whereas invaded parasites are not assessable to the antibody and thus have no staining. To analyse attachment, 15 fields of views were counted for attached and invaded parasites. Those numbers were standardised to wild-type parasites. To determine penetration, 300 parasites were analysed if they were attached or invaded into the host cell.

2.9.8.3 Invasion/Replication assay

Replication assays were performed to investigate if genetically modified *Toxoplasma* tachyzoites were affected concerning their ability to replicate. Therefore, 1 x 10^5 parasites were inoculated on HFF cell growing on glass slips in 24 well plates. After allowing them to invade for 1 hour, the cover slips were washed harshly by dipping them ten times into 1 x PBS to remove all attached parasites. Afterwards, the cover slip was transferred into a fresh 24 well plate containing DMEM media and incubated under normal growth conditions for 24 h. Following fixation with 4 % PFA for 20 minutes a standard immunofluorescence assay was performed using either α-IMC or α-GAP45 antibody to stain for intracellular parasites. To quantify replication the parasites per vacuole of 200 vacuoles were counted. To quantify invasion, vacuoles in 25 fields of view were determined.

2.9.8.4 Egress assay

To examine the ability of *Toxoplasma gondii* to egress infected host cells, egress assays were carried out. Therefore, parasites can be tested for natural egress or for calcium ionophore A23187 induced egress. For the latter 5 x 10^4 parasites were inoculated in a duplicate on IFA plates. A duplicate is used so that one coverslip can serve as a control while the other cover slip will be induced. This was done to make sure the parasites were not egressing naturally and solely because of the ionophore. The parasites were allowed to grow under standard condition for 24 hours. After this time period media without any serum added is warmed to 37°C. The cover slips were washed once with this media to remove all serum since this is inhibiting the Ca^{2+} Ionophore. To one of the cover slips

serum free media was added whereas the other cover slip was treated with the media supplemented with 2 µM Ca^{2+} Ionophore A23187 to artificially induce egress. The parasites were incubated for 5 min at standard condition and then fix with 4 % PFA for 20 minutes. Afterwards an immunflourescence analysis using α-Sag1 antibody was perfomed to stain for extracellular parasites. To quantify the data set 200 vacuoles were counted if they egressed or not. To test for natural egress 5 x 10^4 and 1 x 10^4 parasites were inoculated on HFF cells and fixed after different time points (24, 36, 48, 72, 96 and 120 h). After performing an immunoflourescence assays using α-IMC1, the experiment was analysed microscopic and documented.

2.9.8.5 Trail deposition assays

Gliding motility of *T. gondii* is substrate dependant and can be inhibited by calcium, since calcium triggers microneme release. While parasites glide on HFFS or on FBS coated cover slips, they deposit traces of the major surface antigen 1, Sag1.Those so called trails can be visualised through IFA using α-Sag1 antibody. With the help of this assay the gliding motility of different parasite strains can be determined. Therefore glass cover slips are added inside the wells of a 24 well plate, coated with 50 % FBS in 1 x PBS and incubated over night at 4°C on a shaker. Before starting the experiment 1 x PBS and Hank's Balanced Salt Solution (HBSS) (HBSS supplemented with 1 mM EGTA and 12.5 mM HEPES) were pre heated to 37°C. The FBS coated cover slips were washed three times with 1 x PBS before adding the pre heated HBSS buffer. Artificially released parasites were washed once with HBSS buffer and 1 x 10^6 parasites in 0.5 ml HBSS buffer were added to each cover slip. The parasites were left at room temperature for 15 minutes to settle down and then they were incubated for 30 minutes at 37°C and 5 % CO_2 to allow them to glide. Afterwards, the parasites were fixed in 2.5 % PFA for 20 minutes. Subsequent removal of the PFA the cover slips were air dried for 5 minutes. An immunofluorescence analysis was performed without permeabilising and stained with α-Sag1 antibody to visualise the gliding trails. To quantify the assay 200 parasites were counted for the presence or absence of trails.

2.9.9 Immunoflurescence assay

The localisation of proteins can be determined by using an Immunofluorescence analysis (IFA). For immunofluorescence analysis, HFF cells grown on cover slips were inoculated with *T. gondii* parasites in absences or presence of 1 mM Shld-1 for 24-48 hours depending on the protein. Cells were fixed either with 4% w/v paraformaldehyde in phosphate buffered saline (PBS) for 20 min at room temperature or -20 °C cold methanol for 10 min depending on the primary antibodies that are used. Fixed cells were washed once with 1x PBS and then permeabilised with 0.2 % Triton X-100 in PBS for 20 min followed by blocking in 2 % w/v bovine serum albumin (BSA) in PBS for 20 min to saturate unspecific binding sites. After that the incubation with the primary antibodies for 60 min was performed. To remove unspecific bound antibodies, three washing steps à 5 min with 1x PBS were carried out. This is followed by incubation with secondary Alexa Fluor 488 or Alexa Fluor 594 conjugated antibodies for another 60 min (1:3000, Invitrogen-Molecular Probes). After three more washing steps the cover slips were mounted upside down using DAPI Fluoromount from Southern Biotech.

2.9.10 Sample preparation for electron microscopy

Monolayer of HFF, grown on 6 cm dishes, were infected with parasites and cultured for 24 hours in absence or presence of 1 mM Shld-1. After that the intracellular parasites were detached using trypsin/EDTA, carefully resuspended in 1x PBS and centrifuged for 10 min at 2000 rpm. After this step the pellet was fixed with 2.5 % glutaraldehyde in 0.1 M phosphate buffer pH 7.4. The analysis and documentation of the fixed samples was performed by David J. P. Ferguson (Nuffield Department of Pathology, University of Oxford, United Kingdom).

2.9.11 Microscopy equipment and settings

For image acquisition z–stacks of 1.5-2 µm increments were collected using a UPLSAPO 100 x oil (1.40NA) objective on a Deltavision Core microscope (Image Solutions–Applied Precision, GE) linked to a CoolSNAP HQ2 CCD camera. Deconvolution was achieved using SoftWoRx Suite 2.0 (Applied Precision, GE). Image acquisition was also conducted using a 100X and 63X oil objective on a Zeiss Axioskope 2 MOT+ microscope attached to an Axiocam MRm CCD camera

using Volocity software, Images were processed using ImageJ 1.34r software and Photoshop (Adobe Systems Inc., USA).

2.9.12 Time lapse microscopy

Gliding time-lapse microscopy was performed with the DeltaVision® Core microscope using a 20X objective. Normal growth conditions were retained during the experiment (37 °C; 5 % CO_2). To evaluate gliding kinetics, parasites were prepared analogous to the trail deposition assay. Extracellular parasites were pelleted, washed in pre-warmed PBS and re-suspended to a concentration of 1 × 10^6 per 800 µl in pre-warmed HBSS. Afterwards, parasites were added to FBS-coated glass dishes (Ibidi µ-Dish$^{35mm,\ high}$) and gliding was recorded for 30 min at one frame per second using SoftWoRx® software after parasites have settled. For examination, 19 parasites were manually tracked using the manual tracking plugin for ImageJ 1.34r software and average speed were determined.

2.10 Biochemistry

2.10.1 Preparation of *T. gondii* cell lysates for SDS PAGE

To prepare parasite lysates for SDS PAGE extracellular parasites (either freshly egressed or artificially released from host cells) were centrifuged at 1200 rpm for 10 minutes. The supernatant was removed and the parasite pellet resuspended in 1 ml 1 x PBS. The amount of parasites was determined using a Neubauer counting chamber. While counting the parasites were centrifuged again and the pellet resuspended in RIPA buffer (150 mM NaCl, 1% Triton X-100, 0,5% DOC, 0,1% SDS, 50 mM Tris, pH 8,0, 1 mM EDTA) for lysis. The mix is incubated on ice for 5 minutes and afterwards centrifuged in a table top centrifuged at 14.000 rpm for 1 hour at 4°C. By this means, the protein solution is separated from contamination like cell components. The supernatant was transferred to a clean tube and either immediately stored at -80°C or supplemented with appropriate amount of NuPAGE 4 x LDS buffer (life sciences) and NuPAGE 10 x reducing agent (life sciences) for prompt usage. The samples were boiled at 95°C for 5 minutes prior to performing SDS PAGE.

2.10.2 Sodium dodecyl sulphate polyacrylamide gel electrophoreses

Separation of proteins was achieved by Sodium dodecyl sulphate polyacrylamide gel electrophoreses (SDS-PAGE) according to Laemmli (Laemmli 1970). With the help of SDS PAGE proteins can be separated according their molecular weight. This is possible since addition of Dithiothreitol (DTT) and sodium dodecyl sulphate (SDS) is reducing the proteins so that they gain a negative charge instead of their own charge. Polyacrylamide gels are build by co-polymerization of acrylamid and bis-acrylamide (N', N'-methylene-bis-acrylamide). This reaction is initiated by a free radical-generating system. The polymerisation is catalysed by APS (ammonium persulfate) and TEMED (tetramethylethylenediamine). The persulfate free radicals change acrylamide monomers to free radicals reacting with activated monomers to start the polymerisation chain reaction. The elongating polymer chains are randomly crosslinked by bis, resulting in a gel with distinct porosity that depends on the polymerisation condition and polyacrylamide amount. According to the system from Laemmli the gel consists of a large pore sized stacking gel (5 % acrylamide, pH 6.8) and a small pore sized resolving gel (8 %-12 % acrylamide depending on the protein of interest, pH 8.8). Upon applying an electrical field the proteins wander in direction of the anode, while first being concentrated in the stacking gel and secondly being separated according their molecular weight in the resolving gel. With the help of a protein ladder, Page Ruler Prestained Protein Ladder (Fermentas), the size of the proteins can be determined. SDS-PAGE was carried out with the Mini-Trans-Blot Cell system from BioRad according to manufacturer's instructions. For all buffers and solutions see chapter 2.6. Parasite lysates (see chapter 2.10.1.) and 10 µl of protein ladder were loaded and the gel ran in 1 x SDS PAGE running buffer at 100 V while in the stacking gel and then at 140 V while in the resolving gel. After electrophoresis, gels were used for western blots.

2.10.3 Transfer of proteins from SDS gel to nitrocellulose membrane

After separation by SDS-PAGE, the proteins were transferred onto a nitrocellulose membrane (Hybond ECL, GE Healthcare). A Transblot semi-dry transfer system (Biorad) was used according to manufacturer's instructions. The

gel, the membrane and the filter papers were equilibrated in transfer buffer (48mM Tris , 39mM glycine, 20% methanol) for 15 20 minutes. Next the sandwich for blotting was assembled (1x extra thick filter, membrane, gel, 1x extra thick filter) and the blot was run for 30 min at 13 V.

2.10.4 Verification of proteins using Ponceau-S-staining

To detect proteins on nitrocellulose membranes Ponceau-S was used. Ponceau S is a negative stain which binds reversible to the positively charged amino groups of the proteins. For the staining the membrane was incubated with Ponceau-S for 5 minutes and subsequently washed with ddH_2O until red stained protein bands were visible.

2.10.5 Immunoblot analysis

After Ponceau-S staining, blotted membranes were blocked in 5 % (w/v) skimmed milk powder (Marvel) in 1 x PBS/ 0.2 % Tween20 (v/v) for either overnight at 4°C or for 1 hour at room temperature. Primary antibodies were diluted to the appropriate concentration in blocking solution. After blocking the membrane was placed within a wet chamber (petri dish 150 mm x150 mm with a wet paper towel at the bottom) and the prepared antibody was added. The membrane is between two pieces of parafilm and 1 ml of antibody solution is sufficient to cover the membrane. The membrane was incubated with the primary antibodies for 1 hour at room temperature or overnight at 4°C. After that the membrane was rinsed once in 1 x PBS and washed three times for 10 minutes in 1 x PBS/ 0.2 % Tween20 (v/v). Horseradish peroxidase (HRP) labelled secondary antibodies were diluted 1:50.000 in blocking solution. Depending on the detection Kit used the membrane was incubated for either 2 hours or 30 minutes with the secondary antibodies at room temperature. When ECL Plus was used as detection reagent the membrane was incubated for 2 hours with the secondary antibodies and washes afterwards three times for 10 minutes with 1 x PBS/ 0.2 % Tween20 (v/v). When the more sensitive ECL Prime was used for detection the secondary antibody was only incubated for 30 minutes and it was washed six times for 5 minutes. HRP conjugated secondary antibodies were detected with the Amersham ECL kits and visualized by exposing the western blots to X-ray films.

3 Biogenesis of the Inner Membrane Complex

3.1 Introduction

The apicomplexan parasite *Toxoplasma gondii* belongs to a group of protists referred to as the Alveolata. These protists contain membranous sacs (alveoli) beyond the plasma membrane, termed the Inner Membrane Complex (IMC) in the case of *T. gondii*. Interestingly, apicomplexan parasites replicate within the host cell via a unique mechanism, best described as internal budding. In the event of *T. gondii* two daughter parasites are formed within the mother cell in a process called endodyogeny. Apicomplexan parasites invade their host cell through an active process that depends on gliding motility. The motor for gliding motility, referred to as the MyoA motor complex, is anchored to the IMC of the parasite and is assembled in a stepwise process. While early components of the MyoA motor complex, such as the Gliding Associated Proteins 40 and 50 (GAP40, GAP50), are probably transported to the IMC during its biogenesis, late components MyoA, GAP45 and MLC1, are assembled during cytokinesis of daughter parasites. It is generally believed that components of this complex are not directly involved in parasite replication, as conditional mutants for MyoA or GAP45 do not show any defect in intracellular parasite growth (Meissner *et al*. 2002, Frenal *et al*. 2010). However, overexpression of the tail of MyoA in *T. gondii* leads to a severe block in host cell invasion and intracellular replication of the parasite. This block can be attributed to a defect in IMC maturation, similar to the phenotypes observed in mutants of Rab11-GTPases (Agop-Nersesian *et al*. 2009, Agop-Nersesian *et al*. 2010), indicating a possible role for myosin motors in the Rab11-dependent vesicular transport to the IMC and plasma membrane. Given the shown association of *P. falciparum* with MTIP (Myosin A tail domain interacting protein; TgMLC1 homologue) it was suggested that MLC1/MTIP interacts with an unconventional myosin to provide motile force for vesicle delivery to the IMC. Hence overexpression of the MyoA-tail domain might lead to a competition between the tail domain and endogenous myosins (MyoA and/or other myosins) for formation of functional motor complexes requiring MLC1 or other proteins interacting with MyoA (Agop-Nersesian *et al*. 2009). Therefore it will be analysed in the following chapters if the IMC defect occurs due to overexpression of a mutated version of MyoA or depletion of one of the interaction partners.

3.2 Verification of Myosin A tail overexpressing parasites

Overexpression of the Myosin A tail results in a dominant negative phenotype with a severe defect in the formation of the Inner IMC (Figure 3-1) (Agop-Nersesian *et al*. 2009). The ddFKBP system was used to generate this mutant. This system allows the rapid regulation of protein stabilisation by adding the ligand, Shield-1 (Herm-Gotz *et al*. 2007). Moreover, the overexpression of MyoA-tail has a dual phenotype. While expression in extracellular parasites results in a significant reduction in invasion, expression in intracellular parasites causes a severe block in replication (Agop-Nersesian *et al*. 2009). The MyoA-tail was overexpressed in an attempt to compete with endogenous myosins (MyoA and possibly other myosins) for the formation of functional motor complexes, which require MLC1. It is hypothesised that overexpression may result in deregulation of myosin function, similar to reports for yeast myosin V (Reck-Peterson *et al*. 1999). Former studies have shown that both a conditional knockdown (KD) and a conditional knockout (KO) of Myosin A in parasites demonstrates critical functions for this protein in gliding motility, egress and invasion of the host cells; however, intracellular replication of the parasites is unaffected (Meissner *et al*. 2002, Andenmatten *et al*. 2013). This result implies that overexpression of the tail domain does not result in a MyoA KO phenotype, but rather influences the function of one of the interacting partners of this domain. Therefore, one of the aims of this study was to identify the molecular mechanism(s) that cause this impressive phenotype.

As a first approach, the phenotype after overexpression of the tail domain of MyoA as described by Agop-Nersesian *et al*. (2009) was confirmed. The ddFKBPmycMyoA-tail expressing parasites were inoculated onto HFF cells growing on cover slips for 24 hours in the presence and absence of 1 µM Shield-1. Then, parasites were fixed with 4 % PFA and immunofluorescence analysis (IFA) performed to stain for the IMC (α-IMC1), expression of MyoA-tail (α-myc) and the nuclei of the parasites (DAPI). In the absence of the ligand a weak background expression of MyoA-tail could be detected mainly at the apical and basal poles of the parasites, indicating incomplete degradation of the protein (Figure 3-1). However, in the presence of Shield-1 the expression level of MyoA-tail was significantly higher compared to non-induced parasites due to the stabilisation of the protein thus leading to a strong overexpression of the MyoA-tail. This

overexpression results in and confirms the previously reported defect in IMC biogenesis (Agop-Nersesian *et al.* 2009). Other studies using the ddFKBP system showed that treatment with Shield-1 generally has no impact on IMC morphology (van Dooren *et al.* 2009, Kremer *et al.* 2013). Interestingly, while the IMC itself showed a completely deformed morphology, IMC formation still appeared to initiate during endodyogeny since daughter buds were observed (Figure 3-1; white arrows).

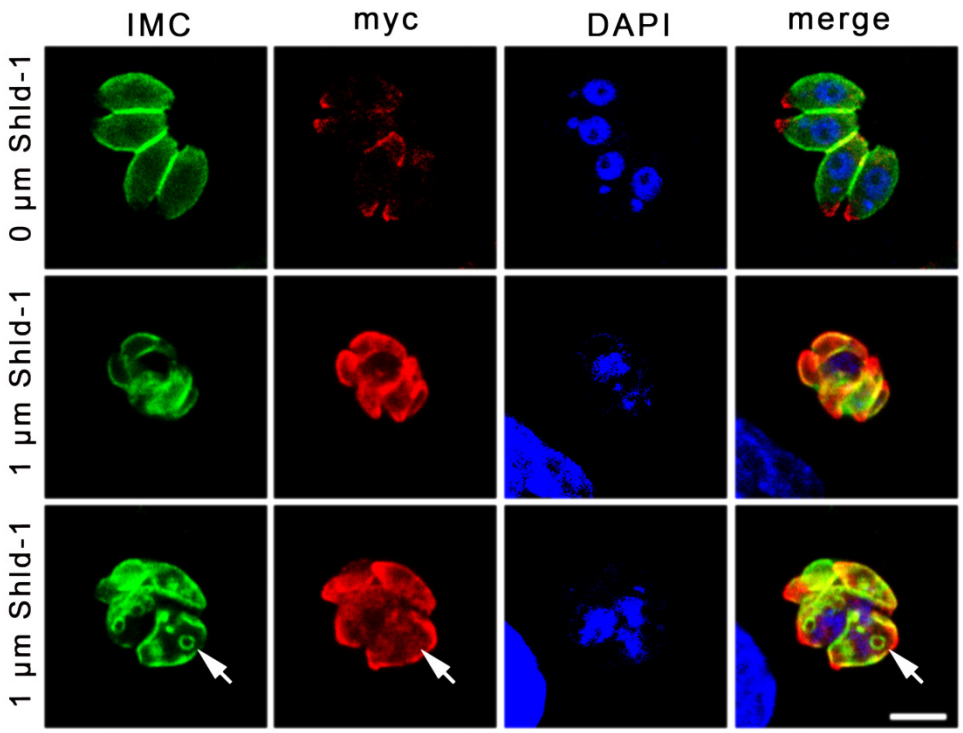

Figure 3-1: Localisation and phenotype of MyoA-tail over-expressing parasites. The upper panel shows the background expression of MyoA-tail (myc) if the ligand is not added. The middle and lower panel show the expression of MyoA-tail after addition of Shield-1. Myo-A co-localises with the IMC and a clear effect on IMC formation can be observed. The IMC of daughter parasites was formed, but the parasites were not able to mature (see arrows). Scale bar represents 5 µm.

Standard transfection of DNA in the RH strain of *T. gondii* results in random integration of the DNA into the genome. Depending on the locus, the expression level of the inserted DNA varies. In case of ddFKBPmycMyoA-tail the severity of the phenotype increased with the expression level as seen in transient transfections where the MyoA-tail DNA integrated into different loci or multiple integrations occurred (Prof Markus Meissner, personal communication; my own observation). Since the ddFKBP system allows a regulation of different expression levels by simply changing the protein stability through different doses of the inducer Shield-1, a concentration course (0-1 µM Shield-1) was used to examine the dependency of protein expression and phenotype severity (Figure 3-2). First, the ability of the parasites to grow in media supplemented with and

without Shield-1 was evaluated. Hence 200 parasites for each condition were inoculated on HFF cells, cultured for seven days prior to fixation with minus 20°C methanol and stained with Giemsa. As anticipated no growth defect was observed for wild-type parasites or the non-induced mutant line. While for 0.1 and 0.25 µM Shield-1 a few very small plaques were observed, no plaque formation was achieved with concentrations higher than that, emphasizing the lethality of this mutant (Figure 3-2A). Second, the protein amount was examined by immunoblot. Therefore, wild-type parasites (RHΔ*hxgprt*) and the MyoA-tail mutant were exposed to varying concentrations of Shield-1 for 24 hours prior generating parasite lysates. Aldolase antibody served as a loading control whereas α-myc was used to detect MyoA-tail. As expected, no protein could be detected in wild-type parasites (RHΔhxgprt) using the myc antibody (Figure 3-2B; left-hand panel), but an obvious band for the non-induced MyoA-tail strain was observed with the myc antibody indicating insufficient degradation of the protein in absence of the ligand (Figure 3-2B; right-hand panel). More striking was that as little as 0.1 µM Shield-1 was sufficient enough to stabilise the maximal quantity of protein since higher amounts of protein could not be detected with higher concentrations of ligand. Expression of transgenic, full-length MyoA results in notable downregulation of endogenous MyoA (Hettmann *et al*. 2000, Herm-Gotz *et al*. 2007). To evaluate if overexpression of MyoA-tail is enough to cause this effect, the western blot was additionally probed with a MyoA antibody. Unlike full-length MyoA, overexpression of the tail domain alone did not result in a significant post-translational downregulation (Figure 3-2B). A well-known interaction partner of MyoA is its light chain, MLC1, that is thought to be important for stabilising the motor complex (Herm-Gotz *et al*. 2002). Thus the influence of the highly expressed, non-functional MyoA-tail on MLC1 protein levels was investigated next. Against expectation no direct connection between MyoA-tail expression and the protein amount of MLC1 could be observed (Figure 3-2B). After noticing that as low as 0.01 µM Shield-1 is enough to lead to a significant stabilisation of MyoA-tail protein, the impact of different Shield-1 concentrations on IMC biogenesis was analysed by IFA using an IMC1 antibody. Although a concentration of 0.01 µM Shield-1 was sufficient to stabilise the protein, this amount was not enough to cause a severe IMC defect (Figure 3-2C); concentrations of 0.1 µM and higher were required to affect the biogenesis of

the IMC. Despite reaching protein stability with 0.1 µM of Shield-1, the impact on the IMC became more severe with increasing concentrations of Shield-1.

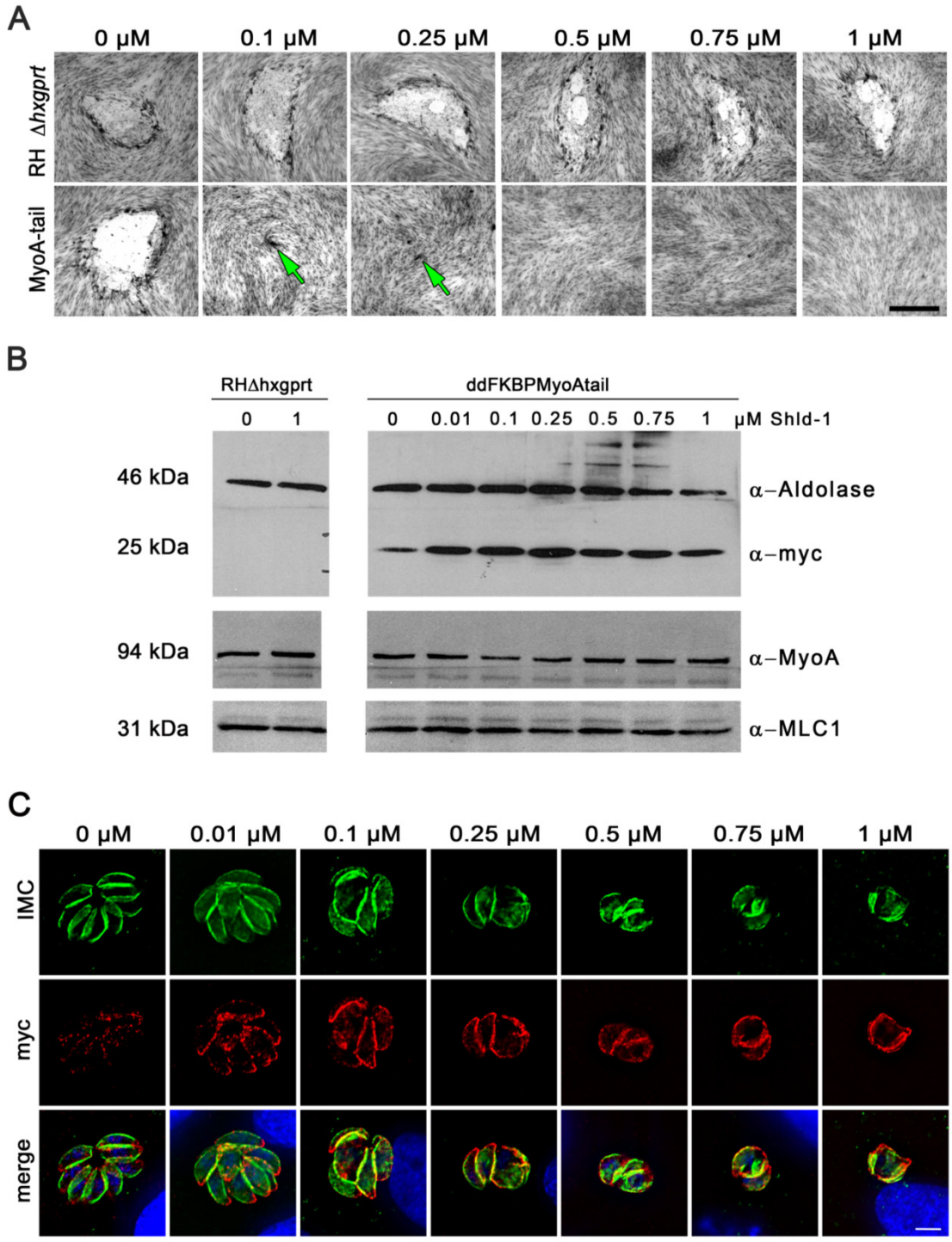

Figure 3-2: Correlation of MyoA-tail expression level with severity of the IMC defect. A) Growth assays of parasites expressing MyoA-tail. 0.25 µM Shield-1 is sufficient to cause a block in intracellular parasite growth. Scale bar represents 500 µm. B) Western blot analysis to verify protein level after induction with different Shield-1 concentrations for 24 h. Aldolase was used as a loading control, whereas the protein of interest, MyoA-tail, was detected by a myc antibody. Surprisingly, a quite high amount of mycMyoA-tail can be detected in the absence of the ligand Shield-1. Complete protein stability was reached with 0.1 µM of Shield. No significant down-regulation of either MyoA or MLC1 was observed. C) IFA of MyoA-tail expressing parasites induced with increasing concentrations of Shield-1. A clear effect on IMC formation was observed using Shield-1 concentrations of 0.1 µM and higher. Scale bar represents 5 µm.

3.3 Specificity of the IMC defect

In *T. gondii*, cell division includes a number of consecutive, highly coordinated processes where DNA replication and nuclear division precedes cytokinesis. Furthermore, the processes of daughter cell budding and nuclear division are not coupled to each other (Shaw *et al*. 2001, Morrissette and Sibley 2002, Gubbels *et al*. 2008). Overexpression of the tail domain of MyoA caused, in addition to the IMC defect, an impact on karyokinesis and/or DNA segregation (Figure 3-1; Figure 3-3). Because of the misshapen appearance of the parasites, this observed effect might be of a secondary nature. During replication some organelles are duplicated and divided between the forming daughter cells, while others are formed *de novo* (Nishi *et al*. 2008). Due to these characteristics the specificity of the MyoA-tail overexpressor on IMC biogenesis was analysed in great detail by examining both secretory organelles built *de novo* and organelles duplicated in the division process (Figure 3-3). As anticipated, the non-induced strain showed no effect on any organelle, thus proving that the observed background expression of MyoA-tail is not sufficient to cause a phenotype. Note that wild-type parasites treated with Shield-1 show no effect on micronemes, rhoptries, dense granules, endosome like compartment, Golgi apparatus, mitochondrion or the apicoplast (Kremer *et al*. 2013). Next, the effect of MyoA-tail overexpressing parasites on *de novo* synthesis of the secretory organelles, rhoptries (ROP5), micronemes (MIC3) and dense granules (GRA9) was investigated. Results indicate that organelle segregation and biogenesis are not affected as the number of organelles detected represents more than one parasite. Nevertheless, the specific localisation of these organelles at the apical pole appeared to be lost. This observation might be explained due to the deformed shape of the parasites and the loss of polarity after overexpression of MyoA-tail. Hereafter the influence of MyoA-tail on duplication of several organelles during endodyogeny was determined. To begin with, parasites stained against proM2AP, a marker for endosomal like compartments (ELC) (Harper *et al*. 2006), showed no defect on this special compartment. Markers for the apicoplast (FNR-RFP) (van Dooren *et al*. 2009), mitochondrion (HSP60-RFP) (van Dooren *et al*. 2009) and Golgi apparatus (GRASP-RFP) (Pfluger *et al*. 2005) were stably transfected into non-induced ddFKBPMyoA-tail parasites for analysis. In MyoA-tail overexpressing parasites, the apicoplast and Golgi are still duplicated, although it is impossible

to say if the number of apicoplasts and Golgi stacks visualised corresponds to the number of parasites within the parasitophorous vacuole since the deformed morphology prohibits an exact prediction of the number of parasites. An effect on mitochondrion duplication/segregation cannot be excluded as the mitochondria look more fragmented in the presence of the inducer than in its absence, but again this might just be a secondary consequence because of the severe replication defect caused by MyoA-tail overexpression. In summary, these results show that overexpression of MyoA-tail indeed leads to a specific defect on IMC biogenesis.

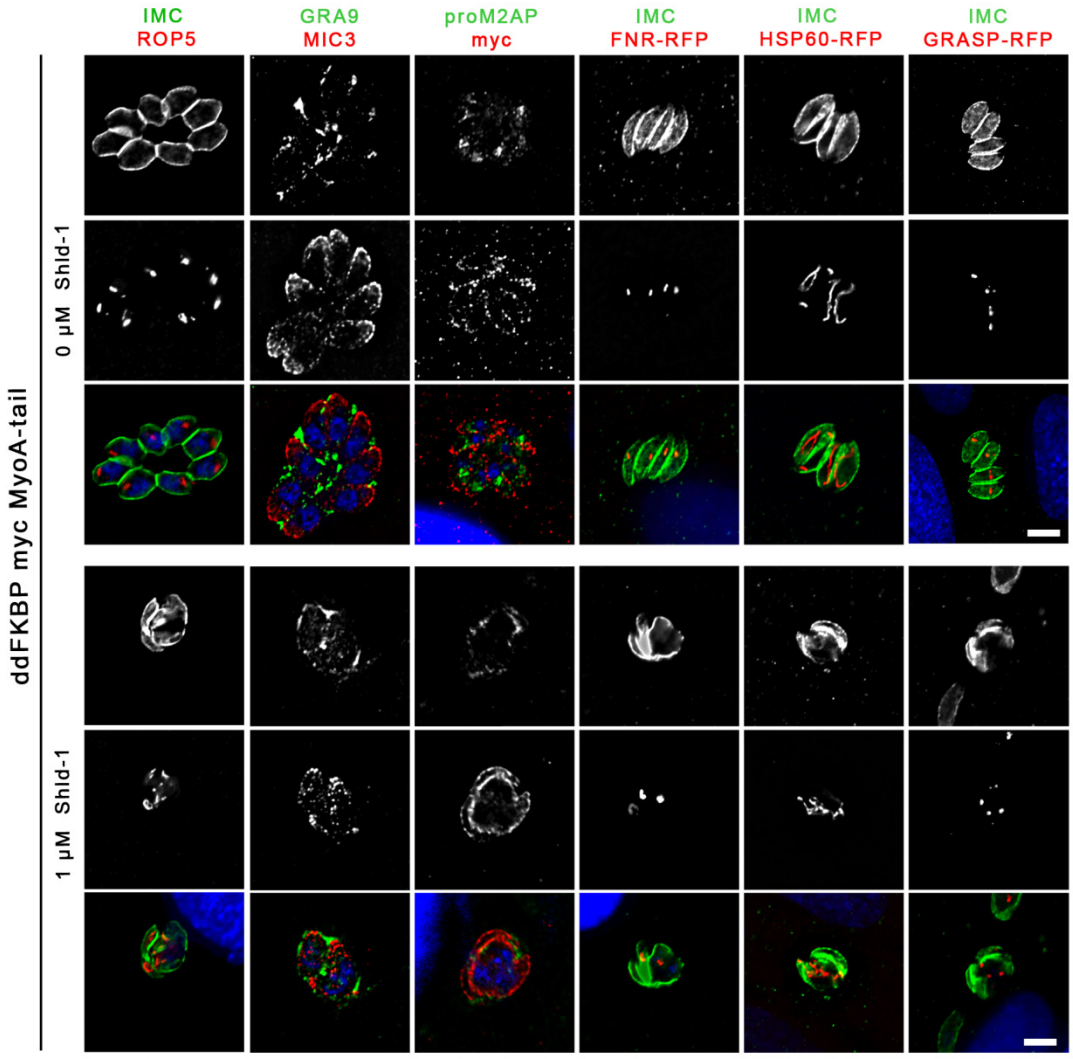

Figure 3-3: Localisation studies of different organelle markers in the MyoA-tail overexpressing parasites. The biogenesis of all secretory organelles seemed not to be affected by overexpression of the MyoA-tail. Nevertheless, they showed an unusual localisation after overexpression of the MyoA-tail. Neither rhoptries (ROP5), micronemes (MIC3) nor dense granules (GRA9) seemed to be normally located. All of them were randomly distributed when the MyoA-tail was overexpressed. No obvious effect was observed on the duplication of several organelles like the apicoplast, Golgi apparatus and mitochondrion, although the latter looked more fragmented in the MyoA mutant parasite line. Scale bars represent 10 µm.

3.4 Overexpression of MyoA-tail causes a block in IMC maturation

The phenotype obtained by overexpression of MyoA-tail, shows similarities to phenotypes observed by overexpression of Rab11A and Rab11B (Agop-Nersesian *et al*. 2009, Agop-Nersesian *et al*. 2010). Rab11B is known as one of the earliest proteins detectable during the initiation phase of daughter cell budding (Anderson-White *et al*. 2012). Components of the MyoA motor complex begin to appear during different phases of daughter bud formation. While GAP40 and GAP50 are integrated into the IMC during the early budding phase, the recruitment of MLC1 and MyoA through GAP45 happens in the late stage. So far the IMC phenotype generated by MyoA-tail overexpression had only been determined by using an antibody against IMC1, a protein that is expressed from early budding onwards. Endogenous MyoA forms a stable complex with GAP40, GAP50, GAP45 and MLC1 and is implied to be the motor driving the transport of the GAP45-MLC1-MyoA complex to the periphery of the parasite (Agop-Nersesian *et al*. 2009). Therefore, the influence of the MyoA-tail mutant on the biogenesis of the components of the MyoA motor complex should be investigated by IFA using different, stably transfected fluorescent markers or by using antibodies. As expected, all components showed the typical peripheral localisation in the absence of Shield-1. In its presence, despite having a completely deformed morphology it seemed that the early components, GAP40 and GAP50, still maintain their peripheral localisation (Figure 3-4A,C), indicating that transport of those proteins to the IMC might not be influenced by the MyoA-tail mutant.

Similarly, the late components of the MyoA motor complex (GAP45, MLC1 and MyoA) displayed no obvious change in localisation hence indicating that the assembly of the MyoA motor complex is not dependent on a functional MyoA (Figure 3-4A,B,D,E). Interestingly, co-expression of YFP-MyoA caused downregulation of MyoA-tail comparable to results described previously (Herm-Gotz *et al*. 2007) suggesting tight post-translational regulation of MyoA (Figure 3-4D). Furthermore, the consequence of the overexpression of MyoA-tail on the major surface antigen 1 (SAG1) was analysed. The localisation of SAG1 was as expected at the plasma membrane without addition of the ligand. After incubation with Shield-1, the localisation of SAG1 was still at the periphery since a complete co-localisation with YFPMyoA at the plasma membrane was observed

(Figure 3-1F). Summarising, all components of the MyoA motor complex showed equivalent defects after overexpression of MyoA-tail. Thereby, absolutely no differences between early (IMC1, GAP40, GAP50) and late components (MyoA, MLC1, GAP45) could be identified. Thus the MyoA-tail phenotype resembles more the phenotype of a dominant negative version of Rab11B than Rab11A, since Rab11A only affects the late components and SAG1 (Agop-Nersesian *et al*. 2009, Agop-Nersesian *et al*. 2010).

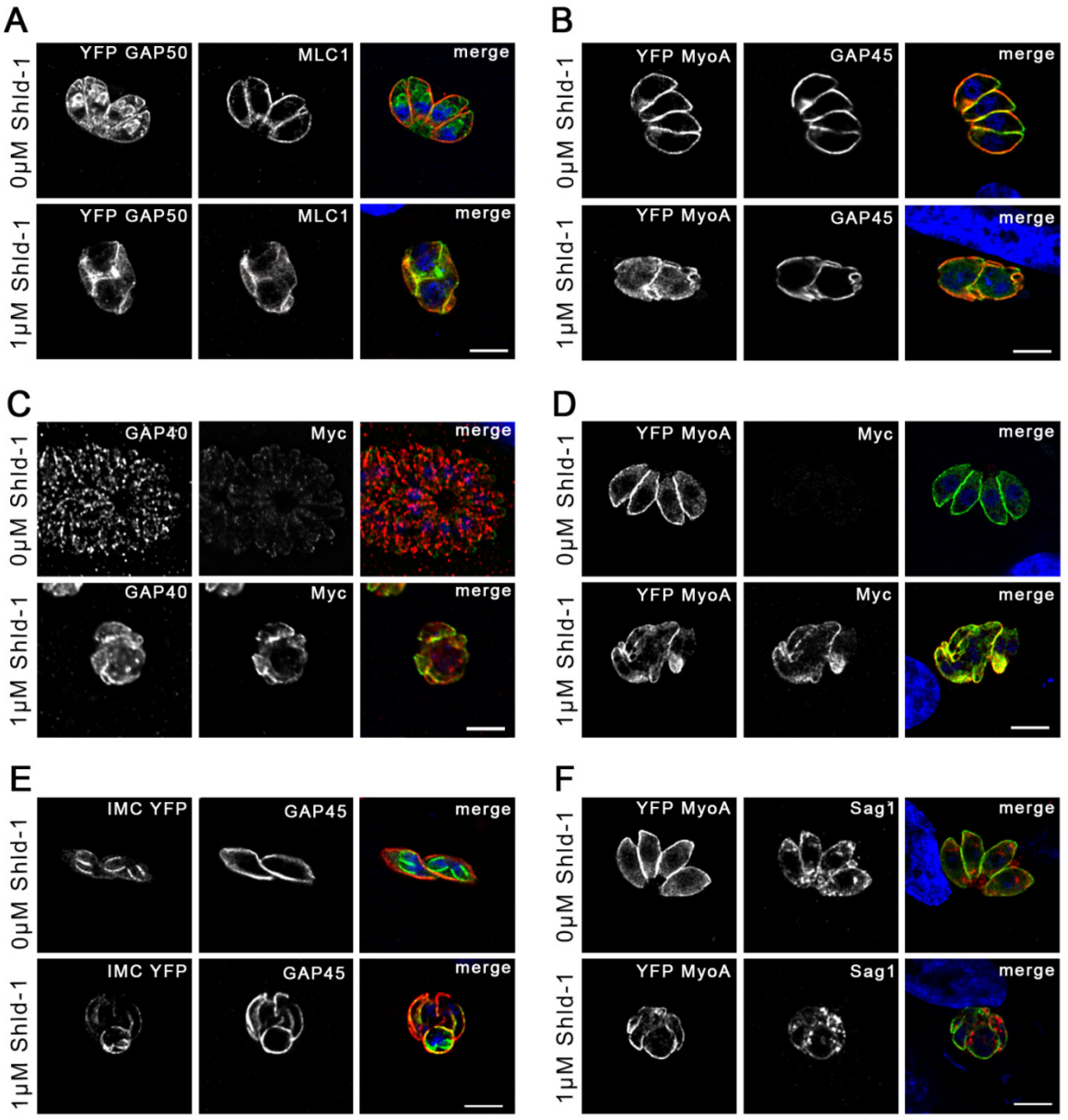

Figure 3-4: Effect of MyoA-tail overexpression on components of the MyoA motor complex. An effect on all components of the MyoA motor complex involved in IMC formation could be observed. No remarkable differences between the early (GAP50, GAP40 and IMC1; A, C, E) and late components (MLC1, GAP45 and MyoA; A-F) of IMC formation could be observed. All components showed the typical peripheral localisation although MyoA-tail overexpression leads to a severe defect on parasite morphology. Additionally, a tight posttranslational regulation of MyoA was confirmed since ddFKBPmycMyoA was downregulated when YFP MyoA was co-expressed (D). Co-localisation of MyoA and SAG1 indicates no detachment of IMC and plasma membrane (F). Scale bars represent 5 µm.

3.5 Complementation studies of Myosin A tail overexpressing parasites

The overexpression of the tail domain of MyoA results in a phenotype that is characterised by an incorrect formation of the IMC. Eleven unconventional myosin heavy chains are known in *T. gondii*, but only seven myosin light chains (Foth *et al*. 2006, Polonais *et al*. 2011), indicating that some myosins are either functional without a light chain or share the same light chain. Because of this, it should next be investigated, if the phenotype caused by overexpression of MyoA-tail occurs due to loss of function of MyoA or due to a limited dilution of one of its interacting partners. In the last scenario, it should be possible to rescue the phenotype by additionally overexpressing the respective interacting partner. There are several known interacting partners of MyoA such as MLC1, GAP45, GAP50, GAP40 and ELC1 (Gaskins *et al*. 2004, Frenal *et al*. 2010, Nebl *et al*. 2011). For complementation analysis different constructs were stable transfected in the overexpressor line. The vector P5RT70mycGFP was used as a control. The phenotype caused by overexpression of the MyoA-tail was not affected by additionally expressing GFP (green fluorescent protein), which is shown by IFA of parasites incubated with and without the ligand Shield-1. The typical phenotype of the MyoA-tail overexpressor can be observed.

To complement the phenotype with functional MyoA, MyoA-tail expressing parasites were stably transfected with the construct P5RT70TyMyoAfulllengthWT. However, it was not possible to complement the IMC defect with functional MyoA, indicating the phenotype is not due to the loss of function of MyoA itself. Furthermore, the vectors P5RT70MycGFPGAP45, P5RT70GAP50YFP, P5RT70ELC1ty and P5RT70GAP40ty were introduced into the MyoA-tail parasites to determine if the reason for the observed phenotype could be attributed to the loss of interacting partners of MyoA for endogenous components, like other myosins. The principle is depicted in Figure 3-5A. Additionally, wildtype versions of the GTPases Rab11A and Rab11B were transfected into MyoA-tail expressing parasites, since it was thought that Rab11A delivers vesicle to the plasma membrane in a MyoA dependent manner and Rab11B has a strikingly similar phenotype (Agop-Nersesian *et al*. 2009, Agop-Nersesian *et al*. 2010). None of the above mentioned constructs were able to restore the IMC defect (Figure 3-5B and data not shown). Next, the plasmid

P5RT70MLC1ty was transfected into MyoA-tail overexpression parasites. The localisation of MLC1 was as expected, in the absence of ligand. After incubation with Shield-1, MLC1 negative parasites still showed an IMC defect whereas MLC1 expressing parasites had an intact IMC and were able to replicate (Figure 3-5B). Co-expression of MLC1 in the MyoA-tail overexpressor rescued the IMC phenotype. The specificity of MLC1 was tested using another myosin light chain, MLC7, as a control. Unlike MLC1, MLC7 could not rescue the phenotype.

However, more detailed analysis of the MLC1 complementation revealed that the restoration was only partial and that after 3-4 rounds of replication the IMC defect reappeared. No parasite rosettes with more than 16 intact parasites could be found (Figure 3-5C and D). This would indicate that the phenotype is partially based on a competition of MyoA-tail and other endogenous myosins for MLC1. There are several reasons for why no full complementation could be achieved: first, the timing of expression of MLC1 could be incorrect since MLC1 is not under control of the endogenous promoter but the constitutive tubulin promoter. Second, the expression of MLC1 was too low to achieve a full rescue of the phenotype. Third the C-terminal ty tag could interfere with some of the functions of MLC1. Finally, it is possible that some additional, unknown factor might directly interact with the tail of MyoA and cause the phenotype of MyoA-tail overexpressor. Moreover, it is possible that multiple proteins are affected in the MyoA-tail mutants, and so complementation with only a single protein would not be able to rescue the phenotype.

Given that a clear conclusion could not be reached with the complementation studies, a new approach to investigate the reason for the MyoA-tail overexpression phenotype was required. Since the phenotype probably occurs due to depletion of one of the interacting partners of MyoA for other endogenous proteins, conditional knockouts of most of the components of the MyoA motor complex were generated using the recently established inducible DiCre system (Andenmatten *et al*. 2013).

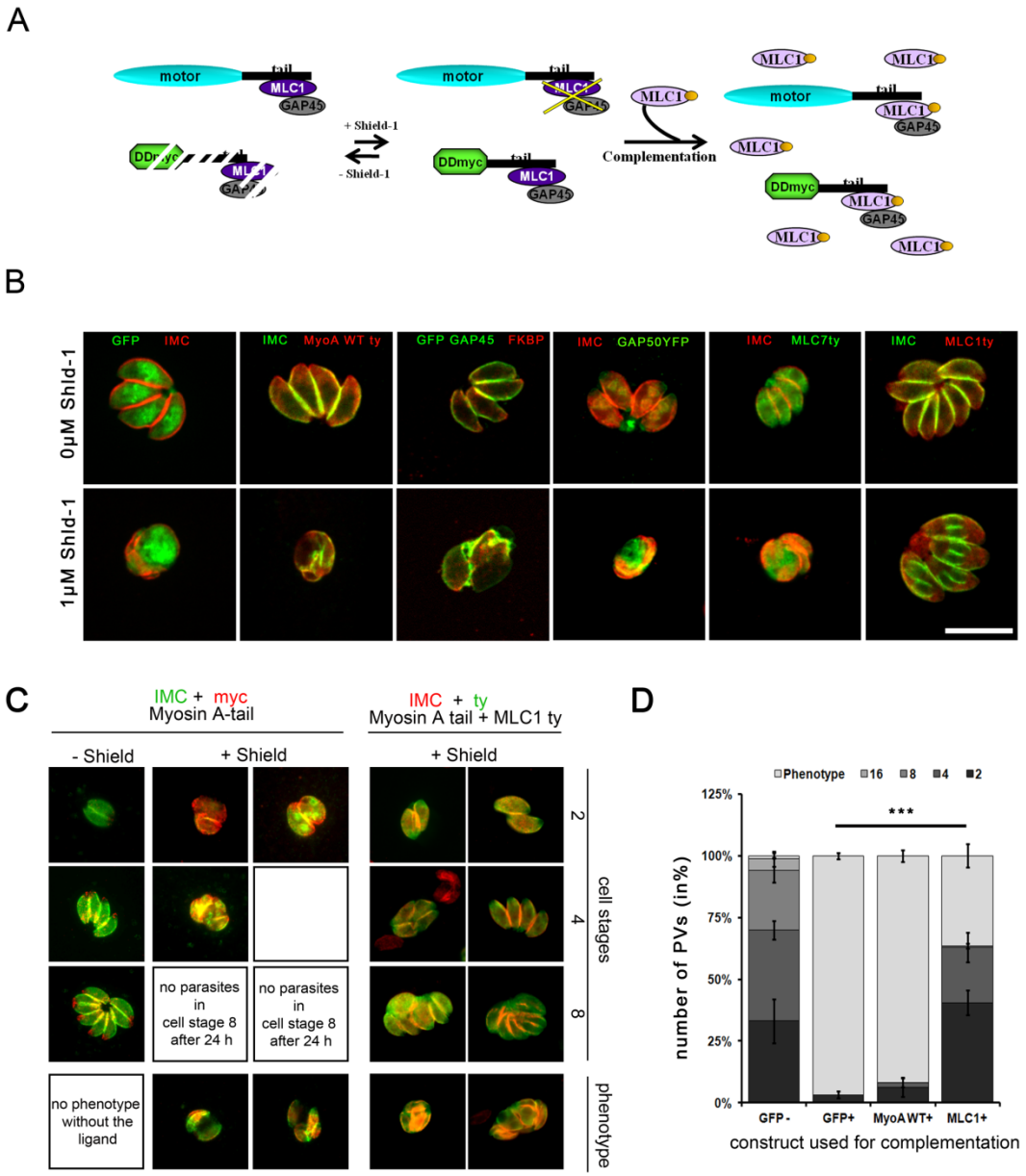

Figure 3-5: Complementation studies of the MyoA-tail overexpressor. A) Schematic illustration of the complementation strategy. B) For complementation analysis, different constructs were introduced in the MyoA-tail expressing parasites and IFAs were performed. Transfection of GFP and MLC7 in MyoA expressing parasites served as controls. As expected, no complementation could be observed; likewise, no complementation was achieved by functional, fulllength MyoA, mycGFP-GAP45 or GAP50YFP. Transfection of MLC1ty in the MyoA-tail overexpressing parasites revealed that the typical phenotype could be complemented by overexpressing MLC1. The parasites were able ato replicate and form normal daughter cell IMCs during the first rounds of endodyogeny. Scale bar represents 10 µm. C) IFA of the complemented parasites at different cell stages with various phenotypes. The parasites replicate normally in the absence of the ligand Shield-1. After adding the ligand all MyoA-tail expressing parasites show a phenotype, but some managed to get into cell stage 4. After co-expression of MLC1 most of the parasites were in cell stage 2-4, but some also in 8. However, no full complementation could be achieved, since a defect in IMC development became apparent after 3-4 rounds of replication, leading to an arrest in parasite replication. No parasite rosettes with more than 16 intact parasites could be found. Scale bar represents 10 µm. D) Quantification of the complementation study. The cell stages of 100 parasites per construct were counted (cell stage 1 was excluded). After expressing of MyoA-tail most of the parasites were arrested in cell stage 1 or showed the typical phenotype. Only parasites expressing MyoA-tail and MLC1 managed to replicate properly.

3.6 Generation of conditional knockouts of MyoA motor complex components

3.6.1 Brief description of the DiCre system

In order to determine if interacting partners of the MyoA-tail have a role during IMC biogenesis, conditional KOs of all known interacting partners were generated using the DiCre system by which the respective gene can be permanently excised in a regulated manner. This system is based on the expression of two inactive Cre fragments (Cre59 and Cre60) that are fused to the rapamycin binding proteins FKBP and FRB, respectively. Addition of rapamycin induces the dimerisation of these two fragments and thus reconstitutes functional Cre recombinase (Jullien *et al*. 2007, Andenmatten *et al*. 2013). The gene of interest (GOI) is flanked by loxP sites. The second loxP site is followed by the open reading frame (ORF) of the yellow fluorescent protein (YFP) which is only expressed if the GOI is excised (Figure 3-6). The addition of 50 nM rapamycin reconstitutes Cre recombinase activity and successful homologous recombination results in the excision and therefore depletion of the GOI. This system will be used to address the genetic and molecular basis for the MyoA-tail overexpression phenotype through the generation of conditional knockouts of the following components of the MyoA motor complex: MLC1, GAP50, GAP45 and GAP40.

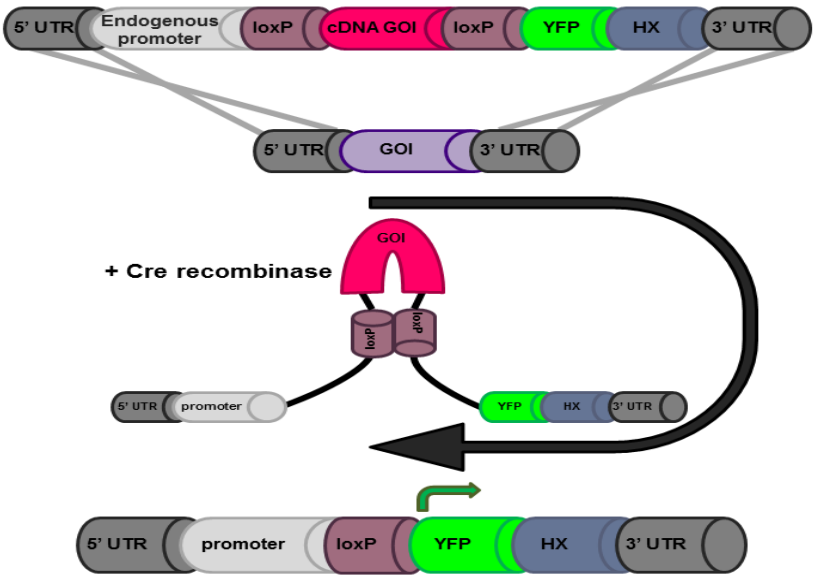

Figure 3-6: Model of the Cre recombinase inducible Knock out system. The cDNA of the gene of interest (GOI) is flanked by loxP sites. After homologous recombination at the endogenous locus of the GOI and expression of the Cre recombinase, the loxP sites recombine to excise the cDNA, which leads to a conditional knockout of the GOI.

3.6.2 Generation and verification of a conditional *mlc1* KO

One of the first discovered interacting partners of MyoA is its regulatory myosin light chain, MLC1. Although it was first detected through co-purification with MyoA over a decade ago (Herm-Gotz *et al*. 2002), a detailed characterisation of this protein has not been done. To shed more light on the functions of MLC1 in the lytic cycle of *T. gondii*, a MLC1 geneswap construct was designed containing the endogenous promoter of *mlc1*, floxed *mlc1* cDNA, *yfp* ORF, *hxgprt* as a selectable marker and 2000 bp of the 3'UTR (untranslated region) of *mlc1*. After transfection into the recipient strain ku80::DiCre that favours homologous recombination over random integration, the endogenous *mlc1* gene is replaced with corresponding fragments of the *mlc1* geneswap plasmid via homologous recombination. Correct integration was confirmed by analytical PCR using three distinct sets of primer pairs (Figure 3-7A). The first primer pair distinguishes between the intact, endogenous *mlc1* and *mlc1* cDNA by annealing to the start sequence of *mlc1* and a sequence within the second exon of *mlc1,* thus generating either 1022 bp (intact, endogenous locus containing introns) or 553 bp (cDNA) fragment sizes. The second primer set consists of a sense oligo that anneals to the *hxgprt* selection cassette and an antisense oligo annealing downstream of the oligo used for cloning the vector, and hence has no homology to the plasmid. As a result, a band of approximately 3400 bp is generated with the conditional loxPMLC1 strain whereas no PCR product is observed with the wildtype strain (ku80::DiCre). No excision occurs in the absence of rapamycin in the conditional *mlc1* KO. These non-induced parasites are termed loxPMLC1 to distinguish between the induced parasites. Upon activation of Cre recombinase, excision of the floxed *mlc1* cDNA was observed in roughly 38% of the population based on YFP expression. This mixed population of non-excised and excised parasites is termed *mlc1* KO throughout this work and was used to confirm the correct integration at the 5'UTR and site-specific recombination after induction with rapamycin. The third primer set anneals upstream of the 5'UTR that was cloned into the geneswap vector, and to the *yfp* ORF. Therefore, ku80::DiCre parasites did not produce a PCR product but the loxPMLC1 parasites yielded a specific 3400 bp fragment. The *mlc1* KO population displayed both the 3400 bp fragment (non-induced) as well as a 2600 bp fragment indicative of site-specific recombination (Figure 3-7A). Expression of MLC1 was analysed by IFA using parasites that had been induced for 4 hour extracellularly with 50 nM rapamycin,

followed by inoculation on HFF cells grown on coverslips and fixed with 4 % PFA 72 hours post-induction. Staining with an antibody against MLC1 revealed that indeed no MLC1 protein could be visualised by IFA (Figure 3-7B). Together, these data show that it was feasible to generate a conditional KO for MLC1 upon treatment of the loxPMLC1 parasites with rapamycin. Although the excision rate was lower than 50%, identification of the KO parasites is straightforward because of their YFP expression.

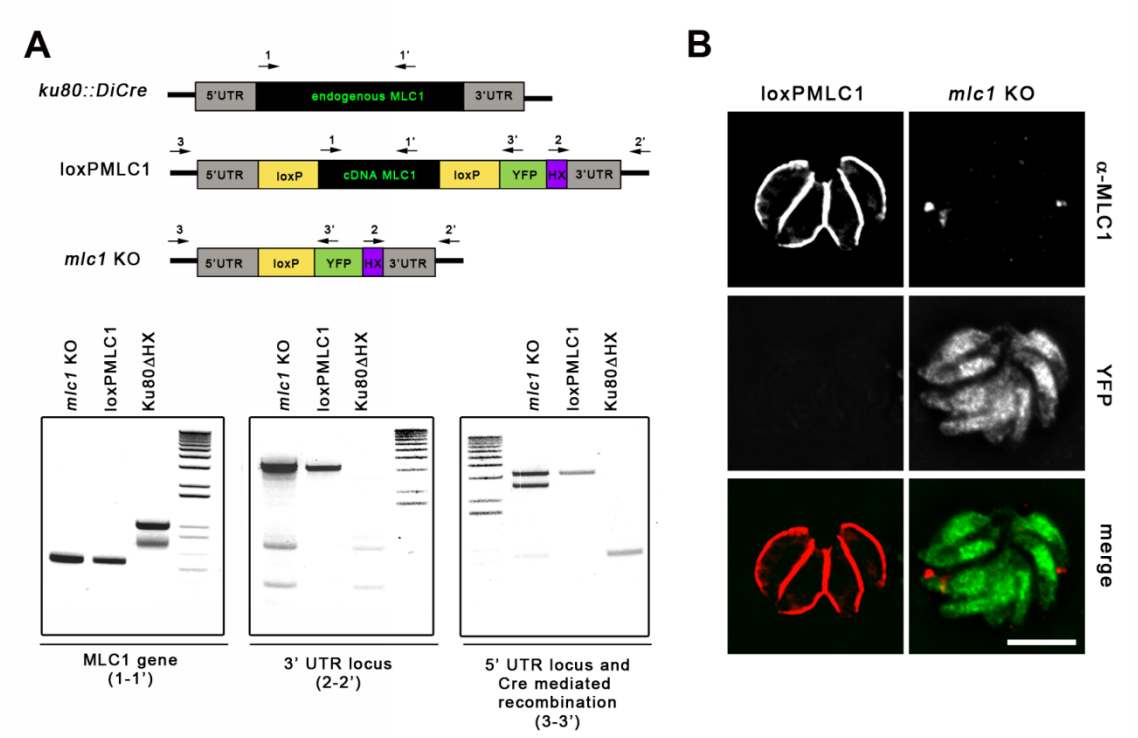

Figure 3-7: Creation of a conditional KO for MLC1. A) Schematic model of analytical PCR to verify correct replacement of the endogenous *mlc1* with the KO construct. Three different primer combinations were used. The replacement of gDNA with cDNA can be seen with primers 1+1'. The oligo pair 2+2' demonstrates that the construct has recombined properly at the 3' UTR. Primer combination 3+3' shows correct integration has occurred at the 5' UTR of the GOI and that the cDNA has been excised after expression of Cre. B) IFA of conditional *mlc1* KO parasites showing regulation of Cre recombinase-mediated excision and thus depletion of MLC1. The parasites were treated with 50 nM rapamycin for 4 h and fixed 96 h post-induction. α-MLC1 was used to show the absence of MLC1 in the *mlc1* KO. Scale bar represents 10 µm.

3.6.3 Generation and verification of a conditional *gap45* KO

Another well-known component of the MyoA motor complex is gliding associated protein 45 (GAP45). Unlike MLC1, GAP45 has been studied in more detail using the tetracycline inducible knockdown system (Frenal *et al.* 2010). While depletion of GAP45 demonstrated important functions of this protein in gliding motility, invasion and egress, no effect on replication was observed. Nonetheless, a conditional knockout of *gap45* using the DiCre system was

generated since the Tet-transactivator system can be subject to leakiness and a minimal amount of GAP45 might be sufficient for daughter cell formation. A GAP45 geneswap construct was built with the endogenous promoter of *gap45*, floxed *gap45* cDNA, *yfp* ORF, *hxgprt* as a selectable marker and 2000 bp of the 3'UTR of *gap45*. This construct was transfected into the recipient strain DiCre Δ*ku80*. Due to the lack of *ku80*, this strain favours homologous recombination over random integration. After endogenous *gap45* was replaced by the *gap45* geneswap vector, analytical PCR was performed to confirm correct integration using two sets of primers analogous to the approach used for *mlc1* in chapter 3.6.2 (Figure 3-8Figure 3-8A). Similarly, the non-induced strain is referred to as loxPGAP45 whereas the induced strain is called *gap45* KO. Since *gap45* has no introns no differentiation between genomic DNA and complementary DNA could be made. Specific integration into the 3'UTR was analysed using the primer pair 2+2'. As expected, no PCR product was amplified for the recipient strain whereas the conditional *gap45* KO revealed a band of ~3300 bp. Induction with rapamycin resulted in a mixed population of non-excised (5%) and excised parasites (95%). This excision rate is considerably higher than the one observed for the *mlc1* KO, but can be explained due to the use of a different recipient strain when generating the conditional KO line. The two recipient strains differ in their level of the Cre recombinase expression, with DiCre Δ*ku80* displaying a much higher level than that of *ku80*::DiCre (Pieperhoff et al. 2014; unpublished). Analytical PCR was performed to show correct integration had occurred at the 5' UTR and to show DiCre-mediated recombination using primer set 3+3'. LoxPGAP45 showed a specific PCR product of ~3300 bp to reflect integration at the 5' UTR, whereas the *gap45* KO showed a smaller band of 2500 bp reflecting successful excision. The expression level of *gap45* KO parasites was assessed by Western blot 72 hours post-induction with 50 nM rapamycin, using antibodies against GAP45 and GFP. RHΔHX and loxPGAP45 parasites served as controls and α-catalase served as an internal loading control. As expected, YFP protein could only be detected in the *gap45* KO parasites, where excision of *gap45* brings *yfp* under the control of the *gap45* promoter. Strikingly, almost complete depletion of GAP45 was observed 72 hours post-induction with only a very faint band detectable, most likely corresponding to the 5% of the *gap45* KO parasite population that did not undergo gene excision (Figure 3-8B). IFA was also performed after Cre-mediated recombination. Parasites were incubated in the

presence and absence of the inducer for 4 hours, and subsequently inoculated on host cells grown on coverslips. After fixation, 72 hours later, IFA was performed by staining with α-GAP45. While loxPGAP45 showed normal localisation of GAP45 and no YFP expression, *gap45* KO parasites exhibited no detectable signal for GAP45, but had strong YFP expression (Figure 3-8C). In summary, it was possible to generate a conditional *gap45* KO line that was tightly controlled by rapamycin, and KO parasites could be easily distinguished from the non-excised population due to the strong expression of YFP.

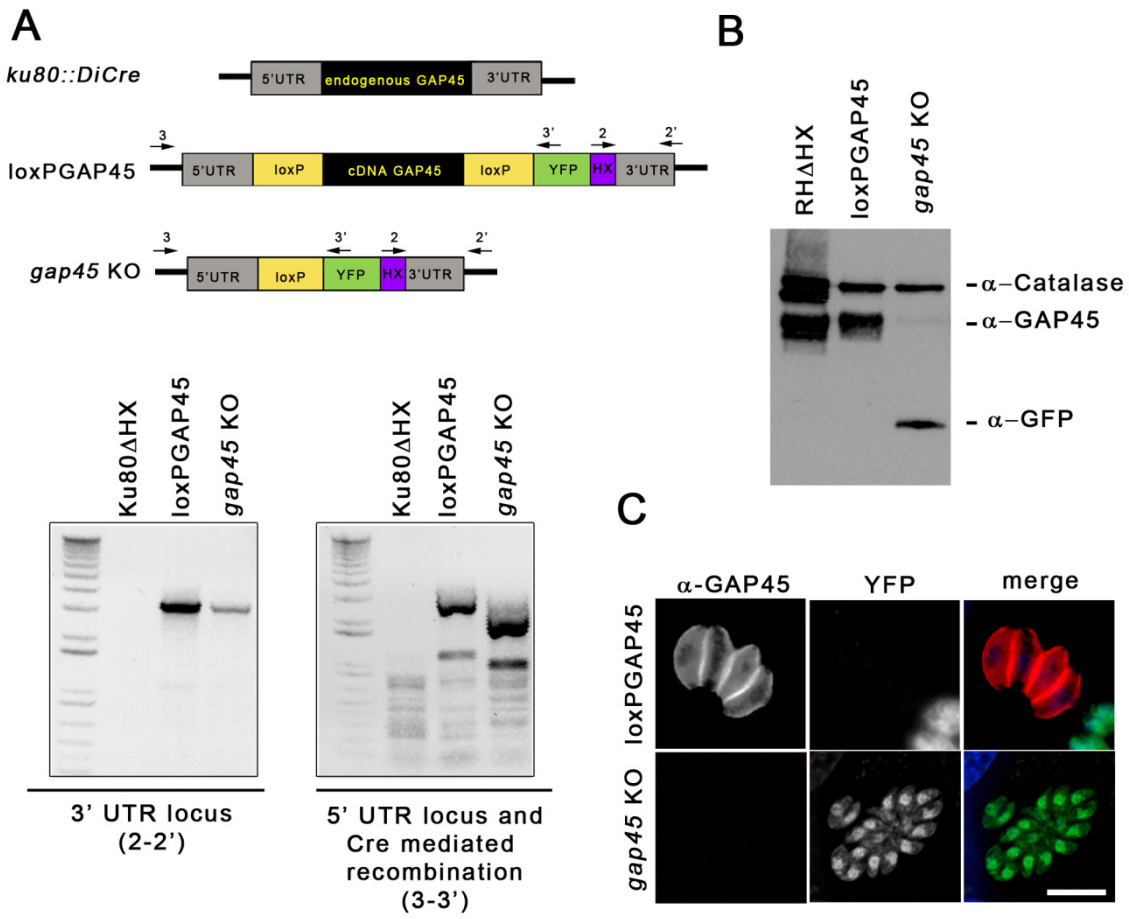

Figure 3-8: Establishment of a conditional KO for GAP45. A) Schematic model of analytical PCR to verify correct replacement of the endogenous *gap45* with the KO construct. Two different primer combinations were used. The oligo pair 2+2' demonstrates that the construct has recombined properly at the 3' UTR. Primer combination 3+3' shows correct integration has occurred at the 5' UTR of the GOI and that the cDNA has been excised after expression of Cre. B) Immunoblot analysis of GAP45 72 h after excision. Antibodies against GAP45 and GFP were used to confirm the absence of GAP45 and examine the expression of YFP. α-Catalase was used as a loading control. C) IFA of conditional *gap45* KO parasites showing regulation of Cre recombinase-mediated excision and thus depletion of GAP45. The parasites were treated with 50 nM rapamycin for 4 h and fixed 72 h post-induction. α-GAP45 was used to show the absence of GAP45 in the *gap45* KO. Scale bar represents 10 µm.

3.6.4 Generation and verification of a conditional *gap40* KO

Gliding associated protein 40 (GAP40) was recently identified as a component of the MyoA motor complex. This protein localises to the IMC and has nine transmembrane domains (Frenal *et al.* 2010), but its precise function is unknown. To generate a conditional *gap40* KO, a geneswap construct was designed comprising the endogenous promoter of *gap40*, floxed *gap40* cDNA, *yfp* ORF, *hxgprt* as a selectable marker and 2000 bp of the 3'UTR of *gap40*. After transfection into the recipient strain DiCre Δ*ku80*, analytical PCR was performed to confirm replacement of endogenous *gap40* with the *gap40* geneswap cassette. The excision rate was comparable with loxPGAP45 at 95%, and as before, the non-induced and induced parasites are referred to as loxPGAP40 and *gap40* KO, respectively. Correct replacement of genomic DNA with complementary DNA was confirmed by analytical PCR (1306 bp *vs.* 1188 bp). The *gap40* geneswap vector integrated at the 3' UTR based on the presence of a 3 kb sized fragment in the conditional *gap40* KO line and the absence of this fragment in the recipient strains. Correct integration at the 5' UTR was shown by the lack of a PCR product in the recipient strain and a specific product of 3.5 kb in loxPGAP40. A band of 2.3 kb in the *gap40* KO parasites indicated efficient excision had taken place (Figure 3-9A). The expression level of GAP40 was evaluated by Western blot, where loxPGAP40 parasites were induced with and without 50 nM rapamycin for 4 hours and parasite lysates were generated 40 hours post-induction. Note that the western blot samples were heated to 50°C for 10 minutes and not boiled at 95°C, since this led to the degradation of transmembrane proteins. Cross reactivity of the GAP40 antibody with the YFP antibody was observed, and so the same sample was loaded onto two different gels to ensure accurate and specific staining with these antibodies; the catalase antibody was used as a loading control. As expected, GAP40 was barely detectable in the *gap40* KO parasites and YFP was expressed (Figure 3-9B). Parasites were also incubated in the presence and absence of 50 nM rapamycin for 4 hours and subsequently inoculated on host cells, fixed after 40 hours and processed for IFA to further assess GAP40 and YFP levels after Cre-mediated excision. The loxPGAP40 parasites displayed typical localisation of GAP40 and no YFP expression, while *gap40* KO parasites lacked GAP40 expression but had a strong YFP signal. In summary, it was feasible to generate a conditional *gap40*

KO line that had a high excision rate and was strongly regulated upon rapamycin treatment.

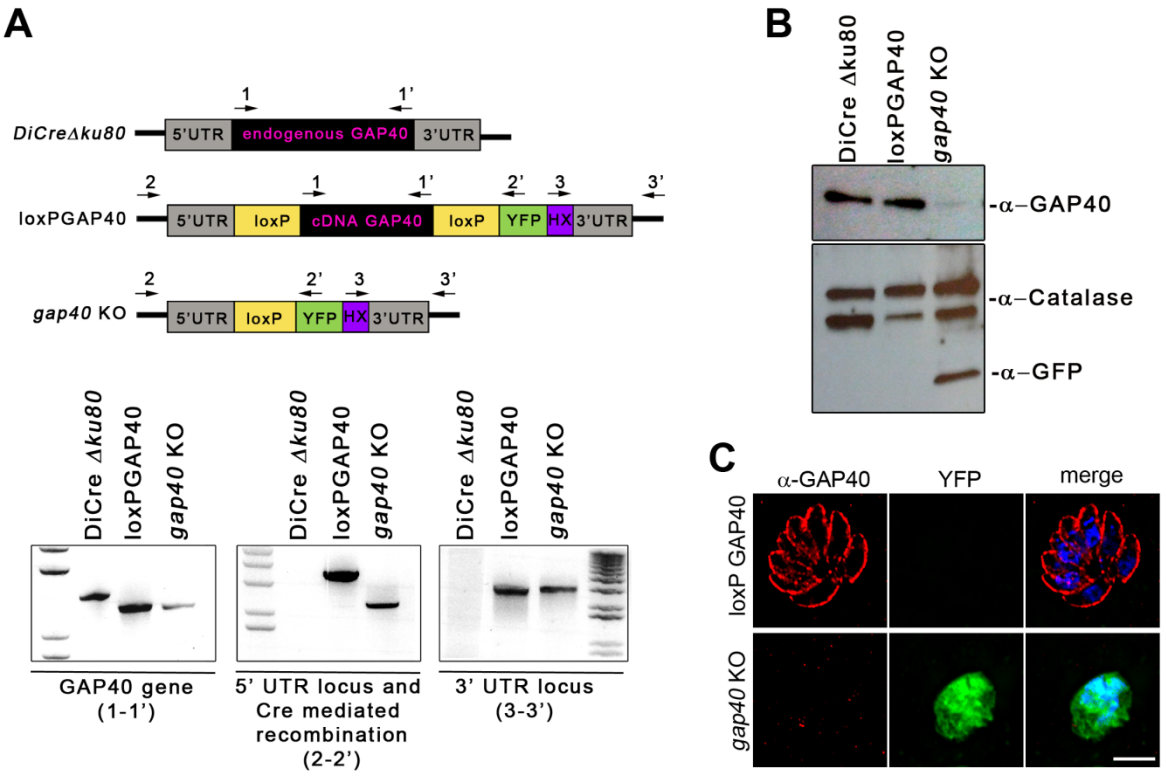

Figure 3-9: Generation of a conditional KO for GAP40. A) Schematic model of analytical PCR to confirm correct replacement of the endogenous *gap40* with the *gap40* geneswap construct. Three different primer sets were used. The replacement of gDNA through cDNA was demonstrated using primer combination 1+1'. Primer combination 2+2' demonstrates that correct integration at the 5' UTR of the GOI has occurred and that the cDNA has been excised after expression of Cre. The primer combination 3+3' shows that the construct has recombined properly at the 3' UTR. B) Immunoblot analysis of GAP40 40 h after recombination. Antibodies against GAP40 and GFP were used to confirm the absence of GAP40 and examine the expression of YFP. The antibody α-catalase was used as a loading control. C) IFA of conditional *gap40* KO parasites to show regulation of Cre recombinase-mediated recombination and thus depletion of GAP40. The parasites were treated with 50 nM rapamycin for 4 h and fixed 40 h post-induction. The antibody α-GAP40 was used to demonstrate the absence of GAP40 in the *gap40* KO. Scale bar represents 5 µm

3.6.5 Generation and verification of a conditional *gap50* KO

The gliding associated protein 50 (GAP50) was first described ten years ago as an internal membrane protein that anchors the MyoA motor complex to the IMC (Gaskins *et al*. 2004). Deglycosylation of GAP50 inhibits its association with other components of the MyoA motor complex (Fauquenoy *et al*. 2011). To analyse this protein in more detail, especially with regards to daughter cell assembly, a GAP50 geneswap vector was designed comprising of the endogenous promoter of *gap50*, floxed *gap50* cDNA, *yfp* ORF, *hxgprt* as a selectable marker and 2000 bp of the 3'UTR of *gap50*. Unfortunately, sequencing of this plasmid revealed a mutation

within the 8 bp spacer region of the first loxP site. Since mutagenesis of loxP is a common tool to change the integration/excision ratio of Cre/loxP systems and different loxP sites can recombine with each other although with lower efficiencies (Siegel *et al*. 2001, Thomson *et al*. 2003), the *gap50* geneswap vector was nevertheless transfected into the recipient strain DiCre Δ*ku80*. The non-induced and induced parasites are referred to as loxPGAP50 and *gap50* KO, respectively. Unlike the *gap45* and *gap40* KOs, the excision rate of the *gap50* KO was roughly 35% 24 hours post-induction indicating that the mutation within the loxP site indeed lowered the recombination rate (to approximately the same levels as that of the *mlc1* KO) but excision still occurred. Correct integration of the *gap50* geneswap construct at the endogenous locus was confirmed as described above. Replacement of genomic DNA with complementary DNA was confirmed (2920 bp vs. 1321 bp). Furthermore, the *gap50* geneswap plasmid was introduced correctly at the 3' UTR since a 2900 bp sized PCR product was amplified in the conditional *gap50* KO parasites whereas no fragment was observed in the recipient strain. Correct integration at the 5'UTR was shown by the lack of a PCR product in the recipient strain and a specific product of 3.8 kb in loxPGAP50. Efficient excision was demonstrated by a 2.4 kb band in the *gap50* KO parasites. Unfortunately, a Western blot could not be performed due to the low excision rate of the *gap50* KO parasites, and the lack of a suitable GAP50 antibody for IFA prevented this method of analysis of GAP50 depletion.

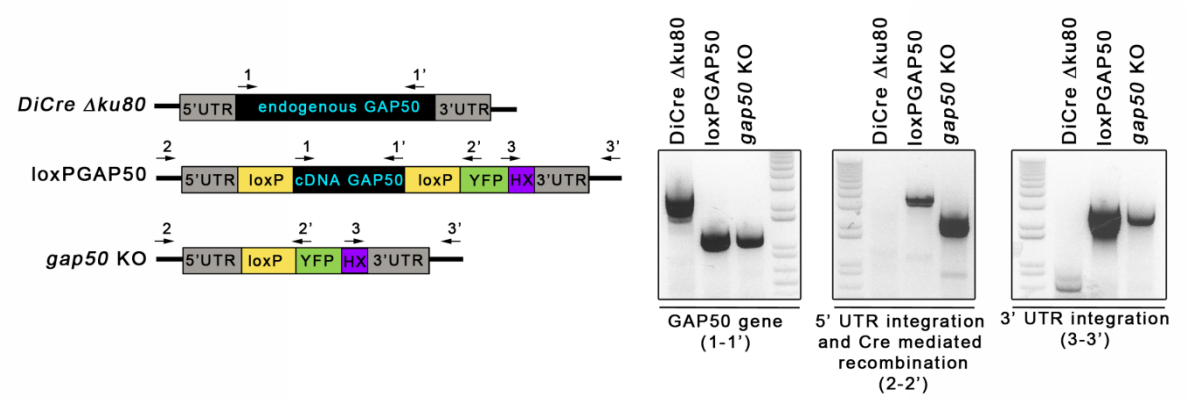

Figure 3-10: Establishment of a conditional KO for GAP50. A) Schematic model of analytical PCR to verify correct replacement of the endogenous *gap50* with the KO construct. Three different primer combinations were used. The replacement of gDNA with cDNA can be seen with primer combination 1+1'. Primer combination 2+2' shows the right integration at the 5' UTR of the endogenous *gap50* locus and as well as if the cDNA has been excised after expression of Cre. The primer pair 3+3' demonstrates that the construct has recombined properly at the 3' UTR.

3.6.6 Generation and verification of a Myosin A/B/C triple KO

So far, the preferred theory for the observed IMC biogenesis phenotype in the MyoA-tail overexpressor is that it is due to depletion of one of the interacting partners of MyoA for other endogenous components, especially other myosins. Although the myosin repertoire is still poorly characterised, two other myosins, MyoB and MyoC, have been implicated to play a role during replication (Delbac *et al*. 2001). These two myosins are encoded by alternatively spliced mRNAs and differ only in their respective C-terminal tail regions. To assess a possible role of MyoB or MyoC during daughter cell budding, a knockout construct was designed in which a bleomycin resistance cassette is flanked by the 5' and 3' UTRs of the *myob/c* gene (Figure 3-11). Since MyoA, MyoB and MyoC may share some interacting partners, redundant roles cannot be ruled out, and therefore the myob/c KO plasmid was transfected into the loxPMyoA parasites to generate an inducible MyoA/B/C KO. Correct replacement of the *myob/c* gene with the bleomycin selectable marker was confirmed by analytical PCR as indicated in the schematic. Correct integration at both the 5'and 3' UTRs was shown by specific PCR products in the loxPMyoA MyoB/C KO parasite line, whereas the wildtype control did not generate a PCR product (primer sets used: 1-1' and 2-2', respectively). Absence of the *myob/c* gene in the conditional MyoA/B/C KO was confirmed using primers binding within this gene. As expected, a specific band was amplified using this primer set only in wild-type parasites. In a brief summary, the establishment of a conditional MyoA/B/C KO was achieved.

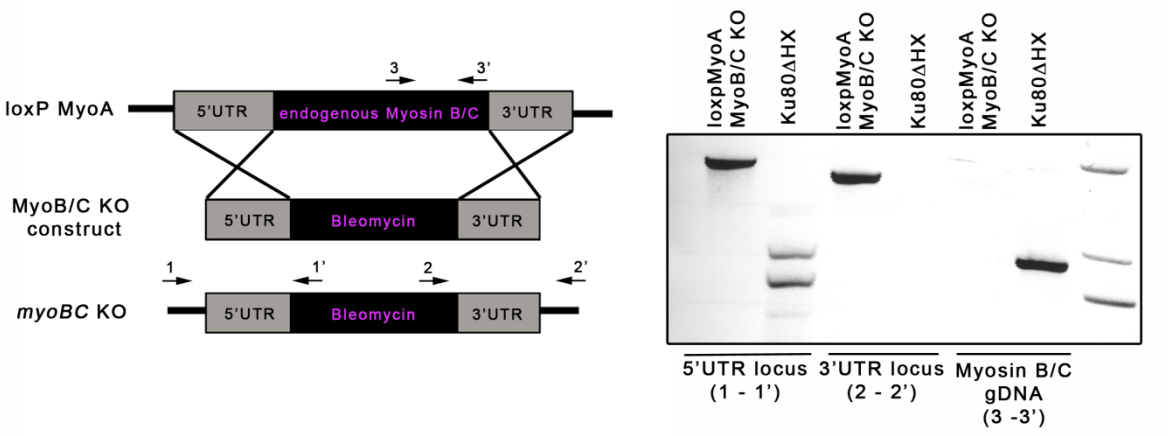

Figure 3-11: Creation of a conditional KO for MyoA/B/C. Strategy for the generation of a MyoB/C KO in the loxPMyoA parasite line and schematic of analytical PCRs to verify correct replacement of the endogenous *myob/c* with the KO construct. Three different Primer combinations were used to show correct integration at the locus for both the 5' and 3' UTRs. Absence of *myob/c* in the KO was validated by failure to amplify a *myob/c*-specific PCR product.

3.7 Components of the Myosin A motor complex have a role during IMC biogenesis

Having generated conditional knockouts for MyoA/B/C, MLC1, GAP45, GAP40 and GAP50, the next step was to address their possible role(s) during IMC biogenesis. For this purpose, loxPMyoA and loxPMyoA-*myoB/C* KO were induced with 50 nM rapamycin for 4 hours and then inoculated on host cells for IFA. After fixation 96 hours post-induction the effect of the loss of these myosins was evaluated by staining against the ty-tag (to detect MyoA) and IMC1. As expected, no IMC defect was observed in the parental line, loxPMyoA, and *myoA* KO parasites (Egarter *et al*. 2014). Neither loxPMyoA-*myoB/C* KO nor the *myoA/B/C* KO showed any influence on IMC biogenesis since parasite morphology and localisation of IMC1 remained intact. Next, the impact on IMC1 biogenesis after depletion of MLC1 and GAP45 was investigated. Parasites were induced with 50 nM rapamycin and IFA was performed 72 hours post-induction using the IMC1 antibody. No noticeable IMC defect could be observed, demonstrating no critical role of MLC1 and GAP45 during daughter cell budding (Figure 3-12). The possible role of GAP40 and GAP50, two membrane proteins anchored within the IMC, was evaluated. IFA was performed 40 hours post-induction with and without 50 nM rapamycin. As expected the non-induced strains loxPGAP40 and loxPGAP50 showed no IMC defect. Strikingly, a severe morphology defect could be observed in parasites lacking either GAP40 or GAP50. Staining against IMC1 revealed that although some IMC structures were still present, the typical localisation at the periphery of the parasite was lost. Instead, the IMC seemed abnormally distributed, similar to the phenotype observed after overexpression of the MyoA-tail. The resemblance of the IMC defect of MyoA-tail overexpressor, *gap*40 KO and *gap*50 KO indicates that MyoA-tail might interfere with GAP40/GAP50 which in turn leads to the MyoA-tail phenotype. Furthermore, the similarities between the Rab11B DN, *gap40* KO and *gap50* KO parasites suggest a common role of those proteins during the early phases of IMC biogenesis. GAP40 and GAP50 will be characterised in more detail in the following subchapters, whereas the components not responsible for IMC biogenesis will be addressed in Chapter 4.

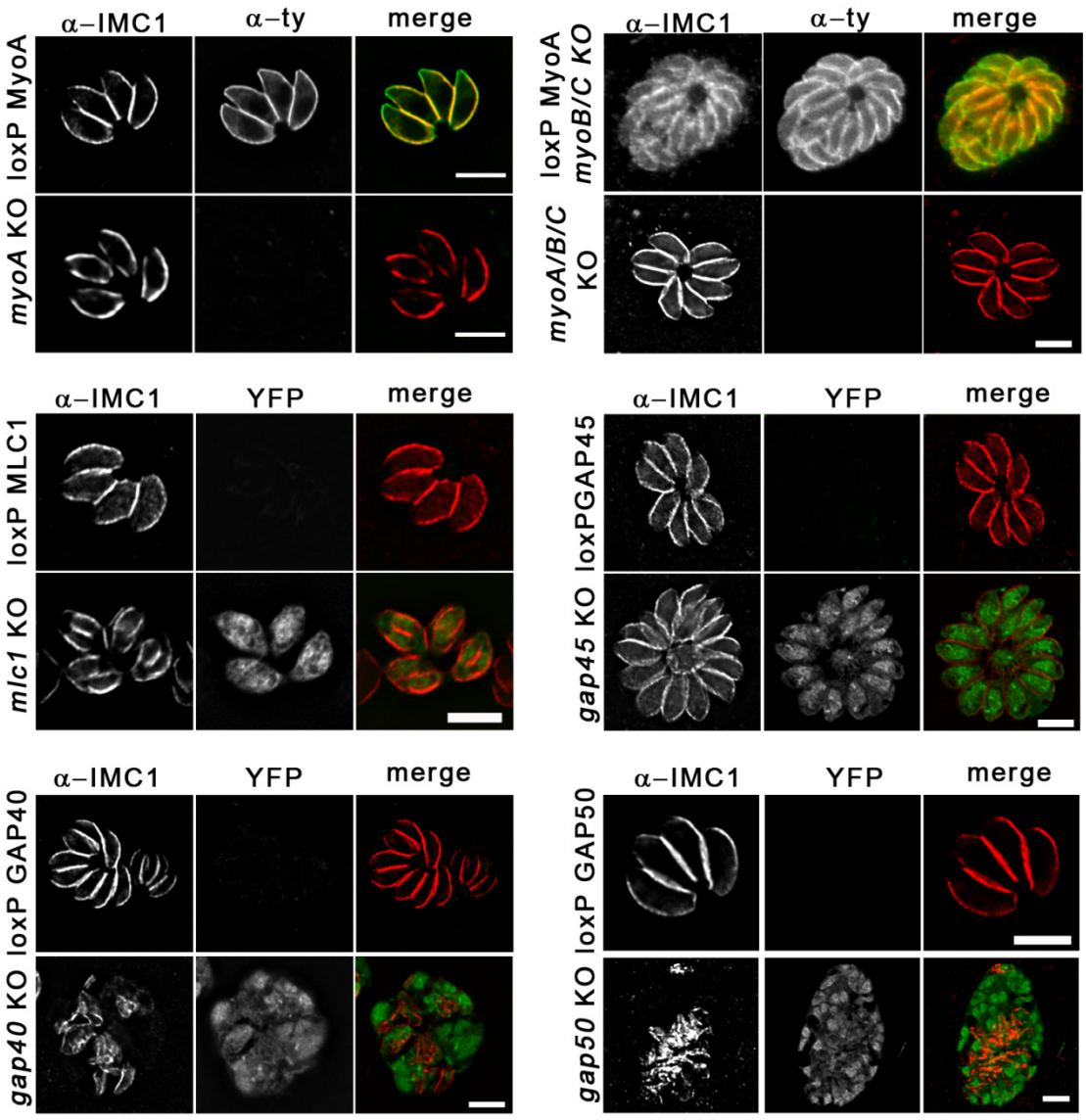

Figure 3-12: Role of the MyoA motor complex during IMC formation. To investigate the role of different proteins, IFA was performed with staining against IMC1. No IMC defect could be observed after depletion of MyoA, MyoB and MyoC. Similarly, MLC1 and GAP45 appear to have no role during IMC formation. However, parasites lacking GAP40 or GAP50 show a severe morphology defect and a clearly mislocalised IMC. Scale bar represents 5 µm.

3.7.1 Characterisation of the *gap40* KO

The depletion of GAP40 resulted in a severe IMC defect 40 hours post-induction with 50 nM rapamycin, and so the *gap40* KO parasites were further characterised. First, the time needed for complete depletion of GAP40 was assessed by IFA. Parasites were incubated in the presence and absence of rapamycin, inoculated on HFF cells and fixed after 18 hours, 24 hours or 40 hours. IFA was performed with staining against GAP40. YFP expressing parasites have excised the *gap40* gene and thus represent *gap40* KOs. A significant downregulation of GAP40 can already be observed at 18 hours post-induction (Figure 3-13A; white arrows). As early as 24 hours post-induction, some vacuoles

were seen lacking GAP40 completely (yellow arrowhead) while others still displayed a weak signal for GAP40 (Figure 3-13A). After 40 hours, large vacuoles were observed with what appeared to be residual, faint GAP40 staining with atypical localisation. Although there was a major defect in IMC biogenesis, some vacuoles still contained GAP40, 40 hours after excision of the gene indicating that *gap40* needs to be formed *de novo* for proper IMC formation. Next, growth analyses were performed. To do this, parasite strains were inoculated onto confluent HFF monolayers and incubated under standard conditions for five days. The cells were then fixed with 4 % PFA and images were taken. As expected, the wildtype strain (DiCre Δ*ku80*) and parental strain (loxPGAP40) showed normal growth behaviour with plaques formed in the host cell monolayers. Parasites lacking *gap40* were incapable of forming any plaques within five days. Instead, they were found in large vacuoles and died intracellularly without ever egressing from the host cell (Figure 3-13B) indicating an essential parasite line.

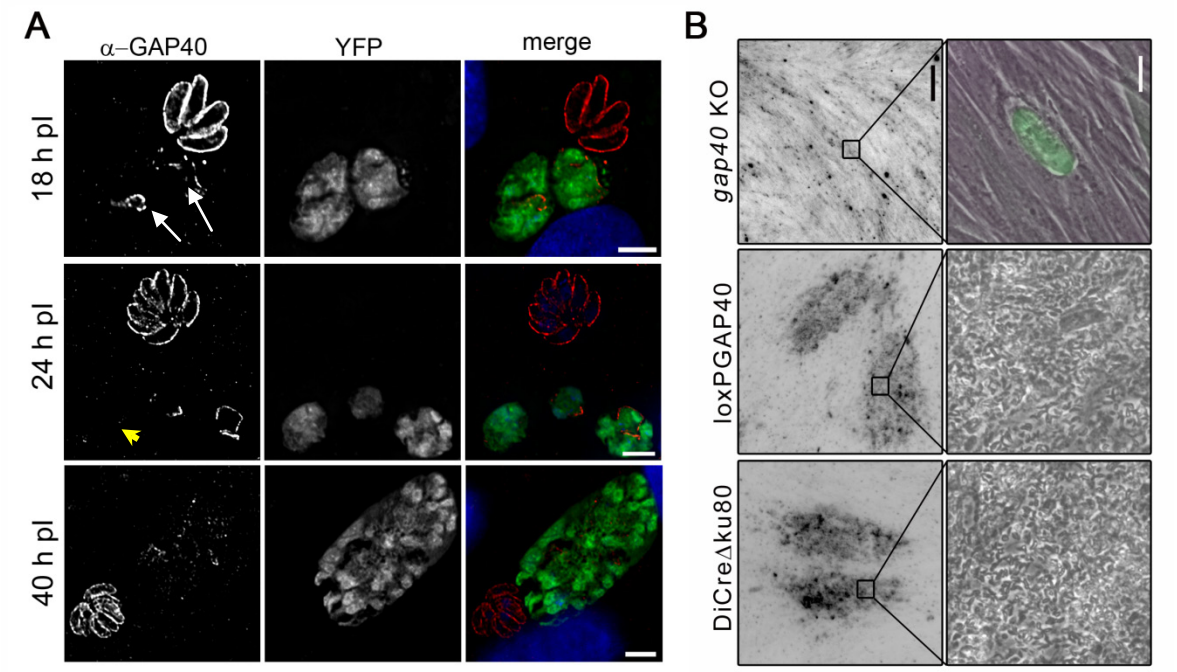

Figure 3-13: Characterisation of *gap40* KO parasites. (A) IFA time course of *gap40* KO parasites stained with α-GAP40 to demonstrate the lack of GAP40. As soon as 24 h post-induction with 50 nM of rapamycin, vacuoles could be detected without any visible GAP40 (yellow arrow). Scale bar represents 5 µm. (B) Growth assays of *gap40* KO parasites. While control parasites showed normal growth behaviour, parasites lacking GAP40 displayed no plaque formation on HFF monolayers. Scale bars represent 20 µm (left panels) and 0.2 mm (right panels), respectively.

Akin to the MyoA-tail overexpressor, the specificity of the IMC defect was investigated by examining different organelles using IFA. The loxPGAP40 parasites were induced with and without 50 nM rapamycin and inoculated onto HFF cells growing on glass coverslips. The parental, non-induced line was fixed

after 40 hours and served as a control whereas *gap40* KO parasites were fixed after either 18 hours or 40 hours. Early and late timepoints were chosen to classify possible effects on organelles as primary or secondary. If an effect was not observed after 18 hours but was present after 40 hours, it could be attributed to a secondary effect due to the severity of the morphology change after loss of GAP40 and not due to the direct loss of GAP40. First, the influence on *de novo* formed secretory organelles, especially rhoptries and micronemes, was analysed using antibodies against ROP2/4 and AMA1. It seemed that *de novo* synthesis of rhoptries and micronemes was not impaired after depletion of GAP40, since the number of organelles stained by the antibody reflects more than one parasite present (Figure 3-14). *Toxoplasma* is a highly polarised organism with micronemes and rhoptries that are localised at the apical end. Although those organelles are still formed in the *gap40* KO parasites, no conclusion could be made about their localisation since the parasites were misshapen. Given that it has nine transmembrane domains and is a component of the MyoA motor complex, a role for anchoring this complex was suggested for GAP40. To pursue this idea, the pellicle was analysed in more detail by IFA staining against the plasma membrane marker, SAG1, as well as MLC1, which is located between the plasma membrane and IMC. While the parental line showed the expected co-localisation of SAG1 and MLC1, IFAs of the *gap40* KO parasites fixed 18 hours post-induction revealed that loss of GAP40 resulted in only a partial co-localisation of SAG1 and MLC1 with some membrane like structures staining for SAG1 but not for MLC1. As an example of an organelle that is not synthesised *de novo* during daughter cell assembly but supplicated and separated in the new forming daughter cells, the apicoplast was chosen for further study. Parasites were stained against the apicoplast protein HSP60 and parasite actin, since actin has been implicated to play a role during apicoplast division (Jacot *et al*. 2013, Mueller *et al*. 2013). After depletion of GAP40, actin showed the typical dotted staining that is also observed in wild-type parasites. Furthermore, the division and segregation of the apicoplast was not affected in the *gap40* KO parasites since more than one apicoplast was found per parasite vacuole.

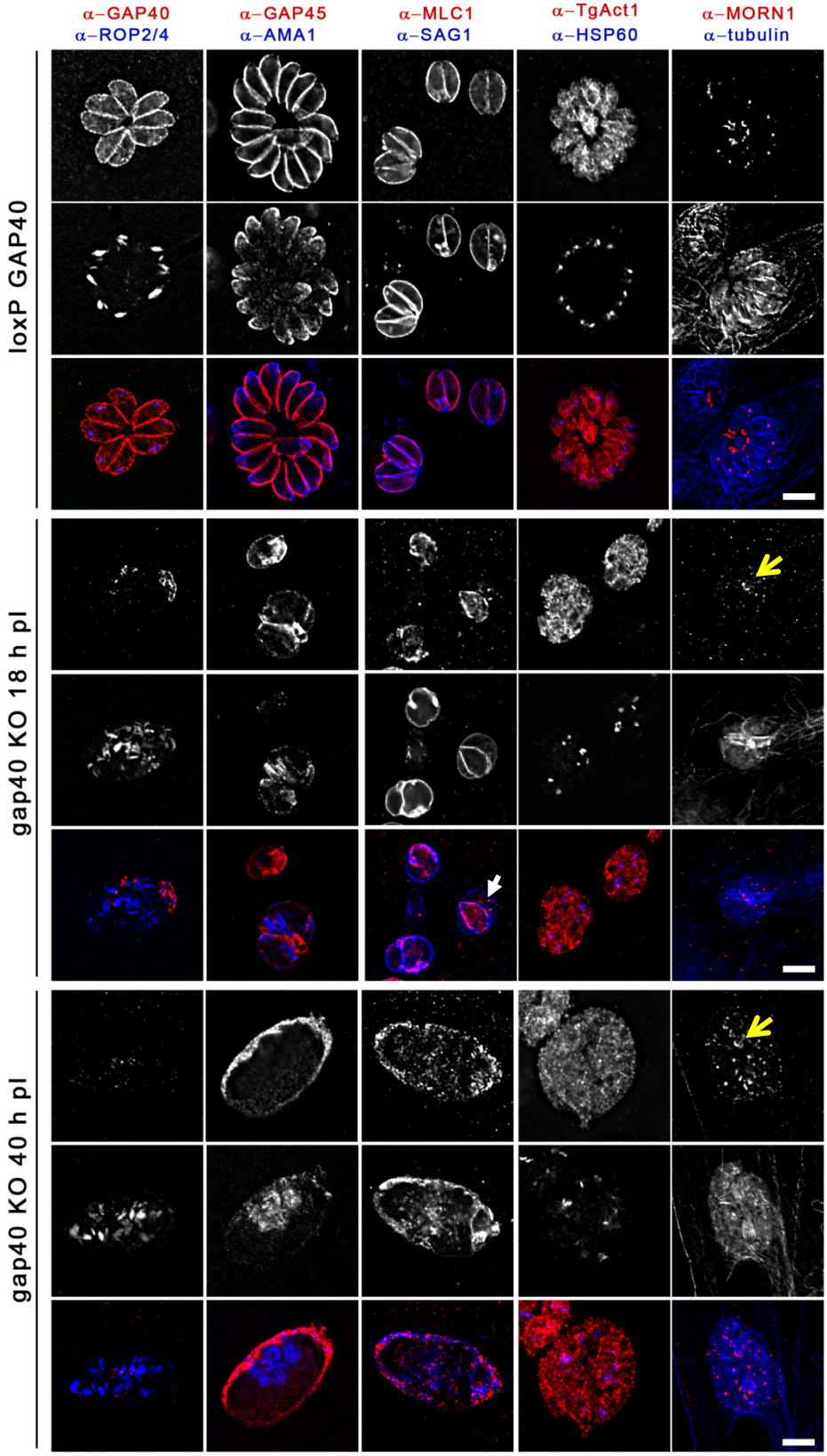

Figure 3-14: IFA of distinct organelles after depletion of GAP40. All antibody used showed their expected localisations in the parental line loxPGAP40. Loss of GAP40 has no influence on *de novo* synthesis of secretory organelles like rhoptries and micronemes (α-ROP2/4; α-AMA1). Interestingly, co-staining with SAG1 and MLC1 showed that although they are both localised at the pellicle they only displayed a partial co-localisation. Organelles like the apicoplast replicated and segregated normally. Daughter cell budding was still initiated and daughter parasites were formed as observed by staining against MORN1 and alpha-tubulin. Scale bar represents 5 µm.

One of the first proteins detected during daughter cell budding is MORN1 (membrane occupation and recognition nexus protein 1). MORN1 localises to the centrocone and to the apical and basal ends of the IMC (Gubbels *et al*. 2006, Lorestani *et al*. 2010) which is nicely reflected in the loxPGAP40 parasites (Figure 3-14). In the *gap40* KO parasites, some structures resembling MORN1 rings were still observed indicating daughter cell formation is still initiated (Figure 3-14; yellow arrows). In addition, budding was still observed by staining with an acetylated tubulin antibody that specifically labels α-tubulin. Taken together, these data suggest the loss of GAP40 results in a specific effect on IMC biogenesis similar to what happens upon overexpression of the tail domain of MyoA.

3.7.2 Characterisation of the *gap50* KO

Akin to GAP40 depletion, the lack of GAP50 caused a strong effect on IMC biogenesis 40 hours after excision of this gene. First, growth analyses were performed. The parasite strains were inoculated on confluent HFF monolayers and incubated under standard conditions for five days. Cells were then fixed with 4% PFA and images were taken immediately. As expected, the recipient parasites (DiCre Δ*ku80*) and parental parasites (loxPGAP50) displayed typical growth behaviour with plaques formed in the host cell monolayers. However, the *gap50* KO parasites showed no plaque formation within five days. Instead, large vacuoles were observed where parasites died intracellularly without ever egressing from the host cell (Figure 3-15), indicating that *gap50* is as essential as *gap40* for parasite survival.

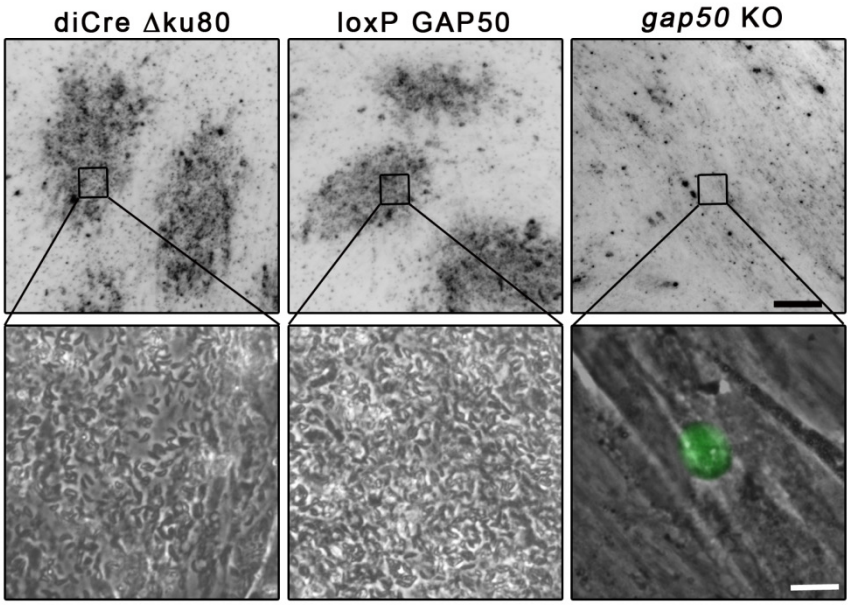

Figure 3-15: Growth assays of parasites lacking GAP50. While control parasites (diCre Δku80) displayed typical growth behaviour, *gap50* KO parasites showed no plaque formation on HFF monolayers indicating that *gap50* is an essential gene in tachyzoites. Scale bars represent 20 µm (bottom panels) and 0.2 mm (top panels), respectively.

Unfortunately no GAP50 antibody is available to perform IFA and determine the exact timepoint that corresponds to complete removal of GAP50. Therefore the same timepoints were chosen as for the *gap40* KO parasites to examine if the observed IMC defect is specific for this organelle. The first organelles analysed were the *de novo* synthesised rhoptries and micronemes using α-ROP2/4 and α-AMA1, respectively. Depletion of *gap50* had no influence on *de novo* synthesis of these organelles, but no conclusion can be drawn concerning their localisation since the loss of *gap50* leads to a severe morphology defect. Based on the likeliness of interaction of GAP40 and GAP50 and the fact that deglycosylation of GAP50 abolishes association with other components of the MyoA motor complex (Fauquenoy *et al*. 2011), the influence of GAP50 depletion on GAP40 was investigated. Surprisingly, GAP40 showed a cytoplasmic localisation rather than an association with a membrane in the *gap50* KO parasites, indicating a possible direct interaction of these two proteins. The effect of SAG1 and MLC1 were analysed next. Similar to the *gap40* KO parasites, no complete co-localisation of SAG1 and MLC1 was achieved in absence of GAP50.

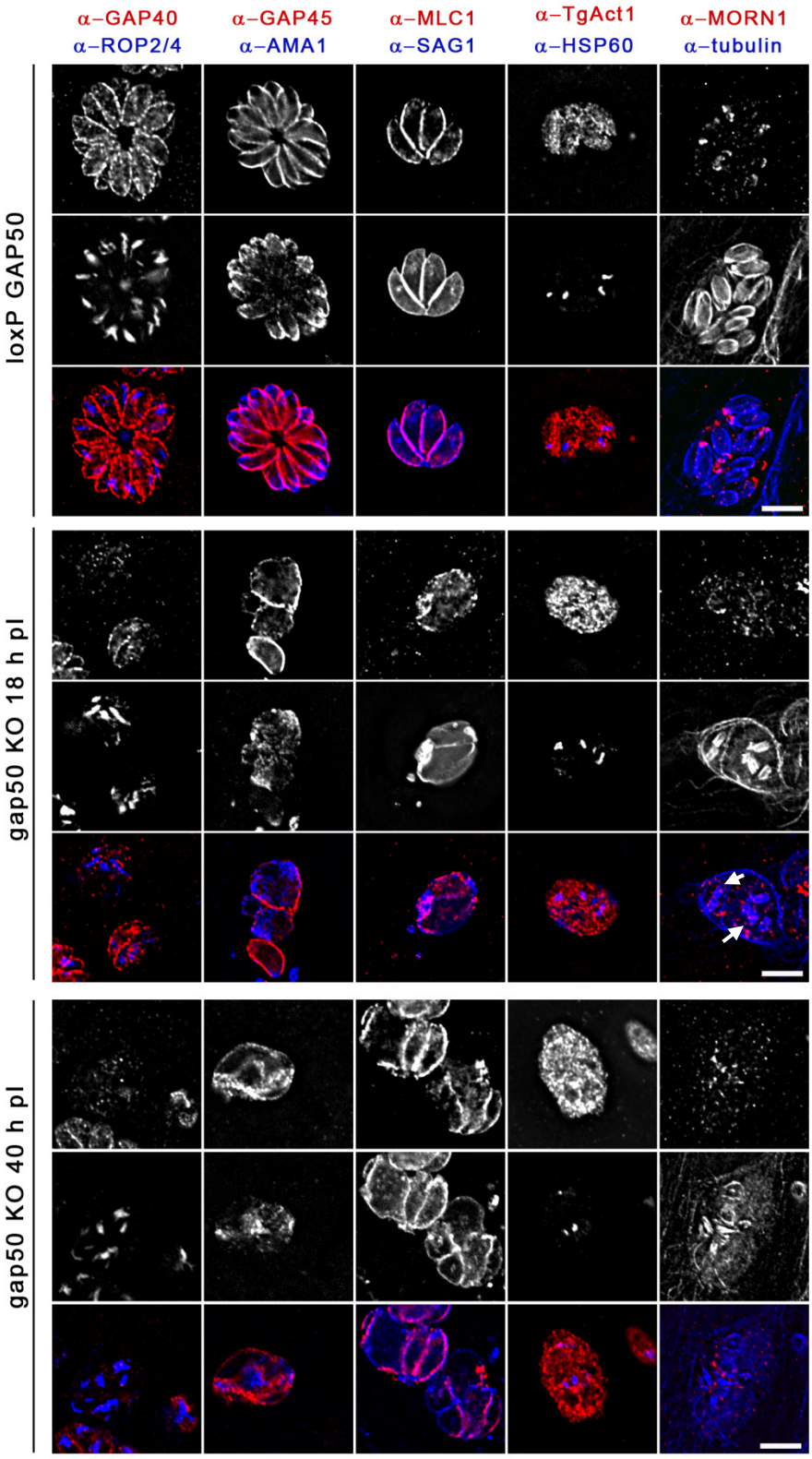

Figure 3-16: IFA of distinct organelles after depletion of GAP50. All antibodies used showed the expected localisation in the parental line loxPGAP50. Loss of GAP50 has no influence on *de novo* synthesis of secretory organelles, like rhoptries and micronmes (α-ROP2/4; α-AMA1). Interestingly, co-staining with SAG1 and MLC1 showed that although they are both localised to the pellicle, they only displayed a partial co-localisation. The apicoplast was able to replicate and segregate normally. Daughter cell budding was still initiated and daughter cells were formed as observed by staining against MORN1 and alpha-tubulin. Scale bar represents 5 µm.

Next, the effect of the *gap50* KO on the apicoplast was determined. Several vacuoles were observed 40 hours post-induction to have a low and uneven number of apicoplasts, indicating a possible effect on apicoplast division and/or segregation. However, 18 hours post-induction this effect was less severe if at all, leading to the conclusion that the effect on apicoplast duplication is a secondary effect caused by the deformed morphology after loss of GAP50. The ability to initiate daughter budding was analysed using the MORN1 antibody. Although a signal was detected using α-MORN1, it was not localised to the basal ends of budding daughter cells, which is marked by alpha tubulin staining, but rather, the signal appeared to be diffusely distributed within the vacuole. The presence of at least five daughter cytoskeletons (Figure 3-16; white arrows) suggests that a minimum of three rounds of daughter cell budding were initiated. Altogether, these data indicate that the observed IMC defect after GAP50 depletion is specific.

3.8 Comparative analysis of Myosin A tail expressing parasites, Rab11B DN, *gap40* KO and *gap50* KO parasites

During parasite replication, the IMC is formed *de novo* within the mother parasite in a process termed internal budding. It was recently discovered that the alveolate specific small GTPase, Rab11B, has a crucial role during IMC biogenesis by transporting Golgi-derived vesicles to the nascent IMC of daughter cells (Agop-Nersesian *et al*. 2010). Since the IMC defect observed with expression of a dominant negative version of Rab11B resembles the phenotypes discovered for the MyoA-tail overexpresser, *gap40* KO and *gap50* KOs, IMC formation of these four strains was examined at the same time. Therefore, loxPGAP40 and loxPGAP50 were induced with 50 nM rapamycin for four hours prior to inoculation on HFF monolayers. At the same time, ddFKBPmycMyoA-tail and ddFKBPmycRab11B-DN (dominant-negative) parasites were inoculated on host cells and supplemented immediately with 1 µM Shield-1 to induce overexpression of the respective protein. Parasites were fixed after 18, 24 and 40 hours and IFA was performed staining against IMC1 for the conditional KOs, or with IMC1 and myc antibodies for the dd-system mutants. Although the DNA amount stained with DAPI increased over time, the nuclei themselves undergo no efficient separation and formed large nuclei in all four mutant lines.

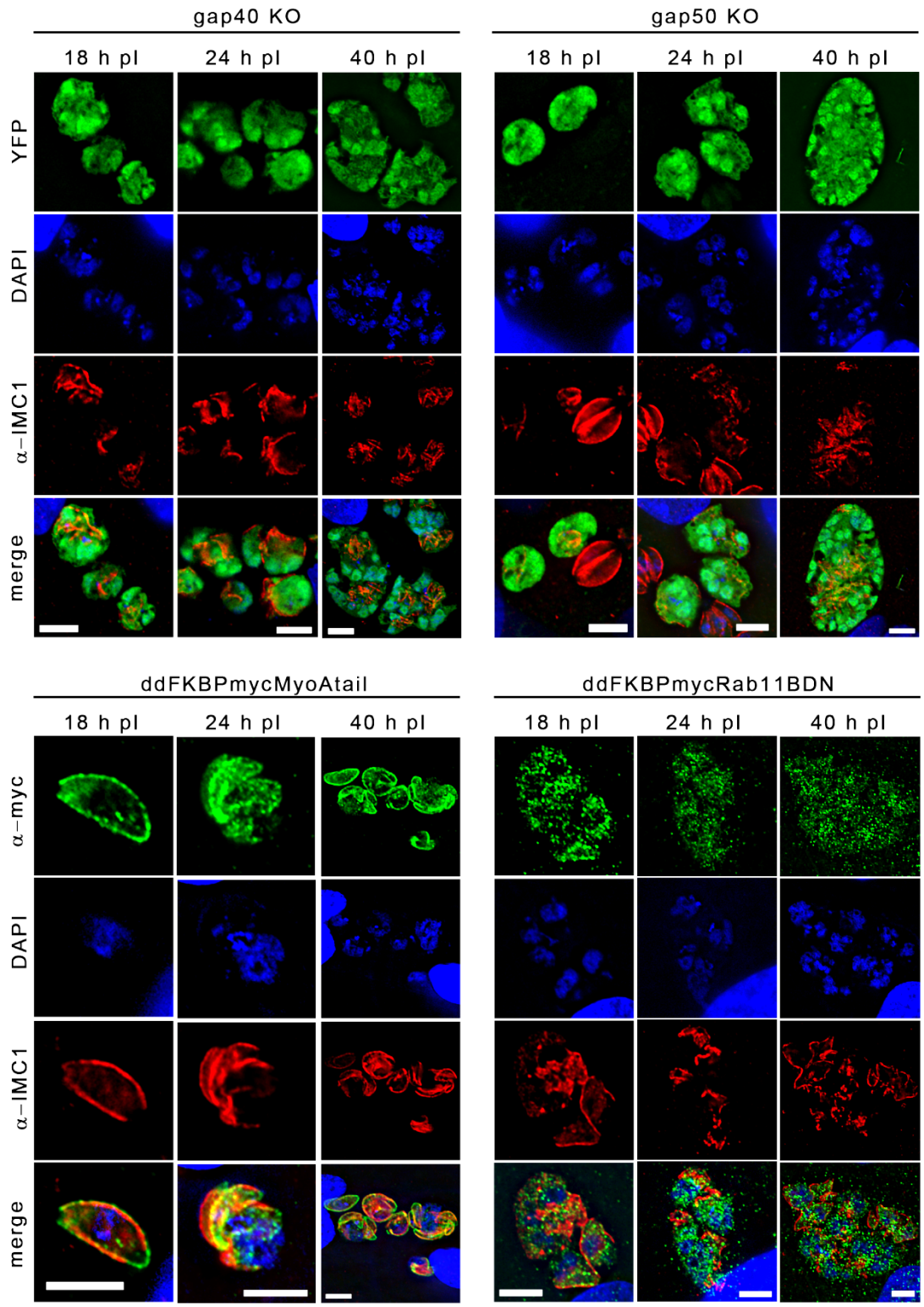

Figure 3-17: Comparative analysis of IMC biogenesis. All four analysed mutant strains (*gap40* KO, *gap50* KO, MyoA-tail overexpressor and Rab11B-DN) showed a severe effect on nuclear division and DNA segregation. All four mutant lines were multinucleated. In addition, the specific defect in IMC biogenesis could be observed as soon as the first replication round was initiated. Although daughter budding began, no mature parasites were detected. A new round of replication was probably initiated since vacuoles increased their size over time, despite not completing cytokinesis. Scale bar represents 5 µM.

A forward genetic screen identified a large number of temperature-sensitive cell cycle mutants (Gubbels *et al.* 2008). These mutants were divided into different

classes depend on their arrest within the cell cycle. Parasites with budding defects showed either early bud arrest or late budding defects. Whereas early and late budding mutants displayed the typical number of nuclei per parasites, a third class, the uncoupling mutants, showed a crucial collapse of the coordination of karyokinesis and cytokinesis resulting in the formation of multiple or very large nuclei within a parasite. This demonstrates that defects in budding are not always directly linked to defects in nuclear division. All four mutants discussed in this chapter resembled the uncoupling mutants, and showed a specific IMC defect as soon as the first round of replication. Whereas *gap40* KO parasites, *gap50* KO parasites and Rab11B-DN expressing parasites already underwent 2-3 rounds of replication judging by the amount of DNA present, MyoA-tail overexpressing parasites were mainly still in the 1 cell stage, likely due to a severe invasion defect (Agop-Nersesian *et al*. 2009) and delayed initiation of replication. Besides the fact that the MyoA-tail overexpressing parasites were a few replication rounds behind, all four mutant strains showed increased vacuole size over time, indicating intracellular growth although none of the replication rounds were completed (Figure 3-17). Note that a direct comparison at distinct time points between the ddFKBP mutants and the KOs cannot be made since the maximal protein stability of after overexpression of MyoA-tail and Rab11B is reached more rapid than depletion of GAP40 and GAP50 after excision of the respective gene. Nevertheless, the overall severity of the IMC defect appeared comparable in the *gap40* KO, *gap50* KO, MyoA-tail overexpressor and Rab11B-DN mutants. Likewise, none of the mutants showed an effect on *de novo* synthesis of secretory organelles. Ultrastructural analysis was performed to examine the MyoA-tail overexpressing, Rab11B-DN, *gap40* KO and *gap50* KO parasites. The non-induced MyoA-tail strain was used as a wildtype control. Parasites replicated by endodyogeny as anticipated. The electron micrographs showed that the Golgi stack was duplicated in the two nascent daughters, the IMC was elongated, the nucleus had begun to separate and secretory organelles could be visualised in the growing daughter parasites. Unlike wild-type parasites, the four analysed mutant strains had multinucleated vacuoles, often with more than four daughter cells present (Figure 3-18) as visualised by either the formation of novel IMC or conoids within the mother cell. This division method resembles more the processes of *Toxoplasma* endopolygeny or *Plasmodium* schizogony where multiple rounds of DNA

replication and mitosis take place before the budding of daughter parasites. These data are in good agreement with the IFA data obtained for each of the four mutants. The ability to synthesise secretory organelles *de novo* within the daughter cells was also confirmed. One of the features of the dominant negative Rab11B was abnormal gaps and overlapping between the plates of the IMC, but the underlying microtubule network appeared normal (Agop-Nersesian *et al*. 2010). Therefore, the microtubules and nascent daughter IMC in the MyoA-tail overexpressor, *gap40* KO and *gap50* KO parasites were analysed in more detail (Figure 3-19). Similar to the Rab11B-DN parasites, daughter budding was initiated in parasites lacking *gap40* or *gap50* respectively and microtubules were observed underneath the IMC. The newly formed daughter IMC appeared to be misaligned and had atypical, large gaps, indicating that the phenotypes observed for the *gap40* KO and Rab11B-DN are indistinguishable. This was also the case with the MyoA-tail mutant. Taken together, the striking resemblance in these data strongly suggests that the phenotypes are closely linked.

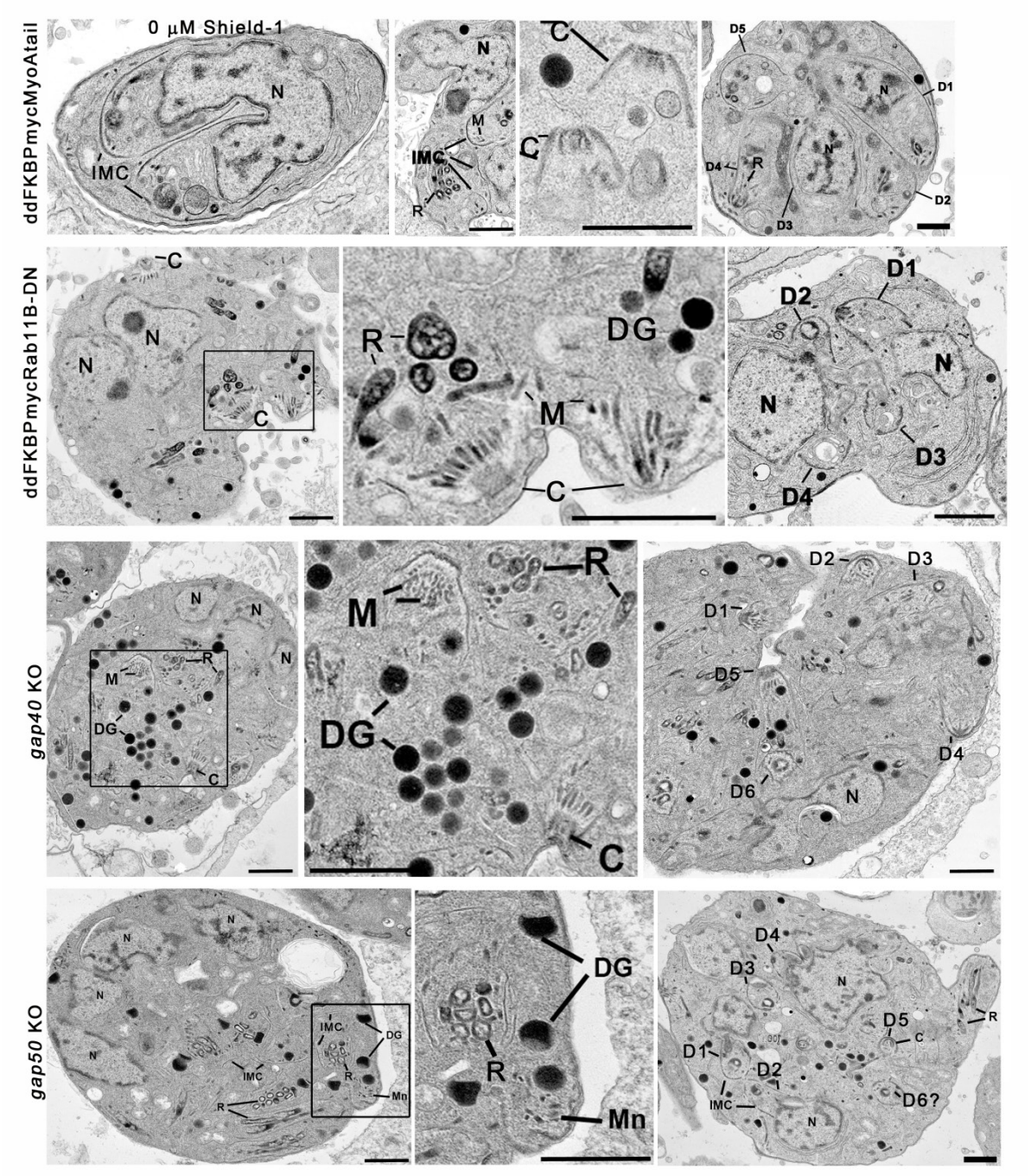

Figure 3-18: Comparison of *gap40* KO, *gap50* KO, Rab11B-DN and MyoA-tail overexpressor at the ultrastructural level. All four parasite lines showed a striking effect on nuclear division. Vacuoles showed multiple nuclei (N) and DNA did not appear to be properly segregated. Vacuoles with more than four daughter buds (D1-D6) were detected by either the formation of daughter cell IMCs or conoids (C). None of the analysed lines showed an effect on *de novo* synthesis of secretory organelles since the micronemes (M), rhoptries (R) and dense granules (DG) were still present. D-daughter parasite, IMC-Inner Membrane Complex, MT- microtubules, N- nucleus, C-conoid, Mn or M- micronemes, R- rhoptries and DG- dense granule. Scale bar represents 1µm.

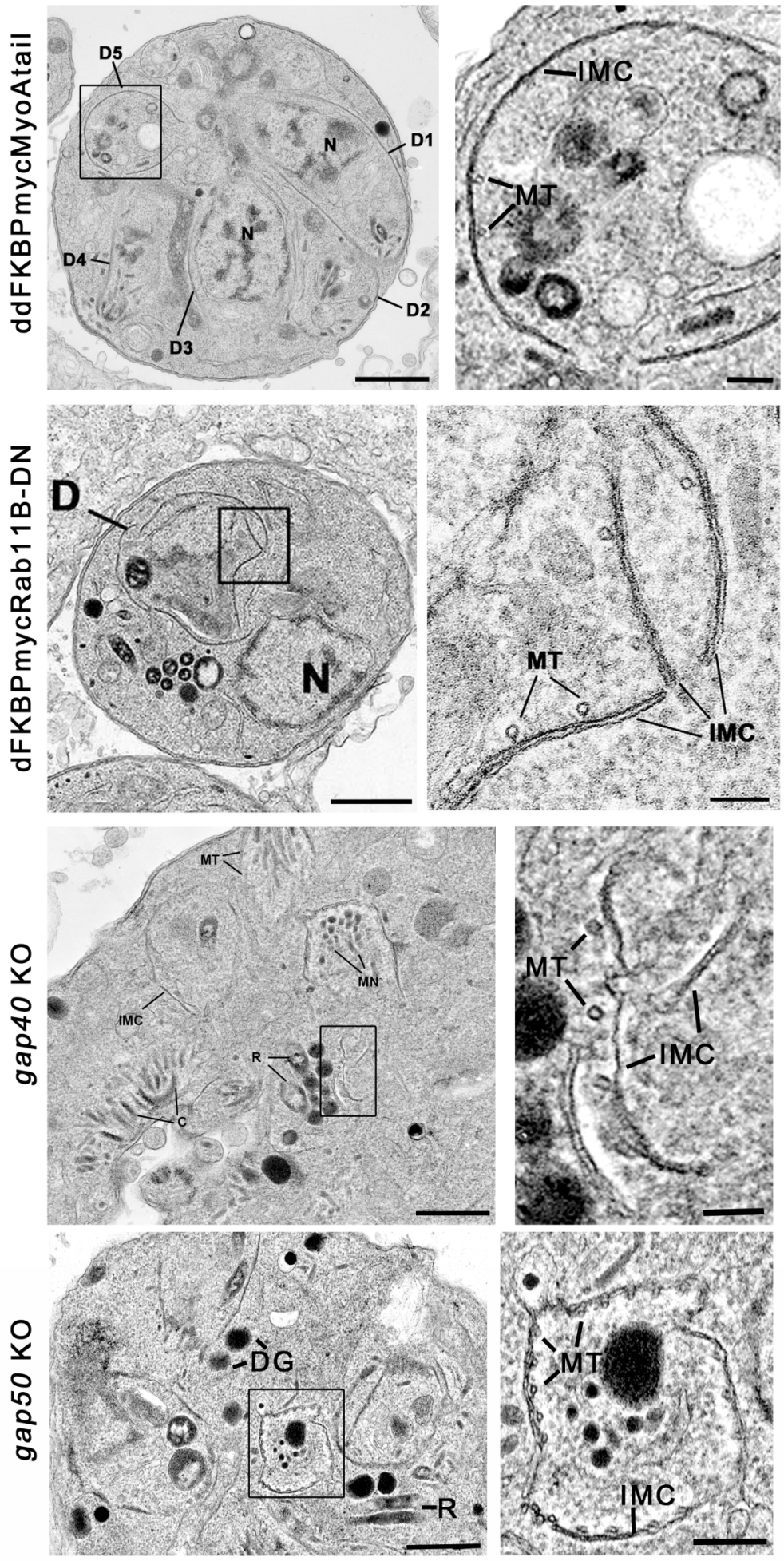
ddFKBPmycMyoAtail
D5
D1
N
N
D4
D2
D3
IMC
MT
dFKBPmycRab11B-DN
D
N
MT
IMC
gap40 KO
MT
MN
IMC
R
C
MT
IMC
gap50 KO
DG
R
MT
IMC

Figure 3-19: Electron micrographs of mutant parasites. MyoA-tail mutant parasites initiated several rounds of replication as shown by the existence of five daughter parasites (D1-D5). The enlargement shows no effect on the microtubules (MT) underlying the IMC. Interestingly, large gaps within the IMC were observed resembling Rab11B-DN mutant parasites undergoing endodyogeny. The inset show that the IMC and underlying microtubules are present; however abnormal gaps and overlapping between the IMC plates were observed. Adapted from Agop-Nersesian *et al*. (2010). Similar to the Rab11B DN parasites, *gap40* and *gap50* KO parasites initiated daughter budding and microtubules were detected underneath the IMC, but atypical gaps and overlapping between the IMC plates of the IMC were observed. D-daughter parasite, IMC-Inner Membrane Complex, MT- microtubules, N- nucleus, C-conoid, MN- micronemes, R-rhoptries and DG- dense granule. Scale bar represents 500 nm and 200 nm, respectively.

3.9 Summary and brief discussion

As a summary, different methods were used to analyse several components of the MyoA motor complex. First, the ddFKBP system was used for a dominant negative approach to generate a strong overexpressor of the tail domain of MyoA (Agop-Nersesian *et al*. 2009). This mutant displayed an IMC defect whereby the severity of the defect increased with the amount of protein stabilised. The IMC biogenesis defect was found to be specific since secretory organelles were still formed *de novo* and other organelles, such as the apicoplast, Golgi and mitochondrion, were duplicated and separated into nascent daughter buds. The effect on IMC biogenesis caused by overexpression of the MyoA-tail was determined to be the early phase of daughter cell budding since early components like GAP40 and GAP50 were already affected. This indicates that overexpression of a mutated version of MyoA resembled the phenotype of the small GTPase Rab11B, while Rab11A affects IMC biogenesis at a later stage (Agop-Nersesian *et al*. 2009, Agop-Nersesian *et al*. 2010). A complementation study where several known interacting partners of MyoA as well as the above mentioned small GTPases were simultaneously expressed in the MyoA-tail overexpressor, revealing that MLC1 was the only protein that could partially rescue the IMC defect. Unfortunately, the complementation study was inconclusive, so conditional KOs for MLC1, GAP45, GAP50, GAP40 and MyoA/B/C were successfully generated. Out of those KOs, *gap40* and *gap50* KO parasites displayed an IMC defect. A comparative study of these IMC biogenesis mutants revealed several shared characteristics: (a) the IMC defect is specific since other organelles were not affected, (b) a severe nuclear division and DNA segregation defect was observed, (c) the IMC defect was detected as soon as the first round of replication had started, (d) initiation of daughter cell budding was not affected, but daughters appeared incapable of maturation, (e) several rounds of replication were initiated without completion of the previous one and (f) the

microtubule network underlying the IMC underlying appeared unaffected, but the IMC itself showing atypical gaps and misalignment. Rab11B is involved in the delivery of vesicles from the Golgi to the nascent IMCs of daughter buds. Although the content of the vesicles is not fully known, a recent study implicated it might be GAP50 (Fauquenoy *et al.* 2011). Given the similarities of the Rab11B-DN, *gap50* KO and *gap40* KO parasites, I propose a model where Rab11B is either involved directly in trafficking both GAP50 and GAP40 to the growing daughter buds or it is an orchestrated process where Rab11A/B delivers vesicles to the IMC and GAP50/40 serve downstream of this route as stabilisation factors or anchoring proteins for delivered vesicles (Figure 3-20).

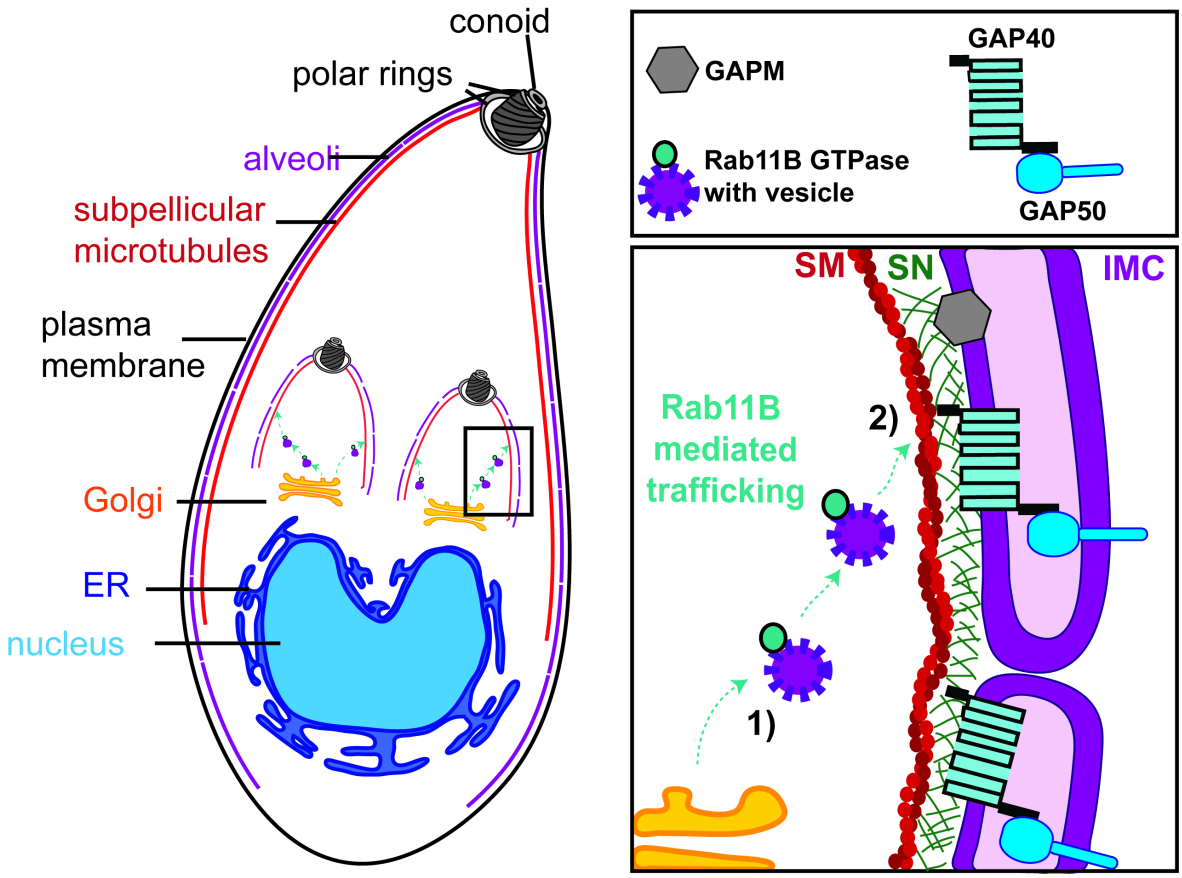

Figure 3-20: Model for involvement of Rab11B, GAP40 and GAP50 during IMC biogenesis. In developing daughter parasites, the nascent IMC forms in a well-coordinated process involving the GTPase Rab11B and the glideosome associated proteins GAP40 and GAP50. First, Rab11B mediates vesicle transport between Golgi and the emerging IMC of daughter cells (green arrow). Although the content of the vesicle has not been identified so far, I speculate that it possible is a component of the IMC/cytoskeleton. In a second step, GAP40/50 stabilise or anchor the delivered vesicle content.

4 Re-dissection of the Myosin motor complex

4.1 Introduction

The locomotion of *Toxoplasma* tachyzoites does not involve cilia, pseudopodia or lamellipodia. Instead, *T. gondii* moves by a unique mechanism termed gliding motility. The mechanism of gliding motility is believed to be driven by an actin-myosin motor (Keeley and Soldati 2004) which is positioned in the supra-alveolar space and anchored between the IMC and plasma membrane (Soldati and Meissner 2004). The components of this motor assemble into a complex consisting of a myosin heavy chain A (MyoA), a myosin light chain 1 (MLC1), an essential light chain 1 (ELC1) and three gliding associated proteins (GAP45, GAP50 and GAP40) (Herm-Gotz *et al*. 2002, Gaskins *et al*. 2004, Frenal *et al*. 2010, Nebl *et al*. 2011). The assembly of the MyoA motor complex is a coordinated process where the interaction of MLC1 with GAP45 transports MyoA to the periphery of the parasite where this pre-complex associates with the conserved carboxy terminal, cytoplasmic domain of GAP50, an integral membrane protein of the IMC (Hettmann *et al*. 2000, Herm-Gotz *et al*. 2002, Gaskins *et al*. 2004). Other components of the invasion and gliding machinery include the actin track on which the motor complex moves, and adhesion molecules (AMA1 and MIC2) that are believed to connect the Acto-myosin system with the parasite cytoskeleton and extracellular substrate (see Figure Figure 1-8). This substrate-dependent motility is an orchestrated process of cell adhesion, concerted action of the MyoA motor and subsequent shedding of surface adhesins (Sibley 2010). Knockdown studies of two core components of the MyoA motor complex (MyoA and GAP45) revealed that while gliding motility was completely eliminated, invasion was not completely blocked, which was thought to be due to background expression of *gap45* and *myoA* respectively (Meissner *et al*. 2002, Frenal *et al*. 2010). Recently, the establishment of a clonal *myoA* KO line demonstrated an important but non-essential role of MyoA during the invasion process (Andenmatten *et al*. 2013), questioning the role of the motor complex and actin during invasion and gliding motility. Therefore, the functions of the components of the MyoA motor complex will be re-dissected in the following chapters.

4.2 Immunofluorescence analysis of conditional KOs for MLC1 and GAP45

MLC1 and GAP45 are well known components of the MyoA motor complex (Herm-Gotz *et al*. 2002, Gaskins *et al*. 2004, Frenal *et al*. 2010). Furthermore, a role in IMC biogenesis of these two proteins was excluded (Chapter 3). In the following chapter, the impact of MLC1 and GAP45 on other organelles will be examined. Immunofluorescence analysis (IFA) of *mlc1* KO and *gap45* KO parasites was performed. LoxPMLC1 and loxPGAP45 parasites were induced with 50 nM rapamycin for four hours, inoculated 96 hours post-induction and fixed 24 hours after inoculation.

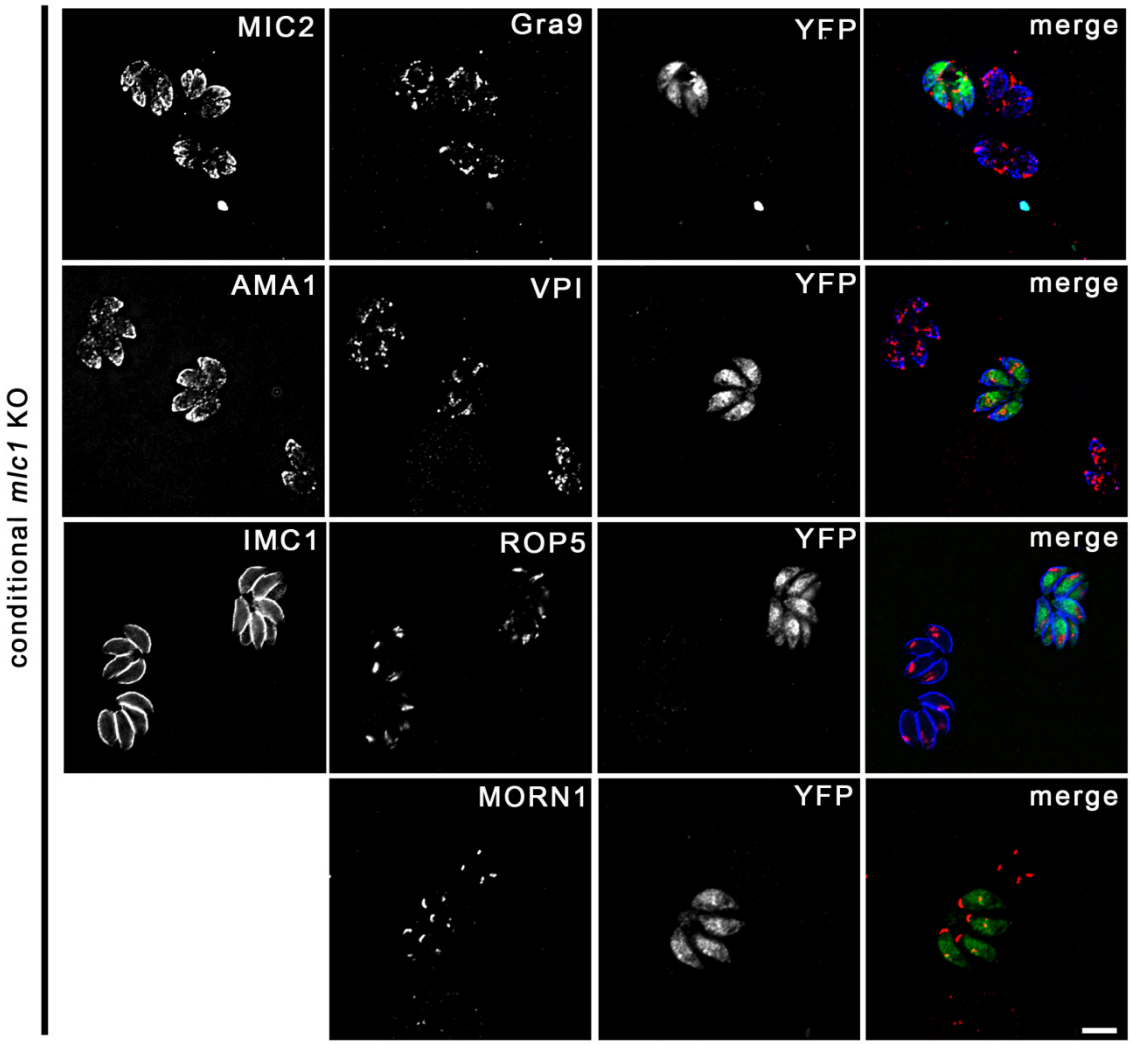

Figure 4-1: IFA of *mlc1* KO parasites. IFA shows a mixed population of loxPMLC1 (YFP negative) and *mlc1* KO (YFP positive) parasites, fixed 120 h post-induction with 50 nM rapamycin. IFA of *mlc1* KO parasites shows that *mlc1* depletion has no impact on the inner membrane complex (IMC1), micronemes (MIC2, AMA1), rhoptries (ROP5), dense granules (GRA9), endosomal like compartment (VPI), or the membrane occupation recognition nexus 1 (MORN1). Scale bar: 5 µm.

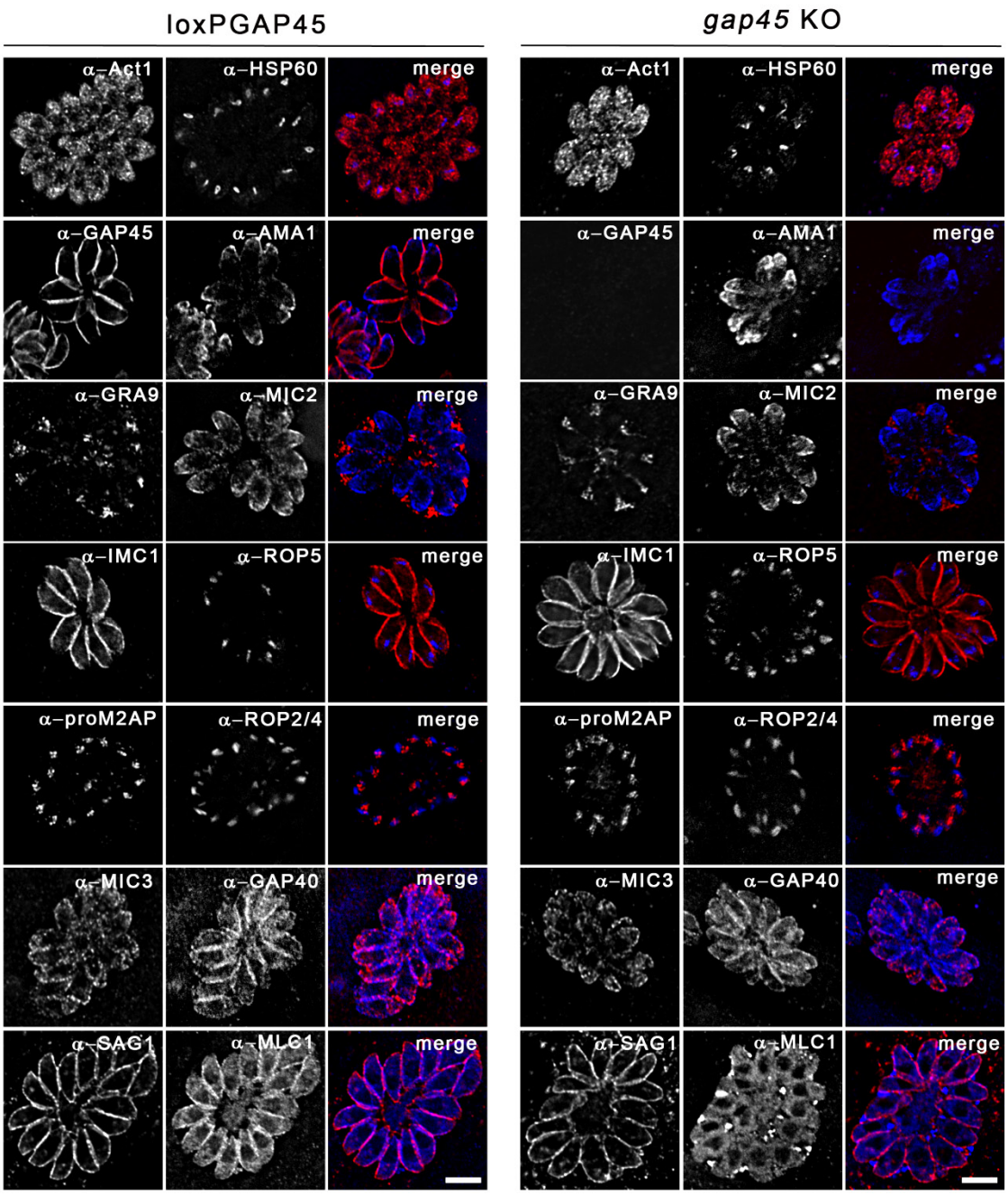

Figure 4-2: IFA of *gap45* KO parasites. The *gap45* KO parasites were fixed 120 h post-induction with 50 nM rapamycin. IFA analysis of *gap45* KO parasites shows that *gap45* removal has no impact on the Inner Membrane Complex (IMC1), micronemes (MIC2, AMA1 and MIC3), rhoptries (ROP5, ROP2/4), dense granules (GRA9), endosomal-like compartment (proM2AP), actin (Act1) or the apicoplast (HSP60). Additionally, MLC1 was re-distributed to the cytosol, confirming previous studies (Frenal *et al*. 2010). Scale bars: 5 µm.

IFA analysis of *mlc1* KO parasites showed that MLC1 depletion has no impact on the inner membrane complex (IMC1), dense granules (GRA9), endosomal-like compartments (VPI), or the membrane occupation recognition nexus 1 (MORN1) (Figure 4-2). MLC1 and GAP45 are components of the MyoA motor complex and implied to have an important role during invasion. Since microneme and rhoptry secretion is a critical step in this process, the micronemes and rhoptries were examined in *mlc1* KO parasites. As depicted in Figure 4-2typical apical signals for

micronemal proteins (AMA1 and MIC2) and club-shaped staining of the rhoptry protein (ROP5) were observed, indicating secretion of micronemes and rhoptries was not affected. Similarly, different organelles were analysed in parasites lacking *gap45*. IFA analysis of *gap45* KO parasites showed that GAP45 has no effect on the inner membrane complex (IMC1), dense granules (GRA9) or the endosomal-like compartment (proM2AP). Furthermore, micronemes (AMA1, MIC2 and MIC3) and rhoptries (ROP5 and ROP2/4) remained intact after the loss of *gap45*. Moreover, removal of *gap45* had no impact on the appearance of the plasma membrane (SAG1) in intracellular parasites. Interestingly, other components of the MyoA motor complex such as GAP40 were not affected by the lack of GAP45, whereas MLC1 was redistributed to the cytosol, confirming previous results (Frenal *et al*. 2010). Therefore, the impact of depleting distinct components of the MyoA motor complex on the other components of the motor complex will be analysed in the next subchapter.

4.3 MyoA motor complex interaction

To study if depletion of one of the components of the MyoA motor complex has an impact on the remaining components, IFA was performed using antibodies against MLC1, MyoA, GAP40 and GAP45. Prior to this a time course analysis was performed for all knockouts to determine complete removal of the gene of interest. Based on this *mlc1* and *gap45* KO parasites were analysed 96 hours post induction whereas *gap40* and *gap50* KOs were analysed 40 hours post induction with rapamycin. The *myoA* KO parasites are a clonal line and so no induction with rapamycin is required (Andenmatten *et al*. 2013). As anticipated, all four proteins localised to the periphery, between the plasma membrane and IMC, in wild-type parasites (Figure 4-3). It should be noted that the MyoA antibody caused a cross reaction, as seen by a signal at the apical end in *myoA* KO parasites. Depletion of MyoA had no influence on the peripheral localisation of MLC1, GAP40 and GAP45 as was observed in previous studies (Andenmatten *et al*. 2013). MLC1 and MyoA were redistributed to the cytosol in *gap45*, *gap40* and *gap50* KO parasites. GAP45 was found at the periphery independently of which component of the MyoA motor complex was depleted. While GAP40 is localised at the periphery of *mlc1* and *gap45* KO parasites, it is re-localised to the cytosol in absence of GAP50.

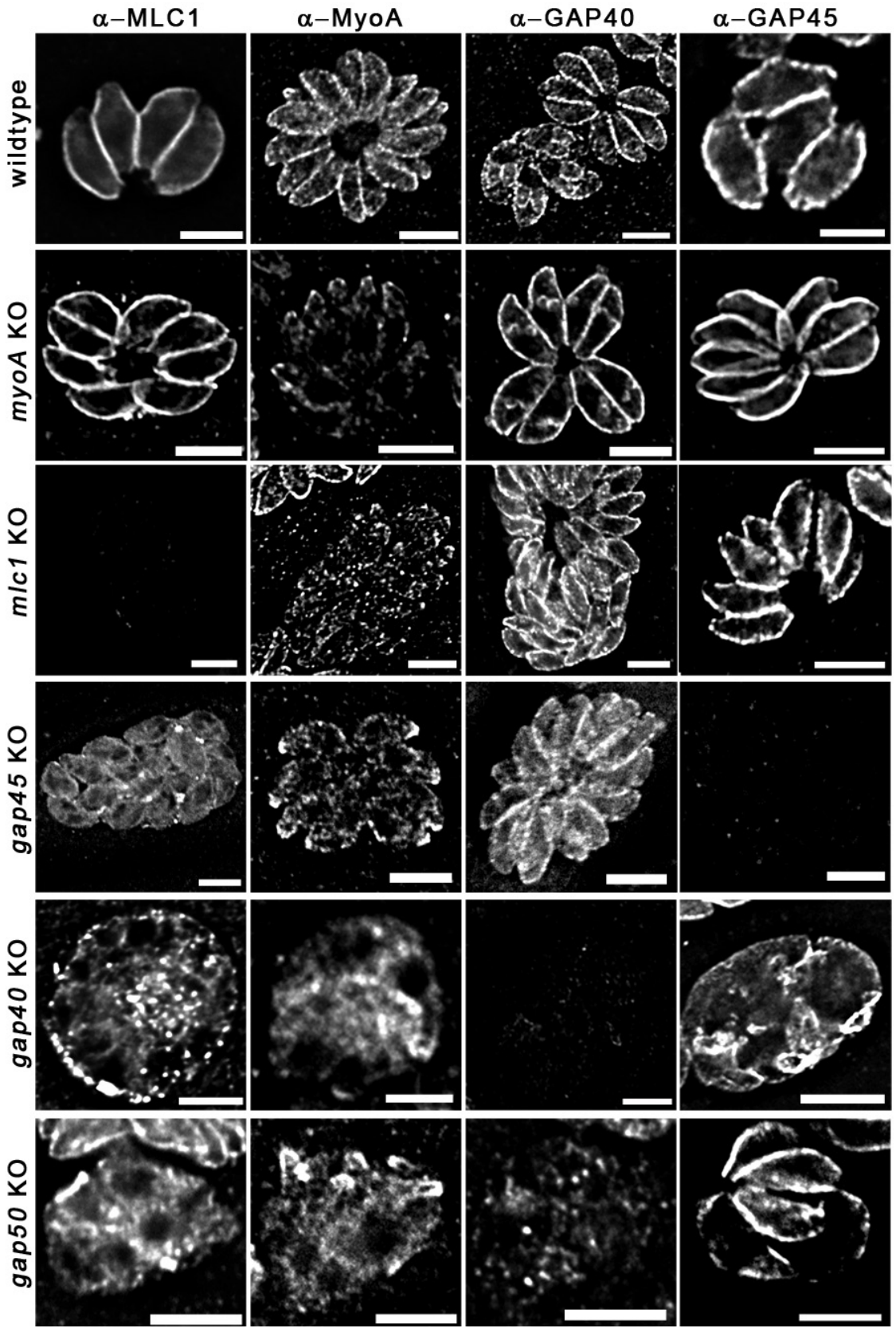

Figure 4-3: Localisation of MyoA motor complex in the various KO strains. The localisation of MLC1 was redistributed to the cytosol in all three *gap* KOs. Deletion of any component of the MyoA motor complex changed the localisation of MyoA from the periphery to the cytosol. Furthermore, GAP40 was only affected when GAP50 was depleted and GAP45 stayed at the periphery in all KOs examined. Scale bar represents 5 µm.

4.4 Characterisation of a conditional *myoA/B/C* KO[1]

Although disruption of *myoA* caused a severe defect on gliding motility, invasion and egress, the *myoA* KO line remained viable in culture (Andenmatten *et al*. 2013, Egarter *et al*. 2014). Surprisingly, *myoA* KO parasites showed short circular movement in the 2D gliding assay with a gliding motility rate of 15 % compared to wild-type parasites. Furthermore, the invasion rate of *myoA* KO parasites was 25 % when standardised to wild-type parasites. Interestingly, overexpression of Ty-MyoC in the *myoA* KO line led to a redistribution of MyoC from its typical localisation at the posterior pole to the periphery of the parasite. Additionally, a partial complementation of the *myoA* KO phenotype was observed. While the overall growth was significantly slower, invasion and 2D gliding appeared to be restored to wildtype levels (Dr Nicole Andenmatten, personal communication).

Because of this observation and based on its close homology to MyoA (Foth *et al*. 2006) the previously generated conditional triple KO for *myoA* and *myoB/C* (see chapter 3.6.6) was used to examine redundancy of these myosins throughout the lytic cycle. First, the growth behaviour of these parasites was examined. 200 parasites for each strain were inoculated on HFF cells and cultured for five days prior to fixation with 4 % PFA. As anticipated, no growth defect was observed for the wild-type line GFPLacZ or the parental line loxPMyoA (see Figure 4-4). Moreover, no growth defect was discovered for loxPMyoA-*myoB/C* KO parasites, indicating that *myoB/C* is not important for parasite survival *in vitro*. Induction of loxPMyoA and loxPMyoA-*myoB/C* KO with 50 nM rapamycin led to the efficient elimination of *myoA* (~60 % of the population, data not shown), resulting in *myoA* KO and *myoA/B/C* KO parasites, respectively. While a clonal *myoA* KO was easily isolated (Egarter *et al*. 2014), several attempts to gain a viable triple knockout failed, indicating that removal of all three myosins is not tolerated by *T. gondii*. Indeed, in growth assays it was observed that parasites lacking *myoA* could form small plaques whereas parasites lacking *myoA/B/C* were not able to form any plaques in a HFF monolayer and died in their vacuoles (Figure 4-4).

[1] Adapted from Egarter *et al* (2014)

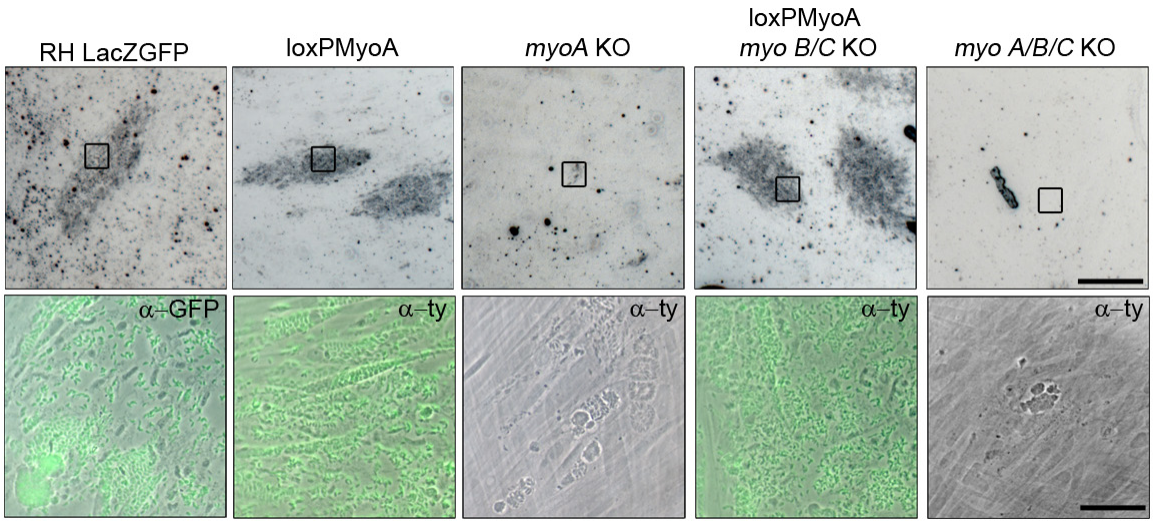

Figure 4-4: Characterisation of the *myoA/B/C* KO. (A) Growth analysis of indicated parasites on HFF monolayers for 5 days. To obtain *myoA/B/C* KOs, the loxPMyoA *myoB/C* KO was treated with 50 nM rapamycin for 4 h prior to inoculation. RHLacZ GFP and loxPMyoA served as controls showing normal growth behaviour. The loxPMyoA-*myoB/C* KOs displayed no growth defect. In contrast, the *myoA* KO and *myoA/B/C* KO parasites showed a severe defect in plaque formation. The absence or presence of *myoA* was determined through staining against Ty-tagged MyoA (in green). Scale bars: 0.2 mm (top panels); 20 µm (bottom panels). Figure adapted from Egarter *et al*. (2014).

Because of this, the next step was to examine the intracellular growth of the parasites. HFF cells were inoculated with parasites (96 hours post-induction with 50 nM rapamycin) for one hour prior to rigorous washing steps with media to remove all loosely attached parasites. Cells were cultured in standard conditions for 24 hours followed by fixation and IFA staining against Ty-MyoA and IMC1 to identify KO parasites that lost Ty-MyoA through excision. Consistent with the growth analysis, loxPMyoA-*myoB/C* KO parasites showed no defect in replication compared to control parasites. Moreover, the *myoA* KO and *myoA/B/C* KO lines replicated slightly slower compared to wild-type lines (Figure 4-5A). Next, host cell egress was analysed. Parasites were treated with or without 50 nM rapamycin for 96 hours prior to artificially triggering egress with calcium ionophore (A23187) for 5 minutes. An increase of intracellular calcium levels led to the secretion of micronemes such as perforin like protein 1, which ruptures the parasitophorous vacuole membrane (Black *et al*. 2000, Kafsack *et al*. 2009). While parasites lacking *myoB/C* showed no effect on host cell egress, *myoA* KO were severely delayed in egress (personal communication with Dr Nicole Andenmatten) and *myoA/B/C* KO parasites were completely blocked in egress (Figure 4-5B).

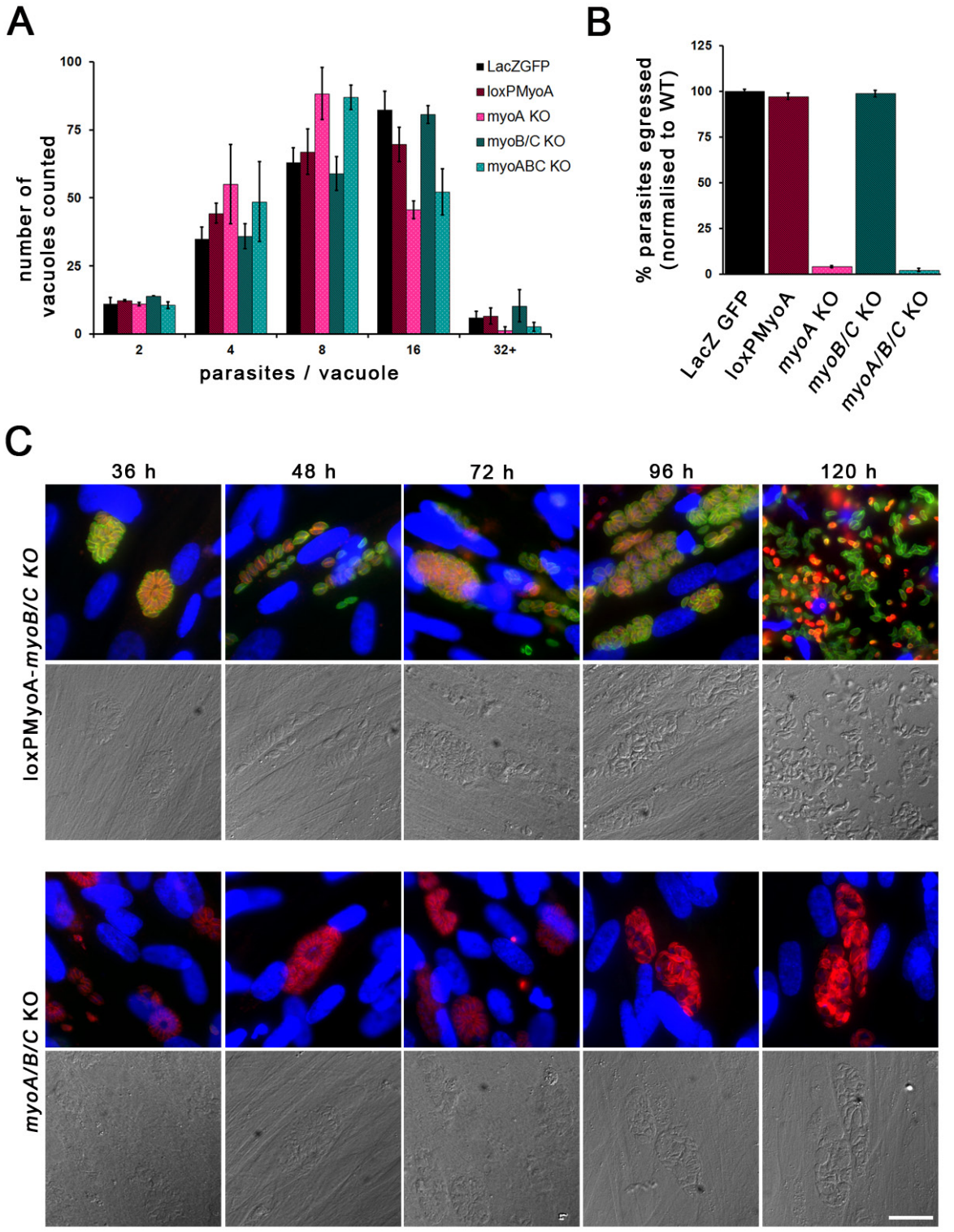

Figure 4-5: Examination of replication and egress in *myoA/B/C* KO parasites. (A) Replication analysis of the indicated parasite lines showed no defect. Mean values of three experiments are shown, ± SEM. (B) Egress analysis of indicated parasites treated ± 50 nM rapamycin 96 h prior to artificially triggering egress with Ca^{2+}-ionophore (A23187) for 5 minutes. For quantification, mean values of three independent experiments are displayed ± SEM. The egress rates were standardised to RHLacZ GFP. (C) Natural egress of loxPMyoA-*myoB/C* KO and *myoA/B/C* KO parasites. Parasites were inoculated on HFF cells and fixed after indicated times. Subsequent IFA was performed using α-IMC1 and DAPI. Whereas parasites lacking *myoB/C* completely lysed the host cells after 120 h, the *myoA/B/C* KO parasites were not capable of egress, and died in their vacuoles. Staining: DAPI (blue), IMC1 (red) and Ty (green). Scale bar represents 20 µm. Figure adapted from Egarter *et al.* (2014).

Next, the ability to naturally egress from host cells was studied in parasites lacking *myoB/C* or *myoA/B/C*. Parasites were inoculated on host cells and fixed after 36, 48, 72, 96 and 120 hours, and samples were processed for IFA using α-IMC1, α-Ty and DAPI. Parasites without *myoB/C* showed intact parasites at all timepoints and parasites were able to egress, re-invade and subsequently lyse the host cell monolayer after 120 hours, indicating they had no defects in egress or invasion. Similarly, *myoA/B/C* KO parasites were structurally intact after 24, 36 and 48 hours (consistent with the replication data in Figure 4-5A) and hence showed no morphological defect that would result in a block in egress. Nevertheless, parasites lacking all three myosins were blocked in natural egress from the host cell and died intracellularly after 96 hours post-inoculation, as observed by deformed IMC and collapsed vacuoles (Figure 4-5C).

Host-cell invasion was investigated next. Parasite lines were allowed to invade HFF cells for 30 minutes followed by fixation and immunostaining with SAG1 and Ty antibodies. While *myoA* KO parasites showed the previously reported invasion rate of 25 % (Andenmatten *et al*. 2013), the invasion rate of parasites lacking *myoA/B/C* was reduced five-fold and dropped to 5 % compared to wild-type parasites (Figure 4-6A). To investigate if *myoA/B/C* KO parasites use the "conventional" route of invasion, parasites were analysed for the formation of a tight junction during invasion. Host cells were infected with a high MOI of parasites, centrifuged at 200 x *g* for two minutes and allowed to invade for five minutes prior to fixation. An IFA against the TJ protein RON4 was performed. As in the *myoA* KO parasites, parasites lacking all three myosins invade through a RON4-positive TJ (Figure 4-6B) suggesting they follow a similar route for host cell entry. Given that *myoA/B/C* KO parasites displayed a decreased invasion rate compared to *myoA* KO, this indicates that MyoA and MyoB/C have overlapping functions. However, it cannot be ruled out that cumulative effects cause a more severe phenotype that is not a direct result of a non-functional myosin complex. Furthermore, additional myosins play a role during the invasion process, but creating multiple KOs for the entire myosin repertoire that can potentially substitute for MyoA and MyoB/C would be technically challenging.

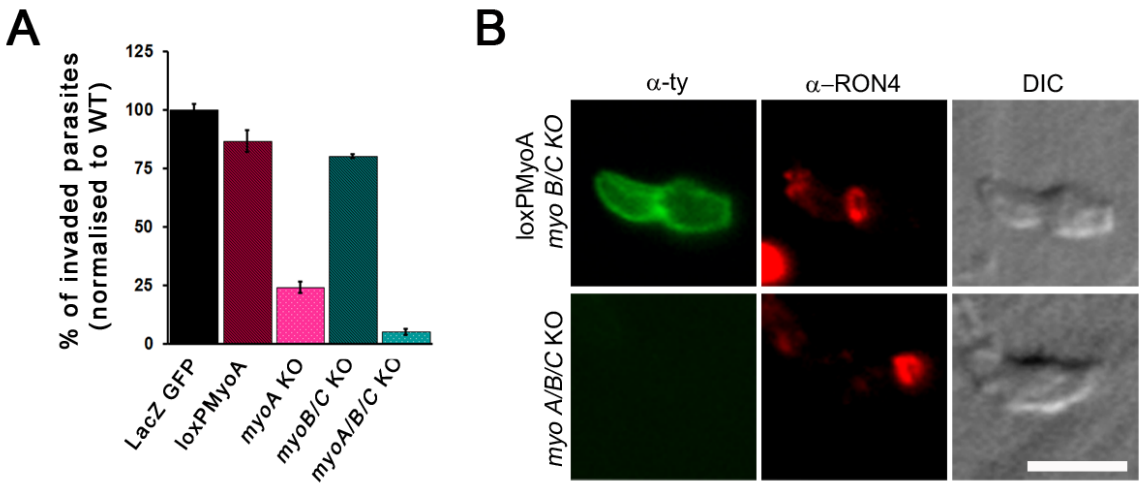

Figure 4-6: Invasion assays and tight junction formation in *myoA/B/C* KO parasites. (A) Invasion assay of parasites treated ± 50 nM rapamycin 96 h prior to invasion. Parasites were allowed to invade for 30 minutes prior to fixation. For quantification, 300 parasites were examined. Mean values of three experiments are displayed, ± SEM. All strains were standardised to RHLacZ GFP. (B) IFA with indicated antibodies of invading parasites demonstrates that parasites lacking all three myosins still form a RON4-positive tight junction (TJ). Scale bar: 5 µm. Figure adapted from Egarter *et al.* (2014).

4.5 Phenotypical characterisation of a conditional *mlc1* KO[2]

At present, seven myosin light chains have been identified in *Toxoplasma gondii* and their localisation has been determined recently (Herm-Gotz *et al.* 2002, Polonais *et al.* 2011). Two of these light chains, MLC1 and MLC2, have a peripheral localisation. While MLC2 interacts with MyoD, MLC1 interacts with the MyoA motor complex and thus is part of the gliding and invasion machinery and consequently a target for development of invasion inhibitors (Herm-Gotz *et al.* 2002, Heaslip *et al.* 2010) (Dr. Jacqueline Leung, personal communication). After successful generation of a conditional *mlc1* KO (see Chapter 3.6.2), the function of MLC1 during the lytic cycle of *Toxoplasma* was examined in more detail. First, growth assays were performed. 200 parasites for each strain were inoculated on HFF cells and cultured for five days prior to fixation with 4 % PFA. Parasites lacking *mlc1* were not able to form plaques in the host cell monolayer (Figure 4-7A). Furthermore, attempts to isolate viable *mlc1* KO parasites were unsuccessful, suggesting that MLC1 is essential for parasite survival *in vitro*. Although MLC1 was not detectable in YFP-positive parasites as early as 48 hours post-induction, phenotypic analysis as illustrated in Figure 4-4 was performed 96 hours after induction with rapamycin to discard the possibility that residual

[2] Adapted from Egarter *et al.* (2014)

MLC1 was present. Additionally, *mlc1* KO parasites could be maintained in culture for up to two weeks when artificially released from infected host cells, before they were outgrown by non-excised parasites in the culture (data not shown). Next, intracellular replication of *mlc1* KO parasites was studied. HFF cells were inoculated with parasites (96 hours post-induction with 50 nM rapamycin) for one hour prior to vigorous washing steps with media to remove non-attached parasites. Cells were cultured with standard conditions for 24 hours followed by fixation and IFA staining against IMC1. No effect on replication was observed in parasites lacking *mlc1* (Figure 4-7B).

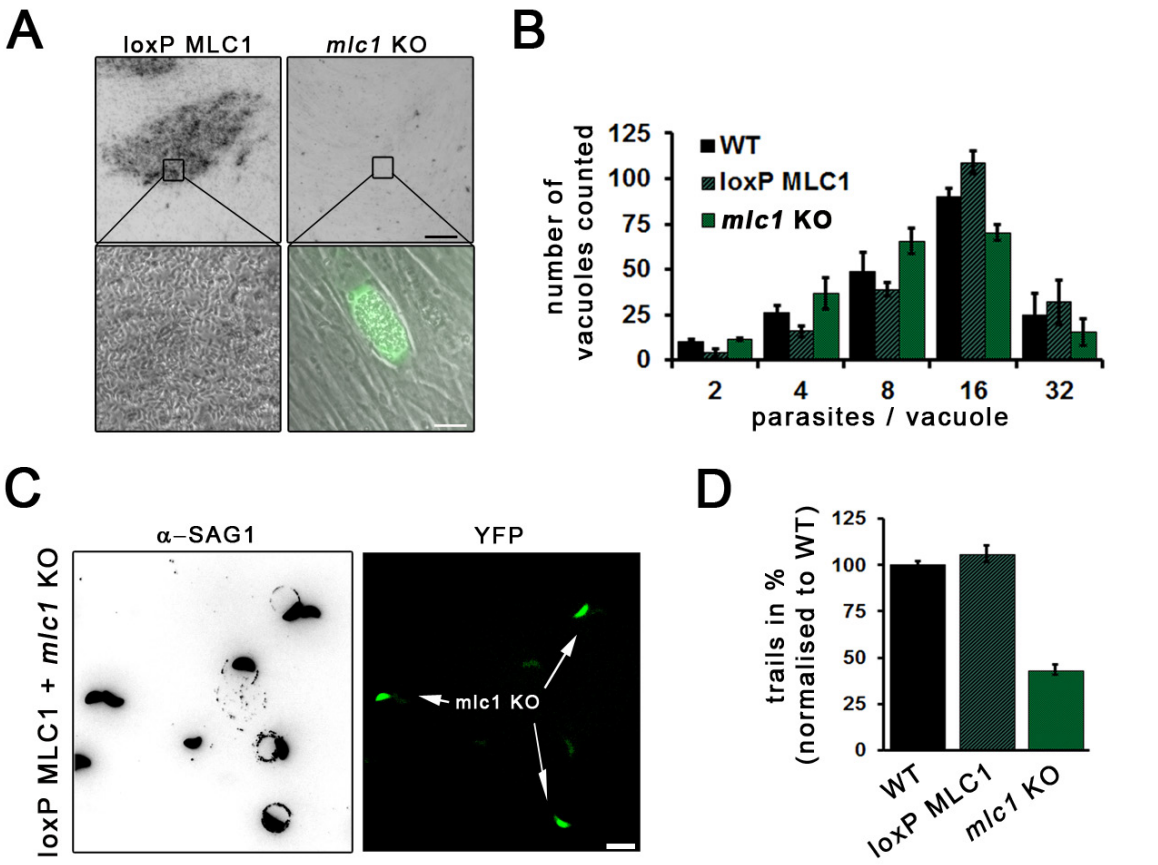

Figure 4-7: Phenotypic characterisation of *mlc1* KO parasites. (A) Plaque formation of indicated parasites was analysed after 5 days. No plaque formation was observed in *mlc1* KO parasites. Scale bars: 0.2 mm (top panels) and 20 µm (bottom panels). (B) Replication analysis of *mlc1* KO parasites was performed 96 h post-induction. Parasites were allowed to invade for 1 h prior to replication for 24 h. For quantification, the number of parasites per parasitophorous vacuole was determined. Mean values of three independent assays are shown ± SEM. (C) Trail deposition assays were performed 96 h post-induction by allowing parasites to glide on FBS-coated coverslips for 30 minutes prior to staining with α-SAG1. Despite the low excision rate of loxPMLC1, *mlc1* deficient parasites can be easily identified due to their YFP expression (see arrows). Scale bar: 10 µm. (D) Quantification of trail deposition assay showed that the motility of *mlc1* KO parasites was 42 % that of the wild-type parasites. Mean values of three independent experiments are shown ± SEM. The number of trails was standardised to wild-type parasites. Figure adapted from Egarter *et al.* (2014).

Next, the ability of *mlc1* KO parasites to move on coated 2D surfaces was examined. *Toxoplasma* tachyzoites display three distinct types of gliding motility referred to as circular, helical and upright twirling (see chapter 1.9.1) (Hakansson *et al*. 1999). During upright twirling, parasites spin with their posterior pole attached to the surface and thus do not travel over a distance. In contrast, the parasites can move along the surface using helical or circular gliding, which can be visualised by IFA using antibodies that recognize shed surface antigens such as SAG1. To analyse the impact on gliding motility in *mlc1*-lacking parasites (96 hours post-induction), trail deposition assays were performed in which parasites were allowed to glide on FBS-coated glass coverslips for 30 minutes prior to fixation and IFA against SAG1. Given the lower excision rate of loxPMLC1 which results in a population of 35 % YFP-positive (*mlc1* KO) and 65 % YFP-negative (non-excised loxPMLC1; parental line) parasites, it was feasible to compare the trails of loxPMLC1 with *mlc1* KO parasites. As anticipated, long circular and helical trails were observed in wild-type parasites. Interestingly, mainly circular trails were detected in the *mlc1* KO parasites, akin to the phenotype observed for *myoA* lacking parasites (Figure 4-7C). Moreover, the overall percentage of parasites forming trails of *mlc1* KO parasites was decreased to approximately 42 % when compared to wild-type parasites (Figure 4-7D).

Since gliding motility is linked to invasion and egress, these two processes were evaluated next. First, the *mlc1* KO parasites were examined for their ability to naturally egress from host cells. LoxPMLC1 and *mlc1* KO parasites were inoculated on host cells and fixed after distinct timepoints (24, 36, 48, 72, 96 and 120 hours) and subsequently stained with IMC1 antibody and DAPI. The parental line, loxPMLC1 showed typical growth behaviour: small vacuoles were observed after 24 hours, and they increased in size until parasites naturally egressed from the host cell and reinvaded neighbouring cells. Several rounds of egress and invasion led to complete lysis of the host cell monolayer after 120 hours. In contrast, although *mlc1* KO parasite-containing vacuoles were structurally intact after 24, 36 and 48 hours (supporting replication data in Figure 4-7B) and hence showed no morphological defect that would result in a malfunction in egress, they were blocked in naturally exiting the host cell and

started to die inside the vacuoles as soon as 72 hours post-inoculation (Figure 4-8A).

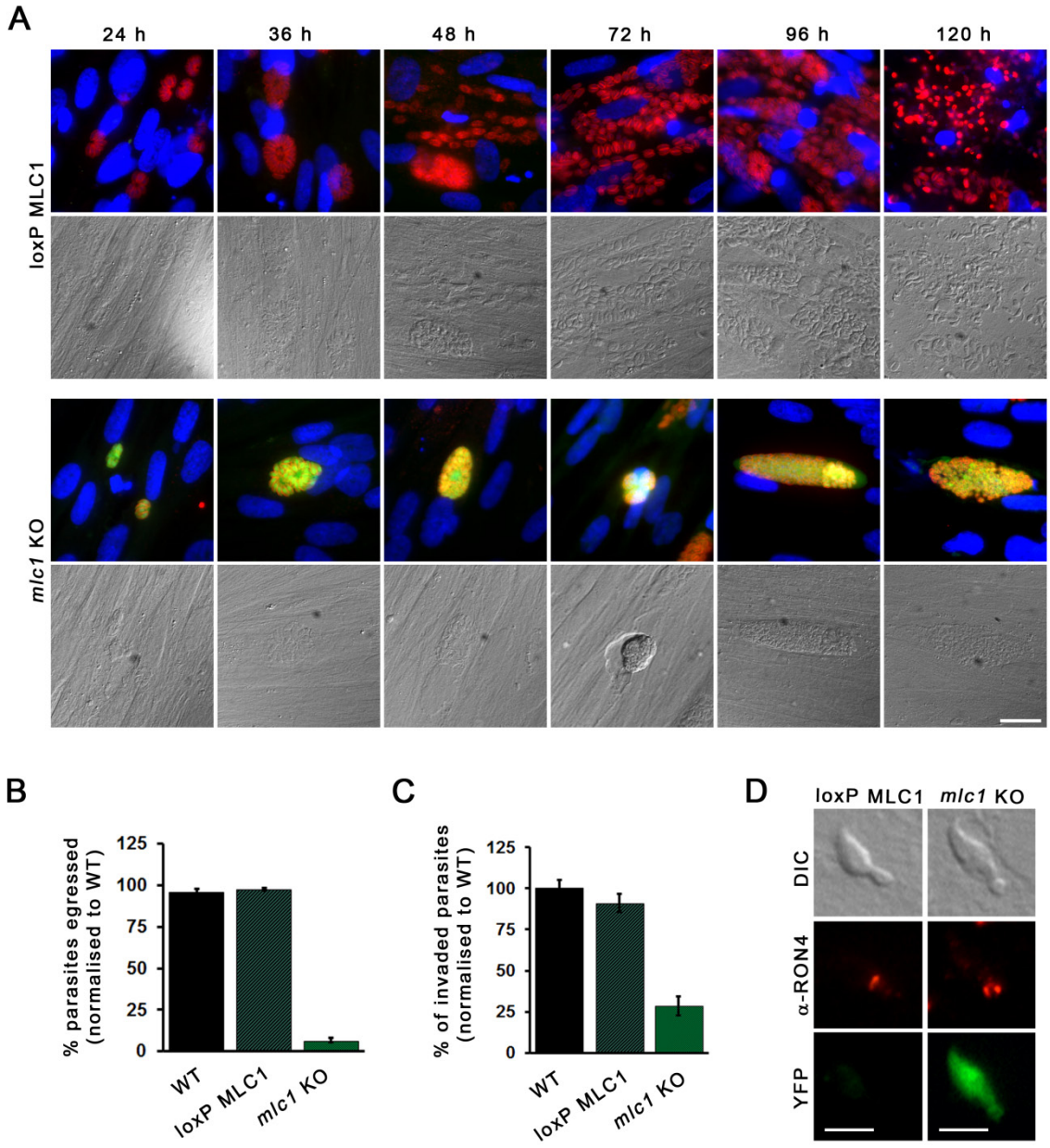

Figure 4-8 Egress and invasion analysis of *mlc1* KO parasites. (A) Natural egress of *mlc1* KO parasites. Parasites were inoculated on HFF cells and fixed after the indicated times. An IFA was then performed staining against IMC1 and DAPI. While the control parasites completely lysed the host cell monolayer after 120 h, the *mlc1* KO parasites were not able to exit the host cell, and died within an intact parasitophorous vacuole. Scale bar represents 20 µm. (B) Egress of loxPMLC1 and *mlc1* KO parasites (96 h post-induction) after artificial induction with Ca^{2+}-ionophore (A23187) for 5 minutes. The egress rates were normalised to wild-type parasites. For quantification of parasite egress, mean values of three independent experiments are shown, ± SEM. (C) Invasion assays of loxPMLC1 and *mlc1* KO parasites were performed 96 h after treatment ± 50 nM rapamycin. Parasites were allowed to invade for 30 minutes. Mean values of three independent assays are displayed ± SEM. (D) IFA of invading parasites using a RON4 antibody demonstrates that parasites lacking *mlc1* were capable of invading the host cell through a typical tight junction (TJ). Scale bar: 5 µm. Figure modified from Egarter *et al.* (2014).

To further investigate this egress phenotype, parasites were treated either with or without 50 nM rapamycin for 96 hours prior to artificially inducing egress with calcium ionophore (A23187) for 5 minutes. As expected, wild-type parasites and loxPMLC1 exited the host cells after addition of calcium ionophore. Analogous to the *myoA/B/C* KO parasites, tachyzoites lacking MLC1 were unable to egress from host cells after calcium ionophore stimulation (Figure 4-8B). Next, host cell invasion was studied. Parasites were allowed to invade HFF cells for 30 minutes followed by fixation and immunostaining against α-SAG1. Interestingly, the invasion rate of *mlc1* KO parasites was 28 % that of wild-type parasites (Figure 4-8C), which is comparable to the observed invasion rate (25 %) of *myoA*-depleted parasites. The *mlc1* KO parasites were then analysed to see if they used the conventional path of invasion via formation of a tight junction. To do this, parasites were added at a high MOI to host cells, centrifuged at 200 x *g* for two minutes and allowed to invade for five minutes prior to fixation and processing for an IFA against the TJ protein RON4. Parasites lacking *mlc1* invaded through a normally appearing TJ (Figure 4-8D). Altogether, *mlc1* is essential for localisation of MyoA at the periphery and host cell egress, but dispensable for gliding motility and invasion of host cells.

4.6 Characterisation of a conditional *gap45* KO[3]

Previously, GAP45 was described as the membrane receptor for the gliding and invasion machinery, and a crucial component to link the MyoA motor complex to plasma membrane and IMC (Gaskins *et al*. 2004). The functions of GAP45 during motility-dependent processes were extensively studied using the tetracycline-inducible knockdown system (Frenal *et al*. 2010). Downregulation of GAP45 led to a redistribution of components of the MyoA motor complex from the periphery to the cytosol in conjunction with the loss of IMC stability. Additionally, *gap45* KD parasites showed a severe effect in egress, a block in gliding motility and a decrease to 25 % of the invasion rate relative to wild-type parasites (Frenal *et al*. 2010). Since this invasion rate could be due to residual expression of GAP45 in the KD line, the DiCre inducible conditional *gap45* KO strain (see chapter 3.6.3) was used to re-dissect the role of GAP45 during these processes. First, growth assays were performed as described above. No plaque formation was

[3] Adapted from Egarter *et al.* (2014)

observed for *gap45* KO parasites (Figure 4-9A). Nevertheless, like the *mlc1* KO line, *gap45* KO parasites could be maintained in culture for up to two weeks when artificially released from the host cells, before they were outgrown by non-excised parasites in the culture (data not shown). However, it was impossible to isolate a viable *gap45* KO clone, indicating that GAP45 is essential for parasite viability *in vitro*. Next, intracellular replication of the *gap45* KO was evaluated. HFF cells were inoculated with parasites (96 hours post-induction with 50 nM rapamycin) for one hour prior to washing with media to remove all loosely attached parasites. Cells were cultured in standard conditions for 24 hours followed by fixation and IFA staining against IMC1. Parasites without GAP45 were not affected in replication (Figure 4-9B).

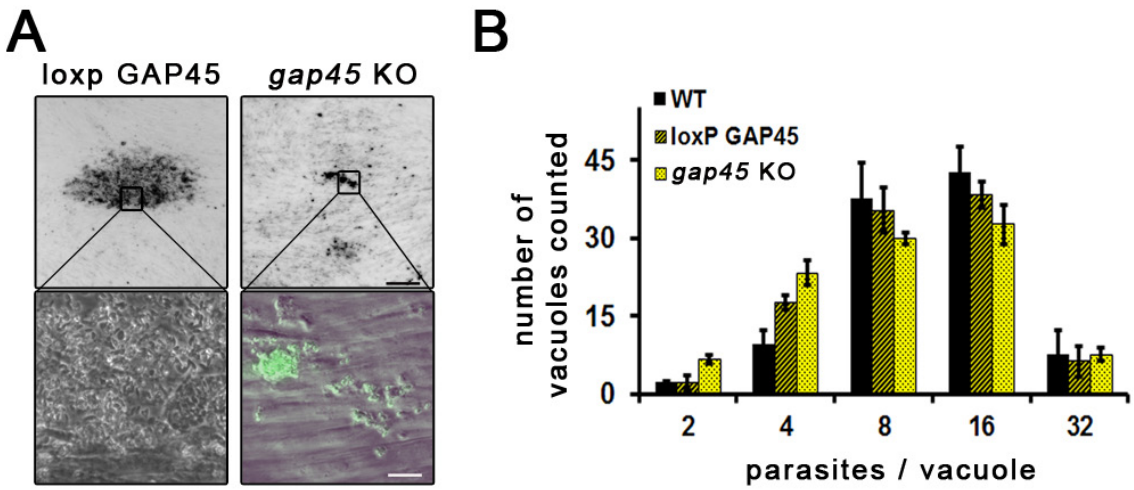

Figure 4-9: Growth analysis of *gap45* KO parasites. (A) Growth of the indicated parasite strains. Plaque formation was analysed after five days. The *gap45* KO parasites were incapable of plaque formation. Scale bars: 0.2 mm (top panels), 20 µm (bottom panels) respectively. (B) Replication analysis of *gap45* KO parasites was performed 96 h post-induction. Parasites were allowed to invade for 1 h before replication for 24 h. To quantify the replication rate, the number of parasites per parasitophorous vacuole was determined. Mean values of three independent assays are shown ± SEM. Figure adapted from Egarter *et al*. (2014).

Unlike depletion of MyoA/B/C or MLC1, removal of GAP45 affected parasite morphology. After host cell egress, *gap45* KO parasites changed from a crescent to a round shape. To investigate this in more detail, IFA of *gap45* KO parasites was performed, stained against IMC1 48 hours after induction with 50 nM rapamycin. Most intracellular parasites were found in typically shaped large vacuoles, with their IMC localising at the periphery as expected. However, some vacuoles had parasites inside that showed abnormal morphology, and had died within the host cell. In addition, rounded, extracellular parasites were identified in which the plasma membrane detached from the IMC (Figure 4-10A; white

arrow). In some cases, no IMC staining could be observed (Figure 4-10A; yellow arrow). Furthermore, ultrastructural analysis was performed 72 hours post-induction with rapamycin and confirmed the IMC detachment from the plasma membrane (Figure 4-10B). This crippled morphology in extracellular parasites recapitulated the descriptions for *gap45* KD parasites (Frenal *et al*. 2010) to a more pronounced extent.

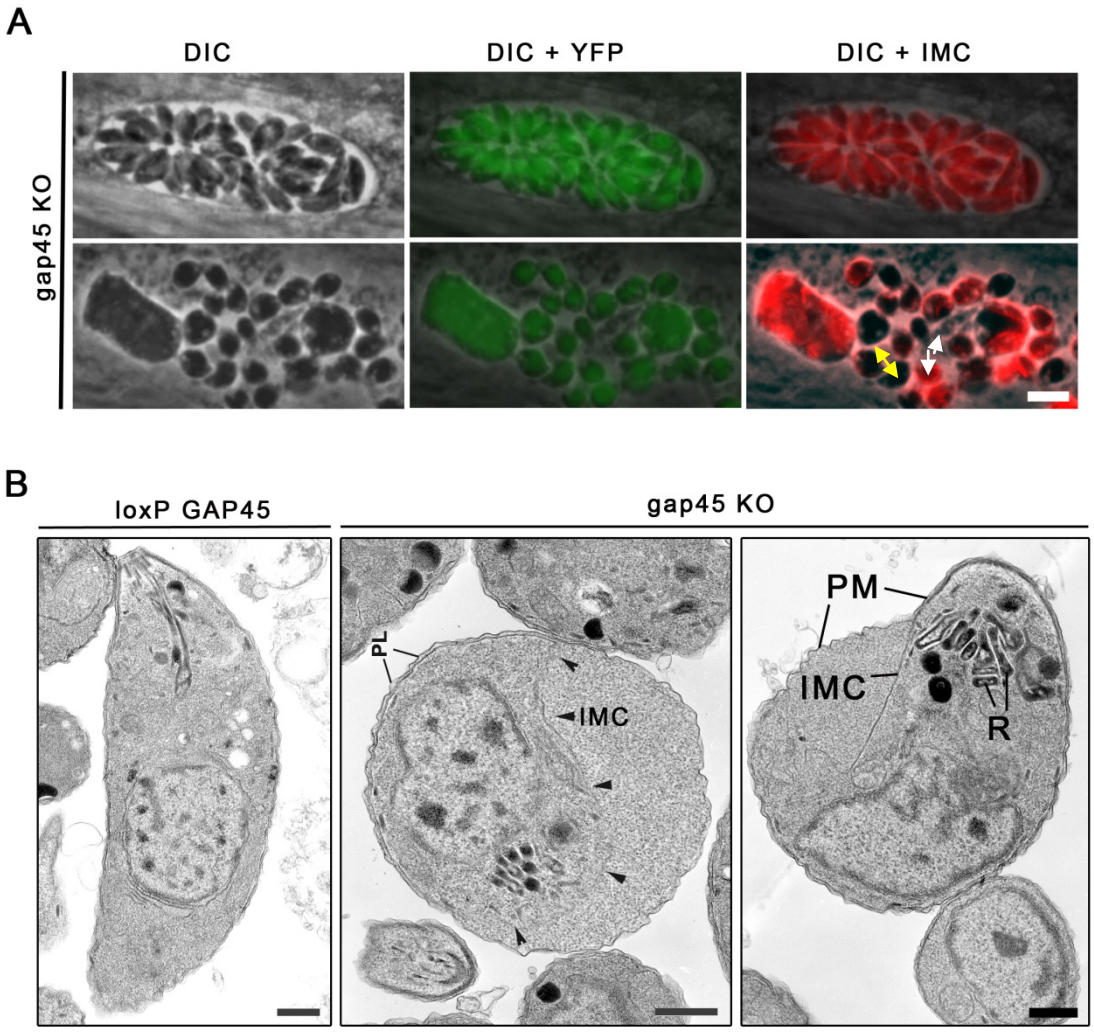

Figure 4-10: Morphology defect of parasites lacking *gap45*. (A) IFA of *gap45* KO staining against IMC1 48 h after induction with 50 nM rapamycin. Most intracellular parasites were found in typically shaped vacuoles with the IMC localising to the periphery. However, several vacuoles had parasites that showed abnormal morphology and had died within the cell. In addition, rounded, extracellular parasites were found in which the plasma membrane had detached from the IMC. In some cases, no IMC staining was observed. Scale bars represent 5 µm. (B) Ultrastructural analysis of extracellular *gap45* KO parasites. The parental line, loxPGAP45, showed the typical crescent shape morphology of *Toxoplasma* tachyzoites. Ultrastructural analysis of extracellular *gap45* KO parasites displayed a change in morphology from a normal crescent shape to a more spherical shape. Detail of a spherically shaped parasite showing the separation of the inner membrane complex (IMC) from the plasma membrane (PL; PM) disrupting the pellicular structure (see arrows). Scale bar represents 500 nm. Figure modified from Egarter *et al*. (2014).

Next, the ability of *gap45* KO and *gap45* KD parasites to glide on surfaces was studied in a similar manner as described for *mlc1* KO (see chapter 4.5). To

analyse the effect on gliding motility in *gap45*-deficient parasites, trail deposition assays were performed in which parasites were allowed to glide on FBS-coated glass coverslips for 30 minutes prior to fixation and staining against SAG1. Surprisingly, both *gap45* KD and *gap45* KO parasites were capable of moving on the coated surface (Figure 4-11A), in contrast to previous findings where a block in gliding was reported (Frenal *et al*. 2010).

Quantitative analysis of gliding motility of parasites lacking *gap45* showed that there was no significant difference in the number of trails formed compared to control parasites (Figure 4-11B). Gliding motility was investigated further by time-lapse microscopy, with 19 circular gliding parasites imaged and manually tracked. Generally, *gap45* KO parasites moved slower and seemed to be arrested for a prolonged period after moving for a semi-circle before starting a new boost of motility. Although *gap45* KO parasites displayed a similar number of trails in trail deposition assays, the gliding speed was severely affected. While wild-type parasites moved with an average speed of 1.7 µm/s, the average speed of parasites lacking *gap45* was more than threefold lower at 0.5 µm/s (Figure 4-11C). Imaging RHΔhxgprt and *gap45* KO parasites for a time span of two minutes revealed that parasites lacking *gap45* require over a minute to complete a full circle whereas wild-type parasites had already started their fourth circle within the same timeframe (Figure 4-11D). Gliding speed appeared to be dependent on parasite morphology, in that more crescent-shaped parasites were capable of gliding more efficiently, while more spherically-shaped parasites had a slower, less efficient motility. Since MyoA localises to the cytosol instead of the periphery in *gap45* KO parasites, the speeds of myoA and *gap45* KO was compared. Intriguingly, parasites lacking MyoA moved even slower, at 0.2 µm/s (Egarter *et al*. 2014).

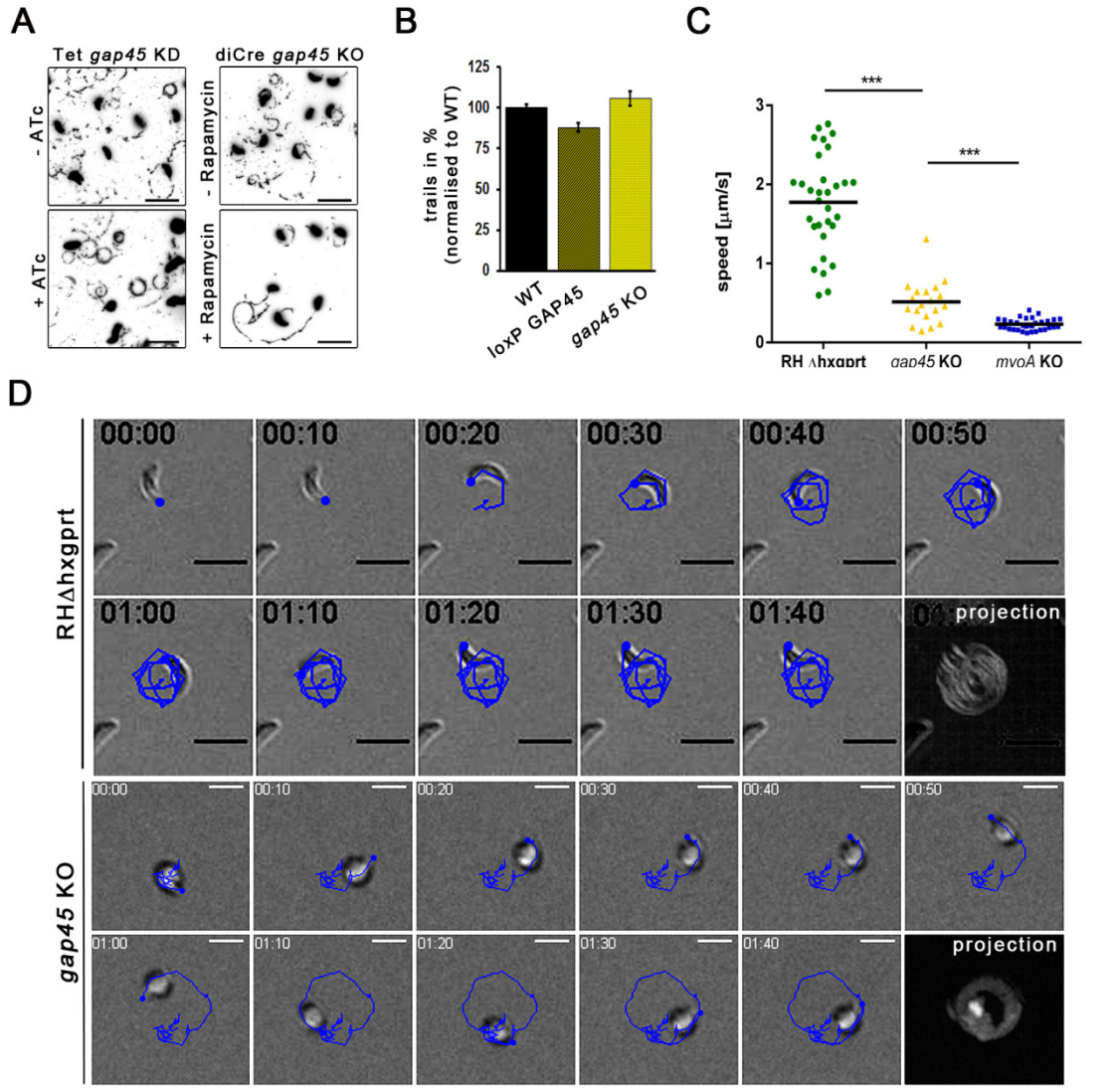

Figure 4-11: Analysis of gliding motility of *gap45* KO parasites. (A) Trail deposition assays were performed by allowing the parasites to glide on FBS-coated coverslips for 30 minutes followed by SAG1 staining. The assays were performed 96 h post-induction ± 50 nM rapamycin. Analysis of the *gap45* knockdown parasites (Frenal et al., 2010) was performed after induction with ATc for 96 h. Scale bars: 20 µm. (B) Quantification of trail deposition assays reveals no gliding defect for *gap45* KO parasites when numbers of trails were scored. Mean values of three independent experiments are shown ± SEM. (C) Kinetics of gliding motility of *gap45* KO parasites. The average speed of 19 manually tracked parasites was analysed. Wild-type parasites moved at a speed of 1.7 µm/s whereas the speed of *gap45* KO parasites was significantly reduced to 0.5 µm/s, ***: p-value < 0.001 in a two tailed student's t-test (D) Time-lapse microscopy of gliding motility of indicated parasites, with the time labelled in seconds. Parasites were manually tracked (blue line). The composite image shows a projection of 110 images acquired at 1 second intervals. Scale bar represents 5 (top two rows) and 10 µm (bottom two rows), respectively. Figure modified from Egarter *et al.* (2014).

Next, host cell egress was analysed. Parasites were incubated with or without 50 nM rapamycin for 96 hours prior to artificially inducing egress with calcium-ionophore (A23187) for five minutes. Depletion of *gap45* caused a severe effect on parasite egress (Figure 4-12A) similar to the effect seen for *mlc1* KO parasites. Host cell invasion was then examined by an invasion replication assay. Parasites were allowed to invade HFF cells for one hour followed by 24 hours of

replication prior to fixation and staining against IMC1. Compared to control parasites, only 6 % of the parasites were capable of invading host cells (Figure 4-12B). Moreover, the invasion rate stayed almost the same (7.5 %) when parasites were allowed to invade for four hours (Figure 4-12C). To investigate if *gap45* KO parasites invade via the conventional way, formation of the tight junction was studied as previously described. Strikingly, even morphologically rounded parasites invaded through a RON4-positive TJ (Figure 4-12E), indicating that key features of the invasion process were conserved. In summary, GAP45 has a crucial role as a structural component of the pellicle. The significant effects observed during egress and invasion may be due to the structural function of GAP45 and not due to its direct role in these processes.

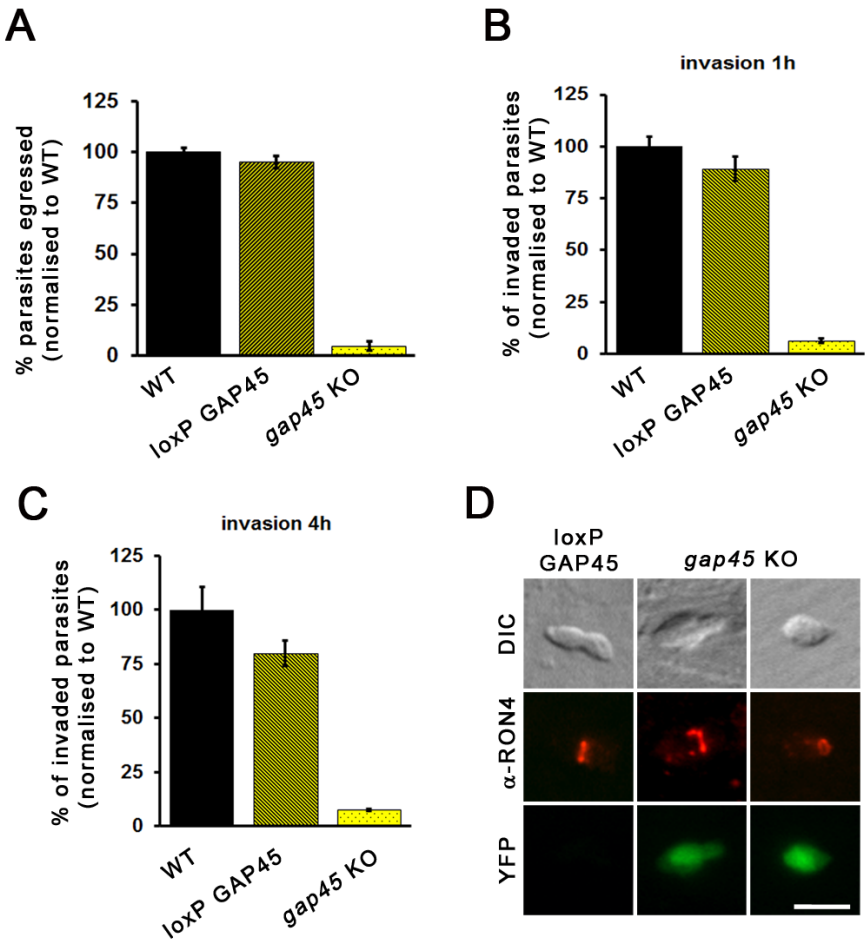

Figure 4-12: Studies of egress and invasion of *gap45* KO parasites. (A) Intracellular parasites were artificially induced with Ca^{2+} ionophore (A23187) for five min to trigger egress. For quantification, mean values of three independent egress assays are shown ± SEM. The egress rates were standardised to wild-type parasites. (B) Invasion assays were performed 96 h after excision of *gap45*. Parasites were allowed to invade for 1 h prior washing the coverslips with PBS to remove all extracellular and loosely attached parasites. Parasites were fixed after 24 h and the number of vacuoles in 25 fields of view was determined. Mean values of three independent assays are shown ± SEM. All strains were standardised to wild-type parasites. (C) Same as in (B) but the invasion time was increased from one to four hours. (D) IFA of invading parasites demonstrates that *gap45* KO parasites are capable of invading the host cell and form a tight junction, as visualised by RON4 staining. Scale bar: 5 µm. Modified from Egarter *et al*. (2014).

4.7 Summary and brief discussion[4]

In this chapter I have analysed the components of the MyoA motor complex in great detail. While it could be demonstrated that that some components affect each other in terms of localisation, others like GAP45 were unaffected. Removal of any component of the MyoA motor complex altered the localisation of MyoA from the periphery to the cytosol. This cytosolic signal appears to be a cross reaction, since it can be detected in *myoA* KO parasites as well, indicating the possibility that MyoA is fully degraded in the absence of MLC1, as observed in the case of *P. berghei*, where depletion of MTIP (the homologue of MLC1) results in the complete loss of MyoA (Sebastian *et al*. 2012).

MLC1 is crucial for host cell egress, but not for gliding motility or invasion of host cells. Together, these data propose that no other myosin light chain can complement MLC1, at least for MyoA function and localisation. Nevertheless, a partial complementation of MyoA motor function through an alternative motor complex cannot be excluded. The recently studied MyoD-MLC2 motor is localised at the periphery (Polonais *et al*. 2011) like MyoA-MLC1, and could be a hypothetical candidate for complementation after loss of MyoA-MLC1.

The data obtained for *gap45* KO parasites show that GAP45 has a crucial, structural role for the attachment of the plasma membrane and IMC, as well as for anchoring the MyoA motor complex to both membranes. However, since the gliding motility rate was not affected and *gap45* KO parasites were able to glide faster than *myoA* KO but still less efficient than wildtype, it appears that *Toxoplasma* can efficiently move even in the absence of a MyoA motor complex that is correctly anchored to the IMC. The decrease of invasiveness is likely a consequence of the morphological defects of these mutants and not caused by impairment of gliding motility as was previously thought. While the study of these MyoA motor mutants indicates that alternative pathways must be in place that can power gliding motility and invasion, an important function of other myosin motors cannot be excluded. However, in the case of the *gap45* KO parasites, this motor must be localised at the apical tip of the parasite which is still intact, meaning the plasma membrane and IMC are not detached, as shown

[4] Adapted from Egarter *et al*. (2014)

by ultrastructural analysis (Figure 4-10B). A summary and comparison of the roles of the components of the MyoA motor complex during motility-dependent processes can be found in Table 4-1. In order to investigate if invasion requires a myosin motor, the role of parasite actin will be examined in more detail in the next chapter, since any myosin motor complex will require polymerised actin in order to perform its function as a motor.

Parasite line	Viability *in vitro*	Intracellular growth	Egress (%) standardised to WT	Invasion (%) standardised to WT	Gliding (%) standardised to WT
***myoA* KO**	Viable	No effect	4 ± 0.6	24 ±0.9	37 %[1]
***myoB/C* KO**	Viable	No effect	98 ±1.8	80 ± 2.4	N.d.
***myoA/B/C* KO**	N.d.	No effect	2 ± 0.9	5 ±1.2	N.d.
***mlc1* KO**	Up to 14 days	No effect	5 ± 0.9	28 ± 4.6	42 ± 2.7
***gap45* KO**	Up to 14 days	No effect	4 ± 1.3	6 ± 1.1	106 ±4.5
***gap40* KO**	Not viable	Blocked	N.d.	N.d.	N.d.
***gap50* KO**	Not viable	Blocked	N.d.	N.d.	N.d.

[1] Data obtained from Egarter *et al*. (2014)

Table 4-1: Summary of KO mutants of the gliding and invasion machinery and their respective phenotypes.

5 Characterisation of a conditional *act1* KO

5.1 Introduction

Actin is a fundamental protein found in almost all eukaryotic cells. The genome of *Plasmodium spp*. encodes for two actin genes and *Toxoplasma gondii* encodes for only one conventional actin gene namely *TgAct1* (Dobrowolski *et al*. 1997). It is believed that these apicomplexan parasites require regulated polymerisation and depolymerisation of actin for gliding motility and active penetration of host cells (Morisaki *et al*. 1995, Hakansson *et al*. 1999, Munter *et al*. 2009). Despite this necessity, the majority (97 %) of actin exists as monomers (G-actin) whereas actin filaments (F-actin) are barely detected. Parasite actins form short, unstable filaments (Wetzel *et al*. 2003, Schmitz *et al*. 2005, Schuler *et al*. 2005, Sahoo *et al*. 2006, Skillman *et al*. 2011). The prerequisite for host cell egress and invasion is a substrate dependant form of locomotion called gliding motility which is an orchestrated process of cell adhesion, coordinated action of the motor and consecutively shedding of surface adhesins (Sibley 2010). Generally most conclusions of actin functions were made using actin disrupting drugs. As off target effects of the used drugs cannot be excluded, a conditional KO for Act1 was generated and will be characterised within this chapter.

5.2 Generation of a conditional *act1* KO

To shed more light on the functions of *Toxoplasma* Act1, an Act1 geneswap construct was generated comprising the endogenous promoter of *act1*, floxed *act1* cDNA, *yfp* ORF, *hxgprt* as selectable marker and approximately 1600 bp of the 3'UTR of *act1* (see Figure 3-6). It needs to be mentioned that a point mutation within the *act1* gene was discovered on the geneswap plasmid. Nevertheless it was continued with transfection of the plasmid. After transfection into the recipient strain ku80::DiCre, that prefers homologous recombination to random integration, homologous recombination occurs, thus replacing the endogenous *act1* gene with the *act1* geneswap plasmid. The correct integration was confirmed by analytical PCR using three distinct sets of primer pairs (Figure 5-1A+B). The first primer pair permits distinction between the intron containing endogenous *act1* and *act1* cDNA by binding to the start and stop sequence of *act1,* thus leading to either 1583 bp or 1145 bp fragment sizes.

The second primer set involved a sense oligo binding to the *hxgprt* selection cassette and an antisense oligo binding downstream of the oligo used for cloning the vector hence has no homology to the plasmid. As a result a band of roughly 2750 bp was amplified for the conditional loxPAct1 strain whereas no PCR product was formed in the wildtype strain (ku80::DiCre) as anticipated. Without rapamycin addition no excision of *act1* occurred. These non-induced parasites were termed loxPAct1 to distinguish between the induced parasites. Upon activation of Cre recombinase, excision of the floxed *act1* cDNA was detected in approximately 15 % of the population determined by YFP expression. This mixed population of non-excised and excised parasites is termed *act1* KO throughout this work and was used to prove the correct integration into the 5'UTR region and the site specific recombination after induction with rapamycin. The used Oligos bind within the 5'UTR upstream of the sequence, referred to as the endogenous promoter, and within the *yfp* ORF. Analytical PCR revealed no PCR product for ku80::DiCre parasites; while a specific fragment of 3500 bp was amplified in loxPAct1 showing specific integration into 5'UTR locus. The *act1* KO displayed in addition a smaller PCR product of 2250 bp confirming site specific recombination (Figure 5-1B). Together these data show that it was possible to generate a conditional KO for Act1, which could be easily regulated upon addition of the inducer. Even though the excision rate was low, the identification of the KO parasites is straightforward because of their YFP expression.

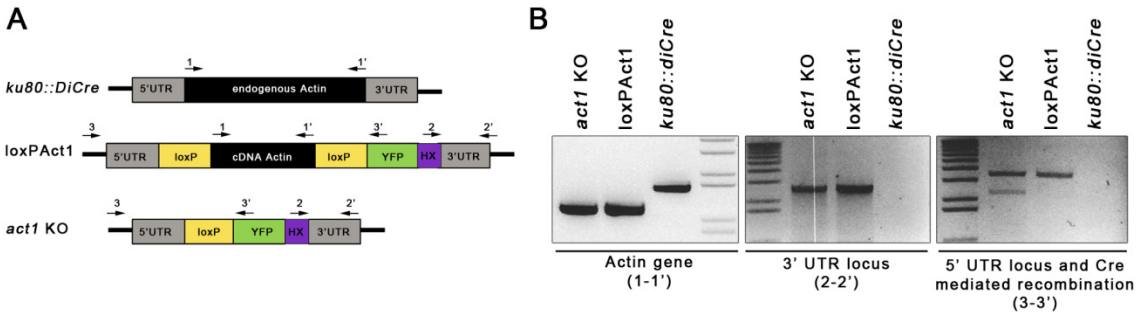

Figure 5-1: Generation of a conditional *act1* KO. A) Schematic model of analytical PCR to verify correct replacement of the endogenous *act1* by the KO construct. (B) Three different Primer combinations were used. The replacement of gDNA through cDNA can be seen by using Primer combination 1+1' The Oligo pair 2+2' demonstrates that the construct has recombined properly within the 3' UTR region. Primer combination 3+3' shows the right integration into the 5' UTR region of the GOI and it shows if the cDNA is excised after expression of Cre. Modified from Andenmatten *et al.* (2013)

5.3 Phenotypic analysis of *act1*KO parasites

5.3.1 Examination of different actin antibodies

After confirming that a conditional *act1* KO was successfully generated, the next step was to examine the depletion of ACT1 on protein level. To perform Immunofluorescence analysis (IFA) on conditional *act1* KO parasites, loxPAct1 parasites were treated with and without 50 nM rapamycin for 4 h, inoculated 96 hours post induction and fixed 120 hours post induction. Afterwards cells were stained using different actin antibodies to demonstrate the absence of ACT1 protein in *act1* KO parasites and confirm the specificity of the particular antibody. It became evident that the commercial antibody (Abcam ACTN05(C4)) that was used in several studies (Dobrowolski and Sibley 1996, Patron *et al*. 2005, Achanta *et al*. 2012), is not specific for *Toxoplasma* Act1 and no downregulation was observed in *act1* KO parasites on IFA level. Next, two antibodies that were raised against *Plasmodium falciparum* actin 1 (PfAct1; epitope–1 (EP1), epitope–2 (EP2)) were examined (Zhang *et al*. 2011). While PfAct1-Ep1 displayed a residual cross reaction at the apical tip of *act1* KO parasites, PfAct1-Ep2 was specific with no signal detectable in parasites lacking ACT1 (Figure 5-2A). Two antibodies against *T. gondii* Act1 were analysed. The first tested *T. gondii* antibody (TgAct1 from Sibley lab) showed an unspecific localisation at the apicoplast and no downregulation of ACT1 protein demonstrating a strong IFA cross-reaction of this antibody. The second antibody (TgAct1 from Soldati lab) was found to be specific as no ACT1 protein was detected in parasites lacking *act1 (*Figure 5-2A). For this reason the antibody kindly provided by Dominique Soldati was used for further analysis on IFA level.

The apicomplexan specific actin antibodies were further analysed on Immunoblot level to examine if antibodies not specific for *Toxoplasma* show additional bands. Therefore, western blot was performed using the wildtype strain RHΔhxgprt as *act1* KO parasites display a too low excision to be examined for ACT1 depletion on western blot level. All used antibodies label a band with the right size for actin at 42 kDa (Figure 5-2B). No significant difference between the *Plasmodium* antibodies was observed hence Ep1 probably binds non-specifically to the apical tip of the parasite.

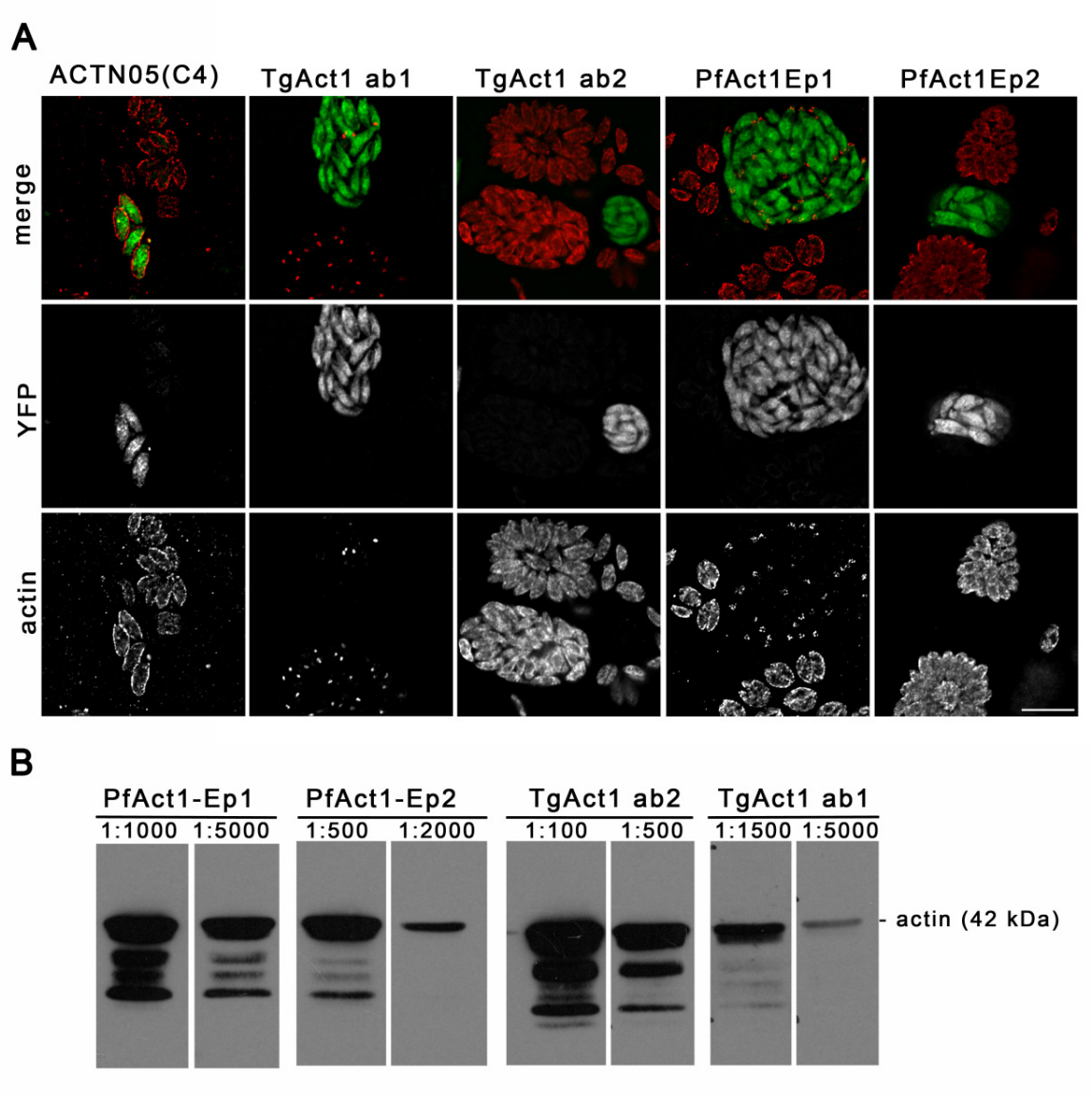

Figure 5-2: Localisation and specificity of different Act1 antibodies.(A) IFA on conditional *act1* KO parasites to show regulation of Cre recombinase mediated excision and thus depletion of ACT1. The parasites are treated with 50 nM rapamycin for 4 h, inoculated 96 hours post induction and were fixed 120 h post induction. Indicated Actin antibodies were used to show the absence of ACT1 and test for specific labelling of the respective antibody. Some antibodies show a strong IFA cross-reaction. Two antibodies raised against *Plasmodium falciparum* actin (epitope-1, epitope-2), two *T.gondii* actin antibodies, and a commercially available antibody (Abcam ACTN05(C4)) were tested. While the first tested *T. gondii* antibody (TgAct1 form Sibley lab) showed an unspecific localisation at the apicoplast, the second antibody (TgAct1 from Soldati lab) seemed specific because no ACT1 protein was detected in parasites lacking *act1*. Moreover PfAct1 Ep1 displayed a residual Act1 staining at the apical tip in *act1* KO parasites whereas Ep2 was specific. The commercial antibody showed no significant down regulation in *act1* KO. Scale bar represents 10 µm. Modified from Andenmatten *et al.* (2013) (B) Immunoblot of wild-type parasites stained against indicated actin antibodies.

5.3.2 *Act1* KO parasites display a delayed death phenotype

Next, an immunofluorescence time-course of *act1* KO parasites was performed to evaluate the time required for ACT1 depletion. Hence, loxPAct1 was induced with 50 nM rapamycin for 4 hours followed by inoculation on HFF cell growing on glass cover slips. Parasites were fixed after 24, 48, 72, 96 and 120 hours and

stained against TgAct1 and the apicoplast marker HSP60. ACT1 protein levels are significantly decreased as early as 24 hours after excision and are undetectable after 72 hours (Figure 5-3). When parasites lacking *act1* were allowed to grow constantly on HFF for 96 hours, they were unable to egress and died intracellular. Although a role of Act1 in parasite replication has been questioned previously (Shaw *et al.* 2000), *act1* removal caused a severe apicoplast (a plastid-like organelle) segregation defect. Furthermore, *act1* KO parasites can be easily identified in the induced loxPAct1 population up to 10 days after induction, suggesting host cell invasion in the absence of *act1*. Indeed, when parasites were artificially released from the host cell 72 hours after induction, parasites lacking *act1* remain capable of infecting host cells (Figure 5-3). Yet, these parasites died within the host cell probably due to apicoplast loss, resulting in a typical delayed death phenotype (Fichera and Roos 1997).

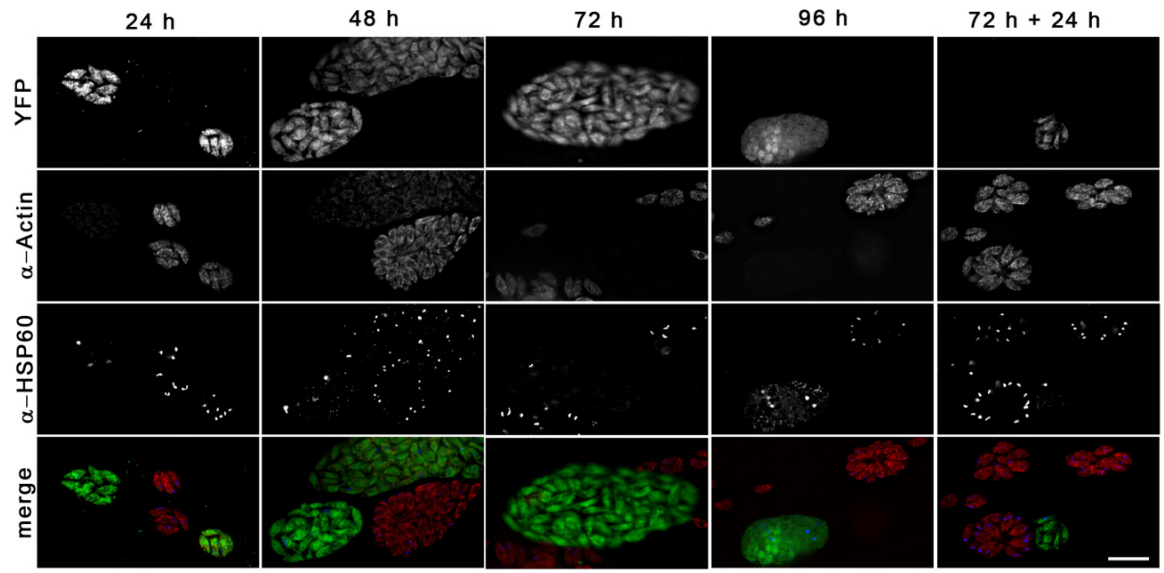

Figure 5-3: Actin is essential for apicoplast replication. LoxPAct1 parasites were treated with rapamycin for 4 h, inoculated on HFF cells, and imaged after the indicated time. Act1 protein levels are significantly reduced *act1* KO parasites after 24 hours and not detectable after 72 hours. The apicoplast, stained with α-HSP60, revealed a replication/segregation defect, resulting in large parasitophorous vacuoles containing few or no plastids. Moreover, 96 hours post induction *act1* KO parasites started dying intracellular. When parasites were artificially released from the host cell after 72 hours, *act1* KO can reinvade the host cell, but fail to replicate the apicoplast (72 h + 24 h). Scale bar: 5 µm. Modified from Andenmatten *et al.* (2013).

5.3.3 Growth analysis of *act1* KO

As actin plays a crucial role in several eukaryotes, the growth behaviour of the indicated lines was studied. Parasites were inoculated on HFF cells and cultured for five days prior to fixation with 4 % PFA. As expected no growth defect was detected for the wildtype line ku80::DiCre or the parental line loxPAct1 (Figure

5-4). Induction of loxPAct1 with 50 nM rapamycin leads to efficient removal of *act1* (~15% of the population) resulting in *act1* KO parasites. Parasites lacking *act1* were not able to form plaques in the host cell layer although large vacuoles were observed (Figure 5-4). Isolation of viable *act1* KO parasites was unsuccessful, suggesting that *act1* is essential for parasite survival *in vitro*.

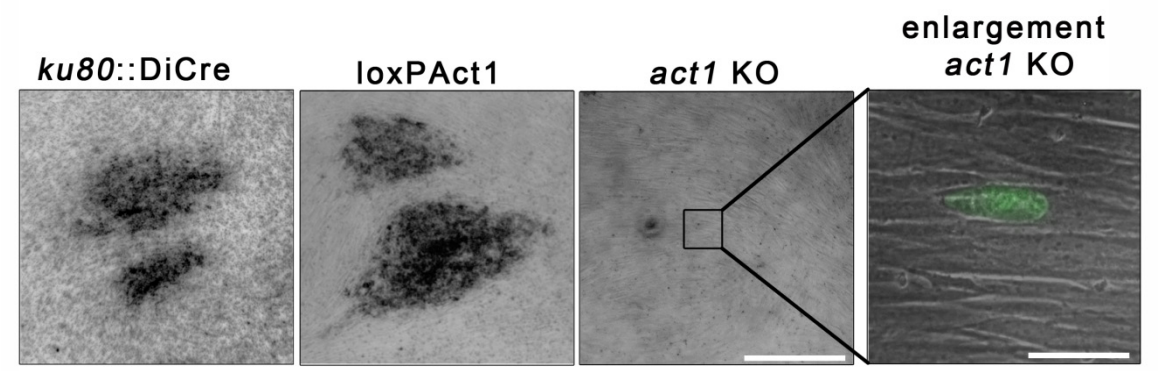

Figure 5-4: Growth analysis of *act1* KO parasites. LoxPAct1 was treated with and without 50 nM rapamycin for 2 h. Parasites were inoculated 24 h post induction. While control parasites displayed typical growth behaviour after 5 days, parasites lacking ACT1 showed no plaque formation on HFF monolayers demonstrating that *act1* is an essential gene in tachyzoites. Scale bars represent 20 µm and 0.2 mm respectively. Adapted from Andenmatten *et al*. (2013).

Next, it was examined if loss of *act1* has an effect on other organelles in addition to the apicoplast. IFA of *act1* KO parasites was performed. LoxPAct1 parasites were induced with 50 nM rapamycin for four hours, inoculated 96 hours post-induction and fixed 24 hours after inoculation. IFA analysis of *act1* KO parasites revealed that ACT1 depletion has no impact on the Inner Membrane Complex (IMC1), dense granules (GRA9), endosomal like compartments (VPI), or the membrane occupation recognition nexus 1 (MORN1). Akin to components of the MyoA motor complex Act1 is implied in having a key role during the invasion procedure. Since microneme and rhoptry secretion is an important step for this process, it was analysed if the micronemes and rhoptries were intact in *act1* KO parasites. Characteristic apical signals for micronemal proteins (AMA1 and MIC2) were detected. Previous studies reported a role of actin for rhoptry positioning which was investigated using the Actin inhibitor Cytochalasin D (Mueller et al 2013).Contrary to this study, typical club-shaped rhoptries (ROP5) were seen in parasites lacking *act1*. Because of the low excision rate of loxPAct1 it was infeasible to investigate the role of Act1 at appropriate times post induction during the lytic cycle, hence a novel conditional actin KO was generated using a different recipient strain to characterise the functions of Act1 and will be described in the following chapters.

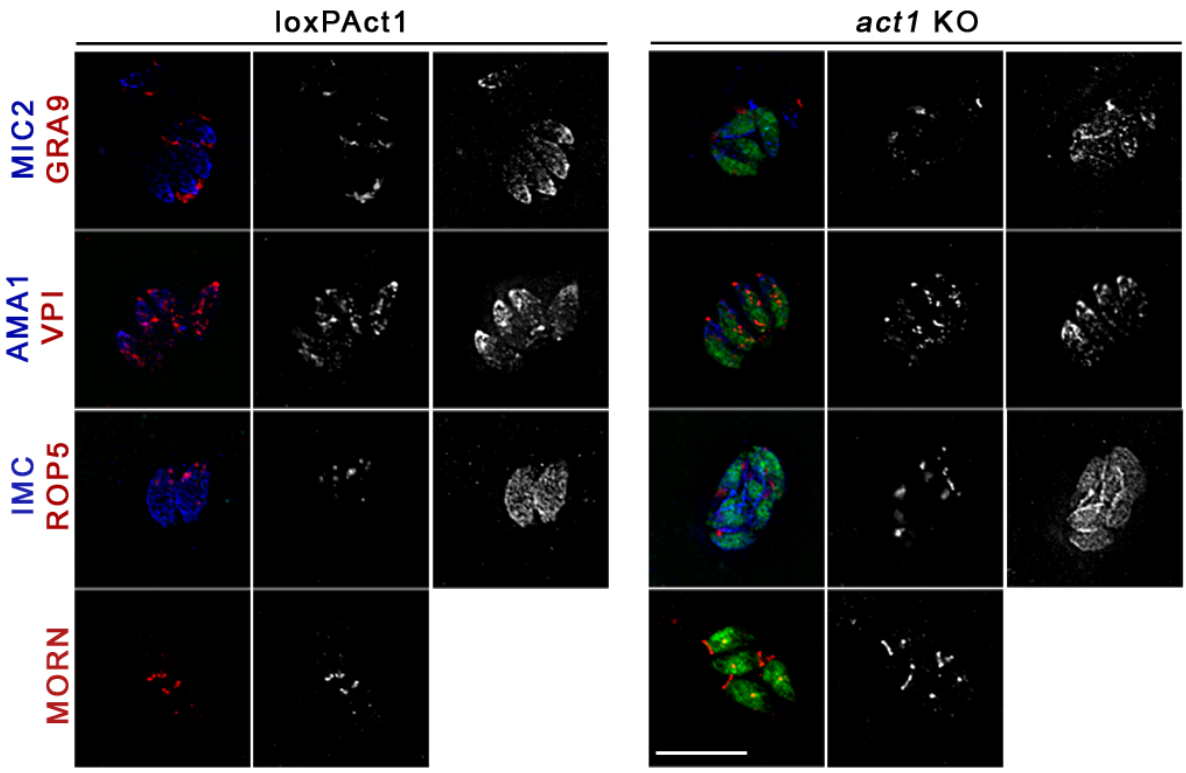

Figure 5-5:IFA of *act1* KO parasites. .IFA shows loxPAct1 (YFP negative) and *act1* KO (YFP positive), fixed 120 h post induction with 50 nM rapamycin IFA analysis of *act1* KO shows that *act1* depletion has no influence on the micronemes (MIC2, AMA1), rhoptries (ROP5), dense granules (GRA9), early endosomes (VPI), the Inner Membrane Complex (IMC1) or the membrane occupation recognition nexus 1 (MORN1). Scale bars: 10 µm. Modified from Andenmatten *et al.* (2013).

5.4 Generation of a more efficient *act1* KO

For the generation of a more efficient conditional *act1* KO, a different DiCre expressing Δku80 strain was used. The expression of DiCre was lower in ku80::DiCre compared to RHDiCre where the DiCre cassette was randomly integrated (Andenmatten *et al.* 2013), which in turn probably affects the excision efficiency. Because of this reason the *ku80* gene was removed in RHDiCre parasites resulting in DiCre *Δku80* (Pieperhoff et al, in preparation). The Act1 geneswap plasmid was transfected into the new recipient strain DiCre *Δku80* and correct integration was confirmed by analytical PCR as described before (see chapter 5.2). Primers binding specifically to the *act1* gene revealed the successful replacement of endogenous *act1* through *act1* cDNA (Figure 5-6A) and a specific PCR product was formed showing correct integration into the 3'UTR locus. As before, no excision of *act1* occurred without rapamycin induction. Importantly, after activation of Cre recombinase, excision of the floxed *act1* cDNA was detected in approximately 95 % of the population judged by YFP expression. This high excision rate is also reflected by PCR where only a

smaller PCR product for site specific recombination was detected in *act1* KO parasites (Figure 5-6A) demonstrating that induction of DiCre results in an almost clonal population of *act1* lacking parasites.

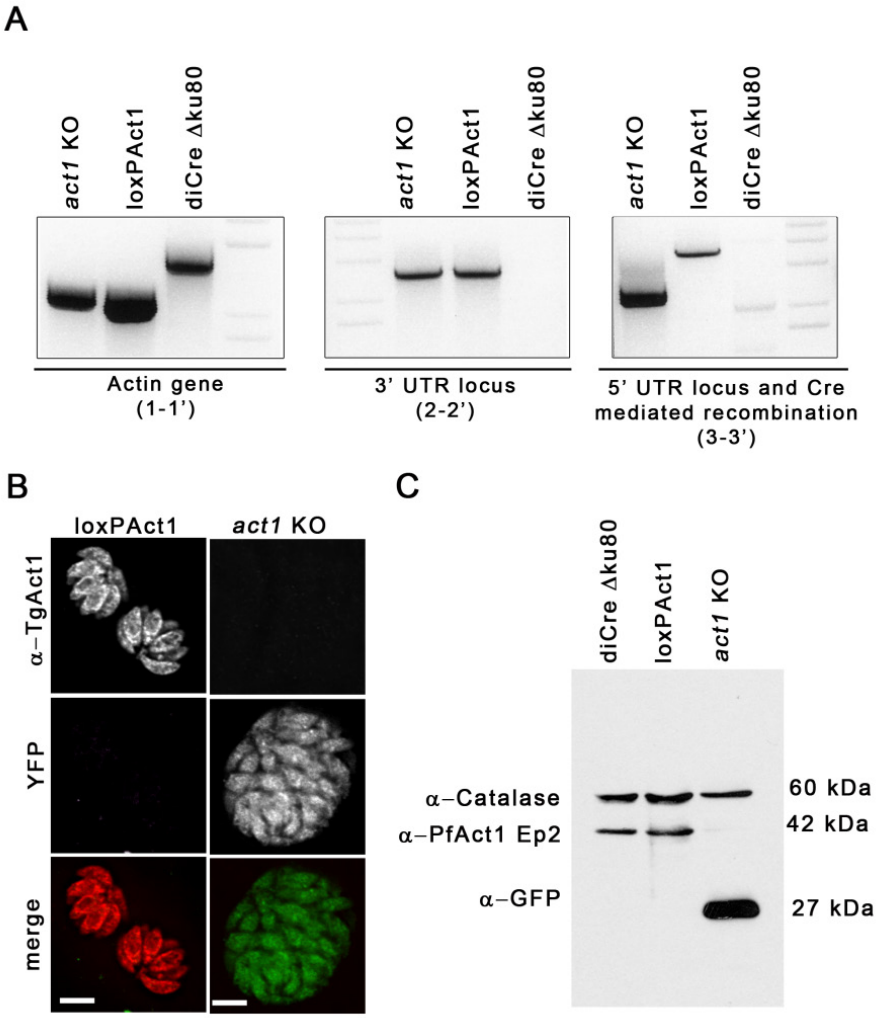

Figure 5-6: Generation of a novel conditional *act1* KO. A) Analytical PCR to verify correct replacement of the endogenous *act1* by the *act1* KO construct. Three different Primer combinations were used. The replacement of gDNA through cDNA can be seen by using Primer combination 1+1' The Oligo pair 2+2' proves that the construct has recombined properly within the 3' UTR region. Primer combination 3+3' displays the right integration into the 5' UTR region of the GOI and it shows if the cDNA is excised after expression of Cre. (B) IFA on conditional *act1*KO parasites shows regulation of Cre recombinase mediated excision and thus depletion of ACT1. The parasites are treated with 50 nM rapamycin for 4 h and are fixed 72 h post induction. α- TgAct1 was used to demonstrate the absence of ACT1 in the *act1*KO. Scale bar represents 10 µm. (C) Immunoblot analysis of ACT1 72 h after excision. Antibodies against ACT1 and GFP were used to validate the absence of ACT1 and study the expression of YFP. α-Catalase served as loading control. Modified from Egarter *et al.* (2013).

Next, the expression level of ACT1 was analysed on protein level 72 hours post induction with 50 nM rapamycin. First, IFA was performed using α-TgAct1. While loxPAct1 displayed typical localisation of Act1 and no YFP expression, *act1* KO parasites showed no detectable signal for ACT1, but exhibited strong YFP

expression (Figure 5-6B). Moreover, expression levels of *act1* KO parasites were evaluated by Western blot using antibodies against ACT1 and GFP respectively. DiCre *Δku80* and loxPAct1 lines served as control parasites and α-Catalase was used as internal control. As anticipated YFP protein can only be detected in *act1* KO parasites, where excision of *act1* brings *yfp* under the control of the Act1 promoter. Strikingly, nearly complete depletion of ACT1 was observed 72 hours post induction with only a very faint band detectable. This is likely corresponding to the 5 % of parasites not having excised the gene (Figure 5-6C). Summarising, it was successful to generate a novel very efficient conditional Act1 KO which can be used to characterise the role of Act1 in great detail.

5.5 Phenotypic characterisation of new *act1* KO

To confirm that the newly obtain conditional *act1* KO displays the same phenotype as the previous one, IFAs were repeated (see chapter 5.3.3). Parasites were induced with 50 nM rapamycin for 4 hours, inoculated 72 hours post induction and fixed 24 hours later. Analogous to the findings above, distinct organelles were analysed in parasites lacking *act1*. IFA analysis of *act1* KO parasites displayed that Act1 has no effect on the Inner Membrane Complex (IMC1), dense granules (GRA9) or the endosome like compartment (proM2AP). Furthermore, micronemes (AMA1, MIC2) and rhoptries (ROP5 and ROP2/4) stayed intact after loss of *act1*, although in some cases it was difficult to draw conclusions about typical localisation because the *act1* KO parasites form unorganised vacuoles and no typical rosettes. Moreover, removal of *act1* had no impact on the morphology of the plasma membrane (SAG1) and components of the MyoA motor complex (GAP45, MLC1 and MyoA). Additionally, the apicoplast replication/segregation defect was confirmed. Together this data proves that both conditional *act1* KOs behave alike.

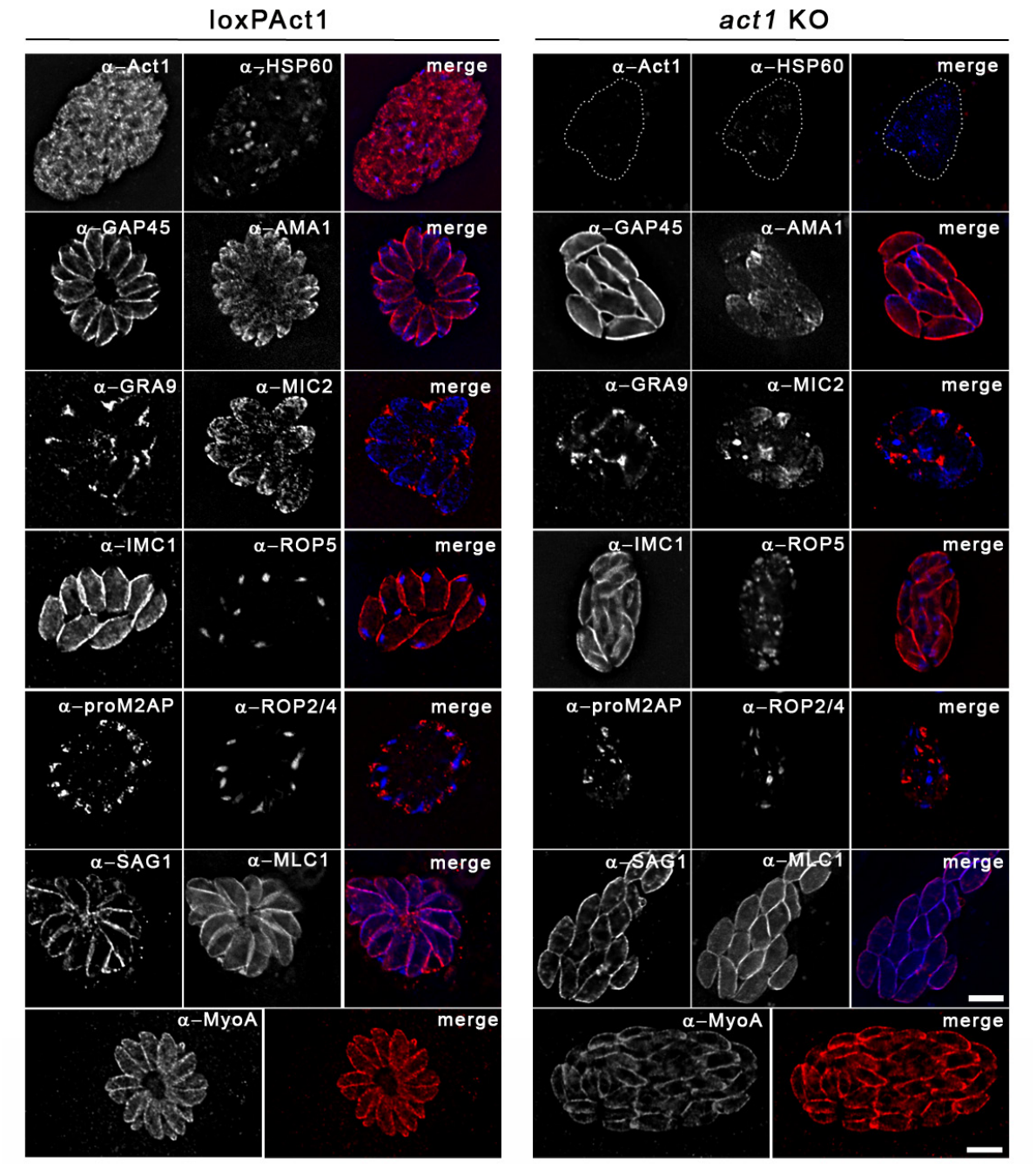

Figure 5-7: IFA of *act1* KO parasites. Act1 KO parasites were fixed 96 h post excision. IFA analysis of *act1* KO displays that *act1* removal has no impact on the Inner Membrane Complex (IMC1) the micronemes (MIC2, AMA1), rhoptries (ROP5, ROP2/4), dense granules (GRA9), endosome like compartment (proM2AP) and component of the MyoA motor complex (GAP45, MLC1 and MyoA). Additionally, the apicoplast phenotype was confirmed. Scale bars: 5 µm.

Ultrastructural analysis was performed 84 hours and 96 hours post induction. Extracellular parasites were examined to determine if all organelles and structures thought to be important for gliding and invasion (conoid, rhoptries and micronemes) were present and intact after loss of *act1* (Figure 5.5-2A). Moreover, staining of the plasma membrane with SAG1 antibody revealed an unexpected morphology defect in extracellular *act1* KO parasites (72 hours post induction). *Act1* depleted parasites seemed to lack a part of their basal end

resulting in a torpedo-like shape (Figure 5.5-2B; white arrows). However, the reason for this change in shape is not known yet.

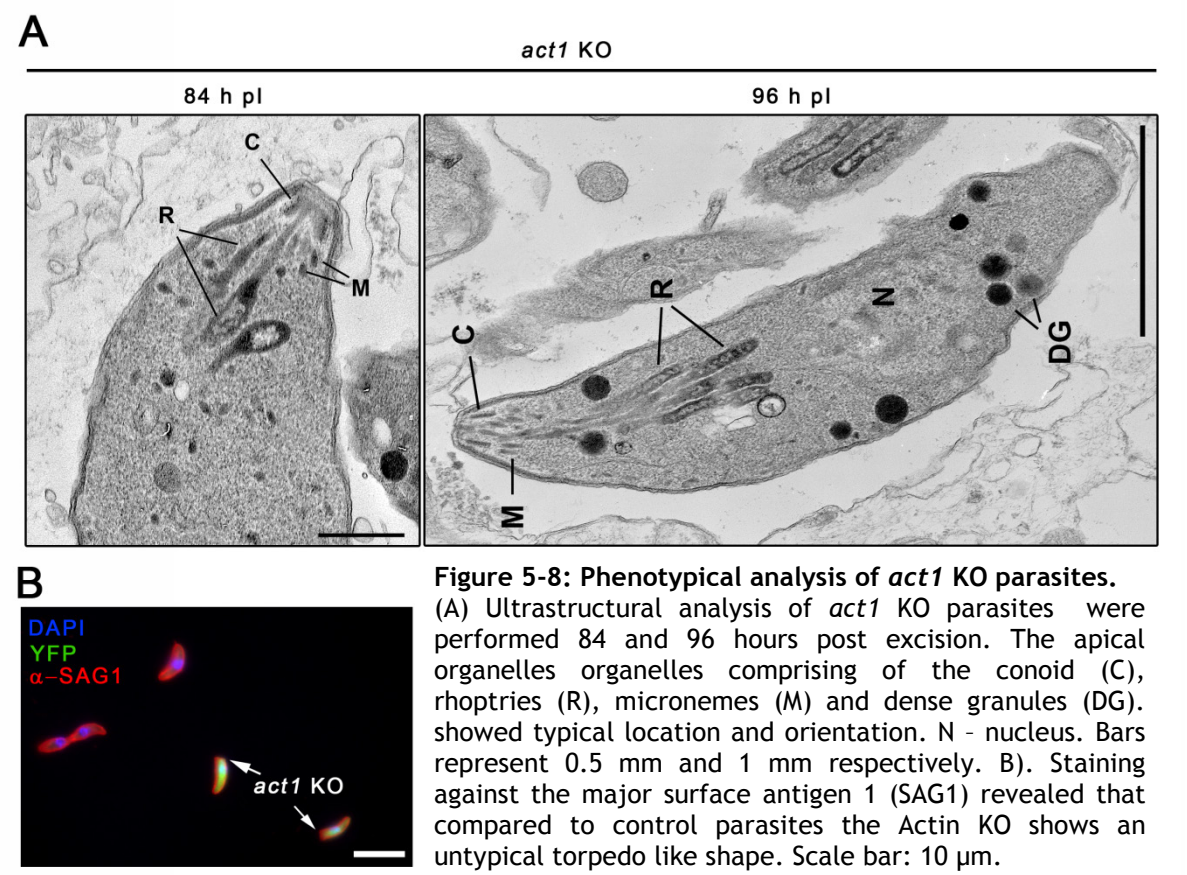

Figure 5-8: Phenotypical analysis of *act1* KO parasites. (A) Ultrastructural analysis of *act1* KO parasites were performed 84 and 96 hours post excision. The apical organelles organelles comprising of the conoid (C), rhoptries (R), micronemes (M) and dense granules (DG). showed typical location and orientation. N – nucleus. Bars represent 0.5 mm and 1 mm respectively. B). Staining against the major surface antigen 1 (SAG1) revealed that compared to control parasites the Actin KO shows an untypical torpedo like shape. Scale bar: 10 µm.

5.6 Growth behaviour of *act1* KO parasites

Akin to previously reported, no plaque formation was observed for *act1* KO parasites after 5 days (Figure 5-9A), but large vacuoles could be detected for parasites lacking *act1*. To further analyse intracellular replication of *act1* KO parasites, HFF cells were inoculated with indicated parasites strains (96 hours post induction with 50 nM rapamycin) for one hour prior to harsh washing steps with media to remove all loosely attached parasites. Cells were cultured at standard conditions for 24 hours followed by fixation and IFA staining against IMC1. Although parasites lacking *act1* were still able to replicate, a slight replication delay was observed (Figure 5-9B). Summarising, Act1 is essential for parasite survival, but not for replication indicating other processes of the lytic cycle are affected by loss of *act1* and will be analysed in the following chapters.

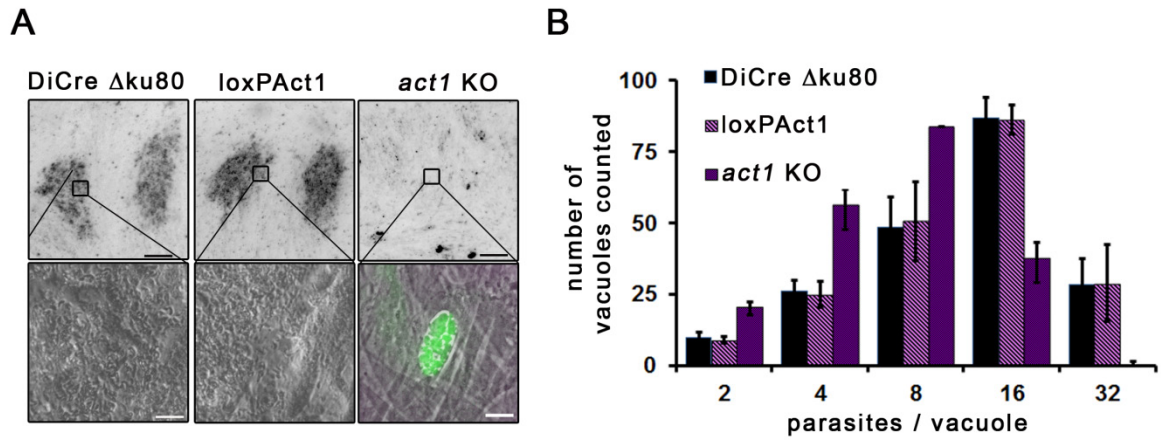

Figure 5-9: Growth behaviour of *act1* KO parasites. (A) Growth of indicated parasite strains. Plaque formation of was analysed after 5 days. The *act1* KO parasites were incapable of plaque formation. Scale bars: 0.2 mm, 20 µm respectively (B) Replication analysis of *act1* KO parasites was performed 96 h post induction. Parasites were allowed to invade for 1 h before replication for 24 h. To quantify the replication rate the number of parasites per parasitophorous vacuole was determined. Parasites lacking *act1* are delayed in replication. Mean values of three independent assays are shown ± SEM. Modified from Egarter *et al.* (2013).

5.7 *Act1* KO parasites are not blocked in gliding motility

Parasite actin is believed to play an important role during the substrate dependant locomotion of apicomplexan parasites which is referred to as gliding motility. Hence, the ability of *act1* KO parasites to glide on surfaces was examined. In general *Toxoplasma* displays three distinct types of gliding motility referred to as circular, helical and upright twirling (see chapter 1.9.1) (Hakansson *et al.* 1999). When parasites move along the surface they shed surface antigens such as SAG1 which can be visualised by immunofluorescence. To study the impact on gliding motility in *act1* lacking parasites (96 hours post induction), trail deposition assays were performed in which parasites were allowed to glide on FBS-coated glass cover slips for 30 minutes prior to fixation and IFA against SAG1. As expected, long circular and helical trails were observed in wild-type parasites. Interestingly, mainly circular trails were seen for *act1* KO parasites, similar to the phenotype observed for *myoA* or *mlc1* lacking parasites (Figure 5-10A). Moreover a decrease of overall gliding motility was detected for *act1* KO parasites when compared to wild-type parasites (Figure 5-10). Trail deposition assays were performed at different time points post induction (36 h, 72h and 96 h) to analyse if a correlation between actin depletion and gliding motility rate exists. Most *act1* KO parasites showed a residual expression of ACT1 36 hours post induction. Nevertheless gliding motility decreased to 13 % when compared to wild-type parasites (Figure 5-10B). 72 hours after removal of *act1*

no Actin protein can be detected and 10 % of the parasites were capable to form trails when normalised to WT parasites (Figure 5-10C). This motility rate stayed the same 96 hours post induction (Figure 5-10D). Summarising this data reveals that identical phenotypes were observed for different time point even when residual actin remained. This indicates that once the actin concentration is below a critical concentration, residual actin levels have no influence on the phenotype. This is also supported by the early loss of the apicoplast, when actin is still easily detectable.

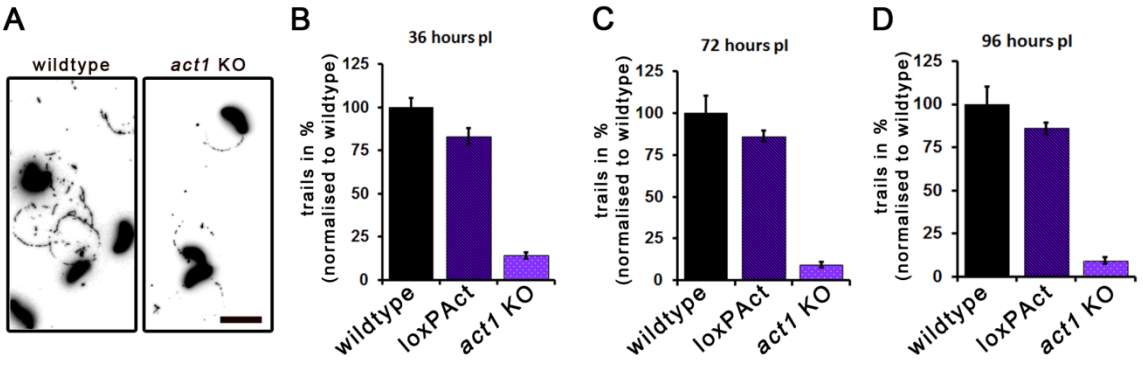

Figure 5-10: Gliding motility of *act1* KO parasites. (A) Trail deposition assays were performed 96 h post induction by allowing indicated parasites to glide on FBS coated cover slips for 30 minutes prior to staining with α-SAG. Scale bar: 10 µm. (B-D) Quantification of gliding motility in *act1* KO parasites 36 h (B), 72 h (C) and 96 h post (D) induction. The number of trails was significantly decreased in *act1* KO parasites to approximately 10 % compared to wild-type parasites. Strikingly, no differences were observed in parasites having residual actin or are completely actin depleted. Mean values of three independent experiments are shown ± SEM. The number of trails was standardised to wild-type parasites. Modified from Egarter *et al.* (2013).

5.8 Characterisation of ability of *act1* KO to egress

Since gliding motility is a requirement for invasion and egress those two processes are assessed next. To begin with, the ability to naturally egress the host cells was studied in *act1* KO parasites. LoxPAct1 and *act1* KO parasites were inoculated on host cells and fixed after distinct time points (24, 36, 48, 72, 96 and 120 hours) and consequently stained against IMC1 and with DAPI. The parental line, loxPAct1 exhibited characteristic growth behaviour. Small vacuoles were observed after 24 hours which increased their size until naturally exiting the host cell prior reinvasion of neighbouring cells. Multiple rounds of egress and invasion result in complete lysis of the host cell monolayer after 120 hours. While *act1* KO parasites were structurally intact after 24 to 36 hours (supporting replication data in Figure 5-9B) and thus displayed no intracellular defect that would result in a failure in egress, they were blocked in naturally

egressing host cells. Instead they started to die intracellular as soon as 72 hours post inoculation (Figure 5-11A).

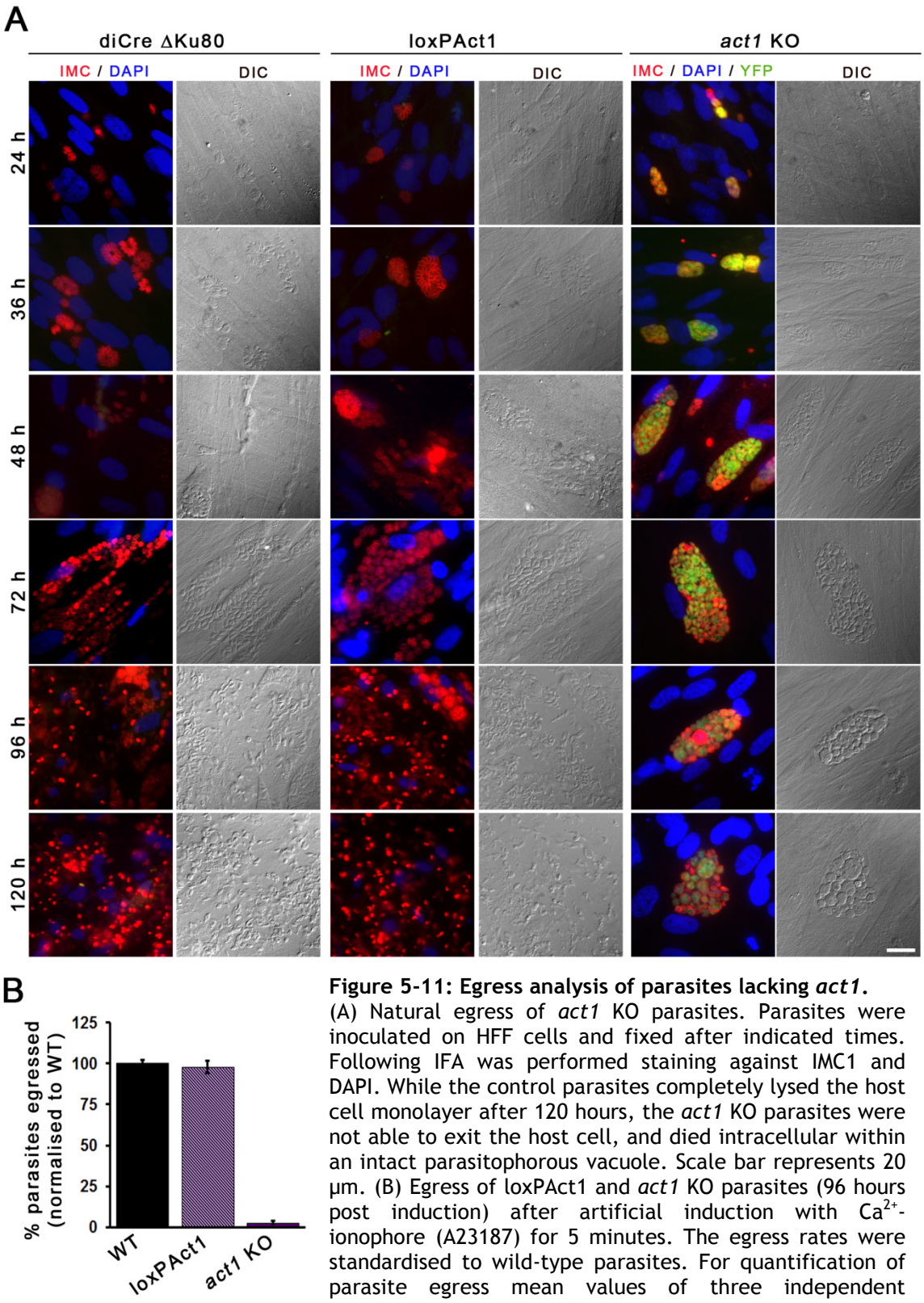

Figure 5-11: Egress analysis of parasites lacking *act1*. (A) Natural egress of *act1* KO parasites. Parasites were inoculated on HFF cells and fixed after indicated times. Following IFA was performed staining against IMC1 and DAPI. While the control parasites completely lysed the host cell monolayer after 120 hours, the *act1* KO parasites were not able to exit the host cell, and died intracellular within an intact parasitophorous vacuole. Scale bar represents 20 µm. (B) Egress of loxPAct1 and *act1* KO parasites (96 hours post induction) after artificial induction with Ca^{2+}-ionophore (A23187) for 5 minutes. The egress rates were standardised to wild-type parasites. For quantification of parasite egress mean values of three independent experiments are shown, ± SEM. Modified from Egarter *et al.* (2013).

To further investigate egress, indicted parasites were treated in absence and presence of 50 nM rapamycin 96 hours before artificially inducing egress with

calcium-ionophore (A23187) for 5 minutes. As anticipated wild-type parasites and loxPAct1 exited the host cells after addition of calcium ionophore. Unlike myoA KO, but analogous to *myoA/B/C* KO, *mlc1* KO and *gap45* KO parasites, tachyzoites lacking *act1* were not capable to egress host cells after calcium ionophore stimulation (Figure 5-11B).

5.9 Act1 is not crucial for host cell invasion

Host cell attachment and invasion was analysed using an attachment/invasion assay. Indicated parasite lines were allowed to invade HFF cells for 30 minutes followed by fixation and staining of extracellular parasites with SAG1 antibody. First, the number of parasites attached and invaded in 15 fields of view was determined to study attachment of the parasites to HFF cells. Attachment was defined as extracellular parasites sticking to cells and intracellular parasites assuming that they must have been attached prior to invasion. Surprisingly, both loxPAct1 and *act1* KO displayed a severe attachment defect with only 50-60 % of parasites attached to cells compared to wild-type parasites (Figure 5-12A). There are different explanation to why an attachment defect was observed in loxPAct1 parasites: (a) the point mutation within *act1* could cause an attachment defect; (b) the *act1* locus is altered through integration of the gene swap plasmid and has for example a different 3'UTR which could cause different expression levels of ACT1 compared to wild-type parasites; (3) expression of DiCre interferes with attachment. The last point appears unlikely because neither loxPMyoA nor loxPGAP45 showed an attachment phenotype (Egarter *et al*. 2014).

Next, the invasion efficiency was quantified. Therefore only attached parasites were considered and 300 parasites were analysed if they were attached or invaded into host cells. While loxPAct displayed a severe attachment, no invasion defect was detected when compared to wild-type parasites. The invasion rate of *act1* KO parasites was reduced to 10 % compared to wild-type parasites, but not as expected completely blocked (Figure 5-12B). Subsequently, to examine if *act1* KO parasites use the conventional path of invasion, formation of tight junction was studied. Parasites were added in excess to host cells, spun at 200 g for 2 minutes and let to invade for 5 minutes prior to fixation. Next, IFA against the TJ protein RON4 was performed. As expected, parasites lacking *act1*

invaded through a normal appearing TJ (Figure 5-12C). Altogether *act1* is essential for parasite survival due to a delayed death phenotype, but dispensable for all gliding motility dependant processes.

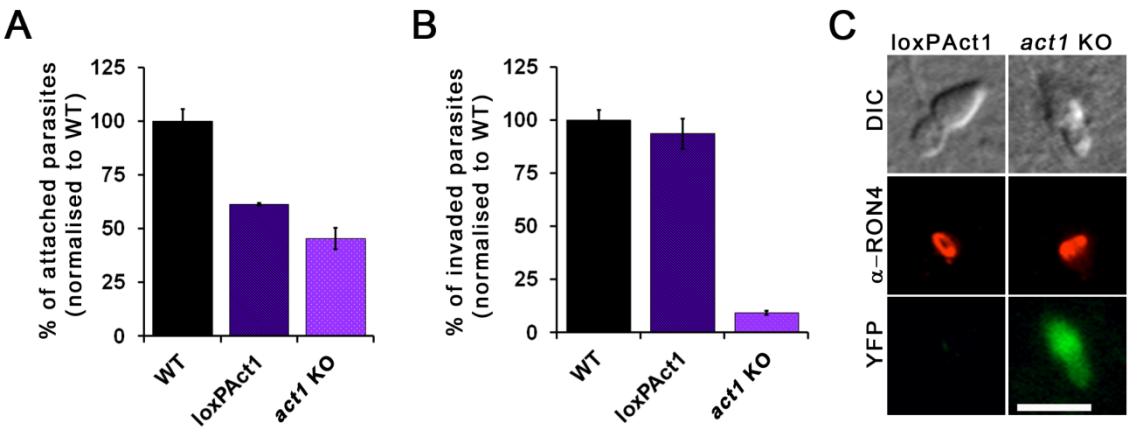

Figure 5-12: Analysis of attachment, invasion and tight junction formation of *act1* KO parasites. (A) Attachment assay of *act1* KO parasites. Parasites were allowed to invade for 30 minutes. Afterwards total amount of parasites in 15 fields of view was scored. Mean values of three independent assays are displayed, ± SEM. (B) Invasion assay of indicated parasites treated ± 50 nM rapamycin 96 h prior to invasion. Parasites were allowed to invade for 30 minutes prior to fixation. For quantification 300 parasites were examined. Mean values of three experiments are displayed, ± SEM. All strains were standardised to WT. (C) IFA with indicated antibodies on invading parasites demonstrates that parasites lacking *act1* still invade through typical appearing tight junction (TJ). Scale bar: 5 µm. Modified from Egarter *et al.* (2013).

5.10 Contribution of host cell actin during invasion and impact of Cytochalasin on gliding motility

Toxoplasma invasion is thought to be an active process that predominantly relies on the parasite's actin. This process can be divided into four distinct steps: (i) initial attachment, (ii) tight attachment and reorientation, (iii) tight junction formation and (iv) active penetration (see chapter 1.9.3) (Carruthers and Boothroyd 2007). The entire process is very fast and completed within 15-30 seconds (Morisaki *et al.* 1995). Several Cytochalasin D (CD) studies were performed in order to investigate the role of the host cell during invasion. CD is an inhibitor of actin polymerisation. Initial CD studies by Ryning and Remington suggested an active role of the host cell during *T. gondii* invasion (Ryning and Remington 1978). In contrast, inhibition studies with CD-resistant parasite and host cell lines indicated that this process was solely driven by parasite actin. A third study proposed that both parasite and host cell actin are important for *Toxoplasma* invasion (Gonzalez *et al.* 2009) (see chapter 1.9.4 for more detail). Because of these inconsistencies and the availability of tools (*i.e.*, CD-resistant host cell lines, CD-resistant parasites and the *act1* KO), the contribution of host

cell actin for the invasion process was re-analysed. Attachment and invasion assays with increasing CD concentrations (0-2 µM) on HFF cells were performed using wild-type parasites (DiCreΔku80), CD-resistant parasites (cytDR) and parasites lacking actin (*act1* KO). All parasite lines were treated with and without indicated concentrations of CD for 7.5 minutes, inoculated on HFF cells, centrifuged for 2.5 minutes at 200 x *g* and allowed to invade for 30 minutes. After fixation, extracellular parasites were stained against the surface antigen SAG1. To examine attachment, the number of parasites attached and invaded in 15 fields of view was determined, and normalised to DiCre *Δku80* without CD treatment. While 0.1 and 0.2 µM CD had little effect on the attachment of wild-type parasites, higher concentrations caused a drop to approximately 50 %. Furthermore, the ability of CD-resistant parasites to attach was only significantly affected at high concentration of CD and like the wild-type parasites, decreased to 50 % with 2 µM CD. Strikingly, addition of CD to *act1*-depleted parasites had no effect on attachment and stayed consistently at 50 % independent of the CD concentration (Figure 5-13A). Altogether these data suggest that CD has an effect on attachment of the parasites, which is contradictory to previous studies (Dobrowolski and Sibley 1996). Interestingly, addition of CD diminished attachment of DiCre *Δku80* and cytDR to *act1* KO levels indicating that actin is indeed important for attachment.

The experiment was adapted to compare penetration rates on HFF cells amongst the three parasite lines. Only attached parasites were considered and 300 parasites were examined for attchment or invasion into HFF cells. At the lowest concentration (0.1 µM CD), neither wild-type nor cytDR parasites showed an effect on the invasion rate (Figure 5-13B). Increasing the CD concentration to 0.2 uM led to a corresponding decrease in invasion events for DiCre *Δku80* until invasion was completely blocked at 2 µM. In contrast, the effect on invasion by cytDR parasites was not noticeable until 0.5 µM CD and not completely blocked at 2 µM CD, indicating they are less sensitive when compared to wild-type parasites but not completely resistant. Surprisingly, while DiCre *Δku80* and cytDR showed no effect on invasion at 0.1 µM CD, the invasion rate of *act1* KO parasites dropped from 10 % to 5 %, suggesting either additional specific target(s) of this drug or a nonspecific off-target effect. Furthermore, invasion was completely blocked in case of *act1* KO parasites when treated with high

doses (1 µM) of CD (Figure 5-13B). Since HFF cells are sensitive to CD and thus the decrease in the invasion rate could be attributed to host cell actin depolymerisation rather than parasite actin, an analogous experiment with CD-resistant host cells (Toyama and Toyama 1984, Toyama and Toyama 1988) was performed. Unexpectedly, *act1* KO and cytDR parasites generally invaded better into this cell line than wild-type parasites. In the absence of CD, *act1* KO parasites invaded at nearly 20% the rate of wildtype, which is double the rate observed in CD-sensitive HFF cells (Figure 5-13C). Although CD-resistant host cells and parasites were used, this actin inhibitor still affected invasion supporting previous concerns of multiple drug targets.

It is thought that gliding motility is the driving force for host cell penetration. Thus, trail deposition was assessed with treatment of different concentrations of CD (0-2 µM). Parasites were pre-treated with CD for 15 minutes in HBSS followed by processing for the trail deposition assay (Hakansson *et al*. 1999). Parasites were fixed and stained against SAG1 and the number of trails was scored. Consistent with the invasion data, the motility rate of wild-type parasites gradually decreased with increasing CD concentrations. No change of the gliding motility rate was observed in cytDR parasites at low doses of CD (0.1 and 0.2 µM). However, the number of trails steadily decreased the higher the CD concentration used to treat parasites. Motility of *act1* KO parasites was almost blocked at 0.5 µM CD and higher, which is consistent with HFF invasion data (Figure 5-13D). Images of trails of all three strains showed a correlation of trail length and CD concentration. In the presence of CD, mainly circular trails were observed (Figure 5-13E). In summary, the data suggest that CD has additional target(s), and so different actin inhibitors should be used to evaluate the contribution of host cells during invasion.

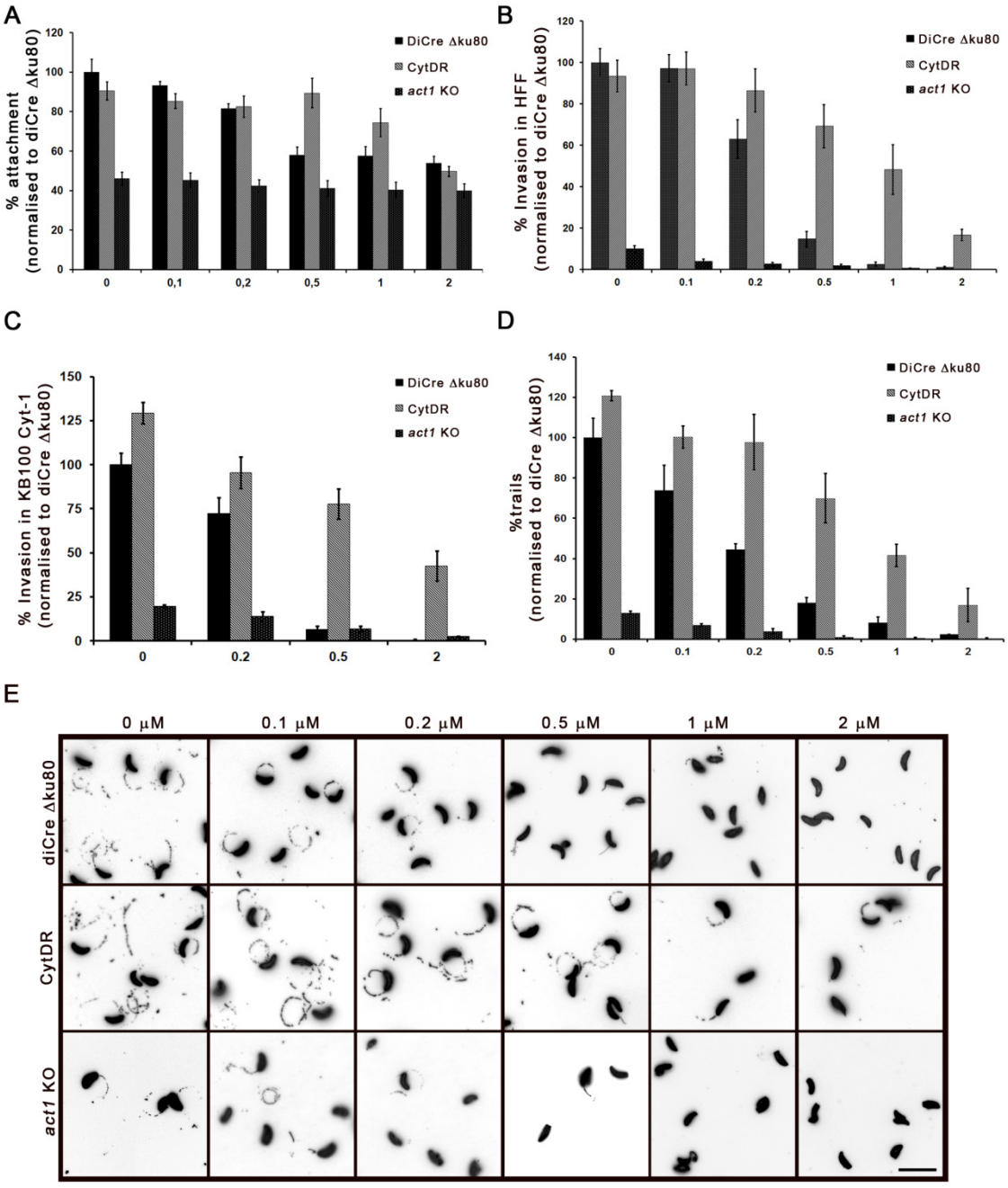

Figure 5-13: Analysis of impact of Cytochalasin D (CD) on host cell invasion and gliding motility. (A) Attachment assay using HFF cells and *act1* KO parasites in the presence of different concentrations of CD. Parasites were allowed to invade for 30 minutes. Afterwards, the total number of parasites in 15 fields of view was scored. Mean values of three independent assays are displayed, ± SEM. (B) Invasion assay of indicated parasites on HFF cells in presence of increasing CD doses. Parasites were treated with CD for 7.5 minutes and then allowed to invade for 30 minutes prior to fixation. For quantification, 300 parasites were examined. Mean values of three experiments are displayed, ± SEM. All strains were standardised to WT. (C) Analogous to (B) but CD-resistant host cells were used. (D) Trail deposition assays using the indicated concentrations of CD. Parasites were allowed to glide on FBS-coated cover slips for 30 minutes prior to staining with α-SAG1. Quantification of gliding motility revealed that the number of trails was significantly decreased with increased concentrations of CD. Mean values of three independent experiments are shown ± SEM. The number of trails was standardised to wild-type parasites not treated with CD. (E) CD had an effect on the number and length of trails and the proportion of helical gliding appeared to be almost abolished. Scale bar: 10 µm.

5.11 Summary and brief conclusion

In summary, it was successfully achieved to generate a highly controllable *act1* KO using the recently established DiCre system (Andenmatten *et al*. 2013). Examination of components of the MyoA motor complex on IFA level revealed that Act1 has no influence on these proteins and rhoptry positioning was not affected in *act1* KO parasites which is in contradiction to a recent study where the actin filament disrupter Cytochalasin D caused mis-localisation of rhoptries (Mueller *et al*. 2013). Moreover, *act1* KO parasites show a severe defect on apicoplast division/segregation which leads to a typical delayed death phenotype, demonstrating that loss of *act1* is essential for the asexual life cycle *in vitro*. While intracellular growth of *act1* KO parasites was not affected, the gliding motility rate decreased to 10 % compared to wild-type parasites. Additionally, invasion was reduced to 10 % as well indicating that Act1 is neither crucial for parasite invasion nor gliding motility. Egress was the only process during the lytic cycle that was found to be completely blocked. In conclusion the *act1* KO demonstrates that the Acto-MyoA motor complex is not essential for parasite invasion and gliding motility.

6 General discussion and future work

6.1 Biogenesis of the Inner Membrane Complex

6.1.1 The MyoA motor complex is associated with IMC biogenesis

Internal budding by apicomplexan parasites can be classified into three different forms: endopolygeny, schizogony and endodyogeny (Striepen *et al*. 2007). During endopolygeny, which is the replication mode used by *Sarcocystis spp*., multiple rounds of DNA replication occur without mitosis taking place, leading to large multinucleated cells. After DNA replication is completed, the nucleus divides and daughter cell budding initiates (Vaishnava *et al*. 2005). Schizogony is used by the malaria causing agent *Plasmodium spp*. to replicate. During this replication form, multiple rounds of asynchronous DNA replication are followed by asynchronous mitosis without cytokinesis taking place. After the last mitosis step, all daughter cells bud from the mother cell at the same time. The final mode of replication, endodyogeny, is used by *Toxoplasma gondii*. Here, a single round of DNA replication is followed by nuclear division and budding of two daughter cells (Striepen *et al*. 2007).

Apicomplexa, together with Ciliates and Dinoflagelates, belong to the super phylum, Alveolates. This phylum is characterised by the presence of membranous vesicles called “alveoli”. The role of these vesicles is generally to strengthen the cytoskeleton, however there are taxon specific functions as well. In Ciliates these flattened vesicles are called alveoli whereas they are called amphiesmal vesicles in dinoflagelates (Morrill and Loeblich 1983, Hausmann and Allen 2010). In these two phyla the vesicles are a mechanism to store calcium. In Apicomplexa, the membranous vesicles are generally referred to as the Inner Membrane Complex (IMC) and serve as crucial scaffold elements during cytokinesis. The IMC architecture varies between the different species of Apicomplexa. In *Toxoplasma* several IMC plates are linked together to build a uniform network of vesicles (Morrissette *et al*. 1997). The same can be observed for non-invasive gamteocytes of *Plasmodium* (Dearnley *et al*. 2012). Interestingly, the IMC of *Plasmodium* merozoites and ookinetes is comprised of only a single vesicle (Kono *et al*. 2012).

Alveolins are a protein family whose homologues are found in all alveolate phyla members making these proteins a unique feature of the infrakingdom (Gould *et al*. 2008, Gould *et al*. 2011). Though much is known about their structure and evolution much less is known about the mechanism of trafficking these proteins to the alveoli or the biogenesis of the membranous sacs.

Toxoplasma daughter budding is an extremely complex process that comprises the coordinated assembly of several elements. In *Toxoplasma gondii* several proteins involved in the budding process and IMC biogenesis have been identified. Amongst these are the membrane occupation and recognition nexus 1 (MORN1), the actin-like-protein 1 (Alp1), and two small Rab GTPases (Rab11A and Rab11B) (Gubbels *et al*. 2006, Gordon *et al*. 2008, Agop-Nersesian *et al*. 2009, Agop-Nersesian *et al*. 2010, Gordon *et al*. 2010). MORN1 is part of the centrocone, a specialised structure of the intranuclear mitotic spindle. Overexpression of this protein causes a defect in nuclear division and formation of daughter cells thus leading to the abolishment of cell division. As a result parasite morphology and IMC seem atypically deformed. Additionally, a MORN1 KD demonstrates a role during the late stages of daughter cell budding as daughter cells mature but fail to complete cytokinesis at their basal ends likely due to the lack of the basal complex (Gubbels *et al*. 2006, Lorestani *et al*. 2010). Unlike MORN1, overexpression of ALP1 causes a block in daughter bud initiation so it might be involved in early IMC biogenesis (Gordon *et al*. 2008). Another protein needed for the completion of cytokinesis is the small GTPase Rab11A that likely delivers vesicles containing SAG1 from the endosome-like compartment to the plasma membrane of the growing daughter cells (Agop-Nersesian *et al*. 2009). Rab11A is also implicated with the maturation of the IMC as late components of the MyoA motor complex fail to be integrated in the IMC in Rab11A dominant negative mutants. The recent discovery that IMC biogenesis is not purely *de novo*, that the mother IMC is also incorporated late during endodyogeny, might implicate Rab11A as a protein involved in mother cell IMC recycling (Dinkorma Ouologuem, 12th congress of toxoplasmosis, 2013). A second Rab GTPAse, Rab11B, is needed for the transport of Golgi derived vesicles to the nascent IMC of the daughter buds during the early phase of IMC biogenesis. IMC formation in this mutant is still initiated but assembled IMC plates seem misaligned and daughter buds are incapable of maturing. Interestingly, a defect

in IMC biogenesis did not disrupt formation of sub-pellicular microtubules, suggesting that formation of subpellicular microtubules occurs independent of IMC biogenesis (Agop-Nersesian *et al*. 2010). Within this work I was able to identify two novel factors crucial for IMC biogenesis, namely the Glideosome associated Proteins, GAP40 and GAP50. This work, for the first time, demonstrates the multi-functionality of components of the MyoA motor complex by identifying their role during replication. Lack of either GAP40 or GAP50 leads to a severe but specific defect on IMC biogenesis as other organelles are unaffected. Comparison of *gap40* KO and *gap50* KO parasites on IFA level displayed no noticeable differences in their phenotype indicating that lack of either protein caused the same effect. Strikingly, electron micrographs of parasites lacking either gap40 or *gap50* revealed large membrane plates of IMC accumulating within the cell without being assembled properly. Nevertheless, the sup-pellicular microtubules appear unaffected. This observation resembles the phenotype observed for expression of a dominant negative version of Rab11B suggesting a functional linkage between these three proteins during early biogenesis. There are two postulations regarding this interaction. Firstly, a direct interaction to traffic IMC material from the Golgi to the nascent daughter buds. Secondly, an orchestrated process where Rab11A/B deliver vesicles to the IMC and downstream of this delivery GAP40/50 stabilise and/or anchor the proteins to the subpellicular matrix (see Figure 3-20).

The function of Rab GTPases is usually linked to three possible types of molecular motors namely myosins, kinesins and dyneins (Ross *et al*. 2008). They have in common that they all use ATP hydrolysis to generate the force for movement (Schliwa and Woehlke 2003, Okten and Schliwa 2007). Kinesins and dyneins use microtubules for their movement and move to the plus- or the minus-end of the microtubule, respectively (Vallee and Sheetz 1996). Myosin motors use actin filaments for their transport and move to the plus end of the filaments with exception of class VI myosin which move to the minus end. There have been many studies in *Toxoplasma* investigating the role of microtubules and actin by treatment with specific actin and microtubule drugs. Treatment with several reagents that disturb the actin cytoskeleton, such as the filament disrupter Cytochalasin D and Latrunculin A and the filament stabiliser Jasplakinolide, reveal that neither disruptors nor stabilisers have major effects

on parasite replication. While daughter cell budding was not disrupted these actin inhibitors show an effect on the turnover of the mother cell organelles visualised by the presence of large residual bodies (Shaw *et al*. 2000). Recently, an effect of Cyotochalasin D on Rhoptry positioning and apicoplast replication was implied (Jacot *et al*. 2013, Mueller *et al*. 2013). Unlike actin inhibitors, some anti-microtubule drugs cause a significant block in parasite replication and the assembly of daughter cell conoids is disrupted. While treatment with nocodazol does not interfere with parasite replication, the microtubule disrupter Oryzalin and the microtubule stabilizer Taxol block the replication step and large abnormal parasite vacuoles are formed (Stokkermans *et al*. 1996, Shaw *et al*. 2000). Microtubule polymerisation is not completely abolished with drug treatment and parasites are still capable of initiating daughter cell budding. Although both mentioned microtubule inhibitors show severe effects on parasite replication their caused phenotypes differ. Oryzalin treatment still produced mature daughter cells with all organelles in place, the only observed phenotype was the lack of incorporation of the nucleus within the daughter parasites. This plant herbicide causes a block in polymerisation of sub-pellicular microtubules and subsequently IMC formation is blocked. It appears that IMC formation depends on the building of the sub-pellicular microtubules but sub-pellicular microtubule generation does not rely on the presence of the IMC. Akin to Oryzalin, Taxol causes a severe effect on nuclear division whereby large membrane sheets of IMC are formed but fail to assemble. Taken together, it seems that disruption of microtubule dynamics resembles the phenotypes observed for *gap40* KO, *gap50* KO and Rab11B-DN. Thus it might indicate that Rab11B delivers vesicles containing GAP40 and / or GAP50 from the golgi to the growing daughter buds using microtubule tracks. Indeed, a conditional KO for TgAct1 displays no defect in parasite replication hence excluding a role of this protein for this process (Andenmatten *et al*. 2013) (see chapter 5). This observation supports the previous findings using actin drugs. Although Act1 has no function during the assembly of the IMC some of the numerous actin-related proteins (ARPs) present in *T. gondii* have been implicated in this process while others are yet to be characterised. The nuclear Actin-related protein ARP4a is known to be required for completion of mitosis, while ALP1, as mentioned above, is needed for daughter cell budding (Gordon and Sibley 2005, Gordon *et al*. 2008, Suvorova *et al*. 2012). Vesicular trafficking depends on either

microtubule or actin filament tracks. Since deletion of *act1*, the only conventional actin gene found in the genome of *T. gondii*, only affects apicoplast segregation it appears unlikely that conventional actin tracks are used for vesicular trafficking in *T. gondii*. Nevertheless, ARPs might fulfil functions during the replication. Indeed, in other eukaryotes the actin-related protein 1 (ARP1) is a key component of the dynactin complex and has a role in microtubule-based transport. The dynactin complex comprises of short of 37 nm long Arp1-filaments and a sidearm which interacts with microtubules and dyneins as motor proteins (Schafer *et al*. 1994, Schroer 2004). Arp1 is capable of ATP hydrolysis and forms filaments that are very stable, short and probably less dynamic compared to conventional actins (Bingham and Schroer 1999). Arp1 filaments are distinct to conventional actin filaments shown by the inaccessibility of Cytochalasin D, the incapability of phallodin binding and the non-reactance with actin specific antibodies (Holleran *et al*. 1996). The function of Arp1 is to attach the kinesin motor to the cargo which are cellular structures such as Golgi membranes (Holleran *et al*. 2001). Orthologues of the chicken Arp1 exist in several apicomplexan parasites such as *Toxoplasma gondii*, *Plasmodium falciparum* and *Cryptosporidium parvum*. Additionally, *T. gondii* encodes for several actin-like proteins (Alps) that are specific for apicomplexan parasites. One could speculate that these Alps evolved to fulfil apicomplexan specific functions or mediate vesicular trafficking of phylum specific structures such as alveoli (IMC). A possible mechanism is that myosin motors could interact with, by means of walking along, Arp or Alp filaments utilising these as tracks. This spectulation is purely hypothetical as no evidence has yet been provided. Interestingly, an interaction of an actin-related protein and a myosin fragment has been reported for the gram negative bacterium *Actinobacillus pleuropneumoniae*. Also, an actin-like protein from *Dictyostelium discoideum* is described to interact with rabbit muscle myosin (Woolley 1972, Guerrero-Barrera *et al*. 1999). Whether or not an interplay of ARPs/ALPs and myosins can mediate vesicle movement during vesicular trafficking in apicomplexan parasites needs to be clarified in the future.

6.1.2 Role of MyoA mutant during replication

Toxoplasma gondii has the largest repertoire of myosins among the apicomplexan group identified so far, whereby 10 genes encode for 11 Myosins

that are divided into five groups depending on their respective head domain (Foth *et al*. 2006). Six myosins were identified in *P. falciparum* and *Cryptosporidium parvum* (Gardner *et al*. 2002, Abrahamsen *et al*. 2004). Six of the myosins (MyoA-E and MyoH) discovered in *Toxoplasma* belong to the apicomplexan specific group XIV. Interestingly, while 11 myosin heavy chains are present in *T. gondii*, only seven Myosin light chains (MLCs) have been identified so far. This suggests that some myosins might share the same light chain (Foth *et al*. 2006, Polonais *et al*. 2011). MyoA is the only Myosin heavy chain identified to interact with MLC1 (Herm-Gotz *et al*. 2002). Overexpression of only the tail domain of this myosin causes a severe IMC specific defect and block in replication (Agop-Nersesian *et al*. 2009). It was thought that the tail domain of MyoA competes with other endogenous myosins for shared interaction partners such as MLC1. Interestingly, two other apicomplexan specific myosins are known to play a possible role during replication. Parasites overexpressing MyoB are delayed in replication and form enlarged residual bodies (Delbac *et al*. 2001). In order to investigate the cause for the observed IMC defect after overexpression of the MyoA-tail different approaches were used. First, it was assessed if a rescue of the phenotype can be achieved by simultaneous over expression of proteins known to interact with MyoA. While none of the transfected constructs were capable of fully restoring the phenotype, overexpression of MLC1 resulted in partial complementation. The *mlc1* DNA used for complementation had a C-terminal Ty tag and was driven by the strong constitutive tubulin promoter P5RT70, which could cause insufficient complementation due to wrong timing of expression or inadequate functioning. Indeed several attempts to tag mlc1 endogenously at the C-terminus failed (data not shown). Therefore, a conditional *mlc1* KO was generated by using the endogenous promoter and no tag at either end of the protein. Although *mlc1* was found to be essential for parasite survival *in vitro*, no defect on the IMC was observed. One explanation could be that overexpressed MLC1ty binds to MyoA-tail and thereby acting as a buffer, neutralising the dominant negative effect of MyoA-tail.

Since overexpression of the tail domain of MyoA caused a dominant negative effect, probably caused by depletion of one of the MyoA interacting proteins, KO mutants for all known components of the MyoA-motor complex were established. Two proteins interacting with the MyoA motor complex were identified having an

IMC defect, GAP40 and GAP50. Although the exact mechanism leading to the MyoA-tail phenotype is not completely understood, its connection with above mentioned MyoA-associated proteins is highly supported, thus attributing the phenotype to depletion of GAP50 and/or GAP40.

6.1.3 Future directions: IMC biogenesis

Although the IMC is a unique compartment, barely anything is known concerning its biogenesis and trafficking of crucial proteins to this important organelle. Within this study two glideosome associated proteins were identified as having a significant role during IMC biogenesis. The interplay of these GAPs with other factors important for IMC formation and their trafficking to the IMC still need to be determined. Although the interaction of GAP40 and GAP50 with the other proteins of the glideosome is well described (Frenal *et al*. 2010), future experiments will be required to dissect the molecular mechanism of their transport pathway. Since the small GTPase Rab11B is involved in transporting vesicles to the nascent IMC of the daughter, an identification of its interaction partners or the content of the vesicles being delivered could shed light on the specifics of the biogenesis of the IMC. To achieve this Co-immunoprecipitations (Co-IP), pull-downs, yeast-two hybrid or vesicle purification could be carried out as in other eukaryotic systems (Huber *et al*. 1993, Christoforidis and Zerial 2000, Kail and Barnekow 2008, Gabernet-Castello *et al*. 2011, Dong and Wu 2013). Additionally, Co-IPs of MyoA-tail overexpression parasites for components of the MyoA motor complex could reveal information about if the tail domain alone is capable of interacting with all known interaction partners of MyoA and hence exclude that the observed phenotype is the outcome of a missing interaction.

Despite being a member of the MyoA motor complex and being integrated within the IMC through nine transmembrane domains, it is not examined yet if direct interaction of GAP40 occurs solely with GAP50 or other components of the glideosome as well. The IMC is a dual membrane layer sandwiched between the plasma membrane and the cytoskeleton network, thus GAP40 could be integrated in either the outer or inner IMC. An interaction with other proteins of the MyoA motor complex additional to GAP50 would only be possible if GAP40 were localised in the outer IMC. Although not falling into their phylogenetic class, GAP40 seems to have similarities to GAPM proteins since GAPM stands for

glideosome-associated protein with multiple-membrane spans which all are features attributed to GAP40. GAPMs are located in the inner IMC and it was suggested that GAPMs anchor the IMC to the cytoskeleton by interacting with alveolins (Bullen *et al*. 2009) hence GAP40 might be localised in the inner IMC building the bridge from the cytoskeleton network to the actin/myosin motor complex. Direct protein-protein interactions of GAP40 with GAP50 or other components of the MyoA motor complex could be investigated using methods such as Fluorescence resonance energy transfer (FRET) or Far Western Blotting (Edmondson and Dent 2001, Sato *et al*. 2011, Aoki *et al*. 2013).

All conclusions concerning the IMC biogenesis effects of *gap40* KO, *gap50* KO, MyoA-tail mutant and Rab11B-DN parasites were drawn dependant on static IFAs and electron microscopy. As this does not give detailed insights into the exact timing when the IMC defect can be observed first, the assessment of these mutants via life microscopy could be the next step to investigate their role in the fate of the IMC further. Unfortunately, depletion using the DiCre system is a rather slow process, thus a faster regulation system such as the Knock-sideway system would be a reasonable alternative (Robinson *et al*. 2010, Robinson and Hirst 2013). The earliest IMC protein detected during daughter bud initiation is IMC15 which co-localises with Rab11B. Therefore amongst others IMC15 would be a good candidate for life microscopy within the mutants. Moreover IMC5, 8, 9 and 13 are detected at the cortical IMC of early daughter buds, but re-localise to the basal end in the late budding phase (Anderson-White *et al*. 2011). Hence it might be interesting to see what happens to these proteins in mutants where the daughter IMC cannot mature. The IMC proteins IMC7, 12 and 14 denote the IMC of the parasites in G1 phase and are not detected in daughter buds, thus a role for these proteins as marker to distinguish mother and daughter IMC for mother IMC disassembly was suggested. Based on the results obtained from the above mentioned IMC mutants, these mutants keep replicating without ever maturating. It would therefore be useful to identify if proteins specific to mature IMC can still be detected. Furthermore it would be attractive to follow the formation of fluorescently labelled tubulin to confirm that IMC biogenesis defects do not necessarily go along with defects on microtubules.

6.2 The functions of the Acto-MyoA motor complex [5]

6.2.1 The Acto-MyoA motor complex is not essential for the asexual lifecycle *in vitro*

Several of the core components of the invasion and gliding machinery were analysed using a tetracycline-inducible transactivator knockdown system and independent results suggest an important role of this machinery for gliding motility and host cell penetration (Meissner *et al*. 2002, Huynh and Carruthers 2006, Plattner and Soldati-Favre 2008, Starnes *et al*. 2009, Buguliskis *et al*. 2010, Daher *et al*. 2010). Interestingly, none of the knockdown mutants of these key players revealed a complete block for the invasion event which was explained due to leaky expression of the respective gene of interest. With the establishment of a conditional DiCre-Knockout system (Andenmatten *et al*. 2013) several core components of the gliding machinery such as the Acto-MyoA motor complex (MyoA, Act1, GAP45, MLC1), the believed force transmitters (AMA1, MIC2) and Rhomboid proteases (ROM4) were re-dissected (Andenmatten *et al*. 2013, Bargieri *et al*. 2013, Egarter *et al*. 2014) (Abstract #175 Molecular Parasitology Meeting, Woods Hole 2013). In agreement with the previous knockdown data, all of the generated knockout mutants were capable invading the host cell in absence of the respective gene. Recent studies on the surface adhesins, AMA1 and MIC2 revealed that both proteins are not essential for parasites survival and parasites are capable of invading the host cell without AMA1 (Bargieri *et al*. 2013) or MIC2 (Andenmatten *et al*. 2013) (Dr Allison Jackson; private conversation). Surprisingly, unlike previously thought AMA1 appears not to be involved in tight junction formation as the RON complex is still formed in absence of AMA1 (Bargieri *et al*. 2013). The glycolytic enzyme aldolase had been described, in a landmark publication, as the essential linker between surface adhesins and parasite actin that is required for force transmission (Jewett and Sibley 2003). Indeed, this early observation has since been validated in numerous, highly influential studies in diverse apicomplexan parasites (Buscaglia *et al*. 2003, Goo *et al*. 2013). Intriguingly, recently the group initially describing this interaction convincingly demonstrated that aldolase has an important function as a glycolytic enzyme, but not as linker (Shen and Sibley 2014). Therefore, the field is now left with a missing link and we cannot be

[5] Adapted from Egarter et al. (2014)

certain how and if force is transmitted via surface adhesins. Detailed analysis of the Acto-MyoA motor complex revealed that while most proteins of this complex were essential for parasite survival, the motor protein, MyoA, was dispensable for the asexual life cycle *in vitro* (Egarter *et al*. 2014). Recent studies on *myoA* KO parasites indicate that MyoA is essential for host cell egress but dispensable for gliding motility and invasion (Andenmatten *et al*. 2013, Egarter *et al*. 2014). Interestingly, gliding and invasion speed were significantly decreased in parasites lacking *myoA*. Moreover, many *myoA* KO parasites invade the host cell in a slow stop and go fashion. Remarkably, a triple KO for *myoA,B/C* exhibits a stronger phenotype when compared to the *myoA* KO, suggesting overlapping functions and/or redundancies of these myosins. Nevertheless, this observation does not explain why other components of the MyoA motor complex (MLC1 and GAP45) are still capable of invading host cells. Depletion of either GAP45 or MLC1 results in re-localisation of MyoA from the periphery to the cytosol, thus indicating that the platform for a functional MyoA motor is absent in these KO lines. Furthermore, initial studies of co-expression of MyoA or MyoC within *mlc1* KO parasites suggests degradation of both myosin motors (my own data, Fernanda Maria Latorre Barragan; unpublished). Removal of *mlc1* results in a phenotype analogous with *myoA* KO parasites in terms of gliding motility and invasion. Surprisingly, the effect of *mlc1* depletion on host cell egress was more pronounced when compared to *myoA* KO parasites. While parasites lacking *mlc1* were almost completely blocked, *myoA* depleted parasites showed rather a delayed egress phenotype. Akin to *myoA* KO, *mlc1* KO parasites show a reduction in gliding motility to a rate of approximately 40 % producing mainly circular trails. Furthermore, *mlc1* KO and *myoA* KO parasites penetrate the host cell with the same efficiency (~25 %) through a typical appearing tight junction. Nevertheless, since MyoA is mislocalised in *mlc1* KO parasites, it seems unlikely that another myosin light chain fulfils the role of MLC1, when MLC1 is absent. However, the substitution through a different motor complex cannot be ruled out. Indeed, the recently studied MyoD-MLC2 motor is localised at the periphery (Polonais *et al*. 2011) akin to MyoA-MLC1 hence presenting a hypothetical candidate for complementing after loss of MyoA-MLC1. Interestingly, removal of *gap45* revealed no effect on the gliding motility rate hence has a less pronounced effect on gliding motility when compared to the *myoA* KO and *mlc1* KO. In the absence of GAP45 the interacting components of the gliding

machinery (MLC1 and MyoA) are redistributed to the cytosol of the parasite and extracellular parasites change their typical crescent shape and swell up. Whereas these data confirm previous findings by Frenal *et al*. 2010, it was an unexpected result that *gap45* KO parasites are able to glide on FBS coated surfaces, although gliding speed was significantly reduced. A possible explanation for the observed inconsistencies could be differences in the conditions of the trail deposition assay, such as different coating substrates that alter the attachment ability. Since the trail deposition assays allows only a qualitative assessment of overall gliding motility, time lapse microscopy was performed to show that *gap45* KO parasites are capable of gliding. Interestingly, *gap45* KO parasites are able to glide twice as fast as *myoA* KO parasites although the motor is not localised at the periphery in the absence of GAP45. This indicates the force for gliding motility can be generated in a MyoA independent manner. Furthermore, invasion of parasites lacking GAP45 is drastically decreased (5 %), possibly due to the observed morphological defects and not due to the absence of gliding motility. Importantly, as observed for *mlc1* KO and *myoA* KO parasites, host cell penetration occurs through a normal appearing TJ. Strikingly, depletion of parasite actin does not cause a complete block of motility and 10 % of *act1* KO parasites are capable of gliding compared to control parasites. Mostly short, circular trails are readily detected in motility assays, suggesting that a residual motility is possible in absence of parasite actin. Additionally, parasites lacking Act1 were still able to invade host cells through a normal appearing TJ, although invasion was significantly reduced. Parasite egress was the only motility dependant process that was completely blocked in parasites lacking *act1*. This result resembles previous studies in which parasites treated with actin inhibiting drugs are unable to exit host cell after artificial stimulation (Shaw *et al*. 2000, Caldas *et al*. 2013).

Intriguingly, when the sensitivity of *act1* KO parasites to the actin disrupting drug Cytochalasin D (CD) was compared to wildtype (DiCre Δku80) and CD resistant parasites (cytdr), it was found that all strains behave similarly and in all cases invasion is almost blocked in presence of 2 µM of CD, as previously shown for CD resistant parasites (Gonzalez *et al*. 2009). In contrast to the study by Dobrowolski and Sibley (1996) the analysis presented here indicates a far less pronounced sensitivity of wild-type parasites to CD and 10-fold higher

concentrations are required (1-2 µM instead of 0.1-0.2 µM). The strongest difference in invasion efficiency between wildtype and cytr parasites can be seen at a concentration of 0.5-1.0 uM CD. Furthermore, invasion of *act1* KO parasites remains sensitive to CD suggesting that invasion of *act1* KO parasites critically depends on host cell actin. Alternatively, CD has a second, not yet identified target in the parasite. Indeed, Dobrowolski and Sibley (1996) isolated a CD resistant parasite line that has no mutation in *act1*. Previous studies implicate a crucial role of host cell actin during invasion (Ryning and Remington 1978, Gonzalez *et al*. 2009, Delorme-Walker *et al*. 2012) leading to the hypothesis that once the TJ is formed host cell actin plays a critical, potentially essential role during invasion of the analysed mutants. Since the current model for gliding motility and invasion seem not to fit to recent data on, an updated model is favoured, where host and parasite actin act in a highly concerted and synergistic manner.

In summary, different explanations would explain the still present gliding motility and invasion Acto-MyoA motor complex mutants: 1) Essential KO lines could have residual protein present which is not detectable on IFA level. 2) Components of the gliding and invasion machinery have multiple redundancies compensating for the loss of a distinct protein. 3) A compensatory invasion mechanism is in place that can substitute for the loss of a functional Acto-MyoA motor complex. 4) Our current model for the molecular mechanisms of gliding motility and host cell invasion requires substantial modification.

6.2.2 Possible redundancies within the MyoA motor complex?

Redundancies are a possible explanation for the residual invasion events of *myoA* KO parasites since parasites lacking myoA, myoB and myoC display a more severe phenotype indicating shared functions. Akin to myosins the collection of micronemal proteins is large and thus redundancies cannot be excluded. Similarly, the repertoire of gliding associated proteins (GAP) comprises five proteins, GAP40, GAP45, GAP50, GAP70 and GAP80 (Gaskins *et al*. 2004, Gilk *et al*. 2009, Frenal *et al*. 2010, Jacot and Soldati-Favre 2012). GAP50 and GAP40 are integrated solely into the IMC and are unlikely substitute for the loss of GAP45. GAP70 and GAP80, on the other hand, were reported to act as an anchor similarly to GAP45 to IMC and PM, but their localisation is restricted to the apical and basal region of the parasites. Although it would be conceivable that GAP70

or GAP80 become redistributed to the whole parasites length, a different motor must generate the force since MyoA-MLC1 is in the cytosol after GAP45 depletion. The only other motor identified at the periphery is MyoD-MLC2, but MyoD is dispensable for tachyzoite survival hence most likely has no important role for gliding and invasion (Herm-Gotz *et al*. 2006, Polonais *et al*. 2011). Since every myosin motor needs actin tracks to generate the force for locomotion, according to the linear motor model, the *act1* KO parasites demonstrate that the observed gliding motility and invasion events, after removal of components of the MyoA motor complex, are unlikely occurring due to redundancies of similar proteins. Therefore, it could be speculated that actin and myosin, although important for motility, are not essential for generation of the force required for gliding and invasion. Their role might be the establishment of the directionality of the movement. It was previously assumed that actin-myosin and micronemes are crucial for the definition and release of attachment sites that direct gliding force in the right direction (Gaskins *et al*. 2004, Munter *et al*. 2009, Andenmatten *et al*. 2013, Hellmann *et al*. 2013). Together the analysis of the key components of the known motility machinery (MyoA, GAP45, MLC1 and Act1) demonstrates that the force required for motility and invasion can be generated differently.

6.2.3 Alternative gliding and invasion mechanism of other Apicomplexa

Since the current linear motor model for gliding motility and the model for invasion of *Toxoplasma gondii* requires revision to fit the latest data for mutants of this machinery, a closer look into alternative gliding and invasion mechanisms of other apicomplexan parasites might reveal new perspectives. *Cryptosporidium parvum* infects enterocytes and causes severe gastrointestinal illnesses. Like most apicomplexan parasites, *C. parvum* approaches new host cell using an actin dependent process called gliding motility (Wetzel *et al*. 2005). Although gliding motility of *C. parvum* is very similar to *T. gondii,* and parasites attach to the host with the apical end orientated towards the host cell, *C. parvum* does not actively invade the cell. Furthermore, no formation of a tight junction has been observed and this parasite lacks homologues of AMA1 or RON2 (Kemp *et al*. 2013). In lieu of active penetration, *C .parvum* facilitates the remodelling of the actin cytoskeleton of the host cell. Different studies show

that host actin modulators (Arp2/3, VASP and N-WASP) are recruited to the parasite entry sites (Elliott and Clark 2000, Chen *et al*. 2004, O'Hara *et al*. 2008). Furthermore, host sodium/glucose co-transporters and aquaporins were recruited to the attachment site (Chen *et al*. 2005). Uptake of glucose leads to water influx and thus subsequently causes an increase in host cell volume at the entry site around the parasite. Hence, cellular invasion depends on host cell actin polymerisation and membrane protrusion at the host-parasite contact site prior to parasite encapsulation. Interestingly, recent work revealed that other apicomplexans like *T. gondii* and *Plasmodium berghei* modulate the host cell actin cytoskeleton at the attachment site of parasite and host cell (Gonzalez *et al*. 2009, Delorme-Walker *et al*. 2012, Gomes-Santos *et al*. 2012), indicating an important role of the host cell. Recent data showed that siRNA against host cortactin and other F-actin regulators as well as destabilisation of host microtubules decreased the invasion rate of *T .gondii* (Sweeney *et al*. 2010, Delorme-Walker *et al*. 2012, Gaji *et al*. 2013). Additionally, both host actin and microtubules accumulated at the TJ during invasion (Baum *et al*. 2008, Takemae *et al*. 2013). Host-mediated internalisation of *T. gondii* might be another explanation for Acto-MyoA independent invasion. Indeed a collar-like structure was found to form between *T. gondii* and non-phagocytotic cell indicating an alternative mechanism (Meissner *et al*. 2013). To which extend other host cell factors might be recruited to the invasion site and contribute to the invasion process needs to be addressed in future.

Another apicomplexan parasite is *Theileria* which is transmitted by ticks and is responsible for east coast fever and theileriosis in cattle. Unlike *Toxoplasma*, *Theileria* sporozoites are non-motile and lack micronemes and a conoid. *Theileria* invasion differs considerably from host cell invasion of other apicomplexans like *Plasmodium* and *Toxoplasma*. *Theileria* is able to invade the host cell in any orientation independently of both parasite and host cell actin (Shaw 1999, Shaw 2003). The initial attachment is a strong binding and not reversible. This is in contrast to *T. gondii* that first loosely attaches then re-orientates itself before invading with its apical end first (Shaw 2003, Carruthers and Boothroyd 2007). This zippering mechanism involves the formation of several firm interaction between the parasites and the host cell (Shaw 2003). Although no tight junction like the one in *Toxoplasma* was observed, homologues of the

tight junction proteins AMA1 and RON2 can be found in the genome of *Theileria spp* (Gardner *et al*. 2005). It remains uncertain if this mechanism is homologous to a zoite that penetrates in an apical orientation, if the zippering mechanism can generate the required force for rapid invasion or if other force-producing mechanisms participate in host cell invasion. Interestingly, it was recently shown that *Theileria* parasites subvert host cell actin dynamics for motility regulation of the host cell and host cell invasiveness (Baumgartner 2011). Recent data demonstrates that *Toxoplasma* is capable to co-opts host cell and to modulate motility of infected dendritic cells (Lambert and Barragan 2010, Koshy *et al*. 2012).

Gregarines are an early branching lineage of apicomplexan parasites and they parasitise invertebrates and urochordates. These parasites approach the host cells by gliding motility (King 1981, Valigurova *et al*. 2013), but unlike other apicomplexan parasites do not invade. Instead they strongly attach and feed on the host cell with their apical pole partially integrated (Valigurova 2012). Gregarines developed elaborate alterations of their apical complex for the uptake of nutrients that include unique secretory organelles. Interestingly, gregarines are the fastest apicomplexan parasites with a gliding motility speed of up to 10 µm per second (King 1988) which is approximately six times fatser than the average speed of *T gondii* although the mechanism is thought to be alike. Contrary to other apicomplexans filamentous actin could be verified by staining with phalloidin (Valigurova 2012), and relatively high doses of Cytochalasin D and Jasplakinolide are required to block gliding motility fully (Valigurova *et al*. 2013).

Concluding, the above findings suggest the existence of distinct invasion mechanism in apicomplexan parasites questioning if some Apicomplexa use the gliding machinery to generate a force at the attachment site allowing access to the host cell. In that case, the question rises whether this mechanism is employed exclusively or additionally to others.

6.2.1 Comparison between apicomplexan motility and amoeboid migration

"Amoeboid migration" refers to a constant alteration of shape while the cell is moving. There are three different known modes for force generation and force transmission to power this type of locomotion: (1) membrane blebbing (see chapter 6.2.2); (2) retrograde actin flow and (3) polymerisation driven membrane deformation (Renkawitz and Sixt 2010).

Retrograde actin flow is the mode used to form lamellipodia for movement, and depends on the force produced and transmitted at the leading edge (Bisi *et al*. 2013). Actin polymerization and Myosin II-mediated contractile and protrusive forces are converted into traction forces via adhesion receptors. This coupling is known as clutch (Hu *et al*. 2007). The force transmitters for this type of locomotion belong to the integrin family of transmembrane receptors and are key players for this adhesion-dependent migration (Arnaout *et al*. 2007). Therefore, retrograde actin flow can only produce force when the actin cortex is mechanically linked to the substrate.

Interestingly, dendritic cells in which all integrins have been depleted show a complete block in adhesion and migration on 2D surfaces, but move with the same speed as wild-type cells in 3D matrices (Lammermann *et al*. 2008). The same study demonstrated that treatment of dendritic cells with the Myosin II inhibitor blebbistatin has no effect on the instantaneous speed of the cells, indicating the disposability of Myosin II dependent gliding in very dense collagen gels. Interestingly, dendritic cells in which actin was disrupted by latrunculin showed no difference in speed, independent of the gel density. Moreover, polymerisation speeds of the actin-myosin network is doubled in the absence of integrins compared to wild-type cells (Renkawitz *et al*. 2009). This third mode of locomotion only occurs in a 3D environment and depends entirely on membrane deformation caused by actin polymerisation.

The linear motor model of apicomplexan parasites works similar to retrograde actin flow. The force for motility is generated by the Acto-MyoA complex and transformed into traction force via the adhesion proteins (MIC2, AMA1) (Soldati and Meissner 2004). Depletion of *act1*, *myoA* , and *mic2* showed a significantly

reduced rate of gliding motility in 2D assays with mainly circular trails that appeared shorter in comparison (Huynh and Carruthers 2006, Egarter *et al*. 2014) to wild-type parasites. Interestingly, analysis of *mic2* KO and *act1* KO parasites in 3D Matrigel revealed that although the fraction of moving parasites motility rate was reduced compared to wild-type parasites, parasites lacking *mic2* or *act1* appeared capable to reach the same speed as the wildtype (Dr Jacqueline Leung, unpublished). Strikingly, removal of *myoA* caused a significantly lower motility rate than seen for *act1* KO parasites and parasites were incapable of moving as fast or as far as wild-type parasites. This indicates that MyoA might be more important than Act1 in a 3D environment similar to the above-mentioned study on dendritic cells (Lammermann *et al*. 2008). Whether or not this is a possibility needs to be clarified in future experiments.

6.2.2 Hypothesis for novel/revised gliding motility model using alternative driving forces [6]

In *Toxoplasma*, parasite actin is a single copy gene (Dobrowolski *et al*. 1997), hence no other conventional actin protein exists that could overtake its role as key player of the gliding machinery (Soldati and Meissner 2004). Because of the findings that parasites were able to glide without act1 present, other possible mechanisms for this movement will be discussed. Actin polymerization and actin-myosin-contraction was believed to be the foundation for force formation in eukaryotic cells. Recent data question this model and suggests a novel model where the cytosol is treated as poroelastic, thus allowing hydrodynamic forces to generate shape changes during motility (Mitchison *et al*. 2008). Supporting this idea, recent studies showed the poroelastic nature of the cytosol (Moeendarbary *et al*. 2013). In this model differences in hydrodynamic pressure generate the force. The pressure can either be generated by actin-myosin activity or by osmogenic ion transporters in the plasma membrane (Mitchison *et al*. 2008) Other organisms use hydrodynamic pressure as the driving force for locomotion. The rice fungus *Magnaporthe oryzae* is able to generate a turgor of 8.0 MPa to invade plant cells (Dagdas *et al*. 2012). Comparable to this invasion mechanism, Alex Mogilner developed a mathematical model, suggesting a gelation-isolation osmotic engine for the locomotion of *T. gondii* (Egarter *et al*. 2014). According

[6] Adapted from Egarter *et al*. (2014)

to this model, a gel-like structure exists at the apical pole of the parasites. This structure comprises actin-like filaments as macromolecules and acidic protein micromolecules secreted by micronemes. In addition, this gel would be coated by immobile heavy and mobile light cations in the cytoplasm (Xian *et al*. 1999). The required osmotic pressure produced by the mobile cations is balanced by tension of the elastic gel. Degradation of macromolecules leads to partial disassembly of the gel which causes the elastic modulus to weaken and subsequently results in gel swelling. As a consequence of the swelling, the leading edge (the apical end) of the parasite is pushed forward providing the gel is connected to the substrate via adhesion sites. The basal end of the parasite will be pulled forward due to membrane tension created by the foregoing force (Ofer *et al*. 2011) and due to cytoplasmic flow, which is generated by the pressure gradient. After the complete disassembly of the old gel, a new one can be formed in order to initiate a new protrusion cycle. In agreement with this proposed model, recent studies demonstrate that rapid locomotion of the parasite depends on quick turnover of adhesion sites as well as cycles of actin filament assembly and disassembly (Munter *et al*. 2009, Hegge *et al*. 2010, Skillman *et al*. 2011, Skillman *et al*. 2013). Other mechanisms that rely on osmotic pressure are also imaginable. The secretion of charged molecules on the apical tip and capping at the rear end can generate a cytoplasmic flow assumed enough water permeability of the parasite membrane. Such a mechanism possibly requires aquaporins for water intake, yet, a respective knockout *in P. berghei* did not affect gliding or invasion (Kenthirapalan *et al*. 2012). Alternatively, pressure could be generated through osmogenic ion transporters in the plasma membrane (Mitchison *et al*. 2008). Indeed several Na^+/H^+ antiporter were shown to be involved in *T. gondii* invasion and egress (Arrizabalaga *et al*. 2004, Karasov *et al*. 2005, Francia *et al*. 2011).

Another mechanism relying on hydrostatic pressure is membrane blebbing (Charras *et al*. 2005, Fackler and Grosse 2008). Generally, blebbing is initiated by extracellular stimuli which cause a spatial destabilisation or depolymerisation of the corical actin meshwork. Consequently the cortex-membrane interaction disrupts and causes a plasma membrane protrusion stimulated by the cell internal cytoplasmic hydrostatic pressure. Thus, bleb development is based on two forces, extracellular osmotic pressure and membrane tension. Interestingly,

a study on *Dictyostelium* cells showed that amoeboid motility involves two mechanically distinct processes, that can be distinguished by the formation of two different cell-surface protrusions namely blebs and filopodia-lamellipodia (Yoshida and Soldati 2006). The same study revealed that increasing the external osmolarity results in blebbing inhibition in wildtype cells but does not affect myosin-II null mutants. Furthermore, blebbing was increased when mechanical resistance in form of high agarose was applied suggesting a solely physical way for bleb stimulation, based on the relief of local membrane stress (Zatulovskiy *et al*. 2014). Although blebbing has not been observed in *T. gondii*, alteration of the actin cytoskeleton using Jasplakinolide, a membrane-permeable actin polymerizing and filament-stabilizing drug, results in apical protrusion which seems energy dependent (Shaw and Tilney 1999, Angrisano *et al*. 2012). Moreover, this process is calcium dependant (Mondragon and Frixione 1996) and can be blocked by Cytochalasin D. Whether or not an osmotic engine could generate the driving forcing for motility and invasion of *T. gondii* needs to be addressed in future.

6.2.3 Future directions: Gliding motility and invasion mechanism

The locomotion of many cells depends on the constant formation and disassembly of adhesion sites (Webb *et al*. 2002). Migrating cells first form a protrusion, build adhesion sites at the leading edge of the protrusion, migrate forward and finally release the attachment site at the rear. Overly tight attachment to the substrate leads to immobility due to failure in adhesion site turnover, whereas loose attachment leads to the inability to produce enough force for locomotion; both situations result in little motility (Kemeny *et al*. 2013). Overall, medium adhesion strength is required for optimal cell spreading and motility as demonstrated through various mathematic models (Barnhart *et al*. 2011, Ziebert and Aranson 2013, Sackmann and Smith 2014). The dynamics of the adhesions sites are reliant on substrate stiffness or adhesiveness.

The movement of *T. gondii* depends on the formation of strong interactions between the parasite's surface and the substrate(s) it is gliding on. Thus, alteration of the substrate in turn changes gliding motility. Recent studies on parasites lacking the subtilisin 1 gene (*sub1*) demonstrate that these parasites are impaired in gliding on substrates such as FBS, heparin and chondroitin

sulphate A (Lagal *et al*. 2010). Interestingly, gliding motility could be restored using Collagen I as substrate although mainly helical gliding was observed and was almost five times more than that observed with FBS coating (Lagal *et al*. 2010). Given my own observations that the gliding rate of GAP45-depleted parasites was not affected when using FBS as a substrate compared to a complete gliding block when using poly-L-lysine as substrate and inducing motility with the calcium ionophore ionomycin (Frenal *et al*. 2010), a next step to analyse gliding motility of Acto-MyoA motor complex KOs would be to compare their gliding abilities on different substrates. Recent studies in *Plasmodium berghei* showed that attachment sites are not evenly distributed over the entire body length of the parasites but form distinct patterns instead. Tractive force and release of contact sites lead to a "stick and slip" movement (Munter *et al*. 2009). Similarly, *T. gondii* tachyzoites seemed to move in a stop and go fashion when circular gliding was observed in live video microscopy. This movement is more pronounced in the *gap45* KO and *myoA* KO parasites, which seem to stop for a relatively long time between motility bursts when compared to wild-type parasites (Egarter *et al*. 2014). One could speculate that the Acto-MyoA motor complex plays an important role during the definition and turnover of attachment sites to the surface. Recent studies on amoeboid cells showed that osmotic pressure and hydrodynamic fluids are critical for locomotion whereas the actin-myosin system appears to be important for formation and release of adhesion sites and the associated traction force (Keren *et al*. 2009). Examination of adhesion turnover dynamics in tachyzoites lacking distinct components of the Acto-MyoA motor complex, using reflection interference contrast microscopy (RICM) and traction force microscopy (TFM), could shed light on the distribution of adhesion sites, when these discrete contacts are formed and when they are disengaged as the parasites are gliding. Another technique to investigate adhesion is to use optical tweezers to manipulate objects and capture organisms in a laser beam. This method has been successfully used to study *P. berghei* sporozoites (Hegge *et al*. 2012) and could be transferred to analyse the *T. gondii* mutants generated in this study. Additionally, flow chambers could be used to measure the adhesion strength of the parasites.

So far penetration and gliding speed was only studied for the *myoA* KO and *gap45* KO parasites. Due to the low invasion rate of *gap45* KO parasites, it was not feasible to analyse invasion kinetics. During several attempts, no parasite was observed to enter the cell in the image field of view. To analyse kinetics pulse invasion assays (Kafsack *et al*. 2007), to synchronise the parasites, in combination with time lapse microscopy could be performed. This would increase the number of parasites penetrating the cell in a field of view. Because of the low excision rate of loxPMLC1 parasites, time lapse microscopy proved to be technically challenging. With the establishment of a highly efficient DiCre recipient strain (DiCre Δ*ku80*), a novel loxPMLC1 strain could be generated in this recipient background to analyse gliding and invasion kinetics. Furthermore, a higher excision rate would allow for western blot analysis, thus the anticipated MyoA depletion after *mlc1* removal could be investigated. Additionally, time lapse microscopy of the *act1* KO parasites should be investigated. Apart from gliding and invasion movies, analysis and comparison of the ability of different mutants to egress after artificial stimulation could be performed using time lapse microscopy. This would be beneficial as this step of the lytic cycle was only assessed using end-point experiments. It might allow to distinguish between different egress phenotypes of the Acto-MyoA motor complex KOs and perhaps lead to hypotheses as to why they behave differently and why it is impossible to generate stable, clonal lines of the *gap45* and *mlc1* KO parasites.

Generally, residual invasion events could be explained by redundancies of the depleted gene. In addition to Myosin A, there are 10 other myosins encoded in the genome of *Toxoplasma*, with five of these belonging to the same myosin class XIV as MyoA. Indeed, it appears there is an overlap between the functions of MyoA, MyoB and MyoC. Similarly, MLC2-MLC7 could complement for MLC1 and GAP70/80 for GAP45 (Frenal *et al*. 2010, Polonais *et al*. 2011). In order to investigate this possibility, co-immunoprecipations could be performed to identify any functionally redundant proteins; *e.g.*, in *myoA* or *mlc1* depleted parasites use an antibody against GAP45 to identify novel interacting partners. It would be expected that if a protein that typically is not associated with the MyoA motor complex overtakes a function within this complex, its expression level will be upregulated. Therefore, mRNA levels of candidate proteins in the respective KO parasites could be measured using quantitative PCR (qPCR) to

identify if other myosins, MLCs or GAPs are upregulated. Interestingly, *myoA* KO parasites adapt over time when kept in *in vitro* culture continuously (Dr Nicole Andenmatten; private communication). However, the expression level of other myosins was not altered compared to the wildtype strain, suggesting that redundancies are probably not the reason for residual invasion events. For the single copy gene act1, I consider it is unlikely that ALPs and ARPs substitute to function as force generators using the linear motor model, however a functional rescue would be possible if the force was generated in a different way such as an osmotic engine. Because of this, qPCR could be used to identify the substituting actin-like protein.

In conclusion, *T. gondii* tachyzoites are capable of invading host cells using an actin-myosin independent mechanism. Elucidation of this highlights the need for future work to determine if the current model needs overall revision or if the parasites have evolved a "backup" mechanism to the linear model to ensure successful invasion and survival.

References

Abrahamsen, M. S., T. J. Templeton, S. Enomoto, J. E. Abrahante, G. Zhu, C. A. Lancto, M. Deng, C. Liu, G. Widmer, S. Tzipori, G. A. Buck, P. Xu, A. T. Bankier, P. H. Dear, B. A. Konfortov, H. F. Spriggs, L. Iyer, V. Anantharaman, L. Aravind and V. Kapur (2004). "Complete genome sequence of the apicomplexan, Cryptosporidium parvum." Science **304**(5669): 441-445.

Achanta, S. S., S. M. Varunan, S. Bhattacharyya and M. K. Bhattacharyya (2012). "Characterization of Rad51 from apicomplexan parasite Toxoplasma gondii: an implication for inefficient gene targeting." PLoS One **7**(7): e41925.

Agop-Nersesian, C., S. Egarter, G. Langsley, B. J. Foth, D. J. Ferguson and M. Meissner (2010). "Biogenesis of the Inner Membrane Complex Is Dependent on Vesicular Transport by the Alveolate Specific GTPase Rab11B." PLoS Pathog **6**(7): e1001029.

Agop-Nersesian, C., B. Naissant, F. Ben Rached, M. Rauch, A. Kretzschmar, S. Thiberge, R. Menard, D. J. Ferguson, M. Meissner and G. Langsley (2009). "Rab11A-controlled assembly of the inner membrane complex is required for completion of apicomplexan cytokinesis." PLoS Pathog **5**(1): e1000270.

Ahn, H. J., S. Kim and H. W. Nam (2005). "Host cell binding of GRA10, a novel, constitutively secreted dense granular protein from Toxoplasma gondii." Biochem Biophys Res Commun **331**(2): 614-620.

Akaki, M. and J. A. Dvorak (2005). "A chemotactic response facilitates mosquito salivary gland infection by malaria sporozoites." J Exp Biol **208**(Pt 16): 3211-3218.

Alexander, D. L., J. Mital, G. E. Ward, P. Bradley and J. C. Boothroyd (2005). "Identification of the moving junction complex of Toxoplasma gondii: a collaboration between distinct secretory organelles." PLoS Pathog **1**(2): e17.

Allen, M. L., J. M. Dobrowolski, H. Muller, L. D. Sibley and T. E. Mansour (1997). "Cloning and characterization of actin depolymerizing factor from Toxoplasma gondii." Mol Biochem Parasitol **88**(1-2): 43-52.

Amino, R., D. Giovannini, S. Thiberge, P. Gueirard, B. Boisson, J. F. Dubremetz, M. C. Prevost, T. Ishino, M. Yuda and R. Menard (2008). "Host cell traversal is important for progression of the malaria parasite through the dermis to the liver." Cell Host Microbe **3**(2): 88-96.

Amino, R., S. Thiberge, S. Shorte, F. Frischknecht and R. Menard (2006). "Quantitative imaging of Plasmodium sporozoites in the mammalian host." C R Biol **329**(11): 858-862.

Andenmatten, N., S. Egarter, A. J. Jackson, N. Jullien, J. P. Herman and M. Meissner (2013). "Conditional genome engineering in Toxoplasma gondii uncovers alternative invasion mechanisms." Nat Methods **10**(2): 125-127.

Anderson-White, B., J. R. Beck, C. T. Chen, M. Meissner, P. J. Bradley and M. J. Gubbels (2012). "Cytoskeleton assembly in Toxoplasma gondii cell division." Int Rev Cell Mol Biol **298**: 1-31.

Anderson-White, B. R., F. D. Ivey, K. Cheng, T. Szatanek, A. Lorestani, C. J. Beckers, D. J. Ferguson, N. Sahoo and M. J. Gubbels (2011). "A family of intermediate filament-like proteins is sequentially assembled into the cytoskeleton of Toxoplasma gondii." Cell Microbiol **13**(1): 18-31.

Angrisano, F., D. T. Riglar, A. Sturm, J. C. Volz, M. J. Delves, E. S. Zuccala, L. Turnbull, C. Dekiwadia, M. A. Olshina, D. S. Marapana, W. Wong, V. Mollard, C. H. Bradin, C. J. Tonkin, P. W. Gunning, S. A. Ralph, C. B. Whitchurch, R. E. Sinden, A. F. Cowman, G. I. McFadden and J. Baum (2012). "Spatial localisation of actin filaments across developmental stages of the malaria parasite." PLoS One **7**(2): e32188.

Aoki, K., Y. Kamioka and M. Matsuda (2013). "Fluorescence resonance energy transfer imaging of cell signaling from in vitro to in vivo: basis of biosensor construction, live imaging, and image processing." Dev Growth Differ **55**(4): 515-522.

Armstrong, C. M. and D. E. Goldberg (2007). "An FKBP destabilization domain modulates protein levels in Plasmodium falciparum." Nat Methods **4**(12): 1007-1009.

Arnaout, M. A., S. L. Goodman and J. P. Xiong (2007). "Structure and mechanics of integrin-based cell adhesion." Curr Opin Cell Biol **19**(5): 495-507.

Arrizabalaga, G., F. Ruiz, S. Moreno and J. C. Boothroyd (2004). "Ionophore-resistant mutant of Toxoplasma gondii reveals involvement of a sodium/hydrogen exchanger in calcium regulation." J Cell Biol **165**(5): 653-662.

Aspenstrom, P. (2010). "Formin-binding proteins: modulators of formin-dependent actin polymerization." Biochim Biophys Acta **1803**(2): 174-182.

Azzouz, N., F. Kamena, P. Laurino, R. Kikkeri, C. Mercier, M. F. Cesbron-Delauw, J. F. Dubremetz, L. De Cola and P. H. Seeberger (2013). "Toxoplasma gondii secretory proteins bind to sulfated heparin structures." Glycobiology **23**(1): 106-120.

Banaszynski, L. A., L. C. Chen, L. A. Maynard-Smith, A. G. Ooi and T. J. Wandless (2006). "A rapid, reversible, and tunable method to regulate protein function in living cells using synthetic small molecules." Cell **126**(5): 995-1004.

Bargieri, D. Y., N. Andenmatten, V. Lagal, S. Thiberge, J. A. Whitelaw, I. Tardieux, M. Meissner and R. Menard (2013). "Apical membrane antigen 1 mediates apicomplexan parasite attachment but is dispensable for host cell invasion." Nat Commun **4**: 2552.

Barnhart, E. L., K. C. Lee, K. Keren, A. Mogilner and J. A. Theriot (2011). "An adhesion-dependent switch between mechanisms that determine motile cell shape." PLoS Biol **9**(5): e1001059.

Baum, J., T. W. Gilberger, F. Frischknecht and M. Meissner (2008). "Host-cell invasion by malaria parasites: insights from Plasmodium and Toxoplasma." Trends Parasitol **24**(12): 557-563.

Baum, J., C. J. Tonkin, A. S. Paul, M. Rug, B. J. Smith, S. B. Gould, D. Richard, T. D. Pollard and A. F. Cowman (2008). "A malaria parasite formin regulates actin polymerization and localizes to the parasite-erythrocyte moving junction during invasion." Cell Host Microbe **3**(3): 188-198.

Baumeister, S., J. Wiesner, A. Reichenberg, M. Hintz, S. Bietz, O. S. Harb, D. S. Roos, M. Kordes, J. Friesen, K. Matuschewski, K. Lingelbach, H. Jomaa and F. Seeber (2011). "Fosmidomycin uptake into Plasmodium and Babesia-infected erythrocytes is facilitated by parasite-induced new permeability pathways." PLoS One **6**(5): e19334.

Baumgartner, M. (2011). "Enforcing host cell polarity: an apicomplexan parasite strategy towards dissemination." Curr Opin Microbiol **14**(4): 436-444.

Beck, J. R., A. L. Chen, E. W. Kim and P. J. Bradley (2014). "RON5 is critical for organization and function of the Toxoplasma moving junction complex." PLoS Pathog **10**(3): e1004025.

Beck, J. R., C. Fung, K. W. Straub, I. Coppens, A. A. Vashisht, J. A. Wohlschlegel and P. J. Bradley (2013). "A Toxoplasma palmitoyl acyl transferase and the palmitoylated Armadillo Repeat protein TgARO govern apical rhoptry tethering and reveal a critical role for the rhoptries in host cell invasion but not egress." PLoS Pathog **9**(2): e1003162.

Beck, J. R., I. A. Rodriguez-Fernandez, J. C. de Leon, M. H. Huynh, V. B. Carruthers, N. S. Morrissette and P. J. Bradley (2010). "A novel family of Toxoplasma IMC proteins displays a hierarchical organization and functions in coordinating parasite division." PLoS Pathog **6**(9): e1001094.

Bement, W. M. and M. S. Mooseker (1995). "TEDS rule: a molecular rationale for differential regulation of myosins by phosphorylation of the heavy chain head." Cell Motil Cytoskeleton **31**(2): 87-92.

Bessoff, K., A. Sateriale, K. K. Lee and C. D. Huston (2013). "Drug repurposing screen reveals FDA-approved inhibitors of human HMG-CoA reductase and isoprenoid synthesis that block Cryptosporidium parvum growth." Antimicrob Agents Chemother **57**(4): 1804-1814.

Besteiro, S., A. Michelin, J. Poncet, J. F. Dubremetz and M. Lebrun (2009). "Export of a Toxoplasma gondii rhoptry neck protein complex at the host cell membrane to form the moving junction during invasion." PLoS Pathog **5**(2): e1000309.

Bingham, J. B. and T. A. Schroer (1999). "Self-regulated polymerization of the actin-related protein Arp1." Curr Biol **9**(4): 223-226.

Bisi, S., A. Disanza, C. Malinverno, E. Frittoli, A. Palamidessi and G. Scita (2013). "Membrane and actin dynamics interplay at lamellipodia leading edge." Curr Opin Cell Biol **25**(5): 565-573.

Black, M., F. Seeber, D. Soldati, K. Kim and J. C. Boothroyd (1995). "Restriction enzyme-mediated integration elevates transformation frequency and enables co-transfection of Toxoplasma gondii." Mol Biochem Parasitol **74**(1): 55-63.

Black, M. W., G. Arrizabalaga and J. C. Boothroyd (2000). "Ionophore-resistant mutants of Toxoplasma gondii reveal host cell permeabilization as an early event in egress." Mol Cell Biol **20**(24): 9399-9408.

Black, M. W. and J. C. Boothroyd (2000). "Lytic cycle of Toxoplasma gondii." Microbiol Mol Biol Rev **64**(3): 607-623.

Blanchoin, L., T. D. Pollard and R. D. Mullins (2000). "Interactions of ADF/cofilin, Arp2/3 complex, capping protein and profilin in remodeling of branched actin filament networks." Curr Biol **10**(20): 1273-1282.

Boothroyd, J. C. and J. F. Dubremetz (2008). "Kiss and spit: the dual roles of Toxoplasma rhoptries." Nat Rev Microbiol **6**(1): 79-88.

Bougdour, A., E. Durandau, M. P. Brenier-Pinchart, P. Ortet, M. Barakat, S. Kieffer, A. Curt-Varesano, R. L. Curt-Bertini, O. Bastien, Y. Coute, H. Pelloux and M. A. Hakimi (2013). "Host cell subversion by Toxoplasma GRA16, an exported dense granule protein that targets the host cell nucleus and alters gene expression." Cell Host Microbe **13**(4): 489-500.

Bougdour, A., I. Tardieux and M. A. Hakimi (2013). "Toxoplasma exports dense granule proteins beyond the vacuole to the host cell nucleus and rewires the host genome expression." Cell Microbiol.

Braun, L., M. P. Brenier-Pinchart, M. Yogavel, A. Curt-Varesano, R. L. Curt-Bertini, T. Hussain, S. Kieffer-Jaquinod, Y. Coute, H. Pelloux, I. Tardieux, A. Sharma, H. Belrhali, A. Bougdour and M. A. Hakimi (2013). "A Toxoplasma dense granule protein, GRA24, modulates the early immune response to infection by promoting a direct and sustained host p38 MAPK activation." J Exp Med **210**(10): 2071-2086.

Brecht, S., H. Erdhart, M. Soete and D. Soldati (1999). "Genome engineering of Toxoplasma gondii using the site-specific recombinase Cre." Gene **234**(2): 239-247.

Breinich, M. S., D. J. Ferguson, B. J. Foth, G. G. van Dooren, M. Lebrun, D. V. Quon, B. Striepen, P. J. Bradley, F. Frischknecht, V. B. Carruthers and M. Meissner (2009). "A dynamin is required for the biogenesis of secretory organelles in Toxoplasma gondii." Curr Biol **19**(4): 277-286.

Brossier, F. and L. David Sibley (2005). "Toxoplasma gondii: microneme protein MIC2." Int J Biochem Cell Biol **37**(11): 2266-2272.

Buguliskis, J. S., F. Brossier, J. Shuman and L. D. Sibley (2010). "Rhomboid 4 (ROM4) affects the processing of surface adhesins and facilitates host cell invasion by Toxoplasma gondii." PLoS Pathog **6**(4): e1000858.

Bullen, H. E., C. J. Tonkin, R. A. O'Donnell, W. H. Tham, A. T. Papenfuss, S. Gould, A. F. Cowman, B. S. Crabb and P. R. Gilson (2009). "A novel family of Apicomplexan glideosome-associated proteins with an inner membrane-anchoring role." J Biol Chem **284**(37): 25353-25363.

Burtnick, L. D., E. K. Koepf, J. Grimes, E. Y. Jones, D. I. Stuart, P. J. McLaughlin and R. C. Robinson (1997). "The crystal structure of plasma gelsolin: implications for actin severing, capping, and nucleation." Cell **90**(4): 661-670.

Buscaglia, C. A., I. Coppens, W. G. Hol and V. Nussenzweig (2003). "Sites of interaction between aldolase and thrombospondin-related anonymous protein in plasmodium." Mol Biol Cell **14**(12): 4947-4957.

Caldas, L. A., W. de Souza and M. Attias (2010). "Microscopic analysis of calcium ionophore activated egress of Toxoplasma gondii from the host cell." Vet Parasitol **167**(1): 8-18.

Caldas, L. A., S. H. Seabra, M. Attias and W. de Souza (2013). "The effect of kinase, actin, myosin and dynamin inhibitors on host cell egress by Toxoplasma gondii." Parasitol Int **62**(5): 475-482.

Carruthers, V. and J. C. Boothroyd (2007). "Pulling together: an integrated model of Toxoplasma cell invasion." Curr Opin Microbiol **10**(1): 83-89.

Carruthers, V. B., S. N. Moreno and L. D. Sibley (1999). "Ethanol and acetaldehyde elevate intracellular [Ca2+] and stimulate microneme discharge in Toxoplasma gondii." Biochem J **342 (Pt 2)**: 379-386.

Carruthers, V. B. and L. D. Sibley (1999). "Mobilization of intracellular calcium stimulates microneme discharge in Toxoplasma gondii." Mol Microbiol **31**(2): 421-428.

Carruthers, V. B. and F. M. Tomley (2008). "Microneme proteins in apicomplexans." Subcell Biochem **47**: 33-45.

Chandramohanadas, R., P. H. Davis, D. P. Beiting, M. B. Harbut, C. Darling, G. Velmourougane, M. Y. Lee, P. A. Greer, D. S. Roos and D. C. Greenbaum (2009). "Apicomplexan parasites co-opt host calpains to facilitate their escape from infected cells." Science **324**(5928): 794-797.

Charras, G. T., J. C. Yarrow, M. A. Horton, L. Mahadevan and T. J. Mitchison (2005). "Non-equilibration of hydrostatic pressure in blebbing cells." Nature **435**(7040): 365-369.

Chen, X. M., B. Q. Huang, P. L. Splinter, J. D. Orth, D. D. Billadeau, M. A. McNiven and N. F. LaRusso (2004). "Cdc42 and the actin-related protein/neural Wiskott-Aldrich syndrome protein network mediate cellular invasion by Cryptosporidium parvum." Infect Immun **72**(5): 3011-3021.

Chen, X. M., S. P. O'Hara, B. Q. Huang, P. L. Splinter, J. B. Nelson and N. F. LaRusso (2005). "Localized glucose and water influx facilitates Cryptosporidium parvum cellular invasion by means of modulation of host-cell membrane protrusion." Proc Natl Acad Sci U S A **102**(18): 6338-6343.

Christoforidis, S. and M. Zerial (2000). "Purification and identification of novel Rab effectors using affinity chromatography." Methods **20**(4): 403-410.

Chtanova, T., S. J. Han, M. Schaeffer, G. G. van Dooren, P. Herzmark, B. Striepen and E. A. Robey (2009). "Dynamics of T cell, antigen-presenting cell, and pathogen interactions during recall responses in the lymph node." Immunity **31**(2): 342-355.

Collins, C. R., S. Das, E. H. Wong, N. Andenmatten, R. Stallmach, F. Hackett, J. P. Herman, S. Muller, M. Meissner and M. J. Blackman (2013). "Robust inducible Cre recombinase activity in the human malaria parasite Plasmodium falciparum enables efficient gene deletion within a single asexual erythrocytic growth cycle." Mol Microbiol **88**(4): 687-701.

Cooper, J. A. and D. A. Schafer (2000). "Control of actin assembly and disassembly at filament ends." Curr Opin Cell Biol **12**(1): 97-103.

Coulliette, A. D., D. E. Huffman, T. R. Slifko and J. B. Rose (2006). "Cryptosporidium parvum: treatment effects and the rate of decline in oocyst infectivity." J Parasitol **92**(1): 58-62.

Dagdas, Y. F., K. Yoshino, G. Dagdas, L. S. Ryder, E. Bielska, G. Steinberg and N. J. Talbot (2012). "Septin-mediated plant cell invasion by the rice blast fungus, Magnaporthe oryzae." Science **336**(6088): 1590-1595.

Daher, W., F. Plattner, M. F. Carlier and D. Soldati-Favre (2010). "Concerted action of two formins in gliding motility and host cell invasion by Toxoplasma gondii." PLoS Pathog **6**(10): e1001132.

Dahl, E. L. and P. J. Rosenthal (2008). "Apicoplast translation, transcription and genome replication: targets for antimalarial antibiotics." Trends Parasitol **24**(6): 279-284.

De La Cruz, E. M. and E. M. Ostap (2004). "Relating biochemistry and function in the myosin superfamily." Curr Opin Cell Biol **16**(1): 61-67.

de Moura, L., L. M. Bahia-Oliveira, M. Y. Wada, J. L. Jones, S. H. Tuboi, E. H. Carmo, W. M. Ramalho, N. J. Camargo, R. Trevisan, R. M. Graca, A. J. da Silva, I. Moura, J. P. Dubey and D. O. Garrett (2006). "Waterborne toxoplasmosis, Brazil, from field to gene." Emerg Infect Dis **12**(2): 326-329.

Dearnley, M. K., J. A. Yeoman, E. Hanssen, S. Kenny, L. Turnbull, C. B. Whitchurch, L. Tilley and M. W. Dixon (2012). "Origin, composition, organization and function of the inner membrane complex of Plasmodium falciparum gametocytes." J Cell Sci **125**(Pt 8): 2053-2063.

Del Carmen, M. G., M. Mondragon, S. Gonzalez and R. Mondragon (2009). "Induction and regulation of conoid extrusion in Toxoplasma gondii." Cell Microbiol **11**(6): 967-982.

Delbac, F., A. Sanger, E. M. Neuhaus, R. Stratmann, J. W. Ajioka, C. Toursel, A. Herm-Gotz, S. Tomavo, T. Soldati and D. Soldati (2001). "Toxoplasma gondii myosins B/C: one gene, two tails, two localizations, and a role in parasite division." J Cell Biol **155**(4): 613-623.

Delorme-Walker, V., M. Abrivard, V. Lagal, K. Anderson, A. Perazzi, V. Gonzalez, C. Page, J. Chauvet, W. Ochoa, N. Volkmann, D. Hanein and I. Tardieux (2012). "Toxofilin upregulates the host cortical actin cytoskeleton dynamics facilitating Toxoplasma invasion." J Cell Sci.

Dharan, N. and O. Farago (2012). "Duty ratio of cooperative molecular motors." Phys Rev E Stat Nonlin Soft Matter Phys **85**(2 Pt 1): 021904.

Dobrowolski, J. M., I. R. Niesman and L. D. Sibley (1997). "Actin in the parasite Toxoplasma gondii is encoded by a single copy gene, ACT1 and exists primarily in a globular form." Cell Motil Cytoskeleton **37**(3): 253-262.

Dobrowolski, J. M. and L. D. Sibley (1996). "Toxoplasma invasion of mammalian cells is powered by the actin cytoskeleton of the parasite." Cell **84**(6): 933-939.

Donald, R. G., D. Carter, B. Ullman and D. S. Roos (1996). "Insertional tagging, cloning, and expression of the Toxoplasma gondii hypoxanthine-xanthine-guanine phosphoribosyltransferase gene. Use as a selectable marker for stable transformation." J Biol Chem **271**(24): 14010-14019.

Donald, R. G. and D. S. Roos (1993). "Stable molecular transformation of Toxoplasma gondii: a selectable dihydrofolate reductase-thymidylate synthase marker based on drug-resistance mutations in malaria." Proc Natl Acad Sci U S A **90**(24): 11703-11707.

Donald, R. G. and D. S. Roos (1995). "Insertional mutagenesis and marker rescue in a protozoan parasite: cloning of the uracil phosphoribosyltransferase locus from Toxoplasma gondii." Proc Natl Acad Sci U S A **92**(12): 5749-5753.

Dong, C. and G. Wu (2013). "G-protein-coupled receptor interaction with small GTPases." Methods Enzymol **522**: 97-108.

Douse, C. H., J. L. Green, P. S. Salgado, P. J. Simpson, J. C. Thomas, G. Langsley, A. A. Holder, E. W. Tate and E. Cota (2012). "Regulation of the Plasmodium motor complex: phosphorylation of myosin A tail-interacting protein (MTIP) loosens its grip on MyoA." J Biol Chem **287**(44): 36968-36977.

Dubey, J. P. (1997). "Bradyzoite-induced murine toxoplasmosis: stage conversion, pathogenesis, and tissue cyst formation in mice fed bradyzoites of different strains of Toxoplasma gondii." J Eukaryot Microbiol **44**(6): 592-602.

Dubey, J. P. (1997). "Survival of Toxoplasma gondii tissue cysts in 0.85-6% NaCl solutions at 4-20 C." J Parasitol **83**(5): 946-949.

Dubey, J. P. (2001). "Oocyst shedding by cats fed isolated bradyzoites and comparison of infectivity of bradyzoites of the VEG strain Toxoplasma gondii to cats and mice." J Parasitol **87**(1): 215-219.

Dubey, J. P., L. R. Ferreira, J. Martins and J. L. Jones (2011). "Sporulation and survival of Toxoplasma gondii oocysts in different types of commercial cat litter." J Parasitol **97**(5): 751-754.

Dubey, J. P. and J. K. Frenkel (1976). "Feline toxoplasmosis from acutely infected mice and the development of Toxoplasma cysts." J Protozool **23**(4): 537-546.

Dubey, J. P., D. S. Lindsay and C. A. Speer (1998). "Structures of Toxoplasma gondii Tachyzoites, Bradyzoites, and Sporozoites and Biology and Development of Tissue Cysts." Clinical Microbiology Reviews **11**(2): 267-299.

Dubey, J. P., N. L. Miller and J. K. Frenkel (1970). "Toxoplasma gondii life cycle in cats." J Am Vet Med Assoc **157**(11): 1767-1770.

Dubey, J. P., N. L. Miller and J. K. Frenkel (1970). "The Toxoplasma gondii oocyst from cat feces." J Exp Med **132**(4): 636-662.

Dubremetz, J. F. (2007). "Rhoptries are major players in Toxoplasma gondii invasion and host cell interaction." Cell Microbiol **9**(4): 841-848.

Dzierszinski, F., M. Mortuaire, M. F. Cesbron-Delauw and S. Tomavo (2000). "Targeted disruption of the glycosylphosphatidylinositol-anchored surface antigen SAG3 gene in Toxoplasma gondii decreases host cell adhesion and drastically reduces virulence in mice." Mol Microbiol **37**(3): 574-582.

Edmondson, D. G. and S. Y. Dent (2001). "Identification of protein interactions by far western analysis." Curr Protoc Protein Sci **Chapter 19**: Unit 19 17.

Egarter, S., N. Andenmatten, A. J. Jackson, J. A. Whitelaw, G. Pall, J. A. Black, D. J. Ferguson, I. Tardieux, A. Mogilner and M. Meissner (2014). "The Toxoplasma Acto-MyoA Motor Complex Is Important but Not Essential for Gliding Motility and Host Cell Invasion." PLoS One **9**(3): e91819.

Elliott, D. A. and D. P. Clark (2000). "Cryptosporidium parvum induces host cell actin accumulation at the host-parasite interface." Infect Immun **68**(4): 2315-2322.

Fackler, O. T. and R. Grosse (2008). "Cell motility through plasma membrane blebbing." J Cell Biol **181**(6): 879-884.

Fauquenoy, S., A. Hovasse, P. J. Sloves, W. Morelle, T. Dilezitoko Alayi, C. Slomianny, E. Werkmeister, C. Schaeffer, A. Van Dorsselaer and S. Tomavo (2011). "Unusual N-glycan structures required for trafficking Toxoplasma gondii GAP50 to the inner membrane complex regulate host cell entry through parasite motility." Mol Cell Proteomics **10**(9): M111 008953.

Ferguson, D. J. (2009). "Toxoplasma gondii: 1908-2008, homage to Nicolle, Manceaux and Splendore." Mem Inst Oswaldo Cruz **104**(2): 133-148.

Fichera, M. E., M. K. Bhopale and D. S. Roos (1995). "In vitro assays elucidate peculiar kinetics of clindamycin action against Toxoplasma gondii." Antimicrob Agents Chemother **39**(7): 1530-1537.

Fichera, M. E. and D. S. Roos (1997). "A plastid organelle as a drug target in apicomplexan parasites." Nature **390**(6658): 407-409.

Field, S. J., K. Rangachari, A. R. Dluzewski, R. J. Wilson and W. B. Gratzer (1992). "Effect of intra-erythrocytic magnesium ions on invasion by Plasmodium falciparum." Parasitology **105 (Pt 1)**: 15-19.

Foth, B. J., M. C. Goedecke and D. Soldati (2006). "New insights into myosin evolution and classification." Proc Natl Acad Sci U S A **103**(10): 3681-3686.

Foth, B. J. and G. I. McFadden (2003). "The apicoplast: a plastid in Plasmodium falciparum and other Apicomplexan parasites." Int Rev Cytol **224**: 57-110.

Fox, B. A., J. G. Ristuccia, J. P. Gigley and D. J. Bzik (2009). "Efficient gene replacements in Toxoplasma gondii strains deficient for nonhomologous end joining." Eukaryot Cell **8**(4): 520-529.

Francia, M. E., S. Wicher, D. A. Pace, J. Sullivan, S. N. Moreno and G. Arrizabalaga (2011). "A Toxoplasma gondii protein with homology to intracellular type Na(+)/H(+) exchangers is important for osmoregulation and invasion." Exp Cell Res **317**(10): 1382-1396.

Frankel, S. and M. S. Mooseker (1996). "The actin-related proteins." Curr Opin Cell Biol **8**(1): 30-37.

Frenal, K., V. Polonais, J. B. Marq, R. Stratmann, J. Limenitakis and D. Soldati-Favre (2010). "Functional dissection of the apicomplexan glideosome molecular architecture." Cell Host Microbe **8**(4): 343-357.

Frevert, U., S. Engelmann, S. Zougbede, J. Stange, B. Ng, K. Matuschewski, L. Liebes and H. Yee (2005). "Intravital observation of Plasmodium berghei sporozoite infection of the liver." PLoS Biol **3**(6): e192.

Fung, C., J. R. Beck, S. D. Robertson, M. J. Gubbels and P. J. Bradley (2012). "Toxoplasma ISP4 is a central IMC sub-compartment protein whose localization depends on palmitoylation but not myristoylation." Mol Biochem Parasitol **184**(2): 99-108.

Gabernet-Castello, C., K. N. Dubois, C. Nimmo and M. C. Field (2011). "Rab11 function in Trypanosoma brucei: identification of conserved and novel interaction partners." Eukaryot Cell **10**(8): 1082-1094.

Gaji, R. Y., M. H. Huynh and V. B. Carruthers (2013). "A novel high throughput invasion screen identifies host actin regulators required for efficient cell entry by Toxoplasma gondii." PLoS One **8**(5): e64693.

Gajria, B., A. Bahl, J. Brestelli, J. Dommer, S. Fischer, X. Gao, M. Heiges, J. Iodice, J. C. Kissinger, A. J. Mackey, D. F. Pinney, D. S. Roos, C. J. Stoeckert, Jr., H. Wang and B. P. Brunk (2008). "ToxoDB: an integrated Toxoplasma gondii database resource." Nucleic Acids Res **36**(Database issue): D553-556.

Gardner, M. J., R. Bishop, T. Shah, E. P. de Villiers, J. M. Carlton, N. Hall, Q. Ren, I. T. Paulsen, A. Pain, M. Berriman, R. J. Wilson, S. Sato, S. A. Ralph, D. J. Mann, Z. Xiong, S. J. Shallom, J. Weidman, L. Jiang, J. Lynn, B. Weaver, A. Shoaibi, A. R. Domingo, D. Wasawo, J. Crabtree, J. R. Wortman, B. Haas, S. V. Angiuoli, T. H. Creasy, C. Lu, B. Suh, J. C. Silva, T. R. Utterback, T. V. Feldblyum, M. Pertea, J. Allen, W. C. Nierman, E. L. Taracha, S. L. Salzberg, O. R. White, H. A. Fitzhugh, S. Morzaria, J. C. Venter, C. M. Fraser and V. Nene (2005). "Genome sequence of Theileria parva, a bovine pathogen that transforms lymphocytes." Science **309**(5731): 134-137.

Gardner, M. J., N. Hall, E. Fung, O. White, M. Berriman, R. W. Hyman, J. M. Carlton, A. Pain, K. E. Nelson, S. Bowman, I. T. Paulsen, K. James, J. A. Eisen, K. Rutherford, S. L. Salzberg, A. Craig, S. Kyes, M. S. Chan, V. Nene, S. J. Shallom, B. Suh, J. Peterson, S. Angiuoli, M. Pertea, J. Allen, J. Selengut, D. Haft, M. W. Mather, A. B. Vaidya, D. M. Martin, A. H. Fairlamb, M. J. Fraunholz, D. S. Roos, S. A. Ralph, G. I. McFadden, L. M. Cummings, G. M. Subramanian, C. Mungall, J. C. Venter, D. J. Carucci, S. L. Hoffman, C. Newbold, R. W. Davis, C. M. Fraser and B. Barrell (2002). "Genome sequence of the human malaria parasite Plasmodium falciparum." Nature **419**(6906): 498-511.

Garrison, E., M. Treeck, E. Ehret, H. Butz, T. Garbuz, B. P. Oswald, M. Settles, J. Boothroyd and G. Arrizabalaga (2012). "A forward genetic screen reveals that calcium-dependent protein kinase 3 regulates egress in Toxoplasma." PLoS Pathog **8**(11): e1003049.

Gaskins, E., S. Gilk, N. DeVore, T. Mann, G. Ward and C. Beckers (2004). "Identification of the membrane receptor of a class XIV myosin in Toxoplasma gondii." J Cell Biol **165**(3): 383-393.

Gendrin, C., A. Bittame, C. Mercier and M. F. Cesbron-Delauw (2010). "Post-translational membrane sorting of the Toxoplasma gondii GRA6 protein into the parasite-containing vacuole is driven by its N-terminal domain." Int J Parasitol **40**(11): 1325-1334.

Gibbons, I. R. and A. J. Rowe (1965). "Dynein: A Protein with Adenosine Triphosphatase Activity from Cilia." Science **149**(3682): 424-426.

Gifford, J. L., M. P. Walsh and H. J. Vogel (2007). "Structures and metal-ion-binding properties of the Ca2+-binding helix-loop-helix EF-hand motifs." Biochem J **405**(2): 199-221.

Gilk, S. D., E. Gaskins, G. E. Ward and C. J. Beckers (2009). "GAP45 phosphorylation controls assembly of the Toxoplasma myosin XIV complex." Eukaryot Cell **8**(2): 190-196.

Giovannini, D., S. Spath, C. Lacroix, A. Perazzi, D. Bargieri, V. Lagal, C. Lebugle, A. Combe, S. Thiberge, P. Baldacci, I. Tardieux and R. Menard (2011). "Independent roles of apical membrane antigen 1 and rhoptry neck proteins during host cell invasion by apicomplexa." Cell Host Microbe **10**(6): 591-602.

Gisselberg, J. E., T. A. Dellibovi-Ragheb, K. A. Matthews, G. Bosch and S. T. Prigge (2013). "The suf iron-sulfur cluster synthesis pathway is required for apicoplast maintenance in malaria parasites." PLoS Pathog **9**(9): e1003655.

Goldstein, L. S. (2001). "Molecular motors: from one motor many tails to one motor many tales." Trends Cell Biol **11**(12): 477-482.

Gomes-Santos, C. S., M. A. Itoe, C. Afonso, R. Henriques, R. Gardner, N. Sepulveda, P. D. Simoes, H. Raquel, A. P. Almeida, L. F. Moita, F. Frischknecht and M. M. Mota (2012). "Highly dynamic host actin reorganization around developing Plasmodium inside hepatocytes." PLoS One **7**(1): e29408.

Gonzalez, V., A. Combe, V. David, N. A. Malmquist, V. Delorme, C. Leroy, S. Blazquez, R. Menard and I. Tardieux (2009). "Host cell entry by apicomplexa parasites requires actin polymerization in the host cell." Cell Host Microbe **5**(3): 259-272.

Goo, Y. K., A. Ueno, M. A. Terkawi, G. Oluga Aboge, Y. Junya, M. Igarashi, J. Y. Kim, Y. C. Hong, D. I. Chung, Y. Nishikawa and X. Xuan (2013). "Actin polymerization mediated by Babesia gibsoni aldolase is required for parasite invasion." Exp Parasitol.

Gordon, J. L., W. L. Beatty and L. D. Sibley (2008). "A novel actin-related protein is associated with daughter cell formation in Toxoplasma gondii." Eukaryot Cell **7**(9): 1500-1512.

Gordon, J. L., J. S. Buguliskis, P. J. Buske and L. D. Sibley (2010). "Actin-like protein 1 (ALP1) is a component of dynamic, high molecular weight complexes in Toxoplasma gondii." Cytoskeleton (Hoboken) **67**(1): 23-31.

Gordon, J. L. and L. D. Sibley (2005). "Comparative genome analysis reveals a conserved family of actin-like proteins in apicomplexan parasites." BMC Genomics **6**: 179.

Gossen, M. and H. Bujard (1992). "Tight control of gene expression in mammalian cells by tetracycline-responsive promoters." Proc Natl Acad Sci U S A **89**(12): 5547-5551.

Gould, S. B., L. G. Kraft, G. G. van Dooren, C. D. Goodman, K. L. Ford, A. M. Cassin, A. Bacic, G. I. McFadden and R. F. Waller (2011). "Ciliate pellicular proteome identifies novel protein families with characteristic repeat motifs that are common to alveolates." Mol Biol Evol **28**(3): 1319-1331.

Gould, S. B., W. H. Tham, A. F. Cowman, G. I. McFadden and R. F. Waller (2008). "Alveolins, a new family of cortical proteins that define the protist infrakingdom Alveolata." Mol Biol Evol **25**(6): 1219-1230.

Graindorge, A. (2013). Toxoplasma gondii MyoH: an essential motor implicated in glideosome functions and conoid protrusion. 12th International Congress of Toxoplasmosis.

Green, J. L., R. R. Rees-Channer, S. A. Howell, S. R. Martin, E. Knuepfer, H. M. Taylor, M. Grainger and A. A. Holder (2008). "The motor complex of Plasmodium falciparum: phosphorylation by a calcium-dependent protein kinase." J Biol Chem **283**(45): 30980-30989.

Gregg, B., B. C. Taylor, B. John, E. D. Tait-Wojno, N. M. Girgis, N. Miller, S. Wagage, D. S. Roos and C. A. Hunter (2013). "Replication and distribution of Toxoplasma gondii in the small intestine after oral infection with tissue cysts." Infect Immun **81**(5): 1635-1643.

Gubbels, M. J., M. Lehmann, M. Muthalagi, M. E. Jerome, C. F. Brooks, T. Szatanek, J. Flynn, B. Parrot, J. Radke, B. Striepen and M. W. White (2008). "Forward genetic analysis of the apicomplexan cell division cycle in Toxoplasma gondii." PLoS Pathog **4**(2): e36.

Gubbels, M. J., S. Vaishnava, N. Boot, J. F. Dubremetz and B. Striepen (2006). "A MORN-repeat protein is a dynamic component of the Toxoplasma gondii cell division apparatus." J Cell Sci **119**(Pt 11): 2236-2245.

Gubbels, M. J., M. White and T. Szatanek (2008). "The cell cycle and Toxoplasma gondii cell division: tightly knit or loosely stitched?" Int J Parasitol **38**(12): 1343-1358.

Guerrero-Barrera, A. L., M. de la Garza, R. Mondragon, C. Garcia-Cuellar and M. Segura-Nieto (1999). "Actin-related proteins in Actinobacillus pleuropneumoniae and their interactions with actin-binding proteins." Microbiology **145 (Pt 11)**: 3235-3244.

Hager, K. M., B. Striepen, L. G. Tilney and D. S. Roos (1999). "The nuclear envelope serves as an intermediary between the ER and Golgi complex in the intracellular parasite Toxoplasma gondii." J Cell Sci **112 (Pt 16)**: 2631-2638.

Hakansson, S., H. Morisaki, J. Heuser and L. D. Sibley (1999). "Time-lapse video microscopy of gliding motility in Toxoplasma gondii reveals a novel, biphasic mechanism of cell locomotion." Mol Biol Cell **10**(11): 3539-3547.

Harper, J. M., E. F. Hoff and V. B. Carruthers (2004). "Multimerization of the Toxoplasma gondii MIC2 integrin-like A-domain is required for binding to heparin and human cells." Mol Biochem Parasitol **134**(2): 201-212.

Harper, J. M., M. H. Huynh, I. Coppens, F. Parussini, S. Moreno and V. B. Carruthers (2006). "A cleavable propeptide influences Toxoplasma infection by facilitating the trafficking and secretion of the TgMIC2-M2AP invasion complex." Mol Biol Cell **17**(10): 4551-4563.

Hartmann, J., K. Hu, C. Y. He, L. Pelletier, D. S. Roos and G. Warren (2006). "Golgi and centrosome cycles in Toxoplasma gondii." Mol Biochem Parasitol **145**(1): 125-127.

Hausmann, K. and R. D. Allen (2010). "Electron microscopy of Paramecium (Ciliata)." Methods Cell Biol **96**: 143-173.

Haynes, J. D., C. L. Diggs, F. A. Hines and R. E. Desjardins (1976). "Culture of human malaria parasites Plasmodium falciparum." Nature **263**(5580): 767-769.

He, C. Y., M. K. Shaw, C. H. Pletcher, B. Striepen, L. G. Tilney and D. S. Roos (2001). "A plastid segregation defect in the protozoan parasite Toxoplasma gondii." EMBO J **20**(3): 330-339.

Heaslip, A. T., J. M. Leung, K. L. Carey, F. Catti, D. M. Warshaw, N. J. Westwood, B. A. Ballif and G. E. Ward (2010). "A small-molecule inhibitor of T. gondii motility induces the posttranslational modification of myosin light chain-1 and inhibits myosin motor activity." PLoS Pathog **6**(1): e1000720.

Hegge, S., S. Munter, M. Steinbuchel, K. Heiss, U. Engel, K. Matuschewski and F. Frischknecht (2010). "Multistep adhesion of Plasmodium sporozoites." FASEB J **24**(7): 2222-2234.

Hegge, S., K. Uhrig, M. Streichfuss, G. Kynast-Wolf, K. Matuschewski, J. P. Spatz and F. Frischknecht (2012). "Direct manipulation of malaria parasites with optical tweezers reveals distinct functions of Plasmodium surface proteins." ACS Nano **6**(6): 4648-4662.

Heintzelman, M. B. and J. D. Schwartzman (1997). "A novel class of unconventional myosins from Toxoplasma gondii." J Mol Biol **271**(1): 139-146.

Hellmann, J. K., N. Perschmann, J. P. Spatz and F. Frischknecht (2013). "Tunable substrates unveil chemical complementation of a genetic cell migration defect." Adv Healthc Mater **2**(8): 1162-1169.

Herm-Gotz, A., C. Agop-Nersesian, S. Munter, J. S. Grimley, T. J. Wandless, F. Frischknecht and M. Meissner (2007). "Rapid control of protein level in the apicomplexan Toxoplasma gondii." Nat Methods **4**(12): 1003-1005.

Herm-Gotz, A., F. Delbac, S. Weiss, M. Nyitrai, R. Stratmann, S. Tomavo, L. D. Sibley, M. A. Geeves and D. Soldati (2006). "Functional and biophysical analyses of the class XIV Toxoplasma gondii myosin D." J Muscle Res Cell Motil **27**(2): 139-151.

Herm-Gotz, A., S. Weiss, R. Stratmann, S. Fujita-Becker, C. Ruff, E. Meyhofer, T. Soldati, D. J. Manstein, M. A. Geeves and D. Soldati (2002). "Toxoplasma gondii myosin A and its light chain: a fast, single-headed, plus-end-directed motor." EMBO J **21**(9): 2149-2158.

Herman, I. M. (1993). "Actin isoforms." Curr Opin Cell Biol **5**(1): 48-55.

Hettmann, C., A. Herm, A. Geiter, B. Frank, E. Schwarz, T. Soldati and D. Soldati (2000). "A dibasic motif in the tail of a class XIV apicomplexan myosin is an essential determinant of plasma membrane localization." Mol Biol Cell **11**(4): 1385-1400.

Hill, D. E., S. Chirukandoth and J. P. Dubey (2005). "Biology and epidemiology of Toxoplasma gondii in man and animals." Anim Health Res Rev **6**(1): 41-61.

Hliscs, M., J. M. Sattler, W. Tempel, J. D. Artz, A. Dong, R. Hui, K. Matuschewski and H. Schuler (2010). "Structure and function of a G-actin sequestering protein with a vital role in malaria oocyst development inside the mosquito vector." J Biol Chem **285**(15): 11572-11583.

Holleran, E. A., L. A. Ligon, M. Tokito, M. C. Stankewich, J. S. Morrow and E. L. Holzbaur (2001). "beta III spectrin binds to the Arp1 subunit of dynactin." J Biol Chem **276**(39): 36598-36605.

Holleran, E. A., M. K. Tokito, S. Karki and E. L. Holzbaur (1996). "Centractin (ARP1) associates with spectrin revealing a potential mechanism to link dynactin to intracellular organelles." J Cell Biol **135**(6 Pt 2): 1815-1829.

Hu, K. (2008). "Organizational changes of the daughter basal complex during the parasite replication of Toxoplasma gondii." PLoS Pathog **4**(1): e10.

Hu, K., L. Ji, K. T. Applegate, G. Danuser and C. M. Waterman-Storer (2007). "Differential transmission of actin motion within focal adhesions." Science **315**(5808): 111-115.

Hu, K., J. Johnson, L. Florens, M. Fraunholz, S. Suravajjala, C. DiLullo, J. Yates, D. S. Roos and J. M. Murray (2006). "Cytoskeletal components of an invasion machine--the apical complex of Toxoplasma gondii." PLoS Pathog **2**(2): e13.

Hu, K., T. Mann, B. Striepen, C. J. Beckers, D. S. Roos and J. M. Murray (2002). "Daughter cell assembly in the protozoan parasite Toxoplasma gondii." Mol Biol Cell **13**(2): 593-606.

Hu, K., D. S. Roos and J. M. Murray (2002). "A novel polymer of tubulin forms the conoid of Toxoplasma gondii." J Cell Biol **156**(6): 1039-1050.

Huber, L. A., S. Pimplikar, R. G. Parton, H. Virta, M. Zerial and K. Simons (1993). "Rab8, a small GTPase involved in vesicular traffic between the TGN and the basolateral plasma membrane." J Cell Biol **123**(1): 35-45.

Hunter, C. A. and L. D. Sibley (2012). "Modulation of innate immunity by Toxoplasma gondii virulence effectors." Nat Rev Microbiol **10**(11): 766-778.

Hutchison, W. M., J. F. Dunachie, J. C. Siim and K. Work (1969). "Life cycle of toxoplasma gondii." Br Med J **4**(5686): 806.

Huynh, M. H. and V. B. Carruthers (2006). "Toxoplasma MIC2 is a major determinant of invasion and virulence." PLoS Pathog **2**(8): e84.

Huynh, M. H. and V. B. Carruthers (2009). "Tagging of endogenous genes in a Toxoplasma gondii strain lacking Ku80." Eukaryot Cell **8**(4): 530-539.

Jacot, D. (2013). Importance of posttranslational modifications in the assembly and regulation of the glideosome. 12th International Congress on Toxoplasmosis, Oxford, United Kingdom.

Jacot, D., W. Daher and D. Soldati-Favre (2013). "Toxoplasma gondii myosin F, an essential motor for centrosomes positioning and apicoplast inheritance." EMBO J **32**(12): 1702-1716.

Jacot, D. and D. Soldati-Favre (2012). "Does protein phosphorylation govern host cell entry and egress by the Apicomplexa?" Int J Med Microbiol **302**(4-5): 195-202.

Jacquet, A., L. Coulon, J. De Neve, V. Daminet, M. Haumont, L. Garcia, A. Bollen, M. Jurado and R. Biemans (2001). "The surface antigen SAG3 mediates the attachment of Toxoplasma gondii to cell-surface proteoglycans." Mol Biochem Parasitol **116**(1): 35-44.

Jewett, T. J. and L. D. Sibley (2003). "Aldolase forms a bridge between cell surface adhesins and the actin cytoskeleton in apicomplexan parasites." Molecular Cell **11**: 885-894.

Johnson, T. M., Z. Rajfur, K. Jacobson and C. J. Beckers (2007). "Immobilization of the type XIV myosin complex in Toxoplasma gondii." Mol Biol Cell **18**(8): 3039-3046.

Joiner, K. A. and D. S. Roos (2002). "Secretory traffic in the eukaryotic parasite Toxoplasma gondii: less is more." J Cell Biol **157**(4): 557-563.

Jomaa, H., J. Wiesner, S. Sanderbrand, B. Altincicek, C. Weidemeyer, M. Hintz, I. Turbachova, M. Eberl, J. Zeidler, H. K. Lichtenthaler, D. Soldati and E. Beck (1999). "Inhibitors of the nonmevalonate pathway of isoprenoid biosynthesis as antimalarial drugs." Science **285**(5433): 1573-1576.

Jones, J. L. and J. P. Dubey (2012). "Foodborne toxoplasmosis." Clin Infect Dis **55**(6): 845-851.

Jullien, N., I. Goddard, S. Selmi-Ruby, J. L. Fina, H. Cremer and J. P. Herman (2007). "Conditional transgenesis using Dimerizable Cre (DiCre)." PLoS One **2**(12): e1355.

Jullien, N., F. Sampieri, A. Enjalbert and J. P. Herman (2003). "Regulation of Cre recombinase by ligand-induced complementation of inactive fragments." Nucleic Acids Res **31**(21): e131.

Jung, C., C. Y. Lee and M. E. Grigg (2004). "The SRS superfamily of Toxoplasma surface proteins." Int J Parasitol **34**(3): 285-296.

Kabsch, W. and K. C. Holmes (1995). "The actin fold." FASEB J **9**(2): 167-174.

Kafsack, B. F., V. B. Carruthers and F. J. Pineda (2007). "Kinetic modeling of Toxoplasma gondii invasion." J Theor Biol **249**(4): 817-825.

Kafsack, B. F., J. D. Pena, I. Coppens, S. Ravindran, J. C. Boothroyd and V. B. Carruthers (2009). "Rapid membrane disruption by a perforin-like protein facilitates parasite exit from host cells." Science **323**(5913): 530-533.

Kail, M. and A. Barnekow (2008). "Identification and characterization of interacting partners of Rab GTPases by yeast two-hybrid analyses." Methods Mol Biol **440**: 111-125.

Karanis, P. and H. M. Aldeyarbi (2011). "Evolution of Cryptosporidium in vitro culture." Int J Parasitol **41**(12): 1231-1242.

Karasov, A. O., J. C. Boothroyd and G. Arrizabalaga (2005). "Identification and disruption of a rhoptry-localized homologue of sodium hydrogen exchangers in Toxoplasma gondii." Int J Parasitol **35**(3): 285-291.

Kardos, R., E. Nevalainen, M. Nyitrai and G. Hild (2013). "The effect of ADF/cofilin and profilin on the dynamics of monomeric actin." Biochim Biophys Acta **1834**(10): 2010-2019.

Karpova, T. S., K. Tatchell and J. A. Cooper (1995). "Actin filaments in yeast are unstable in the absence of capping protein or fimbrin." J Cell Biol **131**(6 Pt 1): 1483-1493.

Keeley, A. and D. Soldati (2004). "The glideosome: a molecular machine powering motility and host-cell invasion by Apicomplexa." Trends Cell Biol **14**(10): 528-532.

Kemeny, S. F., S. Cicalese, D. S. Figueroa and A. M. Clyne (2013). "Glycated collagen and altered glucose increase endothelial cell adhesion strength." J Cell Physiol **228**(8): 1727-1736.

Kemp, L. E., M. Yamamoto and D. Soldati-Favre (2013). "Subversion of host cellular functions by the apicomplexan parasites." FEMS Microbiol Rev **37**(4): 607-631.

Keren, K., P. T. Yam, A. Kinkhabwala, A. Mogilner and J. A. Theriot (2009). "Intracellular fluid flow in rapidly moving cells." Nat Cell Biol **11**(10): 1219-1224.

Kessler, H., A. Herm-Gotz, S. Hegge, M. Rauch, D. Soldati-Favre, F. Frischknecht and M. Meissner (2008). "Microneme protein 8--a new essential invasion factor in Toxoplasma gondii." J Cell Sci **121**(Pt 7): 947-956.

Khan, A., S. Taylor, C. Su, A. J. Mackey, J. Boyle, R. Cole, D. Glover, K. Tang, I. T. Paulsen, M. Berriman, J. C. Boothroyd, E. R. Pfefferkorn, J. P. Dubey, J. W. Ajioka, D. S. Roos, J. C. Wootton and L. D. Sibley (2005). "Composite genome map and recombination parameters derived from three archetypal lineages of Toxoplasma gondii." Nucleic Acids Res **33**(9): 2980-2992.

Kim, K., M. S. Eaton, W. Schubert, S. Wu and J. Tang (2001). "Optimized expression of green fluorescent protein in Toxoplasma gondii using thermostable green fluorescent protein mutants." Mol Biochem Parasitol **113**(2): 309-313.

Kim, K., D. Soldati and J. C. Boothroyd (1993). "Gene replacement in Toxoplasma gondii with chloramphenicol acetyltransferase as selectable marker." Science **262**(5135): 911-914.

Kim, K. and L. M. Weiss (2004). "Toxoplasma gondii: the model apicomplexan." Int J Parasitol **34**(3): 423-432.

Kimata, I. and K. Tanabe (1982). "Invasion by Toxoplasma gondii of ATP-depleted and ATP-restored chick embryo erythrocytes." J Gen Microbiol **128**(10): 2499-2501.

King, C. A. (1981). "Cell surface interaction of the protozoan Gregarina with concanavalin A beads - implications for models of gregarine gliding." Cell Biol Int Rep **5**(3): 297-305.

King, C. A. (1988). "Cell motility of sporozoan protozoa." Parasitol Today **4**(11): 315-319.

Kissinger, J. C., B. Gajria, L. Li, I. T. Paulsen and D. S. Roos (2003). "ToxoDB: accessing the Toxoplasma gondii genome." Nucleic Acids Res **31**(1): 234-236.

Kohler, S., C. F. Delwiche, P. W. Denny, L. G. Tilney, P. Webster, R. J. Wilson, J. D. Palmer and D. S. Roos (1997). "A plastid of probable green algal origin in Apicomplexan parasites." Science **275**(5305): 1485-1489.

Kono, M., S. Herrmann, N. B. Loughran, A. Cabrera, K. Engelberg, C. Lehmann, D. Sinha, B. Prinz, U. Ruch, V. Heussler, T. Spielmann, J. Parkinson and T. W. Gilberger (2012). "Evolution and architecture of the inner membrane complex in asexual and sexual stages of the malaria parasite." Mol Biol Evol **29**(9): 2113-2132.

Koreny, L., M. Obornik and J. Lukes (2013). "Make it, take it, or leave it: heme metabolism of parasites." PLoS Pathog **9**(1): e1003088.

Koshy, A. A., H. K. Dietrich, D. A. Christian, J. H. Melehani, A. J. Shastri, C. A. Hunter and J. C. Boothroyd (2012). "Toxoplasma co-opts host cells it does not invade." PLoS Pathog **8**(7): e1002825.

Kremer, K., D. Kamin, E. Rittweger, J. Wilkes, H. Flammer, S. Mahler, J. Heng, C. J. Tonkin, G. Langsley, S. W. Hell, V. B. Carruthers, D. J. Ferguson and M. Meissner (2013). "An overexpression screen of Toxoplasma gondii Rab-GTPases reveals distinct transport routes to the micronemes." PLoS Pathog **9**(3): e1003213.

Kumar, B., S. Chaubey, P. Shah, A. Tanveer, M. Charan, M. I. Siddiqi and S. Habib (2011). "Interaction between sulphur mobilisation proteins SufB and SufC: evidence for an iron-sulphur cluster biogenesis pathway in the apicoplast of Plasmodium falciparum." Int J Parasitol **41**(9): 991-999.

Kursula, I., P. Kursula, M. Ganter, S. Panjikar, K. Matuschewski and H. Schuler (2008). "Structural basis for parasite-specific functions of the divergent profilin of Plasmodium falciparum." Structure **16**(11): 1638-1648.

Laemmli, U. K. (1970). "Cleavage of structural proteins during the assembly of the head of bacteriophage T4." Nature **227**(5259): 680-685.

Lagal, V., E. M. Binder, M. H. Huynh, B. F. Kafsack, P. K. Harris, R. Diez, D. Chen, R. N. Cole, V. B. Carruthers and K. Kim (2010). "Toxoplasma gondii protease TgSUB1 is required for cell surface processing of micronemal adhesive complexes and efficient adhesion of tachyzoites." Cell Microbiol **12**(12): 1792-1808.

Lamarque, M., S. Besteiro, J. Papoin, M. Roques, B. Vulliez-Le Normand, J. Morlon-Guyot, J. F. Dubremetz, S. Fauquenoy, S. Tomavo, B. W. Faber, C. H. Kocken, A. W. Thomas, M. J. Boulanger, G. A. Bentley and M. Lebrun (2011). "The RON2-AMA1 interaction is a critical step in moving junction-dependent invasion by apicomplexan parasites." PLoS Pathog **7**(2): e1001276.

Lambert, H. and A. Barragan (2010). "Modelling parasite dissemination: host cell subversion and immune evasion by Toxoplasma gondii." Cell Microbiol **12**(3): 292-300.

Lammermann, T., B. L. Bader, S. J. Monkley, T. Worbs, R. Wedlich-Soldner, K. Hirsch, M. Keller, R. Forster, D. R. Critchley, R. Fassler and M. Sixt (2008). "Rapid leukocyte migration by integrin-independent flowing and squeezing." Nature **453**(7191): 51-55.

Lebrun, M., A. Michelin, H. El Hajj, J. Poncet, P. J. Bradley, H. Vial and J. F. Dubremetz (2005). "The rhoptry neck protein RON4 re-localizes at the moving junction during Toxoplasma gondii invasion." Cell Microbiol **7**(12): 1823-1833.

Lekutis, C., D. J. Ferguson, M. E. Grigg, M. Camps and J. C. Boothroyd (2001). "Surface antigens of Toxoplasma gondii: variations on a theme." Int J Parasitol **31**(12): 1285-1292.

Leung, J. M., M. A. Rould, C. Konradt, C. A. Hunter and G. E. Ward (2014). "Disruption of TgPHIL1 Alters Specific Parameters of Toxoplasma gondii Motility Measured in a Quantitative, Three-Dimensional Live Motility Assay." PLoS One **9**(1): e85763.

Levine, N. D. (1988). "Progress in taxonomy of the Apicomplexan protozoa." J Protozool **35**(4): 518-520.

Lim, L. and G. I. McFadden (2010). "The evolution, metabolism and functions of the apicoplast." Philos Trans R Soc Lond B Biol Sci **365**(1541): 749-763.

Lorestani, A., F. D. Ivey, S. Thirugnanam, M. A. Busby, G. T. Marth, I. M. Cheeseman and M. J. Gubbels (2012). "Targeted proteomic dissection of Toxoplasma cytoskeleton sub-compartments using MORN1." Cytoskeleton (Hoboken) **69**(12): 1069-1085.

Lorestani, A., L. Sheiner, K. Yang, S. D. Robertson, N. Sahoo, C. F. Brooks, D. J. Ferguson, B. Striepen and M. J. Gubbels (2010). "A Toxoplasma MORN1 null mutant undergoes repeated divisions but is defective in basal assembly, apicoplast division and cytokinesis." PLoS One **5**(8): e12302.

Lourido, S., J. Shuman, C. Zhang, K. M. Shokat, R. Hui and L. D. Sibley (2010). "Calcium-dependent protein kinase 1 is an essential regulator of exocytosis in Toxoplasma." Nature **465**(7296): 359-362.

Lourido, S., K. Tang and L. D. Sibley (2012). "Distinct signalling pathways control Toxoplasma egress and host-cell invasion." EMBO J **31**(24): 4524-4534.

Lyons, R. E., R. McLeod and C. W. Roberts (2002). "Toxoplasma gondii tachyzoite-bradyzoite interconversion." Trends Parasitol **18**(5): 198-201.

Mann, T. and C. Beckers (2001). "Characterization of the subpellicular network, a filamentous membrane skeletal component in the parasite Toxoplasma gondii." Mol Biochem Parasitol **115**(2): 257-268.

Matuschewski, K., M. M. Mota, J. C. Pinder, V. Nussenzweig and S. H. Kappe (2001). "Identification of the class XIV myosins Pb-MyoA and Py-MyoA and expression in Plasmodium sporozoites." Mol Biochem Parasitol **112**(1): 157-161.

Mazumdar, J., H. W. E, K. Masek, A. H. C and B. Striepen (2006). "Apicoplast fatty acid synthesis is essential for organelle biogenesis and parasite survival in Toxoplasma gondii." Proc Natl Acad Sci U S A **103**(35): 13192-13197.

McCoy, J. M., L. Whitehead, G. G. van Dooren and C. J. Tonkin (2012). "TgCDPK3 regulates calcium-dependent egress of Toxoplasma gondii from host cells." PLoS Pathog **8**(12): e1003066.

McFadden, G. I., M. E. Reith, J. Munholland and N. Lang-Unnasch (1996). "Plastid in human parasites." Nature **381**(6582): 482.

McLeod, R., K. M. Boyer, D. Lee, E. Mui, K. Wroblewski, T. Karrison, A. G. Noble, S. Withers, C. N. Swisher, P. T. Heydemann, M. Sautter, J. Babiarz, P. Rabiah, P. Meier, M. E. Grigg and G. Toxoplasmosis Study (2012). "Prematurity and severity are associated with Toxoplasma gondii alleles (NCCCTS, 1981-2009)." Clin Infect Dis **54**(11): 1595-1605.

Mead, P. S., L. Slutsker, V. Dietz, L. F. McCaig, J. S. Bresee, C. Shapiro, P. M. Griffin and R. V. Tauxe (1999). "Food-related illness and death in the United States." Emerg Infect Dis **5**(5): 607-625.

Mehta, S. and L. D. Sibley (2010). "Toxoplasma gondii actin depolymerizing factor acts primarily to sequester G-actin." J Biol Chem **285**(9): 6835-6847.

Mehta, S. and L. D. Sibley (2011). "Actin depolymerizing factor controls actin turnover and gliding motility in Toxoplasma gondii." Mol Biol Cell **22**(8): 1290-1299.

Meissner, M., S. Brecht, H. Bujard and D. Soldati (2001). "Modulation of myosin A expression by a newly established tetracycline repressor-based inducible system in Toxoplasma gondii." Nucleic Acids Res **29**(22): E115.

Meissner, M., D. J. Ferguson and F. Frischknecht (2013). "Invasion factors of apicomplexan parasites: essential or redundant?" Curr Opin Microbiol.

Meissner, M., D. Schluter and D. Soldati (2002). "Role of Toxoplasma gondii myosin A in powering parasite gliding and host cell invasion." Science **298**(5594): 837-840.

Meissner, M. and D. Soldati (2005). "The transcription machinery and the molecular toolbox to control gene expression in Toxoplasma gondii and other protozoan parasites." Microbes Infect **7**(13): 1376-1384.

Mercier, C., K. D. Adjogble, W. Daubener and M. F. Delauw (2005). "Dense granules: are they key organelles to help understand the parasitophorous vacuole of all apicomplexa parasites?" Int J Parasitol **35**(8): 829-849.

Mercier, C., J. F. Dubremetz, B. Rauscher, L. Lecordier, L. D. Sibley and M. F. Cesbron-Delauw (2002). "Biogenesis of nanotubular network in Toxoplasma parasitophorous vacuole induced by parasite proteins." Mol Biol Cell **13**(7): 2397-2409.

Mercier, C., L. Lecordier, F. Darcy, D. Deslee, A. Murray, B. Tourvieille, P. Maes, A. Capron and M. F. Cesbron-Delauw (1993). "Molecular characterization of a dense granule antigen (Gra 2) associated with the network of the parasitophorous vacuole in Toxoplasma gondii." Mol Biochem Parasitol **58**(1): 71-82.

Mermall, V., P. L. Post and M. S. Mooseker (1998). "Unconventional myosins in cell movement, membrane traffic, and signal transduction." Science **279**(5350): 527-533.

Messina, M., I. Niesman, C. Mercier and L. D. Sibley (1995). "Stable DNA transformation of Toxoplasma gondii using phleomycin selection." Gene **165**(2): 213-217.

Miller, N. L., J. K. Frenkel and J. P. Dubey (1972). "Oral infections with Toxoplasma cysts and oocysts in felines, other mammals, and in birds." J Parasitol **58**(5): 928-937.

Miranda, K., D. A. Pace, R. Cintron, J. C. Rodrigues, J. Fang, A. Smith, P. Rohloff, E. Coelho, F. de Haas, W. de Souza, I. Coppens, L. D. Sibley and S. N. Moreno (2010). "Characterization of a novel organelle in Toxoplasma gondii with similar composition and function to the plant vacuole." Mol Microbiol **76**(6): 1358-1375.

Mital, J., M. Meissner, D. Soldati and G. E. Ward (2005). "Conditional expression of Toxoplasma gondii apical membrane antigen-1 (TgAMA1) demonstrates that TgAMA1 plays a critical role in host cell invasion." Mol Biol Cell **16**(9): 4341-4349.

Mitchison, T. J., G. T. Charras and L. Mahadevan (2008). "Implications of a poroelastic cytoplasm for the dynamics of animal cell shape." Semin Cell Dev Biol **19**(3): 215-223.

Moeendarbary, E., L. Valon, M. Fritzsche, A. R. Harris, D. A. Moulding, A. J. Thrasher, E. Stride, L. Mahadevan and G. T. Charras (2013). "The cytoplasm of living cells behaves as a poroelastic material." Nat Mater **12**(3): 253-261.

Mondragon, R. and E. Frixione (1996). "Ca(2+)-dependence of conoid extrusion in Toxoplasma gondii tachyzoites." J Eukaryot Microbiol **43**(2): 120-127.

Montoya, J. G. and O. Liesenfeld (2004). "Toxoplasmosis." Lancet **363**(9425): 1965-1976.

Morisaki, J. H., J. E. Heuser and L. D. Sibley (1995). "Invasion of Toxoplasma gondii occurs by active penetration of the host cell." J Cell Sci **108 (Pt 6)**: 2457-2464.

Morrill, L. C. and A. R. Loeblich, 3rd (1983). "Ultrastructure of the dinoflagellate amphiesma." Int Rev Cytol **82**: 151-180.

Morrissette, N. S., A. Mitra, D. Sept and L. D. Sibley (2004). "Dinitroanilines bind alpha-tubulin to disrupt microtubules." Mol Biol Cell **15**(4): 1960-1968.

Morrissette, N. S., J. M. Murray and D. S. Roos (1997). "Subpellicular microtubules associate with an intramembranous particle lattice in the protozoan parasite Toxoplasma gondii." J Cell Sci **110 (Pt 1)**: 35-42.

Morrissette, N. S. and L. D. Sibley (2002). "Cytoskeleton of apicomplexan parasites." Microbiol Mol Biol Rev **66**(1): 21-38; table of contents.

Morrissette, N. S. and L. D. Sibley (2002). "Disruption of microtubules uncouples budding and nuclear division in Toxoplasma gondii." J Cell Sci **115**(Pt 5): 1017-1025.

Moudy, R., T. J. Manning and C. J. Beckers (2001). "The loss of cytoplasmic potassium upon host cell breakdown triggers egress of Toxoplasma gondii." J Biol Chem **276**(44): 41492-41501.

Mueller, C., N. Klages, D. Jacot, J. M. Santos, A. Cabrera, T. W. Gilberger, J. F. Dubremetz and D. Soldati-Favre (2013). "The Toxoplasma protein ARO mediates the apical positioning of rhoptry organelles, a prerequisite for host cell invasion." Cell Host Microbe **13**(3): 289-301.

Munter, S., B. Sabass, C. Selhuber-Unkel, M. Kudryashev, S. Hegge, U. Engel, J. P. Spatz, K. Matuschewski, U. S. Schwarz and F. Frischknecht (2009). "Plasmodium sporozoite motility is modulated by the turnover of discrete adhesion sites." Cell Host Microbe **6**(6): 551-562.

Nag, S., M. Larsson, R. C. Robinson and L. D. Burtnick (2013). "Gelsolin: the tail of a molecular gymnast." Cytoskeleton (Hoboken) **70**(7): 360-384.

Nair, S. C., C. F. Brooks, C. D. Goodman, A. Sturm, G. I. McFadden, S. Sundriyal, J. L. Anglin, Y. Song, S. N. Moreno and B. Striepen (2011). "Apicoplast isoprenoid precursor synthesis and the molecular basis of fosmidomycin resistance in Toxoplasma gondii." J Exp Med **208**(7): 1547-1559.

Nebl, T., J. H. Prieto, E. Kapp, B. J. Smith, M. J. Williams, J. R. Yates, 3rd, A. F. Cowman and C. J. Tonkin (2011). "Quantitative in vivo analyses reveal calcium-dependent phosphorylation sites and identifies a novel component of the Toxoplasma invasion motor complex." PLoS Pathog **7**(9): e1002222.

Nichols, B. A. and M. L. Chiappino (1987). "Cytoskeleton of Toxoplasma gondii." J Protozool **34**(2): 217-226.

Nicolle, C. and L. Manceaux (1908). "Sur une infection a corps de Leishman (ou organismes voisons) du gondi." C R Acad Sci **147: 736**.

Nicolle, C. and L. Manceaux (1909). "Sur un protozoaire nouveau du gondi." C R Acad Sci **148: 369**.

Nishi, M., K. Hu, J. M. Murray and D. S. Roos (2008). "Organellar dynamics during the cell cycle of Toxoplasma gondii." J Cell Sci **121**(Pt 9): 1559-1568.

O'Donnell, R. A., P. R. Preiser, D. H. Williamson, P. W. Moore, A. F. Cowman and B. S. Crabb (2001). "An alteration in concatameric structure is associated with efficient segregation of plasmids in transfected Plasmodium falciparum parasites." Nucleic Acids Res **29**(3): 716-724.

O'Hara, S. P., G. B. Gajdos, C. E. Trussoni, P. L. Splinter and N. F. LaRusso (2010). "Cholangiocyte myosin IIB is required for localized aggregation of sodium glucose cotransporter 1 to sites of Cryptosporidium parvum cellular invasion and facilitates parasite internalization." Infect Immun **78**(7): 2927-2936.

O'Hara, S. P., A. J. Small, X. M. Chen and N. F. LaRusso (2008). "Host cell actin remodeling in response to Cryptosporidium." Subcell Biochem **47**: 92-100.

Ofer, N., A. Mogilner and K. Keren (2011). "Actin disassembly clock determines shape and speed of lamellipodial fragments." Proc Natl Acad Sci U S A **108**(51): 20394-20399.

Okten, Z. and M. Schliwa (2007). "Molecular motors: a step dissected." Nature **450**(7170): 625-626.

Pain, A., L. Crossman and J. Parkhill (2005). "Comparative apicomplexan genomics." Nat Rev Microbiol **3**(6): 454-455.

Patron, S. A., M. Mondragon, S. Gonzalez, J. R. Ambrosio, B. A. Guerrero and R. Mondragon (2005). "Identification and purification of actin from the subpellicular network of Toxoplasma gondii tachyzoites." Int J Parasitol **35**(8): 883-894.

Paul, A. S. and T. D. Pollard (2009). "Review of the mechanism of processive actin filament elongation by formins." Cell Motil Cytoskeleton **66**(8): 606-617.

Pelletier, L., C. A. Stern, M. Pypaert, D. Sheff, H. M. Ngo, N. Roper, C. Y. He, K. Hu, D. Toomre, I. Coppens, D. S. Roos, K. A. Joiner and G. Warren (2002). "Golgi biogenesis in Toxoplasma gondii." Nature **418**(6897): 548-552.

Pezzella, N., A. Bouchot, A. Bonhomme, L. Pingret, C. Klein, H. Burlet, G. Balossier, P. Bonhomme and J. M. Pinon (1997). "Involvement of calcium and calmodulin in Toxoplasma gondii tachyzoite invasion." Eur J Cell Biol **74**(1): 92-101.

Pfluger, S. L., H. V. Goodson, J. M. Moran, C. J. Ruggiero, X. Ye, K. M. Emmons and K. M. Hager (2005). "Receptor for retrograde transport in the apicomplexan parasite Toxoplasma gondii." Eukaryot Cell **4**(2): 432-442.

Pieperhoff, M. S., M. Schmitt, D. J. Ferguson and M. Meissner (2013). "The role of clathrin in post-Golgi trafficking in Toxoplasma gondii." PLoS One **8**(10): e77620.

Pinder, J. C., R. E. Fowler, A. R. Dluzewski, L. H. Bannister, F. M. Lavin, G. H. Mitchell, R. J. Wilson and W. B. Gratzer (1998). "Actomyosin motor in the merozoite of the malaria parasite, Plasmodium falciparum: implications for red cell invasion." J Cell Sci **111 (Pt 13)**: 1831-1839.

Pino, P., S. Sebastian, E. A. Kim, E. Bush, M. Brochet, K. Volkmann, E. Kozlowski, M. Llinas, O. Billker and D. Soldati-Favre (2012). "A tetracycline-repressible transactivator system to study essential genes in malaria parasites." Cell Host Microbe **12**(6): 824-834.

Plattner, F. and D. Soldati-Favre (2008). "Hijacking of host cellular functions by the Apicomplexa." Annu Rev Microbiol **62**: 471-487.

Plattner, F., F. Yarovinsky, S. Romero, D. Didry, M. F. Carlier, A. Sher and D. Soldati-Favre (2008). "Toxoplasma profilin is essential for host cell invasion and TLR11-dependent induction of an interleukin-12 response." Cell Host Microbe **3**(2): 77-87.

Pollard, T. D. and G. G. Borisy (2003). "Cellular motility driven by assembly and disassembly of actin filaments." Cell **112**(4): 453-465.

Pollard, T. D. and J. A. Cooper (2009). "Actin, a central player in cell shape and movement." Science **326**(5957): 1208-1212.

Polonais, V., B. Javier Foth, K. Chinthalapudi, J. B. Marq, D. J. Manstein, D. Soldati-Favre and K. Frenal (2011). "Unusual anchor of a motor complex (MyoD-MLC2) to the plasma membrane of Toxoplasma gondii." Traffic **12**(3): 287-300.

Polonais, V., M. Shea and D. Soldati-Favre (2011). "Toxoplasma gondii aspartic protease 1 is not essential in tachyzoites." Exp Parasitol **128**(4): 454-459.

Poupel, O. and I. Tardieux (1999). "Toxoplasma gondii motility and host cell invasiveness are drastically impaired by jasplakinolide, a cyclic peptide stabilizing F-actin." Microbes Infect **1**(9): 653-662.

Radke, J. R., B. Striepen, M. N. Guerini, M. E. Jerome, D. S. Roos and M. W. White (2001). "Defining the cell cycle for the tachyzoite stage of Toxoplasma gondii." Mol Biochem Parasitol **115**(2): 165-175.

Ramakrishnan, S., M. D. Docampo, J. I. Macrae, F. M. Pujol, C. F. Brooks, G. G. van Dooren, J. K. Hiltunen, A. J. Kastaniotis, M. J. McConville and B. Striepen (2012). "Apicoplast and endoplasmic

reticulum cooperate in fatty acid biosynthesis in apicomplexan parasite Toxoplasma gondii." J Biol Chem **287**(7): 4957-4971.

Rayment, I., W. R. Rypniewski, K. Schmidt-Base, R. Smith, D. R. Tomchick, M. M. Benning, D. A. Winkelmann, G. Wesenberg and H. M. Holden (1993). "Three-dimensional structure of myosin subfragment-1: a molecular motor." Science **261**(5117): 50-58.

Reck-Peterson, S. L., P. J. Novick and M. S. Mooseker (1999). "The tail of a yeast class V myosin, myo2p, functions as a localization domain." Mol Biol Cell **10**(4): 1001-1017.

Renkawitz, J., K. Schumann, M. Weber, T. Lammermann, H. Pflicke, M. Piel, J. Polleux, J. P. Spatz and M. Sixt (2009). "Adaptive force transmission in amoeboid cell migration." Nat Cell Biol **11**(12): 1438-1443.

Renkawitz, J. and M. Sixt (2010). "Mechanisms of force generation and force transmission during interstitial leukocyte migration." EMBO Rep **11**(10): 744-750.

Robinson, M. S. and J. Hirst (2013). "Rapid inactivation of proteins by knocksideways." Curr Protoc Cell Biol **61**: 15 20 11-17.

Robinson, M. S., D. A. Sahlender and S. D. Foster (2010). "Rapid inactivation of proteins by rapamycin-induced rerouting to mitochondria." Dev Cell **18**(2): 324-331.

Roiko, M. S. and V. B. Carruthers (2013). "Functional dissection of Toxoplasma gondii perforin-like protein 1 reveals a dual domain mode of membrane binding for cytolysis and parasite egress." J Biol Chem **288**(12): 8712-8725.

Roos, D. S., M. J. Crawford, R. G. Donald, M. Fraunholz, O. S. Harb, C. Y. He, J. C. Kissinger, M. K. Shaw and B. Striepen (2002). "Mining the Plasmodium genome database to define organellar function: what does the apicoplast do?" Philos Trans R Soc Lond B Biol Sci **357**(1417): 35-46.

Ross, J. L., M. Y. Ali and D. M. Warshaw (2008). "Cargo transport: molecular motors navigate a complex cytoskeleton." Curr Opin Cell Biol **20**(1): 41-47.

Ryning, F. W. and J. S. Remington (1978). "Effect of cytochalasin D on Toxoplasma gondii cell entry." Infect Immun **20**(3): 739-743.

Sackmann, E. and A. S. Smith (2014). "Physics of cell adhesion: some lessons from cell-mimetic systems." Soft Matter **10**(11): 1644-1659.

Saeij, J. P., J. P. Boyle, S. Coller, S. Taylor, L. D. Sibley, E. T. Brooke-Powell, J. W. Ajioka and J. C. Boothroyd (2006). "Polymorphic secreted kinases are key virulence factors in toxoplasmosis." Science **314**(5806): 1780-1783.

Saeij, J. P., S. Coller, J. P. Boyle, M. E. Jerome, M. W. White and J. C. Boothroyd (2007). "Toxoplasma co-opts host gene expression by injection of a polymorphic kinase homologue." Nature **445**(7125): 324-327.

Sahoo, N., W. Beatty, J. Heuser, D. Sept and L. D. Sibley (2006). "Unusual kinetic and structural properties control rapid assembly and turnover of actin in the parasite Toxoplasma gondii." Mol Biol Cell **17**(2): 895-906.

Sato, Y., M. Kameya, H. Arai, M. Ishii and Y. Igarashi (2011). "Detecting weak protein-protein interactions by modified far-western blotting." J Biosci Bioeng **112**(3): 304-307.

Schafer, D. A., S. R. Gill, J. A. Cooper, J. E. Heuser and T. A. Schroer (1994). "Ultrastructural analysis of the dynactin complex: an actin-related protein is a component of a filament that resembles F-actin." J Cell Biol **126**(2): 403-412.

Schafer, D. A. and T. A. Schroer (1999). "Actin Related Proteins." Annu. Rev. Cell Dev. Biol. **15**: 341-363.

Schliwa, M. and G. Woehlke (2003). "Molecular motors." Nature **422**(6933): 759-765.

Schmitz, S., M. Grainger, S. Howell, L. J. Calder, M. Gaeb, J. C. Pinder, A. A. Holder and C. Veigel (2005). "Malaria parasite actin filaments are very short." J Mol Biol **349**(1): 113-125.

Schoondermark-Van de Ven, E., W. Melchers, W. Camps, T. Eskes, J. Meuwissen and J. Galama (1994). "Effectiveness of spiramycin for treatment of congenital Toxoplasma gondii infection in rhesus monkeys." Antimicrob Agents Chemother **38**(9): 1930-1936.

Schroer, T. A. (2004). "Dynactin." Annu Rev Cell Dev Biol **20**: 759-779.

Schuler, H., A. K. Mueller and K. Matuschewski (2005). "Unusual properties of Plasmodium falciparum actin: new insights into microfilament dynamics of apicomplexan parasites." FEBS Lett **579**(3): 655-660.

Sebastian, S., M. Brochet, M. O. Collins, F. Schwach, M. L. Jones, D. Goulding, J. C. Rayner, J. S. Choudhary and O. Billker (2012). "A Plasmodium calcium-dependent protein kinase controls zygote development and transmission by translationally activating repressed mRNAs." Cell Host Microbe **12**(1): 9-19.

Seeber, F. and J. C. Boothroyd (1996). "Escherichia coli beta-galactosidase as an in vitro and in vivo reporter enzyme and stable transfection marker in the intracellular protozoan parasite Toxoplasma gondii." Gene **169**(1): 39-45.

Seeber, F. and D. Soldati-Favre (2010). "Metabolic pathways in the apicoplast of apicomplexa." Int Rev Cell Mol Biol **281**: 161-228.

Sellers, J. R. and H. V. Goodson (1995). "Motor proteins 2: myosin." Protein Profile **2**(12): 1323-1423.

Shaw, M. K. (1999). "Theileria parva: sporozoite entry into bovine lymphocytes is not dependent on the parasite cytoskeleton." Exp Parasitol **92**(1): 24-31.

Shaw, M. K. (2003). "Cell invasion by Theileria sporozoites." Trends Parasitol **19**(1): 2-6.

Shaw, M. K., H. L. Compton, D. S. Roos and L. G. Tilney (2000). "Microtubules, but not actin filaments, drive daughter cell budding and cell division in Toxoplasma gondii." J Cell Sci **113 (Pt 7)**: 1241-1254.

Shaw, M. K., D. S. Roos and L. G. Tilney (2001). "DNA replication and daughter cell budding are not tightly linked in the protozoan parasite Toxoplasma gondii." Microbes Infect **3**(5): 351-362.

Shaw, M. K. and L. G. Tilney (1999). "Induction of an acrosomal process in Toxoplasma gondii: visualization of actin filaments in a protozoan parasite." Proc Natl Acad Sci U S A **96**(16): 9095-9099.

Sheffield, H. G. and M. L. Melton (1968). "The fine structure and reproduction of Toxoplasma gondii." J Parasitol **54**(2): 209-226.

Sheiner, L., J. L. Demerly, N. Poulsen, W. L. Beatty, O. Lucas, M. S. Behnke, M. W. White and B. Striepen (2011). "A systematic screen to discover and analyze apicoplast proteins identifies a conserved and essential protein import factor." PLoS Pathog **7**(12): e1002392.

Sheiner, L., J. M. Santos, N. Klages, F. Parussini, N. Jemmely, N. Friedrich, G. E. Ward and D. Soldati-Favre (2010). "Toxoplasma gondii transmembrane microneme proteins and their modular design." Mol Microbiol.

Sheiner, L., J. M. Santos, N. Klages, F. Parussini, N. Jemmely, N. Friedrich, G. E. Ward and D. Soldati-Favre (2011). "Toxoplasma gondii transmembrane microneme proteins and their modular design." Mol Microbiol.

Shen, B. and L. D. Sibley (2014). "Toxoplasma aldolase is required for metabolism but dispensable for host-cell invasion." Proc Natl Acad Sci U S A **111**(9): 3567-3572.

Sibley, L. D. (2010). "How apicomplexan parasites move in and out of cells." Curr Opin Biotechnol **21**(5): 592-598.

Sibley, L. D. and J. C. Boothroyd (1992). "Construction of a molecular karyotype for Toxoplasma gondii." Mol Biochem Parasitol **51**(2): 291-300.

Siegel, R. W., R. Jain and A. Bradbury (2001). "Using an in vivo phagemid system to identify non-compatible loxP sequences." FEBS Lett **505**(3): 467-473.

Silacci, P., L. Mazzolai, C. Gauci, N. Stergiopulos, H. L. Yin and D. Hayoz (2004). "Gelsolin superfamily proteins: key regulators of cellular functions." Cell Mol Life Sci **61**(19-20): 2614-2623.

Skillman, K. M., W. Daher, C. I. Ma, D. Soldati-Favre and L. D. Sibley (2012). "Toxoplasma gondii profilin acts primarily to sequester G-actin while formins efficiently nucleate actin filament formation in vitro." Biochemistry **51**(12): 2486-2495.

Skillman, K. M., K. Diraviyam, A. Khan, K. Tang, D. Sept and L. D. Sibley (2011). "Evolutionarily divergent, unstable filamentous actin is essential for gliding motility in apicomplexan parasites." PLoS Pathog **7**(10): e1002280.

Skillman, K. M., C. I. Ma, D. H. Fremont, K. Diraviyam, J. A. Cooper, D. Sept and L. D. Sibley (2013). "The unusual dynamics of parasite actin result from isodesmic polymerization." Nat Commun **4**: 2285.

Soldati, D. and J. C. Boothroyd (1993). "Transient transfection and expression in the obligate intracellular parasite Toxoplasma gondii." Science **260**(5106): 349-352.

Soldati, D. and M. Meissner (2004). "Toxoplasma as a novel system for motility." Curr Opin Cell Biol **16**(1): 32-40.

Starnes, G. L., M. Coincon, J. Sygusch and L. D. Sibley (2009). "Aldolase is essential for energy production and bridging adhesin-actin cytoskeletal interactions during parasite invasion of host cells." Cell Host Microbe **5**(4): 353-364.

Stokkermans, T. J., J. D. Schwartzman, K. Keenan, N. S. Morrissette, L. G. Tilney and D. S. Roos (1996). "Inhibition of Toxoplasma gondii replication by dinitroaniline herbicides." Exp Parasitol **84**(3): 355-370.

Stommel, E. W., K. H. Ely, J. D. Schwartzman and L. H. Kasper (1997). "Toxoplasma gondii: dithiol-induced Ca2+ flux causes egress of parasites from the parasitophorous vacuole." Exp Parasitol **87**(2): 88-97.

Straub, K. W., S. J. Cheng, C. S. Sohn and P. J. Bradley (2009). "Novel components of the Apicomplexan moving junction reveal conserved and coccidia-restricted elements." Cell Microbiol **11**(4): 590-603.

Straub, K. W., E. D. Peng, B. E. Hajagos, J. S. Tyler and P. J. Bradley (2011). "The moving junction protein RON8 facilitates firm attachment and host cell invasion in Toxoplasma gondii." PLoS Pathog **7**(3): e1002007.

Striepen, B., M. J. Crawford, M. K. Shaw, L. G. Tilney, F. Seeber and D. S. Roos (2000). "The plastid of Toxoplasma gondii is divided by association with the centrosomes." J Cell Biol **151**(7): 1423-1434.

Striepen, B., C. Y. He, M. Matrajt, D. Soldati and D. S. Roos (1998). "Expession, selection, and organellar targeting of green fluorescent protein in Toxoplasma gondii." Mol Biochem Parasitol **92**: 325-338.

Striepen, B., C. Y. He, M. Matrajt, D. Soldati and D. S. Roos (1998). "Expression, selection, and organellar targeting of the green fluorescent protein in Toxoplasma gondii." Mol Biochem Parasitol **92**(2): 325-338.

Striepen, B., C. N. Jordan, S. Reiff and G. G. van Dooren (2007). "Building the perfect parasite: cell division in apicomplexa." PLoS Pathog **3**(6): e78.

Su, C., D. K. Howe, J. P. Dubey, J. W. Ajioka and L. D. Sibley (2002). "Identification of quantitative trait loci controlling acute virulence in Toxoplasma gondii." Proc Natl Acad Sci U S A **99**(16): 10753-10758.

Suvorova, E. S., M. M. Lehmann, S. Kratzer and M. W. White (2012). "Nuclear actin-related protein is required for chromosome segregation in Toxoplasma gondii." Mol Biochem Parasitol **181**(1): 7-16.

Suzuki, Y., Q. Yang, S. Yang, N. Nguyen, S. Lim, O. Liesenfeld, T. Kojima and J. S. Remington (1996). "IL-4 is protective against development of toxoplasmic encephalitis." J Immunol **157**(6): 2564-2569.

Sweeney, K. R., N. S. Morrissette, S. LaChapelle and I. J. Blader (2010). "Host cell invasion by Toxoplasma gondii is temporally regulated by the host microtubule cytoskeleton." Eukaryot Cell **9**(11): 1680-1689.

Takemae, H., T. Sugi, K. Kobayashi, H. Gong, A. Ishiwa, F. C. Recuenco, F. Murakoshi, T. Iwanaga, A. Inomata, T. Horimoto, H. Akashi and K. Kato (2013). "Characterization of the interaction between Toxoplasma gondii rhoptry neck protein 4 and host cellular beta-tubulin." Sci Rep **3**: 3199.

Taylor, S., A. Barragan, C. Su, B. Fux, S. J. Fentress, K. Tang, W. L. Beatty, H. E. Hajj, M. Jerome, M. S. Behnke, M. White, J. C. Wootton and L. D. Sibley (2006). "A secreted serine-threonine kinase determines virulence in the eukaryotic pathogen Toxoplasma gondii." Science **314**(5806): 1776-1780.

Thomson, J. G., E. B. Rucker, 3rd and J. A. Piedrahita (2003). "Mutational analysis of loxP sites for efficient Cre-mediated insertion into genomic DNA." Genesis **36**(3): 162-167.

Tilney, L. G. and M. S. Tilney (1996). "The cytoskeleton of protozoan parasites." Curr Opin Cell Biol **8**(1): 43-48.

Tonkin, M. L., M. Roques, M. H. Lamarque, M. Pugniere, D. Douguet, J. Crawford, M. Lebrun and M. J. Boulanger (2011). "Host cell invasion by apicomplexan parasites: insights from the co-structure of AMA1 with a RON2 peptide." Science **333**(6041): 463-467.

Toyama, S. and S. Toyama (1984). "A variant form of beta-actin in a mutant of KB cells resistant to cytochalasin B." Cell **37**(2): 609-614.

Toyama, S. and S. Toyama (1988). "Functional alterations in beta'-actin from a KB cell mutant resistant to cytochalasin B." J Cell Biol **107**(4): 1499-1504.

Trager, W. and J. B. Jensen (1976). "Human malaria parasites in continuous culture." Science **193**(4254): 673-675.

Tran, J. Q., J. C. de Leon, C. Li, M. H. Huynh, W. Beatty and N. S. Morrissette (2010). "RNG1 is a late marker of the apical polar ring in Toxoplasma gondii." Cytoskeleton (Hoboken) **67**(9): 586-598.

Tyler, J. S., M. Treeck and J. C. Boothroyd (2011). "Focus on the ringleader: the role of AMA1 in apicomplexan invasion and replication." Trends Parasitol **27**(9): 410-420.

Tyska, M. J. and D. M. Warshaw (2002). "The myosin power stroke." Cell Motil Cytoskeleton **51**(1): 1-15.

Vaishnava, S., D. P. Morrison, R. Y. Gaji, J. M. Murray, R. Entzeroth, D. K. Howe and B. Striepen (2005). "Plastid segregation and cell division in the apicomplexan parasite Sarcocystis neurona." J Cell Sci **118**(Pt 15): 3397-3407.

Valigurova, A. (2012). "Sophisticated adaptations of Gregarina cuneata (Apicomplexa) feeding stages for epicellular parasitism." PLoS One **7**(8): e42606.

Valigurova, A., N. Vaskovicova, N. Musilova and J. Schrevel (2013). "The enigma of eugregarine epicytic folds: where gliding motility originates?" Front Zool **10**(1): 57.

Vallee, R. B. and M. P. Sheetz (1996). "Targeting of motor proteins." Science **271**(5255): 1539-1544.

van Dooren, G. G., A. T. Kennedy and G. I. McFadden (2012). "The use and abuse of heme in apicomplexan parasites." Antioxid Redox Signal **17**(4): 634-656.

van Dooren, G. G., S. B. Reiff, C. Tomova, M. Meissner, B. M. Humbel and B. Striepen (2009). "A novel dynamin-related protein has been recruited for apicoplast fission in Toxoplasma gondii." Curr Biol **19**(4): 267-276.

van Dooren, G. G. and B. Striepen (2013). "The algal past and parasite present of the apicoplast." Annu Rev Microbiol **67**: 271-289.

Vanderberg, J. P. (1974). "Studies on the motility of Plasmodium sporozoites." J Protozool **21**(4): 527-537.

Vaughan, A. M., M. T. O'Neill, A. S. Tarun, N. Camargo, T. M. Phuong, A. S. Aly, A. F. Cowman and S. H. Kappe (2009). "Type II fatty acid synthesis is essential only for malaria parasite late liver stage development." Cell Microbiol **11**(3): 506-520.

Vaughan, K. T. (2005). "Microtubule plus ends, motors, and traffic of Golgi membranes." Biochim Biophys Acta **1744**(3): 316-324.

Volkmann, K., C. Pfander, C. Burstroem, M. Ahras, D. Goulding, J. C. Rayner, F. Frischknecht, O. Billker and M. Brochet (2012). "The alveolin IMC1h is required for normal ookinete and sporozoite motility behaviour and host colonisation in Plasmodium berghei." PLoS One **7**(7): e41409.

Waller, R. F., P. J. Keeling, R. G. Donald, B. Striepen, E. Handman, N. Lang-Unnasch, A. F. Cowman, G. S. Besra, D. S. Roos and G. I. McFadden (1998). "Nuclear-encoded proteins target to the plastid in Toxoplasma gondii and Plasmodium falciparum." Proc Natl Acad Sci U S A **95**(21): 12352-12357.

Waller, R. F., P. J. Keeling, G. G. van Dooren and G. I. McFadden (2003). "Comment on "A green algal apicoplast ancestor"." Science **301**(5629): 49; author reply 49.

Wanger, M., T. Keiser, J. M. Neuhaus and A. Wegner (1985). "The actin treadmill." Can J Biochem Cell Biol **63**(6): 414-421.

Webb, D. J., J. T. Parsons and A. F. Horwitz (2002). "Adhesion assembly, disassembly and turnover in migrating cells -- over and over and over again." Nat Cell Biol **4**(4): E97-100.

Wetzel, D. M., S. Hakansson, K. Hu, D. Roos and L. D. Sibley (2003). "Actin filament polymerization regulates gliding motility by apicomplexan parasites." Mol Biol Cell **14**(2): 396-406.

Wetzel, D. M., J. Schmidt, M. S. Kuhlenschmidt, J. P. Dubey and L. D. Sibley (2005). "Gliding motility leads to active cellular invasion by Cryptosporidium parvum sporozoites." Infect Immun **73**(9): 5379-5387.

White, M. W., M. E. Jerome, S. Vaishnava, M. Guerini, M. Behnke and B. Striepen (2005). "Genetic rescue of a Toxoplasma gondii conditional cell cycle mutant." Mol Microbiol **55**(4): 1060-1071.

Wichroski, M. J., J. A. Melton, C. G. Donahue, R. K. Tweten and G. E. Ward (2002). "Clostridium septicum alpha-toxin is active against the parasitic protozoan Toxoplasma gondii and targets members of the SAG family of glycosylphosphatidylinositol-anchored surface proteins." Infect Immun **70**(8): 4353-4361.

Wiesner, J. and H. Jomaa (2007). "Isoprenoid biosynthesis of the apicoplast as drug target." Curr Drug Targets **8**(1): 3-13.

Wilson, R. J., P. W. Denny, P. R. Preiser, K. Rangachari, K. Roberts, A. Roy, A. Whyte, M. Strath, D. J. Moore, P. W. Moore and D. H. Williamson (1996). "Complete gene map of the plastid-like DNA of the malaria parasite Plasmodium falciparum." J Mol Biol **261**(2): 155-172.

Woolley, D. E. (1972). "An actin-like protein from amoebae of dictyostelium discoideum." Arch Biochem Biophys **150**(2): 519-530.

Xian, W., J. X. Tang, P. A. Janmey and W. H. Braunlin (1999). "The polyelectrolyte behavior of actin filaments: a 25Mg NMR study." Biochemistry **38**(22): 7219-7226.

Xie, X., D. H. Harrison, I. Schlichting, R. M. Sweet, V. N. Kalabokis, A. G. Szent-Gyorgyi and C. Cohen (1994). "Structure of the regulatory domain of scallop myosin at 2.8 A resolution." Nature **368**(6469): 306-312.

Yarmola, E. G. and M. R. Bubb (2009). "How depolymerization can promote polymerization: the case of actin and profilin." Bioessays **31**(11): 1150-1160.

Yeh, E. and J. L. DeRisi (2011). "Chemical rescue of malaria parasites lacking an apicoplast defines organelle function in blood-stage Plasmodium falciparum." PLoS Biol **9**(8): e1001138.

Yoshida, K. and T. Soldati (2006). "Dissection of amoeboid movement into two mechanically distinct modes." J Cell Sci **119**(Pt 18): 3833-3844.

Zatulovskiy, E., R. Tyson, T. Bretschneider and R. R. Kay (2014). "Bleb-driven chemotaxis of Dictyostelium cells." J Cell Biol **204**(6): 1027-1044.

Zhang, Q., Y. Huang, Y. Zhang, X. Fang, A. Claes, M. Duchateau, A. Namane, J. J. Lopez-Rubio, W. Pan and A. Scherf (2011). "A critical role of perinuclear filamentous actin in spatial repositioning and mutually exclusive expression of virulence genes in malaria parasites." Cell Host Microbe **10**(5): 451-463.

Ziebert, F. and I. S. Aranson (2013). "Effects of adhesion dynamics and substrate compliance on the shape and motility of crawling cells." PLoS One **8**(5): e64511.